

DISSERTATION ZUR ERLANGUNG DES DOKTORGRADES
DER FAKULTÄT FÜR CHEMIE UND PHARMAZIE
DER LUDWIG-MAXIMILIANS-UNIVERSITÄT MÜNCHEN

**NITROGEN-RICH ENERGETIC MATERIALS BASED
ON 1,2,4-TRIAZOLE DERIVATIVES**

ALEXANDER ARMIN DIPPOLD

aus

Rosenheim

2013

Erklärung:

Diese Dissertation wurde im Sinne von § 7 der Promotionsordnung vom 28. November 2011 von Herrn Professor Dr. Thomas M. Klapötke betreut.

Eidesstattliche Versicherung:

Diese Dissertation wurde eigenständig und ohne unerlaubte Hilfe erarbeitet.

München, den~~01.08.2013~~.....

.....

(Alexander Armin Dippold)

Dissertation eingereicht am:~~01.08.2013~~.....

1. Gutachter: Prof. Dr. Thomas M. Klapötke

2. Gutachter: Prof. Dr. Konstantin Karaghiosoff

Mündliche Prüfung am:~~26.09.2013~~.....

DANKSAGUNG

Mein Dank gilt an erster Stelle Herrn Prof. Dr. Thomas M. Klapötke für die Aufnahme in seinen Arbeitskreis, die finanzielle Unterstützung sowie für sein stets offenes Ohr für alle Belange. Für die uneingeschränkte Unterstützung und das in mich gesetzte Vertrauen möchte ich mich herzlich bedanken.

Herrn Prof. Dr. Konstantin Karaghiosoff möchte ich sowohl für die Übernahme des Zweitgutachtens der Dissertation danken, als auch für die Unterstützung bei zahlreichen NMR Messungen und seinen unerschütterlichen Enthusiasmus („Das ist super!“) und Kennerblick bei der Auswahl und Messung von Einkristallen am X-Ray.

Herrn Akad. ORat Dr. Burkhard Krumm möchte ich für viele erheiternde Diskussionen rund um das Thema Fussball („Was ist denn schon wieder los beim FC Hollywood?“) und für das Anfertigen von zahlreichen NMR Messungen danken.

Frau Irene Scheckenbach danke ich für ihre große Hilfsbereitschaft, Sorgfalt und Mühe in allen bürokratischen Belangen und darüber hinaus. Für zahlreiche fruchtbare Diskussionen und eine hervorragende Arbeitsatmosphäre (inklusive Laborausflug und – halbe) möchte ich meinen Laborkollegen Dr. Franziska Betzler (Sooo flauschig!), Dr. Davin Piercey (Mr. „Pain in the ass“) sowie Dr. Niko und Dennis Fischer („Woisch is des schee!“) danken. Letzteren danke ich im Besonderen für die Bekanntschaft mit „Aktien Hell“ und die Versorgung mit zahlreichen kulinarischen Delikatessen der Firma „Fischer Feinkost GmbH“. Für die stets verlässliche und oft spontane Hilfe bei kniffligen Kristallstrukturen danke ich Frau Dr. Karin Lux und Herrn Dr. Peter Mayer. Eine ganze Schar von Bachelor- und Forschungs-Praktikanten hat durch viel Fleiß und Engagement einen wesentlichen Beitrag zu dieser Arbeit geleistet. Bei Michael Feller, Alexander Barthel, Patrick Nimax, Nils Winter, Manuel Dachs, Marcel Holler, Julius Neß, Michaela Oswald und Jakob Gaar möchte ich mich für die ausgesprochen gute und produktive Atmosphäre während der Zusammenarbeit herzlich bedanken.

Besonders danken möchte ich Dr. Franz Martin, der durch die hervorragende Betreuung und Unterstützung während der Masterarbeit den Grundstein für diese Arbeit gelegt hat und zu einem guten Freund geworden ist.

Für ihre Unterstützung und die großartige Zeit voller unvergesslicher Aktionen weit entfernt von jeglicher Chemie danke ich dem gesamten Arbeitskreis.

Meinen Studienkollegen und Freunden die sich an meiner Seite durch das Chemiestudium und die Promotion gekämpft haben verdanke ich viele unvergessliche Lernabende, Serientage, Biergartenbesuche, Eispausen, Grillabende, Mittagessen sowie eine kurzweilige Freizeit- und Abendgestaltung und vieles mehr..!

Ein ganz besonderer Dank geht an meine gesamte Familie für ihre unerschütterliche und selbstverständliche Unterstützung während des gesamten Studiums, welche weit über das Finanzielle hinaus geht und ohne deren Rückhalt diese Arbeit und vieles mehr nicht möglich gewesen wäre.

TABLE OF CONTENTS

1. INTRODUCTION	1
1.1 History & Background	1
1.2 Definition & Classification of Energetic Materials.....	2
1.3 Requirements for Modern Explosives.....	5
1.4 Strategies in Energetic Materials Design.....	6
1.5 Motivation and Objectives.....	8
1.6 References	9
2. CONCLUSIONS	11
3. CHAPTER 3: SYNTHESIS AND CHARACTERIZATION OF BIS(TRIAMINO GUANIDINIUM) 5,5'-DINITRIMINO-3,3'-AZO-1 <i>H</i> -1,2,4-TRIAZOLATE – A NOVEL INSENSITIVE ENERGETIC MATERIAL	19
4. CHAPTER 4: SYNTHESIS AND CHARACTERIZATION OF 3,3'-BIS(DINITROMETHYL)- 5,5'-AZO-1 <i>H</i> -1,2,4-TRIAZOLE	53
5. CHAPTER 5: NITROGEN-RICH BIS-1,2,4-TRIAZOLES – A COMPARATIVE STUDY OF STRUCTURAL AND ENERGETIC PROPERTIES	65
6. CHAPTER 6: INSENSITIVE NITROGEN-RICH ENERGETIC COMPOUNDS BASED ON THE 3,3'-DINITRO-5,5'-BIS-1,2,4-TRIAZOLATE ANION	95
7. CHAPTER 7: ASYMMETRICALLY SUBSTITUTED 5,5'-BISTRIAZOLES – NITROGEN RICH MATERIALS WITH VARIOUS ENERGETIC FUNCTIONALITIES	123
8. CHAPTER 8: A STUDY OF DINITRO-BIS-1,2,4-TRIAZOLE-1,1-DIOL AND DERIVATIVES – DESIGN OF HIGH PERFORMANCE INSENSITIVE ENERGETIC MATERIALS BY THE INTRODUCTION OF N-OXIDES	147
9. CHAPTER 9: SYNTHESIS AND CHARACTERIZATION OF 5-(1,2,4-TRIAZOL-3- YL)TETRAZOLES WITH VARIOUS ENERGETIC FUNCTIONALITIES	169

10. CHAPTER 10: A STUDY OF 5-(1,2,4-TRIAZOL-C-YL)TETRAZOL-1-OLS: COMBINING THE BENEFITS OF DIFFERENT HETEROCYCLES FOR THE DESIGN OF ENERGETIC MATERIALS	195
11. CHAPTER 11: A COMPARATIVE STUDY ON INSENSITIVE ENERGETIC DERIVATIVES OF 5-(1,2,4-TRIAZOL-C-YL)-TETRAZOLES AND THEIR 1-HYDROXY-TETRAZOLE ANALOGUES	221
12. APPENDIX	245
12.1 List of Abbreviations	245
12.2 Supporting information.....	247
12.3 Curriculum Vitae.....	271
12.4 Bibliography.....	272

1. INTRODUCTION

1.1 HISTORY & BACKGROUND

The chemistry of explosives, their development and application are as old as 220 years BC, when blackpowder was accidentally discovered by the Chinese. The history of energetic materials is well chronicled and therefore only a small look on milestone developments is given.^[1] Knowledge of blackpowder in Western Europe was considerably later when it was independently found by the German monk Berthold Schwartz in the 14th century. The next major milestone came with the development of nitroglycerine (NG) in the 19th century by Ascanio Sobrero, however NG was initially only used as medication for heart disease. The explosive properties were noticed very soon after its discovery and led to the first industrial process development for high explosives by Alfred Nobel in the 1860s. Sensitivity was always an issue with the production of nitroglycerine and many accidents occurred during its preparation. After the repeated occurrence of severe explosions during its manufacturing, nitroglycerine was mixed with kieselguhr forming a dough-like material (“dynamite”), which is far less sensitive and easier to handle than pure nitroglycerine. The growing use of explosives in coal mining also brought a corresponding increase on the number of gas and dust explosions, mandating replacement of the used explosives and promoting the development of new explosives such as picric acid or trinitrotoluene (TNT). While picric acid was suffering from substantial drawbacks like the formation of highly sensitive heavy metal complexes, the much less sensitive TNT was used as the standard explosive in the 1st World War. Research in the field of higher performing explosives for military use commenced and by the 2nd World War both pentaerythritol tetranitrate (PETN) and cyclotrimethylenetrinitramine (RDX) were investigated. RDX found greater use because it is less sensitive and more powerful than PETN.

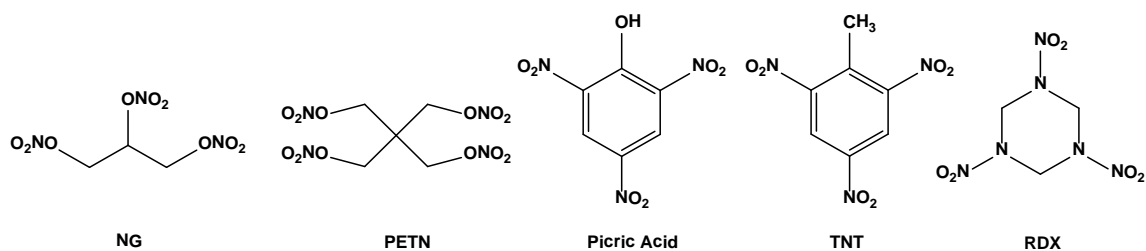


Figure 1: Common explosives and their structures.

While other major explosives have been developed for specialized uses such as higher performance or a high degree of insensitivity, none have gained as wide use as RDX in the 20th century.

The final progress in the last century in explosives science is the process of plastification as an approach to make the handling of these materials safer. While in the beginnings inert, non-energetic binders such as polystyrene were used, the trend was to replace inert binders by energetic binders, which in most cases are based on covalent azides or nitrate esters. Nowadays, not only the application for military purposes is studied, but the utilization of energetic materials for civilian use in mining, construction, demolition and safety equipment such as airbags, signal flares and fire extinguishing systems is extensively studied. The most recent developments in energetic materials concentrate on the synthesis of compounds with either outstanding thermal or mechanical stability or a very high explosive performance like highly cage strained molecules containing nitro- and nitramino moieties. The academic research mainly focuses on the work with novel energetic systems to determine factors affecting stability and performance and to bring new strategies into the design of energetic materials. The main challenge is the desired combination of a large energy content with a maximum possible chemical stability to ensure safe synthesis and handling.

1.2 DEFINITION & CLASSIFICATION OF ENERGETIC MATERIALS

Many different applications have drawn attention and can be reached by the use of energetic materials. A definition of these materials and their subsequent classification is therefore necessary in order to clarify the wide area of application and development. In general, an energetic material is “a metastable compound or mixture capable of the rapid release of stored potential energy.”^[2] The entirety of energetic materials is defined by the American Society for Testing and Material as “...a compound or mixture of substances which contains both the fuel and the oxidizer and reacts readily with the release of energy and gas...”^[3] Energetic materials themselves are then divided into three unique classes: explosives, propellants and pyrotechnics. The class of explosives can be divided further into primary and secondary explosives.

Primary explosives are very sensitive explosives, which can be easily initiated by friction, impact, spark or heat. The initiation of primary explosives leads to a fast deflagration to detonation process with a shock wave formed, which is able to set off the less sensitive charge (main charge, secondary explosive) of an explosive device. They undergo a very fast deflagration to detonation transition (DDT) and are therefore used in initiating devices. Common primary explosives are lead(II) azide, lead(II) styphnate and mercury fulminate (Figure 2). The obvious disadvantage of these compounds is the toxicity of the heavy metal cations. Therefore, new less toxic primary explosives based on organic, metal free compounds were investigated and developed. Besides the development of metal free organic primaries, the replacement of the toxic cations with less toxic metals like silver, iron or copper is another topic of current interest.

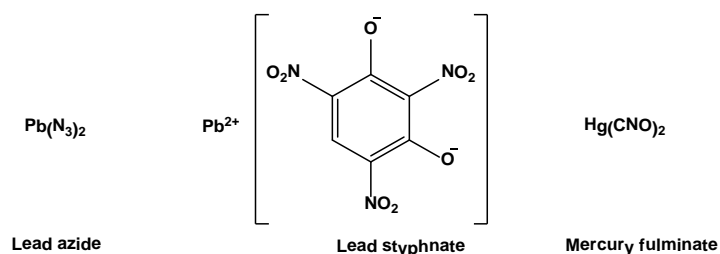


Figure 2: Common primary explosives

Secondary explosives are not only much more stable in terms of friction, impact and electrostatic discharge, but also kinetically stable (metastable) compounds. Hence, they have to be ignited by much larger stimuli, mostly generated by a primary charge. After initiation by the detonation shockwave of primary explosives, the secondary explosive generates a shockwave which promotes the reaction front through the unreacted material. Although they need a much higher impetus to be detonated, secondary explosives exhibit much higher performances than primary explosives. Common secondary explosives are TNT, RDX, HMX, TATB and NQ (Figure 3).

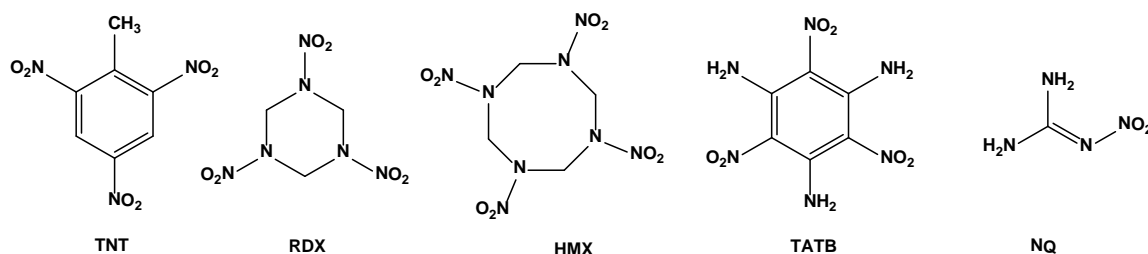


Figure 3: Common secondary explosives

Propellants, in contrast to primary and secondary explosives, are not meant to detonate, but only burn or deflagrate. Basically there are two main classes of propellants, which are propellant charges and rocket propellants. Propellant charges mostly consist of formulations including both oxidizer and fuel. A common propellant used in ammunition is nitrocellulose (single-based propellant), because the advantageous ratio of oxygen to carbon leads to a residue-free burning of the compound. In order to improve the performance, double-based and triple-based propellants were developed based on nitrocellulose. Double based propellants like nitrocellulose and nitroglycerine compositions possess an enhanced performance, unfortunately accompanied by a higher erosion of the gun barrel due to their higher combustion temperature. In order to decrease the erosion, triple-based propellants consisting of nitrocellulose, nitroglycerine and nitroguanidine were developed. Whereas the single-based propellant nitrocellulose is sufficient for ammunition of guns and pistols, the double- and triple-based propellants are used in tank and naval artillery ammunition.

The required properties of rocket propellants differ from that of propellants for ammunition. Rocket propellants can be divided into solid and liquid propellants. Solid propellants are either homogenous mixtures of one or more macroscopically indistinguishable ingredients (e.g. nitrocellulose and nitroglycerine), or heterogeneous mixtures (composite propellants, e.g. ammonium perchlorate and aluminum). Liquid propellants are divided in monopropellants (hydrazine) and bipropellants, which are mixtures of an oxidizer and fuel (e.g. HNO_3 and hydrazine/monomethyl-hydrazine).

Pyrotechnics can be divided into three areas. The heat generating, the smoke generating and the light emitting pyrotechnics. Heat generating pyrotechnics are used for priming charges, detonators, incendiary compositions or matches. Smoke generating pyrotechnics are used for camouflage and signaling purposes. The light emitting pyrotechnics are used either for illumination (visible and infrared), fireworks or decoy flares. The discussion of pyrotechnic systems is omitted, since the primary objective of this thesis is the synthesis and characterization of secondary explosives and, to a certain extent, propellant systems.

1.3 REQUIREMENTS FOR MODERN EXPLOSIVES

Many of the energetic materials, which are in use today, suffer from manifold drawbacks such as high toxicity or high sensitivity, which makes intensive research in possible replacements necessary. In the field of secondary explosives, the widely used RDX as well as its degradation and decomposition products reveals hazards like the toxicity for plants, microorganisms and microbes. RDX itself is toxic to organisms at the base of the food chain such as earthworms and also TNT and its degradation products are ecologically toxic. In general, improved physicochemical properties such as detonation parameters and stabilities outperforming the commonly used RDX are desired. The required properties for new energetic materials as RDX replacements are summarized in Table 1. The detonation velocity should exceed 9000 ms^{-1} and the detonation pressure should be higher than 380 kbar. The thermal stability of a newly synthesized material should exceed 180°C in addition to a high long term thermal stability for the safe storage of explosives.

Besides the performance properties, the desired criteria for a new material in order to become widely accepted are also insensitivity towards destructive stimuli such as electrostatic discharge, heat, friction, and impact to ensure safe handling procedures and enhance controllability of kinetic energy release. Further, a low water solubility and high hydrolytic stability is necessary for environmental reasons.

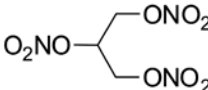
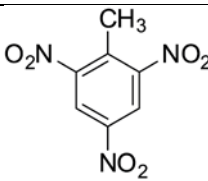
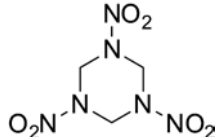
Table 1: Goals for the preparation of new High Energy Density Materials (HEDM)

Performance	detonation velocity	$D > 9000 \text{ m s}^{-1}$
	detonation pressure	$P > 380 \text{ kbar}$
	heat of explosion	$Q > 6200 \text{ kJ kg}^{-1}$
Stability	thermal stability	$T_{\text{dec.}} \geq 180^\circ\text{C}$
	impact sensitivity	$IS > 7 \text{ J}$
	friction sensitivity	$FS > 120 \text{ N}$
	electrostatic sensitivity	$ESD > 0.2 \text{ J}$
Chemical properties	hydrolytically stable, compatible with binder and plasticizer, low water solubility (or non-toxic), smoke-free combustion, long-term stable (> 15 years under normal conditions)	

1.4 STRATEGIES IN ENERGETIC MATERIALS DESIGN

There are three major methods of introducing potentially explosive energy into a molecule: fuel and oxidizer being contained in the same molecule, compounds possessing ring or cage strain, and high heat of formation compounds. Classical secondary explosives like 2,4,6-trinitrotoluene (TNT) and nitroglycerine (NG) derive all their energy from the oxidation of the carbon backbone. Both compounds exhibit negative heats of formation and hence much lower performance rates than RDX. RDX itself obtains its energy from the oxidation of the carbon backbone but as well from the formation of dinitrogen due to the N–N bonds in the nitramine moieties. Therefore, a positive heat of formation is generated, which results (together with the higher density) in significantly higher performance values. The performance values and structures of NG, TNT and RDX are compiled in Figure 1.

Table 2: Classical explosives and their performance characteristics. Values are taken from Ref.^[4]

			
Name systematic	1,2,3-Propanetrioltrinitrate (NG)	2,4,6-Trinitrotoluene (TNT)	1,3,5-Trinitro-1,3,5-triazinane (RDX)
T _m (°C)	13	80	204
T _{dec} (°C)	200	300	210
N (%)	18.5	18.5	37.8
Ω (%)	3.5	−73.9	−21.6
ρ (g cm ^{−3})	1.591	1.654	1.82
ΔH _f ⁰ (kJ mol ^{−1})	−349.7	−49.7	89.2
Impact sensitivity (J)	0.2	15	7.5
Friction Sensitivity (N)	> 360	353	120
V _{det} (m s ^{−1})	7600	6900	8750

The examples of TNT and RDX reveal the features necessary for modern explosives. They should have high positive heats of formation, paired with high densities and well balanced oxygen content.^[5] Positive heats of formation can be obtained by the introduction of nitrogen, either catenated like in heterocyclic ring systems or in the form of nitramine and nitro groups. The backbone of new energetic materials with high heats of formation is often a five or six membered nitrogen heterocycle. Regarding those five

membered rings from pyrrole to pentazole as well as the six membered rings from pyridine to hexazine, there is a wide spectrum of possible energy content and stabilities.

Another very important point is the cage strain eminent in heterocyclic ring systems and structures, which additionally increases the energy of formation. When a caged or cyclic explosive compound possesses bond strain resulting from the geometry of the compound, this stored energy contributes to the energy released upon detonation. Thus, much more energy can be derived by the combination of the oxidation of carbon together with the energy delivered from the cage strain introduced to the backbone. These concepts led to new materials over the last decade, although one has to consider the expensive and often laborious synthesis of those molecules. Strained cage and ring systems have been developed like TEX (4,10-dinitro-2,6,8,12-tetraoxa-4,10-diazaisowurtzitane), CL-20 (2,4,6,8,10,12-hexanitro-hexaazaisowurtzitane), ONC (octanitrocubane) and TNAZ (1,3,3-trinitroazetene) (Figure 4).

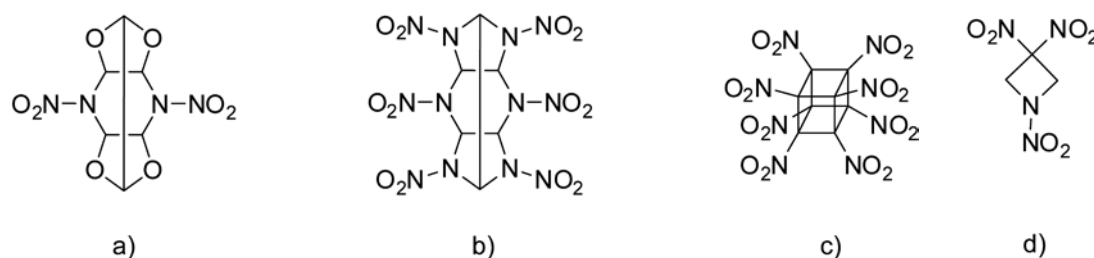


Figure 4: Modern explosives: a) TEX (4,10-dinitro-2,6,8,12-tetraoxa-4,10-diazaisowurtzitane), b) CL-20 (2,4,6,8,10,12-hexanitro-hexaazaisowurtzitane), c) ONC (octa nitrocubane), d) TNAZ (1,3,3-trinitroazetene).

In the design of new energetic materials for practical use, one needs to consider the performance, sensitivities, toxicities as well as cost of production. Of all the driving forces for research on energetic materials, environmental concerns are one of the most powerful. RDX as well as TNT show a high aqua toxicity and due to the overall release of HEDMs to the environment, they are increasingly becoming a soil and ground water contaminant. TNT has been demonstrated to have carcinogenic effects in rats, contaminates water at munition sites and affects male fertility. RDX, HMX, CL-20 and other nitramine containing explosives are no better, being possible human carcinogens.^[6] Fortunately, explosives based on nitrogen-rich compounds are generally less toxic. The detonation products of these compounds are mainly dinitrogen, carbon dioxide and water, which would be the overall goal for a well performing novel explosive.^[7]

1.5 MOTIVATION AND OBJECTIVES

The general area of this thesis is the synthesis and full characterization of novel secondary explosives. Due to the dual-use nature of energetic materials (e.g. RDX is an explosive, but is also capable of being used in propellants), attention at times may briefly turn to the application of these materials in propellants. The concept of new green energetic compounds as explained above is thereby an important topic of this work. The benefits of the development of new high energetic density materials with a high nitrogen content paired with high positive heats of formation are improved performance and also environmental compatibility. With all respect to environmentally friendly compounds and high performance values to be realized, the compounds must exhibit also high thermal stabilities and, for better and safer handling, low sensitivities against impact, friction and electrostatic discharge.

The focus of this thesis is on the synthesis and characterization of compounds composed of either two 1,2,4-triazole moieties or the combination of a triazole ring with a tetrazole ring. The connectivity is either established over an azo functionality or over direct C–C linkage of both heterocycles. The introduction of various energetic moieties like nitro, nitrimino, azido and dinitromethyl at the carbon atom of the triazole moiety leads to the selective tailoring of energetic properties. The effect of the formation of energetic salts on the thermo chemical and physical properties as well as the detonation parameters has also been extensively studied and compared to known secondary explosives.

The development of new HEDMs with high performance as potential RDX replacement, guaranteed through high enthalpies of formation and high densities, combined with high thermal stabilities, was a major scope of this study. The academic research interest mainly focuses on gaining a deeper understanding of factors affecting stability and performance as key to a more rational design of novel compounds with tailored properties.

1.6 REFERENCES

- [1] a) T. M. Klapötke, in *High Energy Density Materials* (Ed.: T. M. Klapötke), Springer: Heidelberg, **2007**, pp. 84–122; b) T. M. Klapötke, *Chemistry of high-energy materials*, 2nd ed., de Gruyter: Berlin, **2012**; c) J. Akhavan, *The chemistry of explosives*, Royal Society of Chemistry: Cambridge, UK, **1998**.
- [2] D. Piercey, *Dissertation*, Ludwig-Maximilians Universität München, **2013**, p. 4.
- [3] www.astm.org.
- [4] J. Köhler, R. Meyer, *Explosivstoffe*, 9th edition, Wiley-VCH: Weinheim, **1998**.
- [5] Calculation of oxygen balance assuming formation of CO₂: $\Omega (\%) = (wO - 2xC - 1/2yH - zS)1600/M$. (w : number of oxygen atoms, x : number of carbon atoms, y : number of hydrogen atoms, z : number of sulfur atoms, M : molecular weight).
- [6] a) M. B. Talawar, R. Sivabalan, T. Mukundan, H. Muthurajan, A. K. Sikder, B. R. Gandhe, A. S. Rao, *J. Hazard. Mater.* **2009**, *161*, 589–607; b) P. Richter-Torres, A. Dorsey, C. S. Hodes, *Toxicological Profile for 2,4,6-Trinitrotoluene*, U.S. Department of Health and Human Services, Public Health Service, Agency for Toxic Substances and Disease Registry, **1995**; c) W. McLellan, W. R. Hartley, M. Brower, *Health advisory for hexahydro-1,3,5-trinitro-1,3,5-triazine*, Technical report PB90-273533; Office of Drinking Water, U.S. Environmental Protection Agency: Washington, DC, **1988**; d) P. Y. Robidoux, J. Hawari, G. Bardai, L. Paquet, G. Ampleman, S. Thiboutot, G. I. Sunahara, *Arch. Environ. Con. Tox.* **2002**, *43*, 379–388; e) W. D. Won, L. H. DiSalvo, J. Ng, *Appl. Environ. Microb.* **1976**, *31*, 576–580; f) J. A. Steevens, B. M. Duke, G. R. Lotufo, T. S. Bridges, *Environ. Toxicol. Chem.* **2002**, *21*, 1475–1482; g) A. Esteve-Núñez, A. Caballero, J. L. Ramos, *Microbiol. Mol. Biol. Rev.* **2001**, *65*, 335–352; h) B. Van Aken, J. M. Yoon, J. L. Schnoor, *Appl. Environ. Microbiol.* **2004**, *70*, 508–517.
- [7] A. K. Sikder, N. Sikder, *J. Hazard. Mater.* **2004**, *112*, 1–15.

2. CONCLUSIONS

In the course of this work, many novel energetic materials based on 1,2,4-triazole derivatives have been developed, leading to new primary and secondary explosives as well as materials with possible applications in the propellants and pyrotechnics sector. The focus of this study is on the synthesis and characterization of compounds composed of either two 1,2,4-triazole moieties or the combination of a triazole ring with a tetrazole ring. The connectivity is either established over an azo functionality or over direct C–C linkage of both heterocycles. The introduction of various energetic moieties like nitro, nitrimino, azido and dinitromethyl at the carbon atom of the triazole moiety leads to the selective tailoring of energetic properties.

CHAPTER 3 deals with the synthesis and characterization of 5,5'-dinitrimino-3,3'-azo-1*H*-1,2,4-triazole and selected nitrogen-rich salts thereof. Since the impact and friction sensitivities for 5,5'-dinitrimino-3,3'-azo-1*H*-1,2,4-triazole are very high with an impact sensitivity of 2 J and an friction sensitivity of 20 N, corresponding nitrogen rich salts have been prepared first in order to decrease the sensitivity and also to increase the thermal stability. Both goals have been achieved for selected salts of 5,5'-dinitrimino-3,3'-azo-1*H*-1,2,4-triazole, showing decomposition temperatures between 212 °C (ammonium) and 261 °C (guanidinium). All impact and friction sensitivities are well above the values of RDX, and hence much less sensitive, while the performance values of the bis(triaminoguanidinium) 5,5'-dinitrimino-3,3'-azo-1*H*-1,2,4-triazolate show promising values very close to RDX.

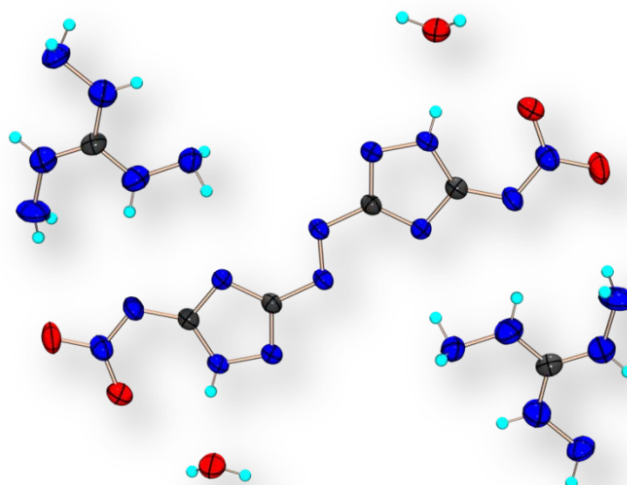


Figure 1: Illustration of bis(triaminoguanidinium) 5,5'-dinitrimino-3,3'-azo-1*H*-1,2,4-triazolate.

CHAPTER 4 contains the synthesis and characterization of 3,3'-bis(dinitromethyl)-5,5'-azo-1*H*-1,2,4-triazole. The performed single crystal X-ray diffraction measurement reveals a tetrahedral coordination at the dinitromethyl moiety typical for sp^3 -carbon atoms (Figure 2). With the high positive heat of formation ($579.5 \text{ kJ mol}^{-1}$) and a detonation velocity of 8433 m s^{-1} , 3,3'-bis(dinitromethyl)-5,5'-azo-1*H*-1,2,4-triazole shows attractive energetic properties. Unfortunately, in contrast to the corresponding nitrimino compound (discussed in chapter 3), the dinitromethyl moiety leads to a very low temperature of decomposition starting at 80°C .

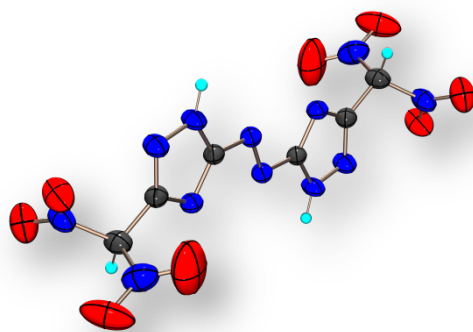


Figure 2: Illustration of 3,3'-bis(dinitromethyl)-5,5'-azo-1*H*-1,2,4-triazole.

CHAPTER 5 is a comparative study of structural and energetic properties of nitrogen-rich bis-1,2,4-triazoles directly connected via C–C bond carrying different energetic moieties like amino, nitro, nitrimino, azido and dinitromethylene groups.

Regarding the stability values and energetic parameters, 3,3'-dinitro-5,5'-bis-1,2,4-triazole (DNBT) shows the highest thermal stability of 251°C together with an insensitivity towards friction and a moderate sensitivity towards impact (10 J). As expected, the nitrimino compound (DNABT) as well as the azido compound (DAzBT) are the most sensitive derivatives. The introduction of the dinitromethyl group (DNMBT) leads to the best detonation parameters (8499 ms^{-1} , 341 kbar), but as it is also the case for the similar azo-bridged compound (see chapter 4), the thermal stability is decreased to 121°C . In summary, the compounds DNBT and DNABT can be considered as nitrogen-rich starting materials for new energetic ionic derivatives in combination with nitrogen-rich cations.

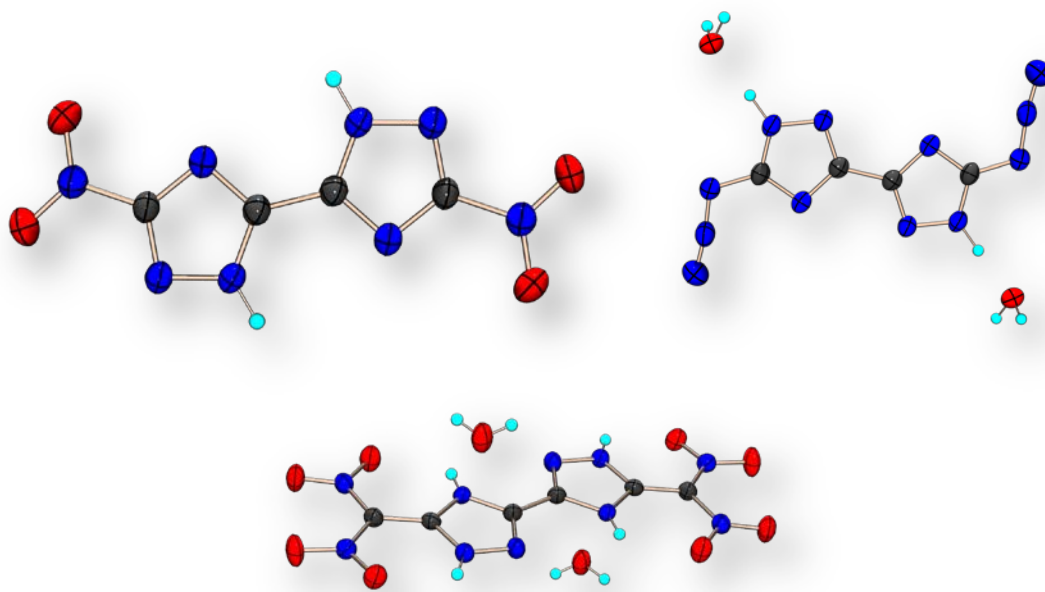


Figure 3: Illustration of bis-1,2,4-triazoles along with selected energetic moieties.

CHAPTER 6 focuses on insensitive energetic compounds based on the 3,3'-dinitro-5,5'-bis-1,2,4-triazolate anion in combination with nitrogen-rich cations. The most interesting compounds regarding the energetic properties are the hydroxylammonium and triaminoguanidinium salt. All of these compounds exhibit decomposition temperatures of above 200 °C and performance values (8477 m s^{-1} and 8365 m s^{-1}) close to RDX. Worth mentioning is the guanidinium salt with a remarkable high decomposition temperature of 335 °C and an insensitivity against friction and impact.

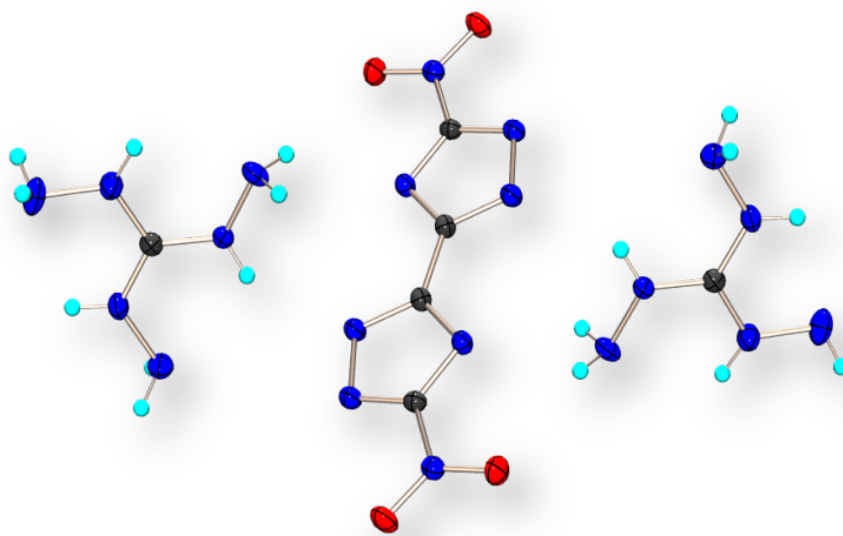


Figure 4: Illustration of bis(triaminoguanidinium) 3,3'-dinitro-5,5'-bis-1,2,4-triazolate.

CHAPTER 7 deals with asymmetrically substituted bistriazoles connected via C–C bond. In this chapter, the synthesis and full structural and spectroscopic characterization of three asymmetrically substituted bis-1,2,4-triazoles, along with different energetic moieties like amino, nitro, nitrimino and azido moieties is presented. Additionally, selected nitrogen-rich ionic derivatives have been prepared and characterized. The amine group of 5-(5-amino-1*H*-1,2,4-triazol-3-yl)-3-nitro-1*H*-1,2,4-triazole was further converted to energetic moieties (nitrimino and azido), which leads to the previously unknown asymmetric energetic bistriazole compounds. Regarding the stability values and energetic parameters, the nitrimino compound (NNBT) and the azido compound are sensitive towards impact sensitivity (8 J) but insensitive towards friction (360 N). With detonation velocities below 8000 ms^{-1} , both compounds are able to compete with commonly used TNT, however, the performance data for RDX are not reached. Energetic ionic compounds were synthesized from NNBT using nitrogen-rich cations,. The most interesting compounds regarding the energetic properties are the hydroxylammonium and triaminoguanidinium compound. Those compounds exhibit decomposition temperatures above $200\text{ }^{\circ}\text{C}$ and performance values in the range of RDX (8706 m s^{-1} and 8707 m s^{-1}).

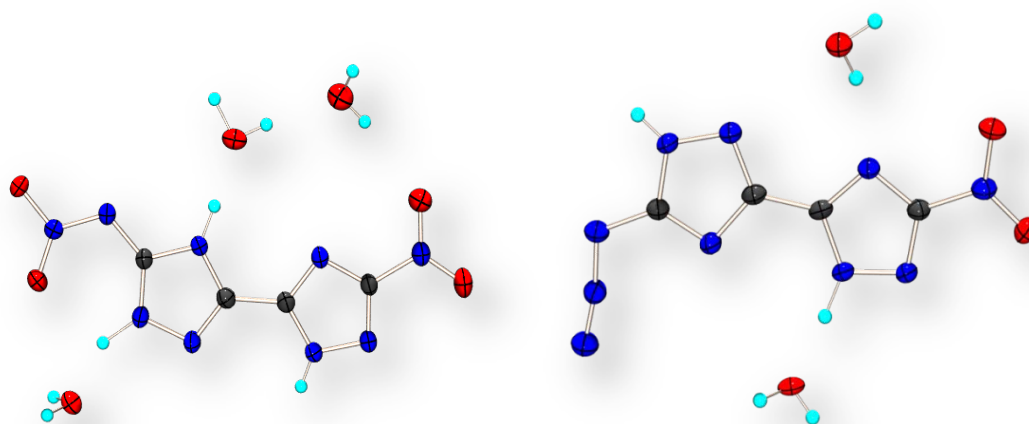


Figure 5: Illustration of asymmetrically substituted bistriazoles.

CHAPTER 8 deals with the design of high performance insensitive energetic materials by the introduction of N-oxides to the triazole moiety. In this chapter, the synthesis and full structural as well as spectroscopic characterization of 3,3'-dinitro-5,5'-bis-1,2,4-triazole-1,1'-diole and nitrogen-rich salts thereof is presented. It is possible to oxidize 3,3'-dinitro-5,5'-bis-1*H*-1,2,4-triazole to the corresponding 1,1'-dihydroxy compound under mild, aqueous conditions in high yield. The simple and straightforward method of

N-Oxide introduction in triazole compounds using commercially available Oxone® improves the energetic properties and reveals a new synthetic pathway towards novel energetic 1,2,4-triazole derivatives. The most striking difference between the N-oxide containing compounds and their parent relatives is a higher crystal density (about 0.1 g cm^{-3}) compared to the corresponding N-oxide free compounds as a consequence of the N-oxide being involved in multiple intermolecular bonding interactions.

The ionic derivatives were found to be high thermally stable, insensitive compounds that are highly powerful but safe to handle and prepare, all compounds show superior performance in comparison to the corresponding ones bearing no N-oxide. The most promising compound for industrial scale up and practical use is the hydroxylammonium salt, which shows a straightforward synthesis including only four cheap and facile steps. Especially the combination of an exceedingly high performance superior to RDX and insensitivity to mechanical stimuli highlights this compound as potential high explosive, which could find practical use as RDX replacement.

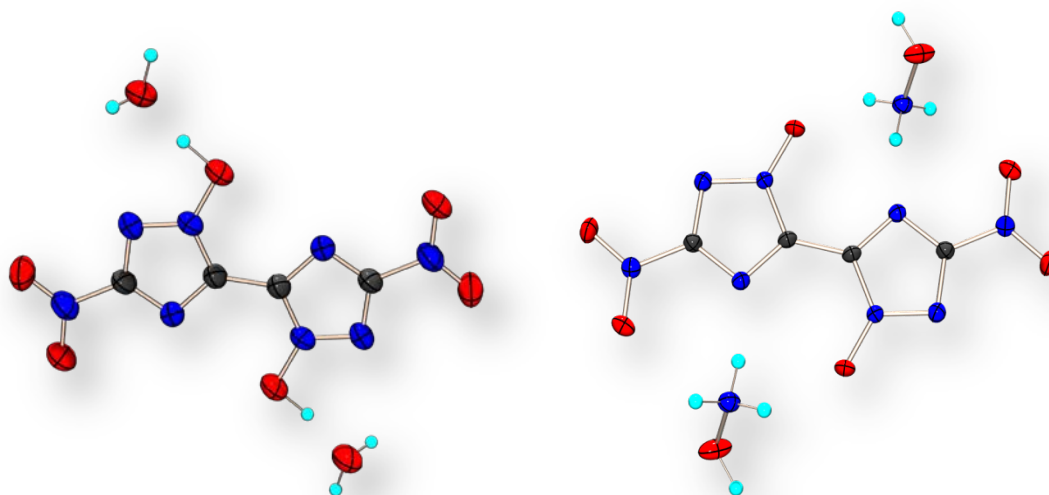


Figure 6: Illustration of 3,3'-dinitro-5,5'-bis-1H-1,2,4-triazole-1,1'-diole and its corresponding hydroxylammonium salt.

CHAPTER 9 contains the combination of a 1,2,4-triazole with a tetrazole via C–C connection. The starting material 5-(5-amino-1*H*-1,2,4-triazol-3-yl)-1*H*-tetrazole (ATT) was converted to energetic derivatives by introduction of nitro- (NTT), nitrimino- (NATT) and azido-moieties (AzTT).

Regarding the stability values and energetic parameters, compounds NATT and NTT show thermal stabilities (215 °C and 211 °C) in the range of RDX. As expected, the nitrimino compound as well as the azido compound are the most sensitive derivatives with an impact sensitivity of less than 1 J and friction sensitivities of 18 N (NATT) and 20 N (AzTT). In contrast, the nitro derivative shows moderate sensitivities towards friction (288 N) and impact (25 J). In general, the connection via C–C bond of a triazole ring with its opportunity to introduce a large variety of energetic moieties and a tetrazole ring implying a large energy content leads to the selective synthesis of precursors for primary and secondary explosives.

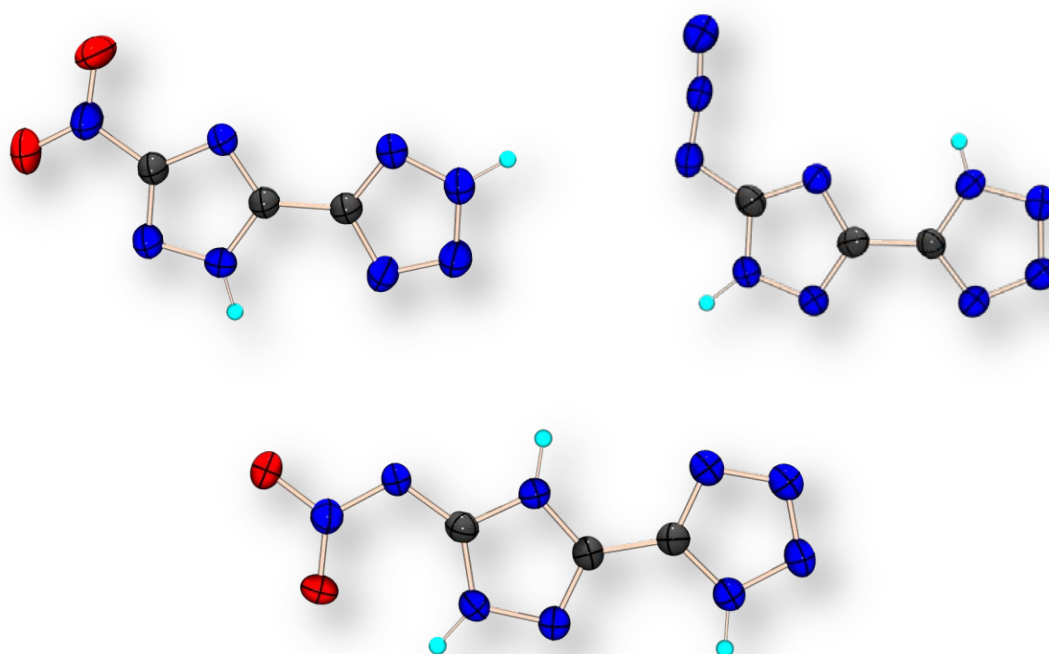


Figure 7: Illustration of 5-(1,2,4-Triazol-3-yl)tetrazoles.

CHAPTER 10 focuses on the C–C connection of a 1,2,4-triazole with a 1-hydroxy-tetrazole. The influence of the variable energetic moieties as well as the C–C connection of a tetrazol-1-ol and a 1,2,4-triazole on structural and energetic properties is investigated. The beneficial influence of a 1-hydroxy-tetrazole on detonation parameters and the tailoring of energetic properties by the introduction of different energetic groups is discussed. In comparison to the corresponding compounds bearing no N-Oxide (chapter 9), the sensitivities are in the same range, however the thermal stability is remarkably lowered. Taking into account the high nitrogen contents of 56.6 % – 72.2 % and high heats of formation, those compounds could be considered as nitrogen rich

environmentally-friendly primary explosives with proper metal cations (AzTT), or be of interest as secondary explosive or propellant ingredient in combination with nitrogen-rich cations (NTT and NATT), respectively. As it is also the case for the tetrazolyl-triazole compounds discussed in chapter 9, the combination of a triazole ring with its opportunity to introduce a large variety of energetic moieties and a 1-hydroxytetrazole ring implying a large energy content leads to the selective synthesis of precursors for nitrogen rich ionic primary and secondary explosives.

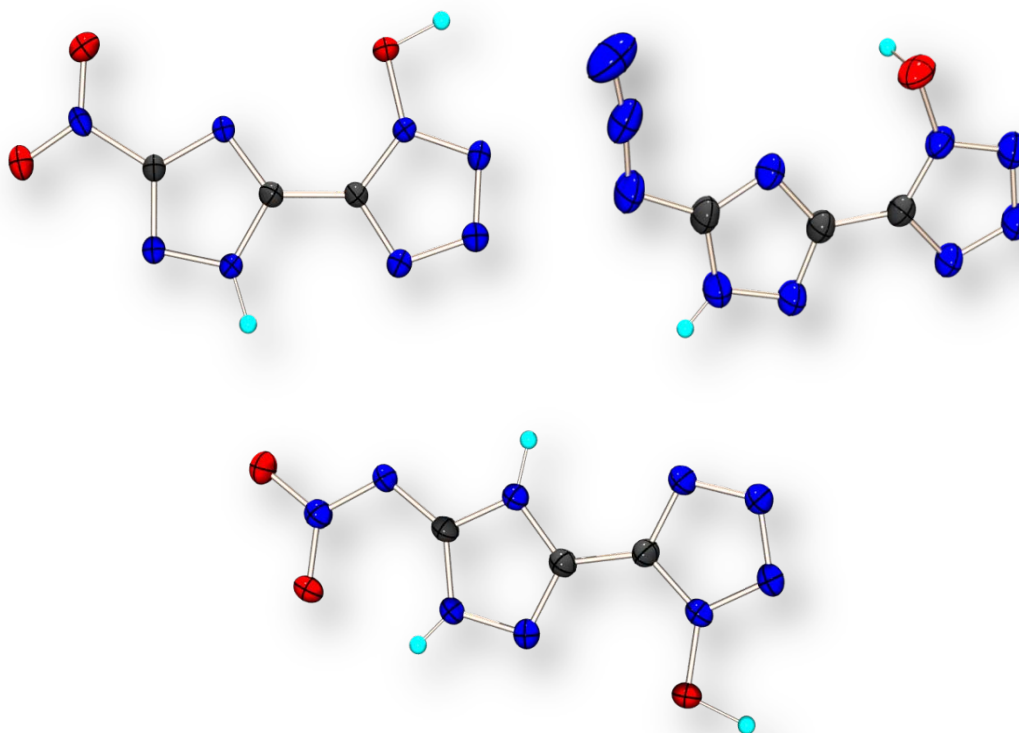


Figure 8: Illustration of 5-(1,2,4-Triazol-C-yl)tetrazol-1-ols.

CHAPTER 11 presents the synthesis and characterization of selected nitrogen-rich salts based on 5-(1,2,4-Triazol-C-yl)tetrazoles and their 1-hydroxy-tetrazole analogues. The main focus is on the energetic properties of those ionic derivatives in comparison to the neutral compounds. Additionally, the positive influence of the introduction of *N*-Oxides in energetic materials is shown. The ionic *N*-Oxid compounds show lower decomposition temperature in comparison to the compounds bearing no *N*-Oxid, however the stability is mainly influenced by the corresponding cation. Most of the compounds show reduced sensitivities in comparison to their neutral precursors, especially the ionic nitrimino-triazolate compounds are much safer to handle, since the stability towards friction and impact was considerably increased. In general, the triazol-C-yl-tetrazoles show lower

performance values in comparison to their 1-hydroxy-tetrazole analogues. For example, the detonation velocities of the hydroxylammonium salts are increased by about 500 ms^{-1} due to the N-Oxide. The introduction of an *N*-Oxide in tetrazole based energetic materials obviously positively influences the detonation parameters due to a higher density and an even greater energy output, however this advantage comes along with lower decomposition temperatures.

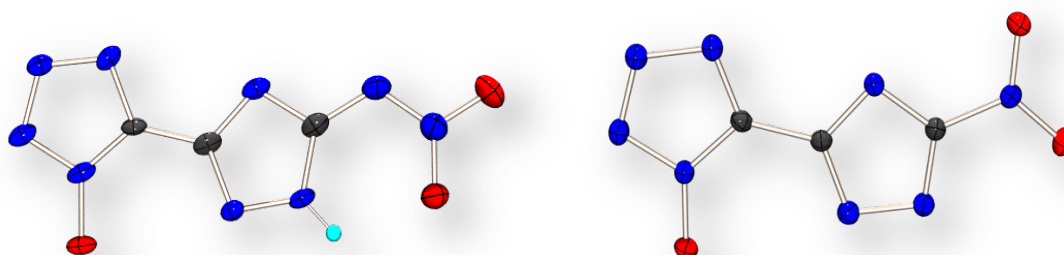
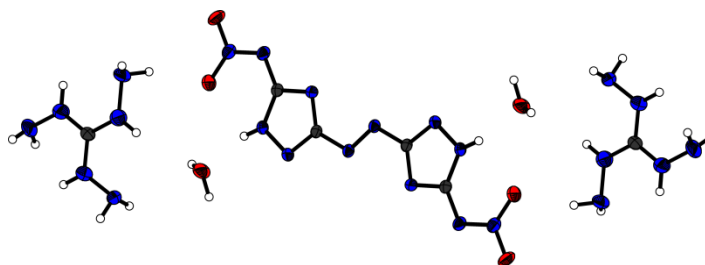


Figure 9: Illustration of 5-(5-Nitramino-1*H*-1,2,4-triazolate-3-yl)tetrazol-1-olate and 5-(3-Nitro-1,2,4-triazolate-5-yl)tetrazol-1-olate anions.

3. SYNTHESIS AND CHARACTERIZATION OF BIS(TRI-AMINOGUANIDINIUM) 5,5'-DINITRIMINO-3,3'-AZO-1*H*-1,2,4-TRIAZOLATE – A NOVEL INSENSITIVE ENERGETIC MATERIAL

As published in:

Zeitschrift für Anorganische und Allgemeine Chemie, **2011**, 637(9), 1181–1193.

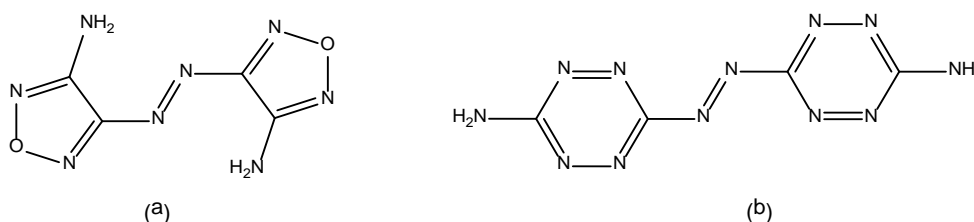


ABSTRACT:

The synthesis of 5,5'-diamino-3,3'-azo-1*H*-1,2,4-triazole (**3**) by reaction of 5-acetylamino-3-amino-1*H*-1,2,4-triazole (**2**) with potassium permanganate is described. The application of the very straightforward and efficient acetyl protection of 3,5-diamino-1*H*-1,2,4-triazole allows selective reactions of the remaining free amino group to form the azo-functionality. Compound **3** is used as starting material for the synthesis of 5,5'-dinitrimino-3,3'-azo-1*H*-1,2,4-triazole (**4**), which was subsequently reacted with organic bases (ammonia, hydrazine, guanidine, aminoguanidine, triaminoguanidine) to form the corresponding nitrogen-rich triazolate salts (**5–9**). All substances were fully characterized by IR and Raman as well as multinuclear NMR spectroscopy, mass spectrometry and differential scanning calorimetry. Selected compounds were additionally characterized by low temperature single crystal X-ray diffraction measurements. The heats of formation of **4–9** were calculated by the CBS-4M method to be 647.7 (**4**), 401.2 (**5**), 700.4 (**6**), 398.4 (**7**), 676.5 (**8**) and 1089.2 (**9**) kJ mol⁻¹. With these values as well as the experimentally determined densities several detonation parameters were calculated using both computer codes EXPLO5.03 and EXPLO5.04. In addition, the sensitivities of **5–9** were determined by the BAM drophammer and friction tester as well as a small scale electrical discharge device.

INTRODUCTION

In recent years, the synthesis of energetic, heterocyclic compounds has attracted an increasing amount of interest, since heterocycles generally offer a higher heat of formation, density and oxygen balance than their carbocyclic analogues.^[1] In combination with the advances of a high nitrogen content such as the high average two electron bond energy associated with the nitrogen-nitrogen triple bond^[2], those compounds are of great interest for investigations. The current widely used nitro-explosives TNT, RDX or HMX per se as well as their transformation products are toxic due to the presence of nitro (-NO₂), nitroso (-NO) or nitrito (-ONO) groups either in the explosives itself or its degradation products.^[3] The development of new energetic materials therefore focuses – besides high performance and stability – on environmentally friendly compounds. Nitrogen-rich compounds mainly generate environmentally friendly molecular nitrogen as end-product of propulsion or explosion, therefore they continue to be the focus of energetic materials research across the globe.^[4] A prominent family of compounds regarding the properties mentioned above are azole-based energetic materials, because they are generally highly endothermic compounds with relatively high densities and a high nitrogen content.^[5] Since modern high energy density materials (HEDM) mostly derive their energy of ring or cage strain as well as of a high heat of formation, a lot of research has been done on explosives containing the azo-functionality. Several heterocyclic compounds like 4,4'-diamino-3,3'-azofurazan (a) and 3,3'-azobis(6-amino-1,2,4,5-tetrazine) (b) have been reported in literature so far (Figure 1).^[6]

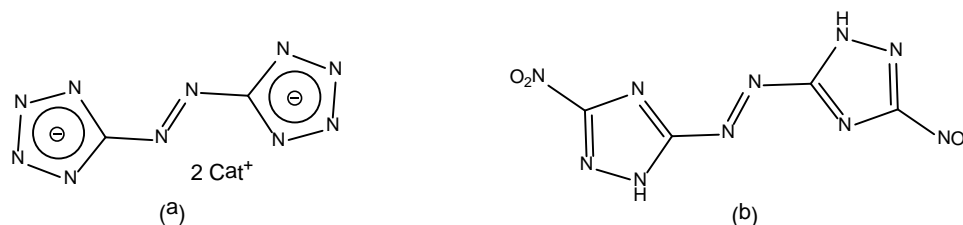


Scheme 1: Formula structures of some heterocyclic compounds containing the azo-functionality.

The combination of a high nitrogen content with a high heat of formation led to the development of azole-based compounds containing the azo-functionality. The recently reported 5,5'-azotetrazolate anion (Figure 2) is such an energetic compound with a very high nitrogen content and therefore suitable for the synthesis of energetic materials. There has been increased interest in the synthesis of energetic salts based on the 5,5'-

azotetrazolate anion, since the neutral compound decomposes at room temperature.^[7] Many 5,5'-azotetrazolate salts have found practical application in combination with nitrogen-rich bases (e.g. guanidinium, triaminoguanidinium, hydrazinium) as propellants,^[8] in gas generators for airbags as well as in fire extinguishing systems.^[9] Heavy metal salts have been used as initiators^[10] and derivatives of 5,5'-azotetrazole are utilized as additives in solid rocket propellants.^[11]

Since triazole derivatives often tend to be thermally and kinetically more stable than their tetrazole analogous, research in this field of azo-bridged azoles shows great promise for energetic materials. For example, 5,5'-dinitro-3,3'-azo-1*H*-1,2,4-triazole and its nitrogen-rich salts have been in the focus as potential insensitive high nitrogen compounds and propellant burn rate modifiers.^[12]



Scheme 2: Formula structures of the 5,5'-azotetrazolate anion (a) and 3,3'-dinitro-5,5'-azo-1*H*-1,2,4-triazole (b).

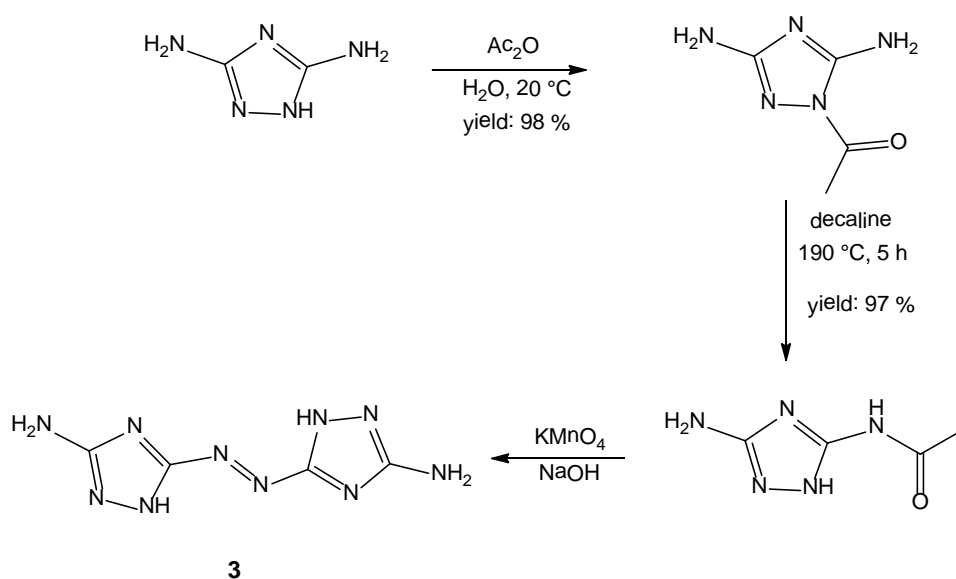
The literature known 5,5'-dinitro-3,3'-azo-1*H*-1,2,4-triazole was first synthesized at Los Alamos National Laboratories by Naud and coworkers in 2003.^[13] Since this molecule and selected nitrogen-rich salts like the triaminoguanidinium compound reveal a high stability and attractive explosive properties,^[14] our goal was the preparation of the corresponding nitrimino-compound as the introduction of this group is known to better the performance characteristics.

RESULTS AND DISCUSSION

SYNTHESIS

The starting material used for nitration, 5,5'-diamino-3,3'-azo-1*H*-1,2,4-triazole (**3**), is not yet known in literature, since it is not accessible using 3,5-diamino-1*H*-1,2,4-triazole as a starting material. The formation of the azo-bridge apparently only works with a unique amino group in the molecule, which necessitates the protection of one amino

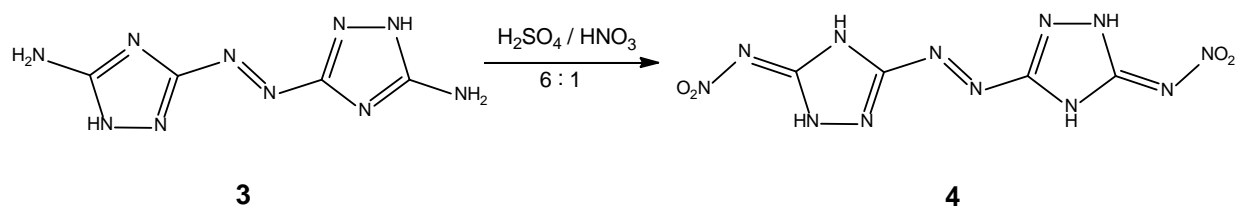
group first. The acetyl protecting group is suitable due to the fact that it is stable even in concentrated acids/bases at room temperature and the amine is not deprotected until using elevated temperatures. Theoretically, acylation of 3,5-diamino-1*H*-1,2,4-triazole can proceed both at the heterocyclic nitrogen atoms and at the two amino groups.^[15] The treatment of 3,5-diamino-1*H*-1,2,4-triazole with acetic anhydride in water provides 1-acetyl-diaminotriazole (**1**) in yields of about 98 %. The desired 5-acetylaminotriazole (**2**) is obtained in nearly quantitative yields via thermal isomerization by heating a suspension of **1** in decaline (Scheme 3) as it is described by Pevzner *et al.*^[16]



Scheme 3: Reaction pathway towards 5,5'-amino-3,3'-azo-1*H*-1,2,4-triazole starting from 3,5-diamino-1*H*-1,2,4-triazole.

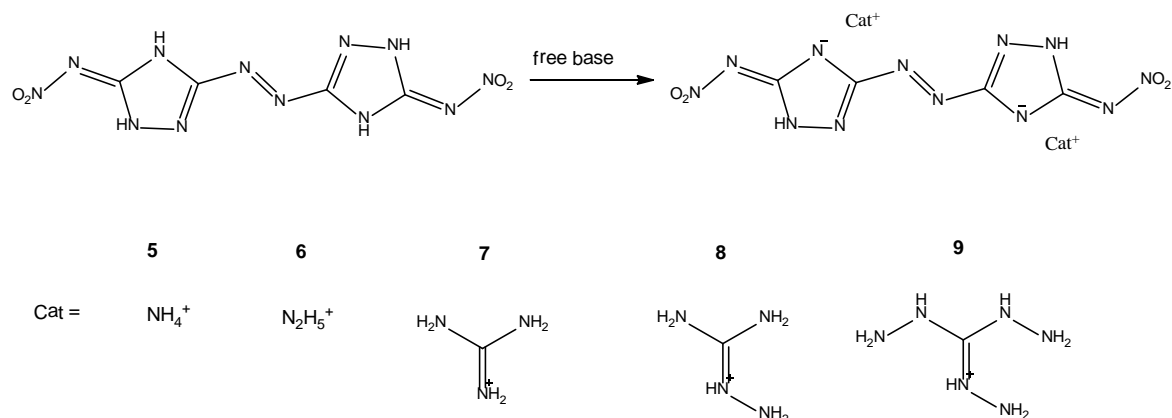
As shown in Scheme 3, the synthesis of 5,5'-diamino-3,3'-azo-1*H*-1,2,4-triazole (**3**) (DAAT) was performed with a stoichiometric amount of potassium permanganate which was added at 0 °C. After removal of the ice bath, the mixture was allowed to warm to room temperature. Subsequent heating to 100 °C for 3 hours completes the formation of the azo-bridge, transforms the remaining permanganate to manganese(IV)-oxide and leads to a complete deprotection of both amine groups. After the removal of the generated manganese oxide by filtration, acidifying the solution to pH 7 leads to the precipitation of compound **3** as an orange solid. Drying at 110 °C over night provides DAAT as elemental analysis pure orange powder. The synthesis of the novel 5,5'-dinitrimino-3,3'-azo-1*H*-1,2,4-triazole (**4**) was accomplished in good yields via nitration of 5,5'-diamino-3,3'-azo-1*H*-1,2,4-triazole (**3**) as it is described for 3-amino-1*H*-1,2,4-triazole by Licht *et. al*^[17]

using a volume ratio $\text{H}_2\text{SO}_4/\text{HNO}_3$ of 6 : 1 and two equivalents of nitric acid per amino group (Scheme 4).



Scheme 4: Synthesis of 5,5'-dinitrimino-3,3'-azo-1H-1,2,4-triazole (**4**) via nitration of **3**.

DNAAT immediately precipitates as a yellow solid while pouring the nitration mixture on ice and can easily be isolated by filtration. After drying at 60 °C, the desired elemental analysis pure nitrimino compound (**4**) was obtained in yields of about 80%. The synthesis of the nitrogen-rich salts (**5–9**) was accomplished as shown in Scheme 5 by adding two equivalents of an organic base (ammonia, hydrazine, guanidine, aminoguanidine, triaminoguanidine) to a suspension of the neutral compound in water.



Scheme 5: Synthesis of nitrogen-rich salts (**5 – 9**) of DNAAT.

The energetic salts of the di-anion DNAAT^{2-} were obtained in good yields as yellow powder while storing the mixture at 5 °C over night. All energetic compounds were fully characterized by IR and Raman as well as multinuclear NMR spectroscopy, mass spectrometry and differential scanning calorimetry. Selected compounds were additionally characterized by low temperature single crystal X-ray spectroscopy.

NMR SPECTROSCOPY

Due to the low solubility of compounds **2** and **3** in common NMR-solvents (but good solubility in bases), NMR spectroscopy was performed in D₂O adding a stoichiometric amount of sodium hydroxide. The NMR signals given in Table 1 correspond to the sodium salts of **2a** and **3a** and present as well the neutral compounds **1** and **2** in [d₆]-DMSO.

Table 1: NMR signals of compounds **1**, **2**, **2a** and **3a**.

compound	¹ H NMR	¹³ C{ ¹ H} NMR			
	CH ₃	C=O	C-NH ₂	C-NHAc (a)	CH ₃
1	2.33	170.5	162.2, 157.0		23.6
2	1.99	169.8	161.6	156.4	22.9
2a	2.03	174.1	162.5	154.1	22.7
3a	–	–	165.0	170.0	–

(a) C-azo in the case of **3a**

In the case of compound **2** (**2a**), two different NMR signals for the triazole carbon atoms could be obtained due to the rearrangement of the acetyl protecting group. The NMR signals of the two carbon atoms of compound **3a** can be found at 170.0 and 165.0 in the ¹³C NMR spectra. The signals of the acetyl protecting group at 2.03 (¹H NMR) and 22.7 (¹³C NMR) could not be obtained anymore, indicating full deprotection of the amine groups. The signals in the NMR spectra for compounds **4–9** were recorded in [d₆]-DMSO and are compiled in Table 2. The neutral compound (**4**) shows two signals for the different carbon atoms at 159.7 and 153.8 ppm, the nitrimino group is visible at –19 ppm in the ¹⁴N NMR-spectra. As expected in the case of compounds **5–9**, all NMR signals are nearly identical. The single proton localized at the triazole ring appears at chemical shifts between 13.5–13.6 ppm in the ¹H NMR spectra, while the signals of the two triazole carbon atoms can be found in the range between 166.9–167.7 ppm and 157.7–158.3 ppm. The nitrimino group is identified by a broad signal at around –15 ppm in the ¹⁴N NMR spectra.

Table 2: NMR signals of compounds **4–9**.

compound	DNAAT ²⁻			cation	
	¹ H	¹³ C{ ¹ H}	¹⁴ N{ ¹ H}	¹ H	¹⁴ N{ ¹ H}
4	/	159.7, 153.8	–19	/	/
5	13.58	167.7, 158.3	–14	7.23	–359
6	13.51	166.9, 157.8	–16	7.28	–359
					¹³ C{ ¹ H}
7	13.53	167.1, 157.9	–14	7.03	157.7
8	13.61	167.0, 157.7	–15	7.89, 4.71	158.9
9	13.48	167.3, 157.8	–14	8.59, 4.49	159.0

VIBRATIONAL SPECTROSCOPY

The isomerization reaction can easily be monitored by IR spectroscopy and is indicated by the shift of the C=O band from 1709 cm^{–1} (**1**) to 1683 cm^{–1} (**2**).

The complete deprotection of the amine groups during the synthesis of **3** can easily be monitored by the missing C=O vibration band at around 1700 cm^{–1} as well as the missing C-H valence vibrations at 2800–3100 cm^{–1} in the IR and Raman spectra. The latter is dominated by the absorption of the azo-moiety at 1348 cm^{–1},^[7c, 18] the infrared spectrum by the deformation mode of the amino groups at 1624 cm^{–1}.

The Raman spectra of **4** is dominated by the vibration of the azo-moiety at 1436 cm^{–1}, the absorption of the amino groups in the infrared spectrum at 1624 cm^{–1} has disappeared. The N-NO₂ groups result in a strong absorption at 1620–1560 cm^{–1} (ν_{asym}(NO₂)) and 1300–1240 cm^{–1} (ν_{sym}(NO₂)).

The symmetric and N=O valence vibrations of all nitrogen-rich salts (**5–9**) can be found at 1530 cm^{–1} (ν_{sym}(NO₂)) and 1335 cm^{–1} (ν_{asym}(NO₂)) in the IR spectrum, accompanied by the fundamental frequencies of the triazole ring in the range of 1300–1500 cm^{–1}.^[19] The N-H stretch modes of the amine group of the cations appear in the range of 3350 cm^{–1} to 3100 cm^{–1} and the -NH₂ deformation vibration at 1630–1680 cm^{–1}. The very intense band of the azo-moiety at 1463 cm^{–1} in the Raman spectrum shows only a marginal shift in comparison to the neutral compound (**4**).

STRUCTURAL CHARACTERIZATION

The single crystal X-ray diffraction data of **4**, **5** and **9** were collected using an Oxford Xcalibur3 diffractometer equipped with a Spellman generator (voltage 50 kV, current 40 mA) and a KappaCCD detector. The data collection was undertaken using the CRYSLIS CCD software^[20] while the data reduction was performed with the CRYSLIS RED software.^[21] The structures were solved with SIR-92^[22] or SHELXS-97^[23] and refined with SHELXL-97^[24] implemented in the program package WinGX^[25] and finally checked using PLATON.^[26] Further information regarding the crystal-structure determination have been deposited with the Cambridge Crystallographic Data Centre^[27] as supplementary publication Nos. 807480 (**4***DMSO), 807481 (**4***THF), 807482 (**5**) and 807483 (**9**).

The crystallization of azo-bridged triazole compounds is very difficult due to the completely planar configuration of the molecules and a lack of possibilities for hydrogen bonding. We were finally able to crystallize **4** from DMSO and also THF, but were not able to record a crystal structure of the neutral compound without incorporated solvent molecules. The same problem occurred with the ionic compounds. Only the ammonium salt (**5**) and the triaminoguanidinium salt (**9**) could be crystallized after a number of tries with different solvents and crystallization conditions. While **5** could only be crystallized with incorporated solvent molecules (DMSO), **9** crystallized with two molecules of crystal water per formula unit. Due to this circumstances, the structures of **4***DMSO, **4***THF and **5***DMSO will not be discussed in detail since no results can be drawn from the discussion of the structure, thus only selected parameters and the asymmetric units of the compounds will be presented. The structure of the title compound **9** will be discussed in detail.

The DMSO adduct of 5,5'-dinitrimino-3,3'-azo-1*H*-1,2,4-triazole (**4**) crystallizes in the monoclinic space group $P2_1/c$ with 4 molecular moieties in the unit cell, while the THF adduct crystallizes in the monoclinic spacegroup $P2_1/n$ with only two molecular moieties in the unit cell. Pycnometer measurements of **4** stated a density of 1.85 g cm^{-3} , while the densities derived from the crystallographic measurements are very low with 1.505 g cm^{-3} for **4***DMSO and 1.374 g cm^{-3} for **4***THF, respectively, owed to the solvent incorporation. The asymmetric units for both adducts are displayed in Figure 1 and Figure 2 together with the numbering scheme and selected bond distances and angles.

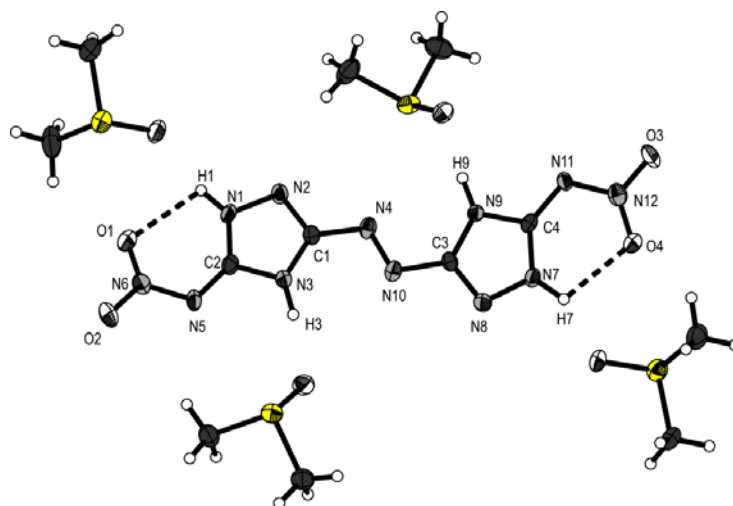


Figure 1: Molecular moiety of **4*DMSO**. Thermal ellipsoids represent the 50% probability level. Selected bond lengths (Å): O1 N6 1.243(3), O2 N6 1.242(3), N1 C2 1.340(3), N1 N2 1.370(3), N1 H1 0.90(2), N2 C1 1.307(3), N3 C2 1.352(3), N3 C1 1.355(3), N3 H3 0.913(16), N4 N10 1.280(3), N4 C1 1.397(3), N5 C2 1.341(3), N5 N6 1.343(3); selected bond angles (°): C2 N1 N2 111.9(2), C2 N1 H1 132.8(16), N2 N1 H1 115.2(16), C1 N2 N1 103.1(2), C2 N3 C1 106.3(2), C2 N3 H3 119.7(15), C1 N3 H3 133.8(16), N10 N4 C1 111.8(2), C2 N5 N6 115.7(2), O2 N6 O1 122.0(2), O2 N6 N5 115.7(3), O1 N6 N5 122.3(3), C4 N7 N8 112.46(19), C4 N7 H7 128.8(15), N2 C1 N3 112.9(2), N2 C1 N4 119.3(3), N3 C1 N4 127.4(2), N1 C2 N5 135.9(2), N1 C2 N3 105.8(2), N5 C2 N3 118.2(3).

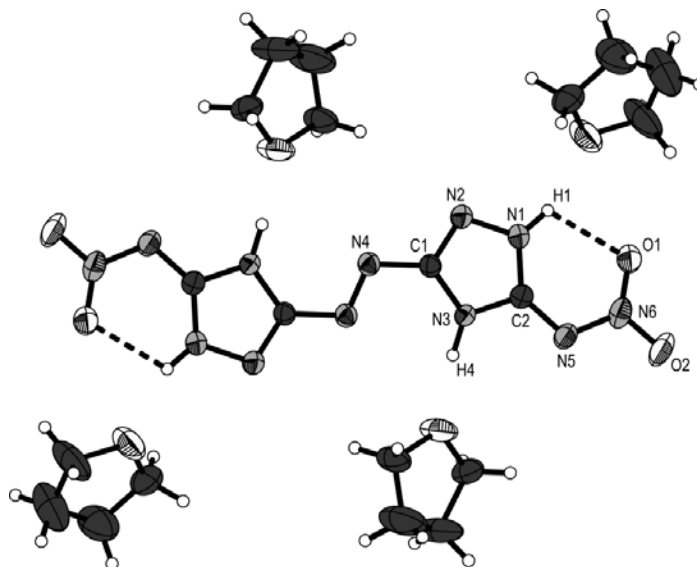


Figure 2: Molecular moiety of **4*THF**. Thermal ellipsoids represent the 50% probability level. Selected bond lengths (Å): C4 C3 1.406(5), C4 C5 1.424(6), N6 1.244(3), N1 C2 1.356(4), N1 N2 1.368(3), N1 H1 0.88(3), N2 C1 1.308(3), N5 C2 1.339(4), N5 N6 1.356(3), N4 N4 1.272(4), N4 C1 1.392(3), N3 C2 1.346(3), N3 C1 1.368(4), N3 H4 0.94(3), N6 O2 1.239(3); selected bond angles (°): C2 N1 N2 111.8(3), C2 N1 H1 129(2), N2 N1 H1 119(2), C1 N2 N1 103.6(2), C2 N5 N6 115.6(3), N4 N4 C1 112.2(3), C2 N3 C1 106.8(2), C2 N3 H4 125(2), C1 N3 H4 128(2), O2 N6 O1 121.5(3), O2 N6 N5 116.0(3), O1 N6 N5 122.4(2), N5 C2 N3 119.8(3), N5 C2 N1 134.8(3), N3 C2 N1 105.5(3), N2 C1 N3 112.3(2), N2 C1 N4 120.8(2), N3 C1 N4 127.0(2).

The DNAAT molecule is nearly planar in both structures, indicating the presence of a delocalized π -electron system, as anticipated for these compounds. Bond lengths and angles are also as expected for this kind of compounds.^[28] The bond length of the azo moiety is in the same range as for the azotetrazole compounds investigated by Hammerl^[7c, 29] while the nitraminogroups also exhibit regular geometrical parameters. The interesting aspect of both structures is the presence of moderately strong intramolecular hydrogen bonds. N1 and N7 are utilized as donor atoms with O1 and O4 function as acceptor atoms respectively for **4*DMSO**, while N1 and O1 build up the hydrogen bond for **4*THF**. Even though, the D–H...A angles are pretty small with 102.15(16)° (N1–H1...O1, **4*DMSO**), 105.8(1)° (N7–H7...O4, **4*DMSO**) and 108.21(23)° (N1–H1...O1, **4*THF**), the D–A distances are very small, ranging between 2.587(1) Å (N1–O1, **4*THF**) and 2.606(4) Å (N1–O1, **4*DMSO**). The hydrogen bonds are considered to be of electrostatic nature rather than being directed.^[30] The build up of a six membered ring between the nitrimino group and the triazole ring, is making the backbone of the molecule more stable, which is also indicated by the very high thermal stabilities, unusual for this class of compounds. In addition the hydrogen atom can only be deprotonated with the use of earth alkaline bases, not with the bases used to form the di-anion. Further, the incorporated solvent molecules take their space due to the formation of hydrogen bonds with each of the four N–H hydrogen atoms. Thus both structures show the mutual number of solvent molecules surrounding each DNAAT molecule.

Bis(ammonium) 5,5'-dinitrimino-3,3'-azo-1*H*-1,2,4-triazolate (**5*DMSO**) crystallizes in the triclinic space group *P*-1, formally with only one molecular moiety occupying the unit cell. The density is as expected very low with only 1.483 g cm⁻³ due to the formation of the DMSO adduct. One molecular moiety together with selected bond length and angles is presented in Figure 3.

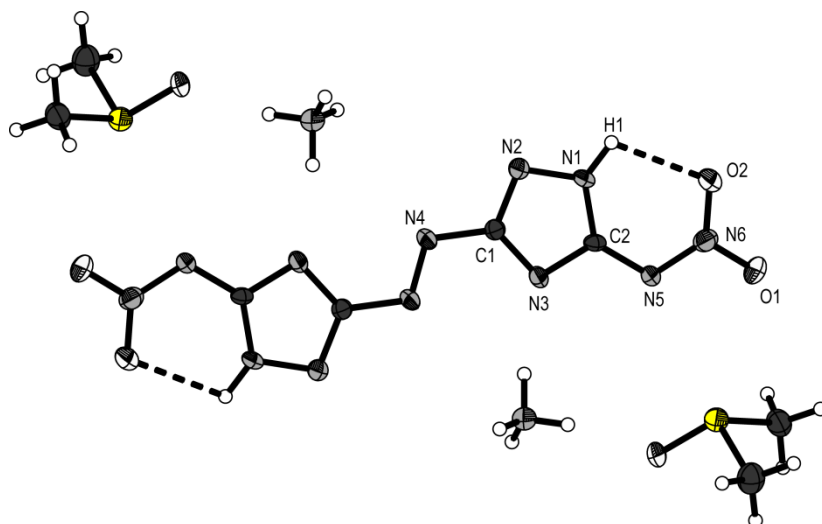


Figure 3: Molecular moiety of **5**. Thermal ellipsoids represent the 50% probability level. Selected bond lengths (Å): O1 N6 1.270(2), O2 N6 1.260(2), N1 C2 1.345(3), N1 N2 1.368(2), N1 H1 0.917(15), N2 C1 1.327(3), N3 C2 1.335(3), N3 C1 1.356(3), N4 N4 1.278(3), N4 C1 1.413(3), N5 N6 1.322(2), N5 C2 1.381(3); selected bond angles (°): C2 N1 N2 110.46(19), C2 N1 H1 133.0(14), N2 N1 H1 116.5(14), C1 N2 N1 101.00(19), C2 N3 C1 102.0(2), N4 N4 C1 112.0(2), N6 N5 C2 116.8(2), O2 N6 O1 120.4(2), O2 N6 N5 123.6(2), O1 N6 N5 116.1(2), N2 C1 N3 116.5(2), N2 C1 N4 117.4(2), N3 C1 N4 126.2(2), N3 C2 N1 110.1(2), N3 C2 N5 117.9(2), N1 C2 N5 132.0(2).

The di-anion is completely planar within the ionic structures with only very slight deviations. The N1–H1•••O2 hydrogen bond builds up the six membered ring again, as seen for the neutral compound, keeping the nitriminogroup perfectly in plane with the triazole ring. Since the thermal decomposition temperature differs only by 3 °C when compared with **4** (209 °C (**4**) compared to 212 °C (**5**)) the formation of this stable configuration seems to have an very important impact on the stability of these compounds. The structure itself is build up from four moderately stable hydrogen bonds, all four of them involving the ammonium cation. An illustration of the surrounding of one ammonium cation is presented in Figure 4, while the parameters of the hydrogen bonds are compiled in Table 4.

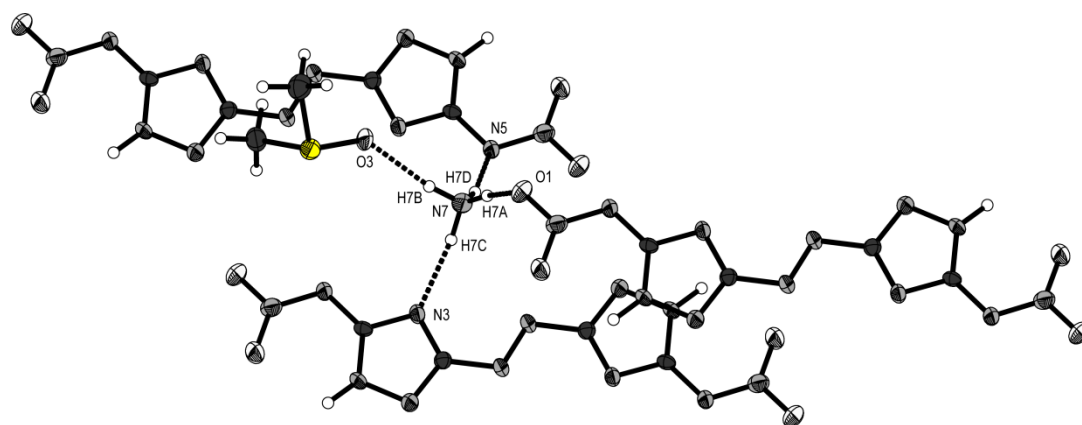


Figure 4: Chemical surrounding of the ammonium cation in **5**, displaying the hydrogen bonds. Thermal ellipsoids represent the 50% probability level.

Table 4: Hydrogen bonds present in the crystal structure of **5**. Since the N–H bonds of the ammonium ion had to be set as restraint, no standard deviation is presented.

Atoms D–H–A	Dist D–H [Å]	Dist. H–A [Å]	Dist. D–A [Å]	Angle D–H–A [°]
N1 – H1 – O3 ⁱ	0.917(15)	1.937(18)	2.786(3)	153.0(19)
N7 – H7a – O1 ⁱⁱ	0.96	2.00	2.929(2)	163.8
N7 – H7b – O3	0.92	1.91	2.811(2)	167.1
N7 – H7c – N3	0.92	1.98	2.872(3)	164.3
N7 – H7d – N5 ⁱⁱⁱ	0.93	2.05	2.951(3)	164.8

Symmetry operators: (i) $x, y-1, z$; (ii) $x+1, y, z$; (iii) $-x+1, -y+1, -z$.

The dihydrate of the bis(triaminoguanidinium) 5,5′-dinitrimino-3,3′-azo-1*H*-1,2,4-triazolate (**9**) crystallizes in the monoclinic space group $P2_1/c$ with two formula units in the unit cell. The density is in the same range as other guanidinium salts of nitrimino-compounds with 1.698 g cm^{-3} . The density is also in good agreement with the experimentally determined density of the anhydrous compound being 1.72 g cm^{-3} (pycnometer measurement). The molecular moiety of **9**, as well as the numbering scheme and selected bond lengths and angles are presented in Figure 5.

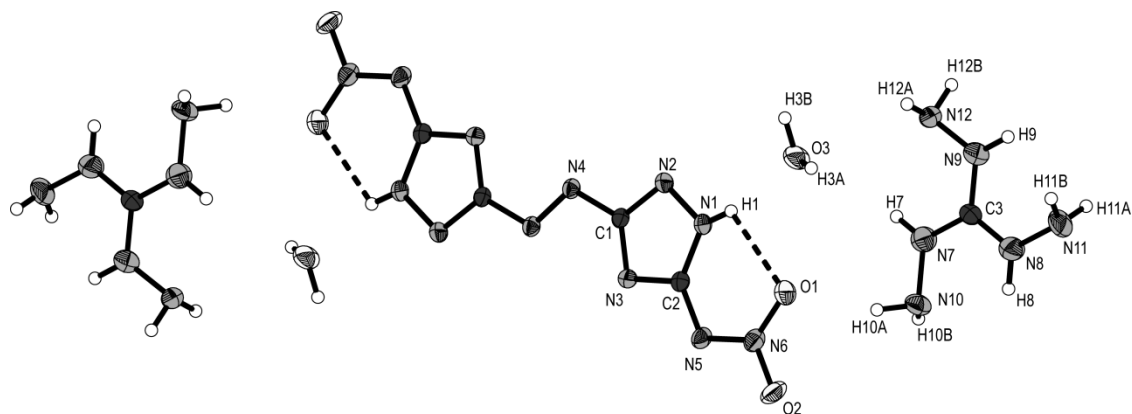


Figure 5: Molecular moiety of **9**. Thermal ellipsoids represent the 50% probability level. Selected bond lengths (Å): O1 N6 1.264(3), O2 N6 1.255(3), N1 N2 1.351(3), N1 C2 1.354(3), N1 H1 0.77(3), N2 C1 1.323(3), N3 C2 1.336(3), N3 C1 1.344(3), N4 N4 1.277(4), N4 C1 1.407(3), N5 N6 1.310(3), N5 C2 1.368(3), N7 C3 1.313(3), N7 N10 1.431(3), N8 C3 1.316(4), N8 N11 1.406(3), N9 C3 1.331(4), N9 N12 1.419(3); selected bond angles (°): N2 N1 C2 110.2(2), N2 N1 H1 116(3), C2 N1 H1 134(3), C1 N2 N1 101.8(2), C2 N3 C1 102.5(2), N4 N4 C1 111.9(3) 3_765, N6 N5 C2 117.7(2), O2 N6 O1 120.8(2), O2 N6 N5 116.9(2), O1 N6 N5 122.2(2), N2 C1 N3 116.2(2), N2 C1 N4 116.7(2), N3 C1 N4 127.1(2), N3 C2 N1 109.4(2), N3 C2 N5 118.2(2), N1 C2 N5 132.4(2), C3 N7 N10 118.3(2), C3 N8 N11 121.9(3), C3 N9 N12 119.0(2).

As seen in the structure of **5**, the DNAAT²⁻ anion is completely planar. The structural motive of two six membered rings, stabilizing the nitrimino groups is also evident in this structure. The donor acceptor distance is in the same range as for **4** and **5** with 2.579(9) Å and with the D–H...A angle of 106.22(31)° of strong electrostatic nature. The complete structure is build up by a strong hydrogen network including 15 non-equivalent hydrogen bonds. All hydrogen bonds are compiled in Table 5 below.

Table 5: Hydrogen bonds present in the crystal structure of **9**. H7, H8 and H9 had to be set restraint, thus no standard deviations are given for the D–H and H–A distances as well as for the D–H–A angles.

Atoms D–H–A	Dist. D–H [Å]	Dist. H–A [Å]	Dist. D–A [Å]	Angle D–H–A [°]
N1 – H1 – O1	0.770(4)	2.256(37)	2.579(9)	106.2(9)
N1 – H1 – O3	0.77(3)	1.98(4)	2.733(3)	165(4)
N7 – H7 – O1 ⁱ	0.88	2.34	2.995(3)	130.9
N8 – H8 – O2 ⁱⁱ	0.88	2.18	2.954(3)	146.3
N9 – H9 – N5 ⁱⁱⁱ	0.88	2.37	3.186(3)	153.7
N10 – H10a – O1	0.96(4)	2.14(4)	3.075(4)	163(3)
N10 – H10b – N10 ⁱⁱ	0.83(4)	2.52(4)	3.198(4)	140(3)
N10 – H10b – O2 ⁱ	0.83(4)	2.57(4)	3.126(3)	125(3)
N11 – H11a – N11 ^{iv}	0.827(19)	2.63(3)	3.142(5)	121(3)
N11 – H11a – O2 ⁱⁱⁱ	0.827(19)	2.54(3)	3.147(3)	131(3)
N11 – H11b – N5 ^v	0.82(4)	2.37(4)	3.176(4)	168(3)
N12 – H12a – N4 ^{vi}	0.82(4)	2.46(4)	3.189(3)	148(3)
N12 – H12b – N3 ⁱⁱⁱ	0.87(4)	2.20(4)	3.000(3)	154(3)
N12 – H12a – O3	0.82(4)	2.71(3)	3.197(9)	119.6(3)
O3 – H3a – N12 ^{vii}	0.73(4)	2.31(4)	3.000(3)	159(4)
O3 – H3b – N2 ^{vi}	0.91(4)	2.04(4)	2.922(3)	163(4)

Symmetry operators: (i) $x, y+1, z$; (ii) $-x+1, y+1/2, -z+1/2$; (iii) $x-1, y+1, z$; (iv) $-x, y+1/2, -z+1/2$; (v) $x-1, y, z$; (vi) $-x+1, -y+1, -z$; (vii) $x, y-1, z$.

The structure consists of coplanar bands, build up from DNAAT²⁻ anions, water molecules and triaminoguanidinium cations located approximately 1 Å below and above the layer spanned up by DNAAT²⁻ anions. The water molecules are located between the DNAAT²⁻ molecules forming strong and directed hydrogen bonds with the triazole rings, namely N1–H1•••O3 and O3–H3b•••N2^{vi}. These hydrogen bonds are well below the sum

of van der Waals radii ($r_w(\text{N}) + r_w(\text{O}) = 3.10 \text{ \AA}$).^[31] The third hydrogen bond is formed by the water molecule as donor, while N12^{vii} functions as the donor. Again, the D–A distance is much shorter than the sum of van der Waals radii and the D–H...A angle is 159° which again indicates a rather directed than only electrostatic interaction. The only weak hydrogen bond build up by the H₂O is N12–H12a...O3, with a donor acceptor distance of $3.197(9) \text{ \AA}$ and therefore longer than the sum of van der Waals radii and an D–H...A angle of only $119.6(3)^\circ$. All other hydrogen bonds formed are using the nitrogen atoms of the triaminoguanidinium cation as donor atoms. The two hydrogen bonds utilizing nitrogen atoms of the DNAAT²⁻ anion as acceptors all show D–A distances smaller than the sum of van der Waals radii ($r_w(\text{N}) + r_w(\text{N}) = 3.2 \text{ \AA}$) at 3.186 \AA (N9 – H9 – N5ⁱⁱⁱ) and 3.000 \AA (O3 – H3a – N12^{vii}), respectively. The corresponding D–H...A angles (around 150°) indicate the bonds being moderately strong but mostly of electrostatic nature. The three hydrogen bonds using oxygen atoms as acceptors are moderately strong with D–A distances between 2.954 and 3.147 \AA and with D–H...A angles between 125° and 131° they are rather of electrostatic nature. The complete hydrogen bonding scheme within the bands is presented in Figure 6.

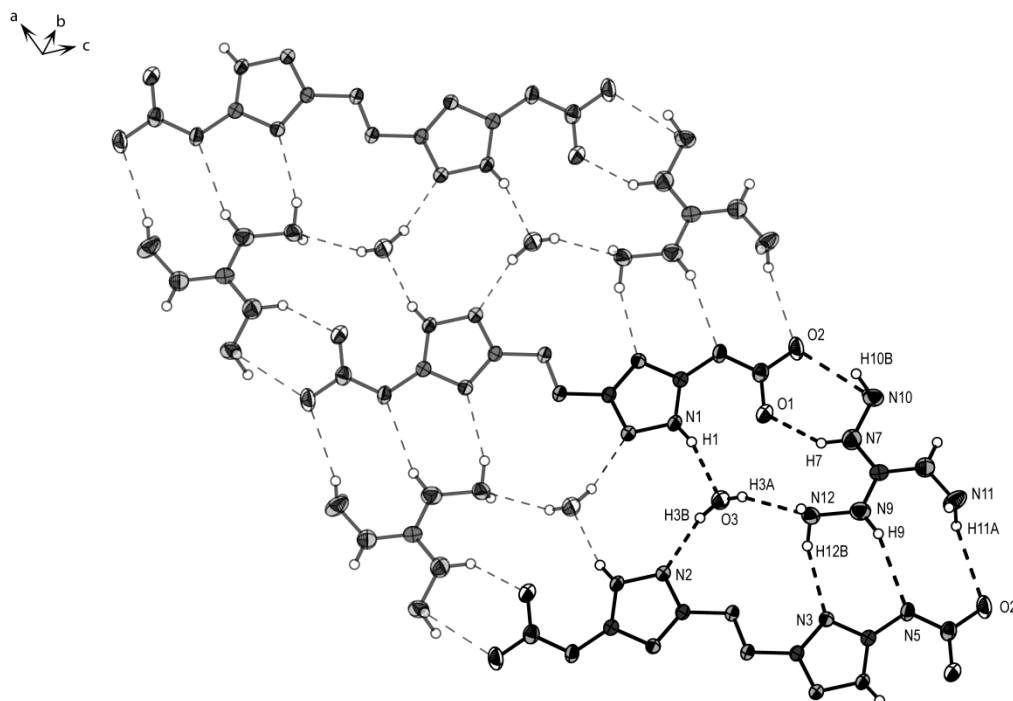


Figure 6: Hydrogen bonding scheme within the band structures of **9**. Thermal ellipsoids represent the 50% probability level.

The distance between the bands is 3.280 Å, while they are stacked along the *b*-axis. The bands are connected via hydrogen bonds formed between the triaminoguanidinium cations and interactions from the triaminoguanidinium cation with the nitramino groups, to form zig-zag layers presenting an angle of 133.99° between the individual bands. The hydrogen bonds involved are namely N11–H11a•••N11^{iv} and N10–H10b•••N10ⁱⁱ, only involving the triaminoguanidinium cations, while N8–H8•••O2ⁱⁱ presents the interaction between the NH group of the triaminoguanidinium cation in one layer with the nitriminogroup of the DNAAT²⁻ anion in the tilted layer. The layer scheme of the structure is displayed in Figure 7 along the *a*-axis.

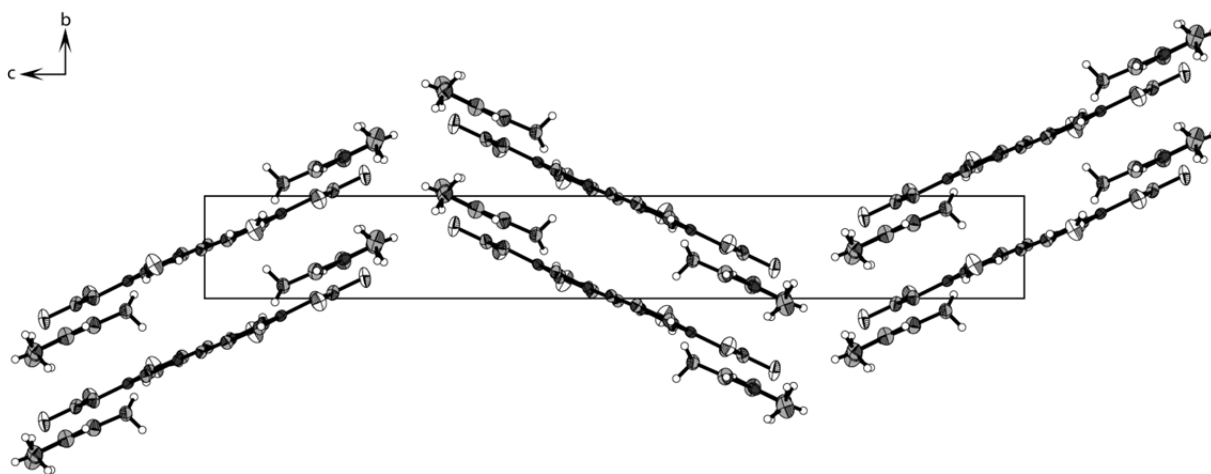


Figure 7: Layer structure of **9**, showing the connectivity of the individual bands along the *a*-axis. Thermal ellipsoids represent the 50% probability level.

The angle between the bands is due to the connectivity over hydrogen bonds formed by the triaminoguanidinium cations. The N10–H10b•••N10ⁱⁱ and N11–H11a•••N11^{iv} hydrogen bonds are rather long with D–A distances of 3.142 and 3.198 Å, respectively, but shorter than the sum of van der Waals radii. D–H•••A angles of only 121° and 140°, respectively, indicate mostly electrostatic interactions. Since the donor atoms are the two amine groups, the angle between the bands is given. The third band connecting hydrogen bond N8–H8•••O2ⁱⁱ is rather short with a D–A distance of 2.954 Å. The bond is mainly of electrostatic nature, but also directed with a D–H•••A angle of 146.43°. The surrounding of one triaminoguanidinium cation is displayed in Figure 8, presenting the complete three dimensional hydrogen bonding network. Three moderately strong hydrogen bonds connect the bands towards the next layer, namely N11–H11b•••N5^v, N12–H12a•••N4^{vi} and N10–H10a•••O1.

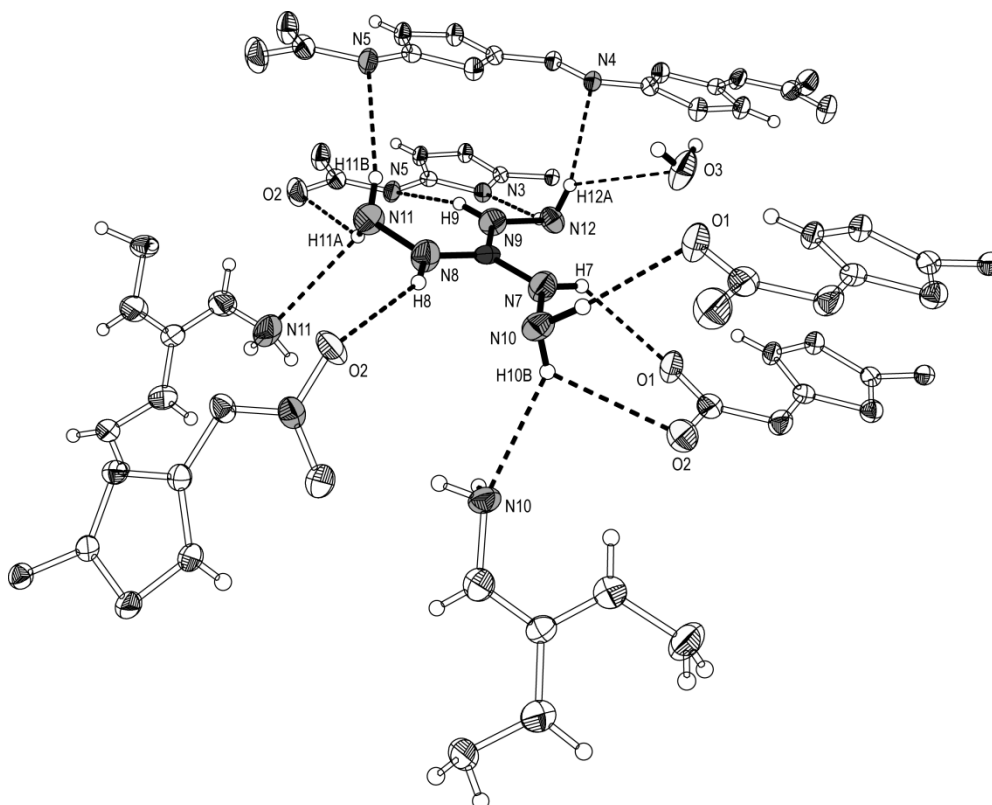


Figure 8: Surrounding of one triaminoguanidinium cation in **9**, showing the connectivity of the structural motive. Non participating atoms are set transparent, molecules are partially omitted for better clarity. Thermal ellipsoids represent the 50% probability level.

THEORETICAL CALCULATIONS

Due to the highly energetic character of **4–9**, bomb calorimetric measurements could only be performed with small amounts, consequently doubtful combustion energies were obtained. Therefore an extensive computational study was accomplished for **4–9**, which is presented in the following section. All calculations were carried out using the Gaussian G03W (revision B.03) program package.^[32] The enthalpies (H) and free energies (G) were calculated using the complete basis set (CBS) method of Petersson and coworkers in order to obtain very accurate energies. The CBS models use the known asymptotic convergence of pair natural orbital expressions to extrapolate from calculations using a finite basis set to the estimated complete basis set limit. CBS-4 begins with a HF/3-21G(d) geometry optimization; the zero point energy is computed at the same level. It then uses a large basis set SCF calculation as a base energy, and a MP2/6-31+G calculation with a CBS extrapolation to correct the energy through second order. A MP4(SDQ)/6-31+(d,p) calculation is used to approximate higher order contributions. In

this study we applied the modified CBS-4M method (**M** referring to the use of Minimal Population localization) which is a re-parametrized version of the original CBS-4 method and also includes some additional empirical corrections.^[33] The enthalpies of the gas-phase species **M** were computed according to the atomization energy method (eq. 1) (Tables 6–8).^[34]

$$\Delta_f H^\circ_{(g, M, 298)} = H_{(Molecule, 298)} - \sum H^\circ_{(Atoms, 298)} + \sum \Delta_f H^\circ_{(Atoms, 298)} \quad (1)$$

Table 6: Results obtained from theoretical calculations at the CBS-4M level of theory.

	point group	$-H^{298} / \text{a.u.}$	<i>NIMAG</i>
DNAAT	C_1	1111.064789	0
DNAAT²⁻	C_s	1110.009835	0
A⁺	T_d	56.796608	0
Hy⁺	C_s	112.030523	0
G⁺	C_1	205.453192	0
AG⁺	C_1	260.701802	0
TAG⁺	C_3	371.197775	0
H		0.500991	0
C		37.786156	0
N		54.522462	0
O		74.991202	0
Cl		459.674576	0

Table 7: Literature values for atomic $\Delta H^\circ_f{}^{298} / \text{kcal mol}^{-1}$

	NIST ^[35]
H	52.1
C	171.3
N	113.0
O	59.6
Cl	29.0

Table 8: Enthalpies of the gas-phase species M.

M	M	$\Delta_f H^\circ(\text{g}, \text{M}) / \text{kcal mol}^{-1}$
DNAAT	$\text{C}_4\text{H}_4\text{N}_{12}\text{O}_4$	743.6
DNAAT ²⁻	$\text{C}_4\text{H}_2\text{N}_{12}\text{O}_4^{2-}$	446.5
A	NH_4^+	151.9
Hy	N_2H_5^+	184.9
G	CH_6N_3^+	136.6
AG	CH_7N_4^+	160.4
DAG	CH_8N_5^+	184.5
TAG	CH_7N_4^+	208.8

The solid state energy of formation (Table 10) of **DNAAT** was calculated by subtracting the gas-phase enthalpy with the heat of sublimation ($22.5 \text{ kcal mol}^{-1}$) obtained by the TROUTON'S rule ($\Delta H_{\text{sub}} = 188 \cdot T_m$) ($T_m = 204^\circ \text{C}$).^[36] In the case of the salts, the lattice energy (U_L) and lattice enthalpy (ΔH_L) were calculated from the corresponding molecular volumes (Table 9) according to the equations provided by Jenkins *et al.*^[37] With the calculated lattice enthalpy (Table 9) the gas-phase enthalpy of formation (Table 8) was converted into the solid state (standard conditions) enthalpy of formation. These molar standard enthalpies of formation (ΔH_m) were used to calculate the molar solid state energies of formation (ΔU_m) according to equation 2 (Table 7).

$$\Delta U_m = \Delta H_m - \Delta n RT \quad (2)$$

(Δn being the change of moles of gaseous components)

Table 9: Lattice energies and lattice enthalpies.

	V_M / nm^3	$U_L / \text{kJ mol}^{-1}$	$\Delta H_L / \text{kJ mol}^{-1}$	$\Delta H_L / \text{kcal mol}^{-1}$
(NH₄)₂DNAAT (5)	298	1306.1	1317.0	314.5
(N₂H₅)₂DNAAT (6)	312	1283.5	1294.4	309.2
(G)₂DNAAT (7)	388	1181.0	1191.9	284.7
(AG)₂DNAAT (8)	464	1102.3	1113.2	265.9
(TAG)₂DNAAT (9)	472	1095.0	1105.9	264.1

Table 10: Solid state energies of formation ($\Delta_f U^\circ$)

	$\Delta_f H^\circ(\text{s}) /$ kcal mol ⁻¹	$\Delta_f H^\circ(\text{s}) /$ kJ mol ⁻¹	Δn	$\Delta_f U^\circ(\text{s}) /$ kJ mol ⁻¹	$M /$ g mol ⁻¹	$\Delta_f U^\circ(\text{s}) /$ kJ kg ⁻¹
DNAAT (4)	154.7	647.7	10	672.5	248.2	2366.3
(NH₄)₂DNAAT (5)	95.8	401.2	14	435.9	318.3	1369.6
(N₂H₅)₂DNAAT (6)	167.3	700.4	16	740.1	348.32	2124.6
(G)₂DNAAT (7)	95.2	398.4	18	443.0	402.4	1101.0
(AG)₂DNAAT (8)	161.6	676.5	20	726.1	432.42	1679.2
(TAG)₂DNAAT (9)	260.1	1089.2	24	1148.7	492.50	2332.3

DETONATION PARAMETERS AND THERMAL PROPERTIES

The calculation of the detonation parameters was performed with the program package EXPLO5 (version 5.03 and 5.04).^[38] The program is based on the chemical equilibrium, steady-state model of detonation. It uses the Becker-Kistiakowsky-Wilson's equation of state (BKW EOS) for gaseous detonation products and Cowan-Fickett's equation of state for solid carbon. The calculation of the equilibrium composition of the detonation products is done by applying modified White, Johnson and Dantzig's free energy minimization technique. The program is designed to enable the calculation of detonation parameters at the CJ point. The BKW equation in the following form was used with the BKWN set of parameters (α , β , κ , θ) as stated below the equations and X_i being the mol fraction of i -th gaseous product, k_i is the molar covolume of the i -th gaseous product^[39]:

$$pV / RT = 1 + x e^{\beta x} \quad x = (\kappa \sum X_i k_i) / [V(T + \theta)]^\alpha$$

$$\alpha = 0.5, \beta = 0.176, \kappa = 14.71, \theta = 6620.$$

The detonation parameters calculated with the EXPLO5 versions V5.03 and V5.04 using the experimentally determined densities (X-ray) are summarized in Table 11.

Table 11: Physico-chemical properties of **4 - 9** in comparison with hexogen (**RDX**).

	DNAAT (4)	(NH ₄) ₂ DNAAT (5)	(N ₂ H ₅) ₂ DNAAT (6)	(G) ₂ DNAAT (7)	(AG) ₂ DNAAT (8)	(TAG) ₂ DNAAT (9)	RDX*
Formula	C ₄ H ₄ N ₁₂ O ₄	C ₄ H ₁₀ N ₁₄ O ₄	C ₄ H ₁₂ N ₁₆ O ₄	C ₆ H ₁₄ N ₁₈ O ₄	C ₆ H ₁₆ N ₂₀ O ₄	C ₆ H ₂₀ N ₂₄ O ₄	C ₃ H ₆ N ₆ O 7
Molecular							
Mass	284.16	318.21	348.12	402.14	432.17	492.38	222.12
[g mol ⁻¹]							
Impact							
sensitivity	2	> 40	10	> 40	> 40	> 40	7
[J] ^a							
Friction							
sensitivity	20	> 360	> 360	> 360	> 360	160	120
[N] ^b							
ESD–test [J]	0.1	0.15	0.05	0.35	0.2	0.2	--
N [%] ^c	59.15	61.62	64.35	62.67	64.80	68.27	37.8
Ω [%] ^d		-45.25	-45.94	-59.65	-59.21	-58.48	-21.6
T _{dec.} [°C] ^e	209	212, 257	154, 228	261	177	219	210
ρ [g cm ⁻³] ^f	1.85	1.70	1.70	1.70	1.70	1.70	1.80
Δ _f H _m ^o [kJ mol ⁻¹] ^g	647.7	401.2	700.4	398.4	676.5	1089.2	70
Δ _f U ^o [kJ kg ⁻¹] ^h	2366.3	1369.6	2124.6	1101.0	1679.2	2332.3	417
EXPLO5 values: V5.03 (V5.04)							
–Δ _E U ^o [kJ kg ⁻¹] ⁱ	5268 (5339)	4473 (4461)	5055 (5026)	3731 (3690)	4202 (4147)	4681 (4602)	6038 (6125)
T _E [K] ^j	4237 (4089)	3362 (3234)	3583 (3475)	2855 (2732)	3048 (2944)	3213 (3087)	4368 (4236)
p _{C-J} [kbar] ^k	337 (298)	259 (267)	290 (294)	242 (241)	267 (262)	300 (290)	341 (349)
V _{Det.} [m s ⁻¹] ^l	8784 (8723)	8156 (8229)	8609 (8575)	8034 (7944)	8391 (8244)	8890 (8596)	8906 (8748)
Gas vol. [L kg ⁻¹] ^m	732 (708)	809 (798)	832 (816)	801 (781)	820 (797)	852 (822)	793 (739)

^[a] BAM drophammer, grain size (75–150 μm); ^[b] BAM friction tester, grain size (75–150 μm); ^[c] Nitrogen content; ^[d] Oxygen balance^[40]; ^[e] Temperature of decomposition by DSC ($\beta = 5$ °C, Onset values); ^[f] X-ray structure, Pycnometer for DNAAT; ^[g] Molar enthalpy of formation; ^[h] Energy of formation; ^[i] Energy of Explosion; ^[j] Explosion temperature; ^[k] Detonation pressure; ^[l] Detonation velocity; ^[m] Assuming only gaseous products; * values based on Ref. ^[41] and the EXPLO5 database; n.d.: not determined.

The neutral compound **4** already shows a remarkably high thermal stability of 209 °C, but a quite high sensitivity towards friction and impact. Since salts of energetic compounds tend to be more stable as the neutral compound, the nitrogen-rich salts of DNAAT are expected to show an improved stability. The decomposition temperatures of the compounds **5–9** are in the range of the neutral compound, those of the ammonium and guanidium as well as the triaminoguanidinium salt are even higher and appear in the range from 212 °C up to 261 °C. The ammonium and the hydrazinium salts show two decomposition points in the DSC with the first decomposition starting at 212 °C and 154 °C, respectively. As expected, the sensitivity values of all nitrogen-rich salts are considerably higher in comparison to the neutral compound. Nearly all compounds are insensitive towards friction, impact and electrostatic discharge, only the hydrazinium salt is slightly sensitive towards impact (10 J) and the triaminoguanidinium salt towards friction (160 N).

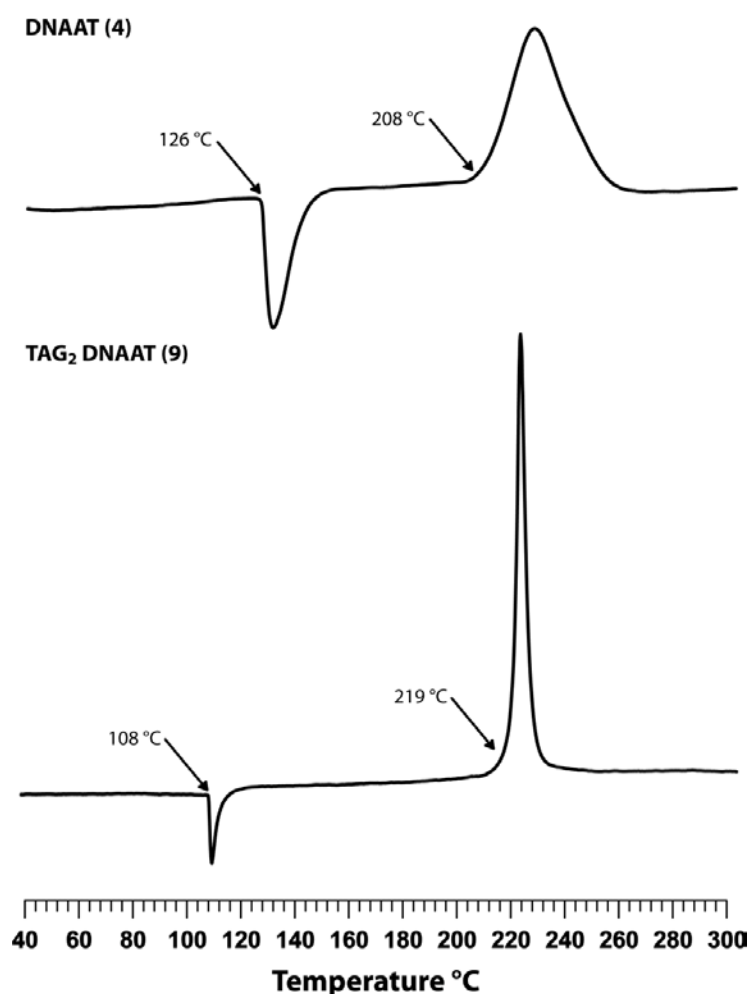


Figure 9: Differential scanning calorimetry (DSC) curves for the neutral nitrimino compound **4** and the bis(triaminoguanidinium) salt of **4** (**9**).

The nitrogen rich salts of DNAAT all exhibit positive heats and energies of formation. The detonation velocities were calculated in the range of 7944 m s^{-1} (**7**) to 8596 m s^{-1} (**9**). The best performance was calculated for the triaminoguanidinium salt (**9**) with a detonation velocity of 8596 m s^{-1} , which is only slightly lower than the performance of RDX. With the excellent sensitivity values for friction (160 N), impact (<40 J) and ESD (0.2 J) in addition to the remarkable high temperature of decomposition (219°C) and a very low solubility in water (2.5 g L^{-1} , 25°C), the triaminoguanidinium salt (**9**) seems to be the best choice in terms of performance and sensitivity and makes this compound suitable as a potential new high explosive. Additionally, the DSC curves of the 5,5'-dinitrimino-3,3'-azo-1*H*-1,2,4-triazole (**4**) and the corresponding bis(triaminoguanidinium) salt (**9**) are displayed in Figure 9.

Since 3,5-diamino-1*H*-1,2,4-triazole was used previously as a starting material resulting in 3,3'-dinitro-5,5'-azo-1,2,4-triazole (DNAT) and its triaminoguanidinium salt,^[13,14] we want to put the results obtained for these compounds into relation to the advances we were able to make. DNAT, synthesized by Naud et al. as mentioned in the introduction, shows a much lower sensitivity towards impact and friction with 12.5 J and 250 N, respectively, while the density is in the same region as observed for DNAAT (**4**) (1.85 g cm^{-3}). DNAT as a neutral compound is therefore much more stable regarding outer stimuli, but shows lower performance characteristics than DNAAT with a detonation velocity of 8500 m s^{-1} (**4**: 8723 m s^{-1}). Hence we were able to increase the performance of the molecule with the exchange of the nitro group with the nitrimino group, but the sensitivity values are much too high which prohibits the use as an energetic material (other than for primary explosives). This relation changes, when comparing the triaminoguanidinium salts of DNAT and DNAAT. In this case TAG₂ DNAAT (**9**) is exceeding the properties of TAG₂ DNAT in every respect: the decomposition temperature of **9** is higher (219°C compared to 202°C) together with the sensitivity values being much better in respect to the impact sensitivity (DNAT: 9.3 J, **9**: > 40J) and close to equal with respect to the friction sensitivity (DNAT: 157 N, **9**: 160 N). The performance characteristics of **9** cannot be compared directly, since they have been calculated at different densities, but we can state an overall increase in performance. At a density of 1.58 g cm^{-3} TAG₂ DNAT shows a detonation velocity of 8200 m s^{-1} and a detonation pressure at the Chapman-Jouguet point of 230 kbar while **9** exhibits a detonation pressure of 8596 m s^{-1} paired with a detonation pressure of 290 kbar at a density of 1.70 g cm^{-3} .

CONCLUSIONS

The application of the very straightforward and efficient acetyl protection of 3,5-diamino-1*H*-1,2,4-triazole allows selective reactions of the remaining free amino group and establishes a basis to a multitude of potential new energetic compounds that are now accessible. The synthesis of 5,5'-diamino-3,3'-azo-1*H*-1,2,4-triazole (**3**) by reaction of 5-acetylamino-3-amino-1*H*-1,2,4-triazole (**2**) with potassium permanganate is described. **3** acts as starting material for other new high energetic materials, since several modifications of the amine groups are possible. The subsequent nitration of **3** leads to the formation of 5,5'-dinitrimino-3,3'-azo-1*H*-1,2,4-triazole (**4**), which was fully characterized in terms of sensitivity and energetic properties as well as by single crystal X-ray diffraction. The molecule reveals promising energetic properties but quite high sensitivities towards friction (20 N), impact (2 J) and electrostatic discharge (0.1 J). Therefore, nitrogen rich salts were synthesized by reaction with high-nitrogen bases (ammonia, hydrazine, guanidine, aminoguanidine, triaminoguanidine). All salts were fully characterized by NMR-, IR- and Raman spectroscopy. Special attention was turned on the thermal stabilities and sensitivities values. The triaminoguanidinium salt (**9**) exhibits a remarkable high temperature of decomposition (219 °C) and detonation velocity (8596 m s⁻¹) and therefore turned out to be the most promising compound in terms of performance and stability. The performance characteristics of **9** exceed the ones of TAG₂ DNAT, which served as a reference molecule, especially when comparing the detonation pressure and sensitivity values.

EXPERIMENTAL PART

Caution: Although all 3,5-diamino-1,2,4-triazolium derivatives reported in this publication are rather stable against friction, impact and electric discharge, proper safety precautions should be taken when handling dinitramide salts. The derivatives are energetic materials and tend to explode under certain conditions, especially under physical stress. Laboratories and personnel should be properly grounded, and safety equipment such as Kevlar gloves, leather coats, face shields and ear plugs are recommended.

General. All chemical reagents, except 3,5-diamino-1,2,4-1*H*-triazole and solvents were obtained from Sigma-Aldrich Inc. or Acros Organics (analytical grade) and were used as supplied. 3,5-diamino-1,2,4-1*H*-triazole was obtained from ABCR. ^1H , $^{13}\text{C}\{^1\text{H}\}$, and ^{14}N NMR spectra were recorded on a JEOL Eclipse 400 instrument in $\text{DMSO-}d_6$ at or near 25 °C. The chemical shifts are given relative to tetramethylsilane (^1H , ^{13}C) or nitromethane (^{14}N) as external standards and coupling constants are given in Hertz (Hz). Infrared (IR) spectra were recorded on a Perkin-Elmer Spectrum BX FT-IR instrument equipped with an ATR unit at 25 °C. Transmittance values are qualitatively described as “very strong” (vs), “strong” (s), “medium” (m) and “weak” (w). Raman spectra were recorded on a Bruker RAM II spectrometer equipped with a Nd:YAG laser (1064 nm) and a reflection angle of 180°. The intensities are reported as percentages of the most intense peak and are given in parentheses. Elemental analyses were performed with a Netzsch Simultaneous Thermal Analyzer STA 429. Melting points were determined by differential scanning calorimetry (Setaram DSC141 instrument, calibrated with standard pure indium and zinc). Measurements were performed at a heating rate of 5 °C/min in closed aluminum sample pans with a 1 μm hole in the top for gas release under a nitrogen flow of 20 mL/min with an empty identical aluminum sample pan as a reference.

For initial safety testing, the impact and friction sensitivities as well as the electrostatic sensitivities were determined. The impact sensitivity tests were carried out according to STANAG 4489^[42], modified according to instruction^[43] using a BAM^[44] drophammer. The friction sensitivity tests were carried out according to STANAG 4487^[45] and modified according to instruction^[46] using the BAM friction tester. The electrostatic sensitivity tests were accomplished according to STANAG 4490^[47] using an electric spark testing device ESD 2010EN (OZM Research) operating with the “Winspark 1.15 software package”.

1-Acetyl-3,5-diamino-1*H*-1,2,4-triazole (1)

According to literature,^[16] acetic anhydride (40.8 mL, 1.2 eq.) was added dropwise under vigorous stirring to a solution of 3,5-diamino-1,2,4-triazole (36.0 g, 0.36 mol) in 130 mL water at room temperature. After stirring for 1 h, the precipitate was filtered off, washed with water and dried at room temperature to yield **1** as a colorless powder (48.3 g, 0.34 mol, 95% 1-acetyl-3,5-diamino-1*H*-1,2,4-triazole).

¹H NMR ([*d*6]-DMSO, 25 °C): δ 7.35 (s, 2H, NH₂), 5.64 (s, 2H, NH₂), 2.33 (s, 3H, CH₃); **¹³C NMR** ([*d*6]-DMSO, 25 °C): δ 170.5 (C=O), 162.2, 157.0, 23.6 (CH₃); **IR** (ATR, 25 °C, cm⁻¹): 3414(m), 3388(vs), 3295(m), 3127(s), 1709(s), 1640(vs), 1568(s), 1448(m), 1393(s), 1365(vs), 1336(s), 1178(m), 1116(m), 1066(m), 1043(m), 973(m), 839(w), 757(w), 699(w), 669(w); **Raman** (200 mW, 25 °C, cm⁻¹): 3418(4), 3403(5), 3220(10), 3183(9), 3132(9), 3022(35), 2989(16), 2934(68), 1711(100), 1641(40), 1568(44), 1549(25), 1459(9), 1425(21), 1396(41), 1375(39), 1340(43), 1182(37), 1155(80), 1118(25), 1037(42), 972(21), 840(25), 767(8), 719(11), 668(49), 590(15), 577(17), 445(50), 399(15), 385(15), 345(39), 245(13), 224(18).

3-Acetyl-amino-5-amino-1*H*-1,2,4-triazole (2)

A mixture of 1-acetyl-3,5-diamino-1,2,4-triazole (**1**) (10.0 g, 70.9 mmol) and 100 mL decaline was refluxed without stirring at 187–190 °C for 6 h. The solid was filtered off, washed with petrol ether (100 mL) and diethyl ether (100 mL) and dried in air to yield **2** as a colorless powder (9.6 g, 68.0 mmol, 96 %).

¹H NMR D₂O, NaOH, 25 °C): δ 2.03 (s, 3H, CH₃); **¹³C NMR** ([D₂O, NaOH, 25 °C): δ 174.1 (C=O), 162.5 (C-NH₂), 154.1 (C-NHAc), 22.7 (CH₃); **IR** (ATR, 25 °C, cm⁻¹): 3426(m), 3251(s), 1682(vs), 1597(vs), 1581(vs), 1451(s), 1295(m), 1269(m), 1080(m), 1026(w), 1010(w), 816(w), 714(m); **Raman** (200 mW, 25 °C, cm⁻¹): 3243(5), 2933(39), 1684(100), 1647(12), 1586(52), 1537(11), 1456(13), 1366(24), 1296(10), 1261(8), 1084(47), 1027(45), 970(28), 818(11), 793(12), 694(4), 590(38), 493(12), 363(12), 324(24). **Elemental analysis:** (C₄ H₇ N₅ O₁): calc: C 34.04, H 5.00, N 49.62; found: C 34.11, H 4.86, N 49.12.

5,5'-Diamino-3,3'-azo-1*H*-1,2,4-triazole (3)

Potassium permanganate (2/3 eq., 1.54 g, 9.7 mmol) was added over a period of 10 minutes to a solution of 3-acetylamino-5-amino-1*H*-1,2,4-triazole (**2**, 2.0 g, 14.2 mmol) in sodium hydroxide (32 %, 15 mL) at 0 °C. The mixture was allowed to warm to room temperature and subsequently refluxed for 3 h after addition of sodium hydroxide (5 mL, 2M). The generated manganese oxide was removed by filtration and the filtrate acidified with concentrated hydrochloric acid to pH = 6. The precipitate was filtered off and 5,5'-diamino-3,3'-azotriazole (**3**) was obtained as an orange solid (0.93 g, 4.8 mmol, 68%).

¹³C NMR (D₂O, NaOH): δ 170.2 (C-N=N), 165.3 (C-NH₂); **IR** (ATR, 25 °C, cm⁻¹): 3452(s), 3351(s), 2677(m), 1624(vs), 1490(m), 1465(m), 1413(w), 1349(m), 1142(m), 1102(m), 1051(m), 880(w), 799(w), 759(w), 708(vw), 676(vw); **Raman** (200 mW, 25 °C, cm⁻¹): 3349(1), 1658(2), 1520(4), 1448(42), 1388(24), 1347(100), 1139(35), 1103(7), 1056(9), 927(2), 912(3). **Elemental analysis**: (C₄ H₁₀ N₁₀ O₂, dihydrate): calc: C 20.87, H 4.38, N 60.85; found: C 21.58, H 3.85, N 59.05;

5,5'-Dinitrimino-3,3'-azo-1*H*-1,2,4-triazole (4)

5,5'-diamino-3,3'-azotriazole (0.35 g, 1.8 mmol) was dissolved in sulfuric acid (conc., 1.75 mL) and nitric acid (conc., 0.30 mL, 7.2 mmol) was added at 0 °C. After stirring at 0 °C for 30 minutes, the mixture was allowed to warm to room temperature, stirred for 1 h and poured on ice (10 g). The precipitate was filtered off, washed with water and dried at 60 °C to obtain **4** as a yellow solid.

DSC (Onset, 5 °C min⁻¹): T_{Dec.}: 209 °C; **¹³C{¹H} NMR** ([*d*6]-DMSO, 25 °C): δ 159.7 (C-N=N), 153.8 (C-N-NO₂); **¹⁴N NMR** ([*d*6]-DMSO, 25 °C): δ -19 (NO₂); **IR** (ATR, 25 °C, cm⁻¹): 3066(s), 1695 (w), 1586(vs), 1542(m), 1522(s), 1493(m), 1436(m), 1273(s), 1238(s), 1139(m), 1075(m), 1039(m), 979(m), 845(w), 770(w), 721(w); **Raman** (200 mW, 25 °C, cm⁻¹): 1538(16), 1493(10), 1436(100), 1354(11), 1307(16), 1145(21), 1091(7), 994(11), 905(4), 847(3), 754(2); **Elemental analysis**: (C₄ H₄ N₁₂ O₄): calc: C 16.91, H 1.42, N 59.15; found: C 18.27, H 1.83, N 58.25; **Sensitivities** (grain size: 100–500 μm): FS: 20 N, IS: 2 J, ESD: 0.1 J.

General synthesis of nitrogen-rich salts of DNAAT

The free nitrogen-rich base (2 eq., 22.8 mmol) was added to a suspension of 5,5'-dinitrimino-3,3'-azo-1*H*-1,2,4-bistriazole (**4**, 3.24 g, 11.4 mmol) in 75 mL water at 60 °C. After cooling to 5 °C, the precipitate was filtered off, washed with cold water and dried at 60 °C to yield the corresponding nitrogen-rich salt of 5,5'-dinitrimino-3,3'-azo-1*H*-1,2,4-triazole (**5–9**) as a yellow solid.

(NH₄)₂DNAAT (5)

yield: 50%; **DSC** (onset, 5 °C min⁻¹): T_{Dec.}: 212 °C; **¹H NMR** ([*d*6]-DMSO, 25 °C): δ 13.58 (s, 2H, N_{ring}-H), 7.23 (NH₄⁺); **¹³C NMR** ([*d*6]-DMSO, 25 °C): δ 167.7 (C-N=N), 158.3 (C-N-NO₂); **¹⁴N NMR** ([*d*6]-DMSO, 25 °C): δ -14 (-NO₂), -359 (NH₄⁺); **IR** (ATR, 25 °C, cm⁻¹): 3171(s), 1692(w), 1641(w), 1594(m), 1530(s), 1474(s), 1432(s), 1380(s), 1316(vs), 1168(m), 1078(s), 1035(w), 1004(m), 861(w), 770(m), 733(w), 698(w); **Raman** (200 mW, 25 °C, cm⁻¹): 1544(25), 1466(100), 1403(53), 1352(84), 1167(30), 1099(17), 1044(8), 1002(41), 924(12), 860(8), 748(6), 397(7); **Sensitivities** (grain size: 100–500 μm): FS: >360 N, IS: >40 J, ESD: 0.15 J.

(N₂H₅)₂DNAAT (6)

yield: 54%; **DSC** (onset, 5 °C min⁻¹): T_{Dec.}: 154 °C; **¹H NMR** ([*d*6]-DMSO, 25 °C): δ 13.51 (s, 2H, N_{ring}-H), 7.28 (N₂H₅⁺); **¹³C NMR** ([*d*6]-DMSO, 25 °C): δ 166.9 (C-N=N), 157.8 (C-N-NO₂); **¹⁴N NMR** ([*d*6]-DMSO, 25 °C): δ -16 (-NO₂), -359 (N₂H₅⁺); **IR** (ATR, 25 °C, cm⁻¹): 3103(s), 1631(m), 1528(s), 1472(m), 1426(s), 1385(m), 1315(vs), 1260(s), 1168(m), 1080(s), 996(m), 859(w), 769(w), 732(vw), 705(w); **Raman** (200 mW, 25 °C, cm⁻¹): 1541(9), 1461(100), 1403(36), 1353(54), 1258(3), 1162(19), 1100(10), 1000(20), 924(7), 859(4), 747(2), 399(2); **Sensitivities** (grain size: 100–500 μm): FS: >360 N, IS: 10 J, ESD: 0.05 J.

G₂DNAAT (7)

yield: 73%; **DSC** (onset, 5 °C min⁻¹): T_{Dec.}: 261 °C; **¹H NMR** ([*d*6]-DMSO, 25 °C): δ 13.53 (s, 2H, N_{ring}-H), 7.03 (s, G⁺); **¹³C NMR** ([*d*6]-DMSO, 25 °C): δ 167.1 (C-N=N), 157.9 (C-N-NO₂), 157.7 (G⁺); **¹⁴N NMR** ([*d*6]-DMSO, 25 °C): δ -14 (-NO₂); **IR** (ATR, 25 °C, cm⁻¹): 3336(m), 3241(m), 3167(m), 2790(w), 1680(m), 1635(s), 1532(m), 1471(m), 1436(m), 1391(m), 1368(m), 1339(vs), 1255(m), 1162(m), 1085(s), 1011(m),

864(w), 770(m), 726(w), 690(w); **Raman** (200 mW, 25 °C, cm^{-1}): 1536(14), 1462(100), 1402(23), 1363(56), 1156(18), 1097(14), 1012(24), 917(8), 862(5), 402(5); **Elemental analysis**: (C₆ H₁₄ N₁₈ O₄): calc: C 17.91, H 3.51, N 62.67; found: C 18.49, H 3.59, N 62.12; **Sensitivities** (grain size: 100–500 μm): FS: >360 N, IS: >40 J, ESD: 0.35 J.

AG₂DNAAT (8)

yield: 87%; **DSC** (onset, 5 °C min^{-1}): T_{Dec.}: 177 °C; **¹H NMR** ([d₆]-DMSO, 25 °C): δ 13.61 (s, 2H, N_{ring}-H), 7.89 (s, AG⁺), 7.12 (s, AG⁺), 4.71 (s, AG⁺); **¹³C NMR** ([d₆]-DMSO, 25 °C): δ 167.0 (C-N=N), 157.7 (C-N-NO₂), 158.9 (AG⁺); **¹⁴N NMR** ([d₆]-DMSO, 25 °C): δ -15 (-NO₂); **IR** (ATR, 25 °C, cm^{-1}): 3435(m), 3341(m), 3252(vs), 3183(s), 2888(w), 1685(vs), 1668(vs), 1530(s), 1475(m), 1436(m), 1386(m), 1346(vs), 1257(m), 1164(w), 1086(s), 1009(m), 864(w), 770(m), 730(w), 692(w); **Raman** (200 mW, 25 °C, cm^{-1}): 1534(16), 1488(12), 1463(100), 1409(22), 1367(51), 1156(20), 1096(12), 1041(5), 1008(29), 918(9), 861(5), 746(4), 403(5); **Elemental analysis**: (C₆ H₁₆ N₂₀ O₄): calc.: C 16.67, H 3.73, N 64.80; found: C 16.87, H 3.73, N 61.97; **Sensitivities** (grain size: 100–500 μm): FS: >360 N, IS: >40 J, ESD: 0.20 J.

TAG₂DNAAT (9)

yield: 85%; **DSC** (onset, 5 °C min^{-1}): T_{Dec.}: 219 °C; **¹H NMR** ([d₆]-DMSO, 25 °C): δ 13.48 (s, 2H, N_{ring}-H), 8.59 (s, TAG⁺), 4.49 (s, TAG⁺); **¹³C NMR** ([d₆]-DMSO, 25 °C): δ 167.3 (C-N=N), 157.8 (C-N-NO₂), 159.0 (TAG⁺); **¹⁴N NMR** ([d₆]-DMSO, 25 °C): δ -14 (-NO₂); **IR** (ATR, 25 °C, cm^{-1}): 3252(s), 1682(s), 1526(s), 1466(m), 1435(s), 1315(vs), 1250(m), 1133(m), 1073(s), 1003(m), 857(w), 771(w), 728(w), 656(w); **Raman** (200 mW, 25 °C, cm^{-1}): 1534(16), 1488(12), 1463(100), 1409(22), 1367(51), 1156(20), 1096(12), 1041(5), 1008(29), 918(9), 861(5), 746(4), 403(5); **Elemental analysis**: (C₆ H₂₀ N₂₄ O₄): calc.: C 14.64, H 4.09, N 68.27; found: C 15.22, H 4.37, N 66.73; **Sensitivities**: (grain size: 100–500 μm): FS: 160 N, IS: >40 J, ESD: 0.20 J.

REFERENCES

- [1] P. F. Pagoria, G. S. Lee, A. R. Mitchell, R. D. Schmidt, *Thermochim. Acta* **2002**, 384, 187-204.
- [2] T. M. Klapötke, in *Structure and bonding* (Ed.: D. M. P. Mingos), Springer-Verlag, Berlin Heidelberg **2007**.
- [3] D. Fournier, A. Halasz, J. Spain, R. J. Spanggord, J. C. Bottaro, J. Hawari, *Appl. Environ. Microb.* **2004**, 70, 1123-1128.
- [4] a) T. M. Klapoetke, J. Stierstorfer, A. U. Wallek, *Chem.Mat.* **2008**, 20, 4519-4530; b) T. M. Klapoetke, C. M. Sabate, *Chem.Mat.s* **2008**, 20, 3629-3637; c) S. Yang, S. Xu, H. Huang, W. Zhang, X. Zhang, *Huaxue Jinzhan* **2008**, 20, 526-537; d) D. E. Chavez, M. A. Hiskey, D. L. Naud, *Propell. Explo. Pyrot.* **2004**, 29, 209-215; e) Y. Huang, H. Gao, B. Twamley, J. n. M. Shreeve, *Eur. J. Inorg. Chem.* **2008**, 2560-2568.
- [5] C. M. Sabate, T. M. Klapoetke, *New Trends in Research of Energetic Materials, Proceedings of the Seminar, 12th, Pardubice, Czech Republic, Apr. 1-3, 2009* **2009**, 172-194.
- [6] a) D. E. Chavez, M. A. Hiskey, R. D. Gilardi, *Angew. Chem. Int. Ed.* **2000**, 39, 1791-1793; b) D. Chavez, L. Hill, M. Hiskey, S. Kinkead, *J. Energ. Mat.* **2000**, 18, 219-236.
- [7] a) T. M. Klapoetke, C. M. Sabate, *New J. Chem.* **2009**, 33, 1605-1617; b) T. M. Klapoetke, C. M. Sabate, *Chem. Mat.* **2008**, 20, 1750-1763; c) A. Hammerl, G. Holl, T. M. Klapotke, P. Mayer, H. Noth, H. Piotrowski, M. Warchhold, *Eur.J. Inorg. Chem.* **2002**, 834-845.
- [8] a) B. C. Tappan, A. N. Ali, S. F. Son, T. B. Brill, *Propell. Explo. Pyrot.* **2006**, 31, 163-168; b) R. Sivabalan, M. B. Talawar, N. Senthilkumar, B. Kavitha, S. N. Asthana, *J. Therm.Anal. Calorim.* **2004**, 78, 781-792.
- [9] M. A. Hiskey, N. Goldman, J. R. Stine, *J.Energ. Mat.* **1998**, 16, 119-127.
- [10] a) M. M. Chaudhri, *J. Mater. Sci. Lett.* **1984**, 3, 565-568; b) D. J. Whelan, R. J. Spear, R. W. Read, *Thermochim. Acta* **1984**, 80, 149-163; c) G. O. Reddy, A. K. Chatterjee, *Thermochim. Acta* **1983**, 66, 231-244; d) M. M. Chaudhri, *Nature (London, United Kingdom)* **1976**, 263, 121-122.
- [11] M. M. Williams, W. S. McEwan, R. A. Henry, *J. Phys. Chem.* **1957**, 61, 261-267.
- [12] D. E. Chavez, B. C. Tappan, 8-ISICP, Los Alamos National laboratory, **2009**.

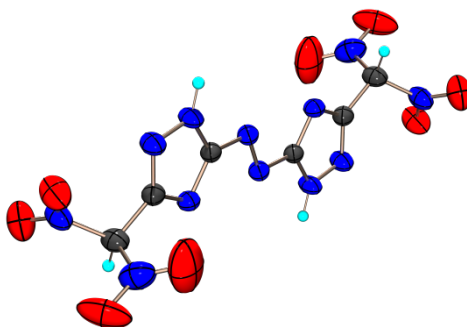
- [13] D. L. Naud, M. A. Hiskey, H. H. Harry, *J. Energ. Mat.* **2003**, 21, 57-62.
- [14] D. E. Chavez, B. C. Tappan, B. A. Mason, D. Parrish, *Propell. Explo. Pyrot.* **2009**, 34, 475-479.
- [15] B. G. van den Bos, *Recueil des Travaux Chimiques des Pays-Bas et de la Belgique* **1960**, 79, 836-842.
- [16] M. S. Pevzner, N. V. Gladkova, T. A. Kravchenko, *Zh. Org. Khim.* **1996**, 32, 1230-1233.
- [17] H.-H. Licht, H. Ritter, *J. Energ. Mat.* **1994**, 12, 223-235.
- [18] N. Biswas, S. Umapathy, *J. Phys. Chem. A* **2000**, 104, 2734-2745.
- [19] F. Billes, H. Endredi, G. Keresztury, *Theochem* **2000**, 530, 183-200.
- [20] *CrysAlis CCD, Oxford Diffraction Ltd., Version 1.171.27p5 beta (release 01-04-2005 CrysAlis171.NET).*
- [21] *CrysAlis RED, Oxford Diffraction Ltd., Version 1.171.27p5 beta (release 01-04-2005 CrysAlis171.NET).*
- [22] A. Altomare, G. Cascarano, C. Giacovazzo, A. Guagliardi, *J. Appl. Cryst.* **1993**, 26, 343-350.
- [23] G. M. Sheldrick, *SHELXS-97, Crystal Structure Solution, Version 97-1; Institut Anorg. Chemie, University of Göttingen, Germany, 1990.*
- [24] G. M. Sheldrick, *SHELXL-97, Program for the Refinement of Crystal Structures. University of Göttingen, Germany, 1997.*
- [25] L. Farrugia, *J. Appl. Cryst.* **1999**, 32, 837-838.
- [26] A. L. Spek, *Platon, A Multipurpose Crystallographic Tool, Utrecht University, Utrecht, The Netherlands, 1999.*
- [27] *Crystallographic data for the structure(s) have been deposited with the Cambridge Crystallographic Data Centre. Copies of the data can be obtained free of charge on application to The Director, CCDC, 12 Union Road, Cambridge CB2 1EZ, UK (Fax: int.code (1223)336-033; e-mail for inquiry: fileserv@ccdc.cam.ac.uk; e-mail for deposition: deposit-@ccdc.cam.ac.uk).*
- [28] F. H. Allen, O. Kennard, D. G. Watson, L. Brammer, A. G. Orpen, R. Taylor, *J. Chem. Soc. Perk. T. 2 (1972-1999)* **1987**, S1-S19.
- [29] A. Hammerl, Ludwig-Maximilians-University (Munich), **2001**.
- [30] G. A. Jeffrey, *An Introduction to Hydrogen Bonding*, Oxford University Press, Oxford **1997**.

- [31] A. F. Hollemann, E. Wiberg, N. Wiberg, *Lehrbuch der anorganischen Chemie*, de Gruyter, New York, **2007**.
- [32] M. J. Frisch et al., *Gaussian 03, Revision B04*, Gaussian Inc., Wallingford, CT, **2004**.
- [33] a) J. W. Ochterski, G. A. Petersson, J. A. Montgomery, Jr., *J. Chem. Phys.* **1996**, *104*, 2598-2619; b) J. A. Montgomery, Jr., M. J. Frisch, J. W. Ochterski, G. A. Petersson, *J. Chem. Phys.* **2000**, *112*, 6532-6542.
- [34] a) L. A. Curtiss, K. Raghavachari, P. C. Redfern, J. A. Pople, *J. Chem. Phys.* **1997**, *106*, 1063-1079; b) E. F. C. Byrd, B. M. Rice, *J. Phys. Chem. A* **2006**, *110*, 1005-1013; c) B. M. Rice, S. V. Pai, J. Hare, *Combust. Flame* **1999**, *118*, 445-458.
- [35] <http://webbook.nist.gov/chemistry>
- [36] a) M. S. Westwell, M. S. Searle, D. J. Wales, D. H. Williams, *J. Am. Chem. Soc.* **1995**, *117*, 5013-5015; b) F. Trouton, *Philos. Mag.* **1884**, *18*, 54-57.
- [37] a) H. D. B. Jenkins, H. K. Roobottom, J. Passmore, L. Glasser, *Inorg. Chem.* **1999**, *38*, 3609-3620; b) H. D. B. Jenkins, D. Tudela, L. Glasser, *Inorg. Chem.* **2002**, *41*, 2364-2367.
- [38] a) M. Sućeska, *EXPLO5.4 program*, Zagreb, Croatia, **2010**; b) M. Sućeska, *EXPLO5.3 program*, Zagreb, Croatia, **2009**.
- [39] a) M. Sućeska, *Mater. Sci. Forum* **2004**, 465-466, 325-330; b) M. Sućeska, *Propell. Explos. Pyrot.* **1991**, *16*, 197-202; c) M. Sućeska, *Propell. Explos. Pyrot.* **1999**, *24*, 280-285; d) M. L. Hobbs, M. R. Baer, in *Proc. of the 10th Symp. (International) on Detonation*, ONR 33395-12, Boston, MA, **July 12-16, 1993**, p. 409.
- [40] Calculation of oxygen balance: $\Omega (\%) = (wO - 2xC - 1/2yH - 2zS)1600/M$. (w : number of oxygen atoms, x : number of carbon atoms, y : number of hydrogen atoms, z : number of sulfur atoms, M : molecular weight).
- [41] J. Köhler, R. Meyer, *Explosivstoffe*, Vol. 9th edition, Wiley-VCH, Weinheim, **1998**.
- [42] i. t. NATO standardization agreement (STANAG) on explosives, no.4489, 1st ed., Sept. 17, **1999**.
- [43] *WIWEB-Standardarbeitsanweisung 4-5.1.02, Ermittlung der Explosionsgefährlichkeit, hier: der Schlagempfindlichkeit mit dem Fallhammer*, Nov. 08, **2002**.
- [44] <http://www.bam.de>.

- [45] *NATO standardization agreement (STANAG) on explosives, friction tests, no.4487, 1st ed., Aug. 22, **2002**.*
- [46] *WIWEB-Standardarbeitsanweisung 4-5.1.03, Ermittlung der Explosionsgefährlichkeit, hier: der Reibempfindlichkeit mit dem Reibeapparat, Nov. 08, **2002**.*
- [47] *NATO standardization agreement (STANAG) on explosives, electrostatic discharge sensitivity tests, no.4490, 1st ed., Feb. 19, **2001**.*

4. SYNTHESIS AND CHARACTERIZATION OF 3,3'-BIS(DINITRO-METHYL)-5,5'-AZO-1H-1,2,4-TRIAZOLE

As published in: *Zeitschrift für Anorganische und Allgemeine Chemie* **2011**, 637, 1453–1457.



ABSTRACT:

The synthesis of 3,3'-bis(dinitromethyl)-5,5'-azo-1H-1,2,4-triazole (**5**) using the readily available starting material 2-(5-amino-1H-1,2,4-triazol-3-yl)acetic acid (**1**) is described. All compounds were characterized by means of NMR, IR and Raman spectroscopy. The energetic compound **5** was additionally characterized by single crystal X-Ray diffraction and DSC measurements. The sensitivities towards impact, friction and electrical discharge were determined. In addition, detonation parameters (e.g. heat of explosion, detonation velocity) of the target compound were computed using the EXPLO5 code based on the calculated (CBS-4M) heat of formation and X-ray density.

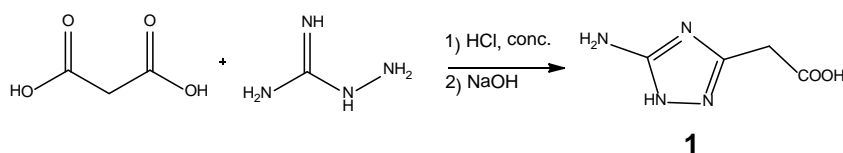
INTRODUCTION

Nitrogen rich heterocycles are traditional building blocks for nitrogen rich energetic materials and have been intensively investigated as high energy density materials [1]. In recent years, the synthesis of energetic, heterocyclic compounds has attracted an increasing amount of interest, since heterocycles generally offer a higher heat of formation, density and oxygen balance than their carbocyclic analogues [2]. In combination with the advances of a high nitrogen content such as the high average two electron bond energy associated with the nitrogen-nitrogen triple bond [3], those compounds are in the focus as propellants [4], in gas generators for airbags [5] as well as

in formulations for use as propellant burn rate modifiers [6]. Triazole derivatives generally exhibit desired properties such as a positive heat of formation, high densities and a high nitrogen content together with low sensitivity towards external forces like impact and friction [7]. Since modern high energy density materials (HEDM) mostly derive their energy of ring or cage strain as well as of a high heat of formation, a lot of research has been done on explosives containing the azo-functionality [8]. Due to its auspicious energetic properties, a variety of azole-based energetic compounds including the dinitromethyl-moiety have already been synthesized [9]. In this work the synthesis and characterization of 3,3'-bis (dinitromethyl)-5,5'-azo-1*H*-1,2,4-triazole (**5**) as potential new nitrogen-rich high energetic material is presented.

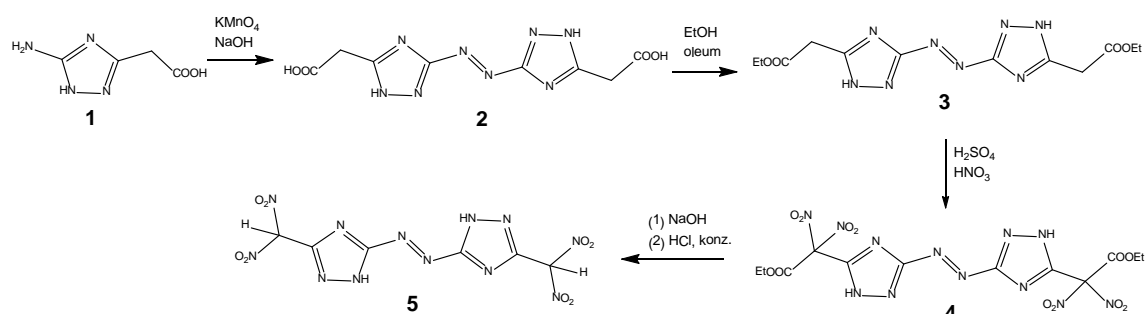
RESULTS AND DISCUSSION

The synthesis of the starting material 2-(5-amino-1*H*-1,2,4-triazol-3-yl)acetic acid (**1**) was performed using malonic acid and aminoguanidinium bicarbonate as described by Chernyshev *et. al* (Scheme 1) [10]. Compound **1** is formed via malonic acid diguanylhydrazide as an intermediate product followed by subsequent cyclisation with 6 m sodium hydroxide solution.



Scheme 1: Synthesis of starting material **1**

As shown in Scheme 2, the resulting 2-(5-amino-1*H*-1,2,4-triazol-3-yl)acetic acid (**1**) was reacted with sodium permanganate to form 2,2'-(3,3'-azo-bis(1*H*-1,2,4-triazol-5-yl))diacetic acid (**2**). The two free acetic acid groups were protected using ethanol and oleum resulting in the formation of **3**. Introduction of the NO₂-moieties was achieved by nitration with sulfuric acid/nitric acid (6:1) to form the nitrated compound **4**.



Scheme 2: Synthetic route towards 3,3'-bis(dinitromethyl)-5,5'-azo-1H-1,2,4-triazole (**5**)

The ethyl ester hydrolyses in basic media and subsequent acidification with concentrated hydrochloric acid leads to the release of CO_2 and the formation of 3,3'-bis(dinitromethyl)-5,5'-azo-1H-1,2,4-triazole (**5**). All compounds were characterized by means of NMR, IR and Raman spectroscopy. The complete decarboxylation of the acetic acid groups during the synthesis of **5** can easily be monitored by the missing $\text{C}=\text{O}$ vibration band at 1766 cm^{-1} as well as the missing C-H valence vibrations in the range of $2800\text{--}3100\text{ cm}^{-1}$ in the IR and Raman spectra. The latter is dominated by the absorption of the azo-moiety at 1462 cm^{-1} [8e, 11]. The neutral compound **5** shows two signals for the different triazole carbon atoms at 169.7 and 149.7 ppm as well as the signal for the dinitromethyl moiety at 124.9 ppm. The nitro groups can be found at -23 ppm in the ^{14}N NMR spectra.

Compound **5** as well as the corresponding sodium salt (**6**) were additionally characterized by low temperature single crystal X-ray spectroscopy. Crystals of 3,3'-bis(dinitromethyl)-5,5'-azo-1H-1,2,4-triazole (**5**) have been obtained by recrystallisation from methanol. Compound **5** crystallizes in the monoclinic spacegroup $P2_1/n$ with two formula units per unit cell and a density of 1.798 g cm^{-3} . The molecular structure is shown in Figure 1.

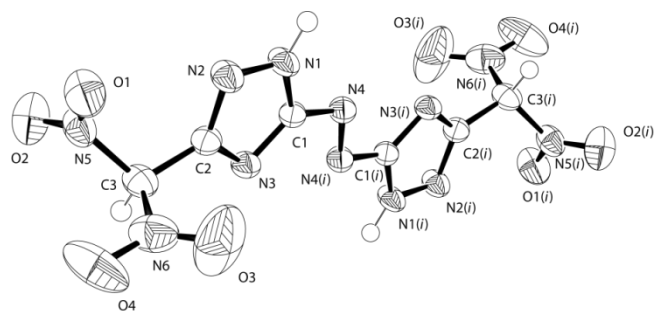


Figure 1: ORTEP representation of the molecular moiety of **5** (DNMAT). Displacement ellipsoids are shown at the 50% probability level; Selected bond lengths (Å): N4–N4(*i*) 1.260(2), N4–C1 1.400(2), N3–C1 1.324(2), N3–C2 1.347(2), N2–C2 1.325(2), N2–N1 1.341(2), N1–C1 1.333(2), N1–H1 0.88(2), C3–C2 1.485(2), C3–N5 1.498(2), C3–N6 1.517(2), C3–H3 0.931(18), O1–N5 1.219(2), N5–O22 1.214(2), N6–O3 1.198(2), N6–O4 1.211(2); Selected bond angles (°): C2–C3–N5 110.3(1), C2–C3–N6 113.3(2), N5–C3–N6 106.2(1), C2–C3–H3 113.4(1), N5–C3–H3 107.6(1), N6–C3–H3 105.5(1); Selected torsion angles (°): N4(*i*)–N4–C1–N3 0.9(3), N4(*i*)–N4–C1–N1 -177.6(2); (*i*) = $-x+1/2, y+1/2, -z+1/2$.

The azo-triazole moiety shows a planar assembly as expected. The proton of the dinitromethyl moiety is not located at the nitrogen atom N3 in the ring but at the carbon atom C3. This leads to a tetrahedral coordination typical for sp^3 carbon atoms and a C2–C3 distance in the range of a C–C single bond (1.485(2) Å) [12]. The proton of the dinitromethyl moiety can easily be deprotonated with common bases such as sodium hydroxide. The molecular structure of **6** including the coordination sphere of the sodium atoms is shown in Figure 2. Atoms within the asymmetric unit are labeled, atoms generated by symmetry are set transparent.

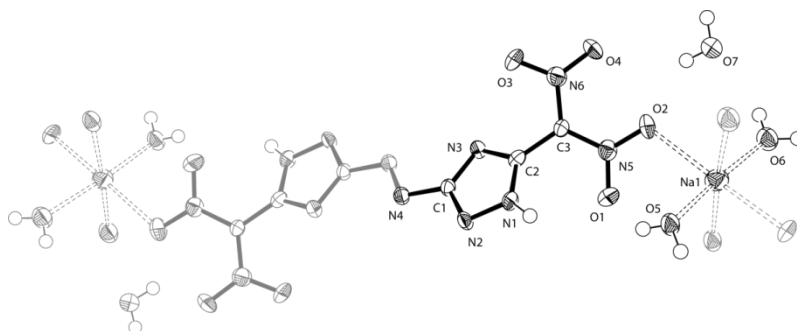


Figure 2: ORTEP representation of the molecular structure of **6** (Na₂DNMAT) including the coordination sphere of the sodium atoms. Displacement ellipsoids are shown at the 50% probability level; atoms generated by symmetry are set transparent. Selected bond lengths (Å): C1–N2 1.326(3), C1–N3 1.359(3), C1–N4 1.408(3), C2–N3 1.324(3), C2–N1 1.340(3), C2–C3 1.457(4), C3–N5 1.382(3), C3–N6 1.405(3), N1–N2 1.356(3), N1–H1 0.81(3), N4–N4(*i*) 1.264(4), N5–O2 1.244(3), N5–O1 1.263(3), N6–O4 1.237(3), N6–O3 1.241(3); Selected bond angles (°): N5–C3–N6 120.9(2), N5–C3–C2 119.9(2), N6–C3–C2 119.2(2); Selected torsion angles (°): N4–C1–N2–N1 -179.3(2), N4–C1–N3–C2 179.2(3).

Crystals of the sodium salt of 3,3'-bis(dinitromethyl)-5,5'-azo-1*H*-1,2,4-triazole (**6**) were obtained by recrystallization from water.

The corresponding di-anion (**6**) shows a shorter C2–C3 distance than **5**, which is in the range of a conjugated C_{sp2}=C_{arom.} double bond (1.457(4) Å) [12], indicating the presence of a delocalized π -electron system as anticipated for anionic azo-triazole derivatives. This leads to an increased thermal stability with a decomposition temperature of 209 °C for compound **6**. Hence, the deprotonation of **5** appears promising for the synthesis of highly stable energetic materials including nitrogen rich cations.

ENERGETIC PROPERTIES

The energetic properties of compound **5** in comparison to RDX are compiled in Table 2.

Table 2: Physico-Chemical Properties of **5** in comparison with hexogen (**RDX**)

	5	RDX*
Formula	C ₆ H ₄ N ₁₂ O ₈	C ₃ H ₆ N ₆ O ₇
FW [g mol ⁻¹]	372.17	222.12
Impact sensitivity [J] ^a	4	7
Friction sensitivity [N] ^b	360	120
ESD-test [J]	0.15	0.2
N [%] ^c	45.2	37.8
Ω [%] ^d	-25.8	-21.6
T _{dec.} [°C] ^e	80	210
ρ [g cm ⁻³] ^f	1.798	1.80
$\Delta_f H_m^\circ$ [kJ mol ⁻¹] ^g	579.5	70
$\Delta_f U^\circ$ [kJ kg ⁻¹] ^h	1557.2	417
EXPLO5.4 values:		
$-\Delta_E U^\circ$ [kJ kg ⁻¹] ⁱ	5831	6125
T _E [K] ^j	4473	4236
p_{C-J} [kbar] ^k	320	349
$V_{Det.}$ [m s ⁻¹] ^l	8433	8748
Gas vol. [L kg ⁻¹] ^m	661.2	739

^[a] BAM drophammer, grain size (75–150 μ m); ^[b] BAM friction tester, grain size (75–150 μ m); ^[c] Nitrogen content; ^[d] Oxygen balance [13]; ^[e] Temperature of decomposition by DSC ($\beta = 5$ °C, Onset values); ^[f] X-ray structure, Pycnometer for DNAAT; ^[g] Molar enthalpy of formation; ^[h] Energy of formation; ^[i] Energy of Explosion; ^[j] Explosion temperature; ^[k] Detonation pressure; ^[l] Detonation velocity; ^[m] Assuming only gaseous products; * values based on Ref. [14] and the EXPLO5 database.

As expected for azo-triazoles, compound **5** exhibits a high positive heat of formation of $579.5 \text{ kJ mol}^{-1}$. With a detonation velocity of 8433 m s^{-1} and a pressure at the C-J point of 320 kbar, the performance of compound **5** is only slightly below RDX. In addition, 3,3'-bis(dinitromethyl)-5,5'-azo-1*H*-1,2,4-triazole is sensitive towards impact (4 J) but insensitive towards friction ($>360 \text{ N}$).

CONCLUSIONS

The synthesis of 3,3'-bis(dinitromethyl)-5,5'-azo-1*H*-1,2,4-triazole (**5**) is straightforward using inexpensive and readily available starting materials. All intermediate compounds were fully characterized by means of IR and Raman as well as multinuclear NMR spectroscopy and differential scanning calorimetry. The target compound **5** as well as the corresponding sodium salt (**6**) were additionally characterized by low temperature single crystal X-ray diffraction measurements. With the high positive heat of formation ($579.5 \text{ kJ mol}^{-1}$) and a detonation velocity of 8433 m s^{-1} , compound **5** reveals attractive energetic properties. The neutral compound shows low sensitivity towards friction, a high sensitivity towards impact paired with a very low temperature of decomposition starting at 80°C . Deprotonation of compound **5** results in a delocalized π -electron system and an increase of the decomposition temperature up to 209°C in the case of the sodium salt (**6**). Since literature known azo-triazole derivatives show excellent properties [8f, 15] the ability of deprotonating 3,3'-bis(dinitromethyl)-5,5'-azo-1*H*-1,2,4-triazole (**5**) to form the corresponding di-anion and its nitrogen-rich or metal salts offers promising opportunities for the synthesis of new ionic and highly stable energetic materials.

EXPERIMENTAL SECTION

General. All chemical reagents, except solvents were obtained from Sigma-Aldrich Inc. or Acros Organics (analytical grade) and were used as supplied. ^1H , $^{13}\text{C}\{^1\text{H}\}$, and $^{14}\text{N}\{^1\text{H}\}$ NMR spectra were recorded on a JEOL Eclipse 400 instrument in $\text{DMSO-}d_6$ at or near 25 °C. The chemical shifts are given relative to tetramethylsilane (^1H , ^{13}C) or nitromethane (^{14}N) as external standards and coupling constants are given in Hertz (Hz). Infrared (IR) spectra were recorded on a Perkin-Elmer Spectrum BX FT-IR instrument equipped with an ATR unit at 25 °C. Transmittance values are qualitatively described as “very strong” (vs), “strong” (s), “medium” (m) and “weak” (w). Raman spectra were recorded on a Bruker RAM II spectrometer equipped with a Nd:YAG laser (1064 nm) and a reflection angle of 180°. The intensities are reported as percentages of the most intense peak and are given in parentheses. Elemental analyses were performed with a Netzsch Simultaneous Thermal Analyzer STA 429. Melting points were determined by differential scanning calorimetry (Linseis PT 10 DSC), calibrated with standard pure indium and zinc. Measurements were performed at a heating rate of 5 °C/min in closed aluminum sample pans with a 1 μm hole in the top for gas release under a nitrogen flow of 20 mL/min with an empty identical aluminum sample pan as a reference.

The single crystal X-ray diffraction data of **5** and **6** were collected using an Oxford Xcalibur3 diffractometer equipped with a Spellman generator (voltage 50 kV, current 40 mA) and a KappaCCD detector. The data collection was undertaken using the CrysAlis CCD software [16] while the data reduction was performed with the CrysAlis Red software [17]. The structures were solved with Shelxs-97 [18], refined with Shelxl-97 implemented in the program package WinGX [19] and finally checked using Platon [20]. Further information regarding the crystal-structure determination have been deposited with the Cambridge Crystallographic Data Centre [21] filed under CCDC numbers 820713 (**5**) and 820714 (**6**).

The heat of formation calculation of compound **5** was performed using the atomization method based on CBS-4M enthalpies described recently in detail in the literature [22].

$$\Delta_f H^\circ_{(\text{g,M},298)} = H_{(\text{Molecule}298)} - \sum H^\circ_{(\text{Atoms}298)} + \sum \Delta_f H^\circ_{(\text{Atoms}298)} \quad (1)$$

All quantum chemical calculations were performed with the Gaussian G03W (revision B.03) program package [23]. The results are compiled in Table 2. The gas phase heat of formation ($\Delta_f H^\circ(\text{g,M})$) was converted into the solid state heat of formation ($\Delta_f H^\circ(\text{s})$) using the Jenkins equations [24].

Compounds **1**, **2** and **3** were synthesized according to known literature procedures [10].

Diethyl-2,2'-(3,3'-azo-bis(1H-1,2,4-triazol-5-yl))2,2'-dinitro-diacetate(4)

Diethyl-2,2'-(3,3'-azo-bis(1H-1,2,4-triazol-5-yl))diacetate (**3**) (3.89 g, 11.6 mmol) was dissolved in sulfuric acid (conc., 25 mL) and nitric acid (fuming, 4.2 mL) was added dropwise at 0 °C. The mixture was allowed to warm to room temperature, stirred for 2 h and subsequently poured on ice. The precipitate was collected by filtration, washed with water and dried at 60 °C to yield diethyl-2,2'-(3,3'-azo-bis(1H-1,2,4-triazol-5-yl))2,2'-dinitro-diacetate (**4**) as yellow solid (4.92 g, 9.5 mmol, 82 %). **¹H NMR** (DMSO-*d*₆): δ = 4.48 (q, $^3J_{\text{HH}}$ = 7.15 Hz, 2H, CH₂-CH₃), 1.30 (t, $^3J_{\text{HH}}$ = 7.15 Hz, 3H, CH₂-CH₃) ppm. **¹³C{¹H} NMR** (DMSO-*d*₆): δ = 162.8 (C=O), 156.4 (C_{Triazol}), 151.8 (C_{Triazol}), 114.0 (CH₂-CH₃), 67.5 (CH₂-C=O), 14.0 (CH₂-CH₃) ppm. **¹⁴N NMR** (DMSO-*d*₆): δ = -23 ppm. **IR**: ν (cm⁻¹) (rel. int.) = 3182 (w), 2360 (w), 2340 (w), 1766 (s), 1720 (w), 1588 (vs), 1444 (w), 1372 (w), 1348 (w), 1302 (m), 1256 (s), 1182 (m), 1106 (s), 1018 (m), 1000 (m), 966 (m), 854 (w), 834 (m), 804 (s), 772 (m), 754 (m), 624 (w). **Raman** (200 mW): ν (cm⁻¹) (rel. int.) = 2983 (2), 2948 (3), 1769 (2), 1721 (3), 1599 (2), 1494 (63), 1448 (17), 1413 (74), 1354 (100), 1177 (20), 1112 (8), 1025 (2), 972 (2), 921 (16), 857 (4), 803 (2), 371 (4), 323 (3). **Sensitivities** (grain size: 100–500 μ m): friction: 360 N, impact: 10 J.

3,3'-Bis(dinitromethyl)-5,5'-azo-1H-1,2,4-triazole (5)

Diethyl-2,2'-(3,3'-azo-bis(1H-1,2,4-triazol-5-yl))2,2'-dinitro-diacetate (**4**) (3.53 g, 6.8 mmol) was dissolved in an aqueous solution of sodium hydroxide (2m, 30 mL) and stirred at room temperature for 2 h. The solution was subsequently acidified under gas evolution with concentrated hydrochloric acid to pH = 1. The precipitate was collected by filtration, washed with ice water and dried at 60 °C to yield 3,3'-bis(dinitromethyl)-5,5'-azo-1H-1,2,4-triazole (**5**) as yellow solid (2.33 g, 6.3 mmol, 92%). **¹H NMR** (DMSO-*d*₆): δ = 14.64 (H_{Triazol}) ppm. **¹³C{¹H} NMR** (DMSO-*d*₆): δ = 169.7 (C_{Triazol}), 149.7 (C_{Triazol}), 124.9 (C(NO₂)₂) ppm. **¹⁴N NMR** (DMSO-*d*₆): δ = -23 ppm. **IR**: ν (cm⁻¹) (rel. int.) = 3610 (vw), 3234 (w), 2360 (vw), 2342 (vw), 1654 (vw), 1542 (m), 1438 (m), 1362 (w), 1348 (w), 1268 (m), 1212 (vs), 1184 (m), 1138 (m), 1122 (m), 1094 (s), 1036 (w), 986 (w), 830 (w), 768 (m), 744 (m), 692 (w). **Raman** (200 mW): ν (cm⁻¹) (rel. int.) = 1541 (16), 1487 (45), 1462 (100), 1413 (44), 1387 (56), 1363 (34), 1337 (88), 1308 (9), 1292 (11), 1233 (14), 1185 (38), 1142 (3), 1104 (7), 1042 (4), 983 (32), 919 (15), 827 (8), 778 (4), 479 (5), 370 (3), 305 (1). **Elemental analysis** (C₆H₄N₁₂O₈): calc.: C 19.36,

H 1.08, N 45.16; found: C 20.33, H 1.13, N 43.77. **DSC** (onset, 5 °C min⁻¹): T_{Dec.}: 80 °C. **Sensitivities** (grain size: 100–500 µm): friction: 360 N, impact: 4 J, ESD: 0.15 J.

Sodium 3,3'-bis(dinitromethyl)-5,5'-azo-1H-1,2,4-triazolate (6)

A solution of sodium hydroxide (0.25 m, 6.4 mL, 1.6 mmol), was added to a solution of 3,3'-bis(dinitromethyl)-5,5'-azo-1H-1,2,4-triazole (0.30 g, 0.8 mmol) in ethanol (50 mL). The precipitate was collected by filtration, washed with ethanol and dried at 60 °C to yield sodium 3,3'-bis(dinitromethyl)-5,5'-azo-1H-1,2,4-triazolate (**6**) as yellow solid (0.26 g, 0.6 mmol, 78%). ¹³C{¹H} **NMR** (DMSO-d₆): δ = 170.6 (C_{Triazol}), 153.8 (C_{Triazol}), 128.3 (C(NO₂)₂) ppm. ¹⁴N **NMR** (DMSO-d₆): δ = -23 ppm. **IR**: ν (cm⁻¹) (rel. int.) = 3484(w), 3325(w), 1632(w), 1517(m), 1450(m), 1427(m), 1388(w), 1366(m), 1204(vs), 1150(s), 1131(vs), 1083(m), 1060(w), 1030(w), 1003(m), 985(w), 835(w), 783(w), 760(m), 755(m), 745(m), 686(vw). **Raman** (200 mW): ν (cm⁻¹) (rel. int.) = 1611(4), 1564(6), 1557(6), 1523(12), 1460(82), 1449(81), 1427(30), 1395(39), 1353(100), 1335(70), 1310(95), 1269(4), 1256(4), 1224(10), 1197(8), 1182(12), 1131(81), 1075(8), 1065(7), 1008(11), 985(16), 937(17), 925(15), 925(15), 832(10), 782(4), 473(5), 457(5), 452(5), 411(4), 361(5). **DSC** (onset, 5 °C min⁻¹): T_{Dec.}: 209 °C. **Sensitivities** (grain size: 100–500 µm): friction: 360 N, impact: 40 J, ESD: 0.5 J.

REFERENCES

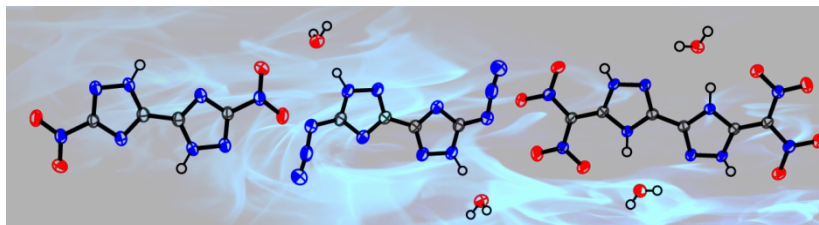
- [1] a) T. M. Klapötke, *Chemistry of high-energy materials*, De Gruyter, Berlin, **2011**;
b) T. M. Klapötke, *Chemie der hochenergetischen Materialien*, de Gruyter, Berlin, **2009**.
- [2] P. F. Pagoria, G. S. Lee, A. R. Mitchell, R. D. Schmidt, *Thermochim. Acta* **2002**, 384, 187.
- [3] T. M. Klapötke, in *High energy density materials. Structure and bonding* (Ed.: D. M. P. Mingos), Springer-Verlag, Berlin Heidelberg **2007**.
- [4] a) B. C. Tappan, A. N. Ali, S. F. Son, T. B. Brill, *Propell., Explos., Pyro.* **2006**, 31, 163; b) R. Sivabalan, M. B. Talawar, N. Senthilkumar, B. Kavitha, S. N. Asthana, *J. Therm. Anal. Calorim.* **2004**, 78, 781.
- [5] M. A. Hiskey, N. Goldman, J. R. Stine, *J. Energ. Mat.* **1998**, 16, 119.
- [6] D. E. Chavez, B. C. Tappan, 8-ISICP, Los Alamos National laboratory, **2009**.
- [7] C. M. Sabate, T. M. Klapoetke, *New Trends Res. Energ. Mater., Proc. Semin., 12th* **2009**, 172.
- [8] a) D. E. Chavez, M. A. Hiskey, R. D. Gilardi, *Angew. Chem.* **2000**, 112, 1861; *Angew. Chem. Int. Ed.* **2000**, 39, 1791; b) D. Chavez, L. Hill, M. Hiskey, S. Kinkead, *J. Energ. Mat.* **2000**, 18, 219; c) T. M. Klapoetke, C. M. Sabate, *New J. Chem.* **2009**, 33, 1605; d) T. M. Klapoetke, C. M. Sabate, *Chem. Mater.* **2008**, 20, 1750; e) A. Hammerl, G. Holl, T. M. Klapoetke, P. Mayer, H. Noth, H. Piotrowski, M. Warchhold, *Eur. J. Inorg. Chem.* **2002**, 834; f) D. L. Naud, M. A. Hiskey, H. H. Harry, *J. Energ. Mat.* **2003**, 21, 57.
- [9] a) T. M. Klapötke, F. X. Steemann, *Propell., Explos., Pyro.* **2010**, 35, 114; b) V. Thottempudi, H. Gao, J. M. Shreeve, *J. Am. Chem. Soc.* **2011**, 133, 6464.
- [10] a) T. P. Kofman, T. A. Uvarova, G. Y. Kartseva, *Zhurnal Organicheskoi Khimii* **1995**, 31, 270; b) V. Chernyshev, A. Chernysheva, V. Taranushich, *Russ. J. Appl. Chem.* **2009**, 82, 276.
- [11] N. Biswas, S. Umapathy, *J. Phys. Chem. A* **2000**, 104, 2734.
- [12] F. H. Allen, O. Kennard, D. G. Watson, L. Brammer, A. G. Orpen, R. Taylor, *J. Chem. Soc., Perkin Trans. 2* **1987**, S1.
- [13] *Calculation of oxygen balance: Ω (%) = $(wO - 2xC - 1/2yH - 2zS)1600/M$. (w: number of oxygen atoms, x: number of carbon atoms, y: number of hydrogen atoms, z: number of sulfur atoms, M: molecular weight).*

- [14] J. Köhler, R. Meyer, *Explosivstoffe*, Vol. 9th edition, Wiley-VCH, Weinheim, **1998**.
- [15] D. E. Chavez, B. C. Tappan, B. A. Mason, D. Parrish, *Propell., Explos., Pyro.* **2009**, 34, 475.
- [16] *CrysAlis CCD*, Oxford Diffraction Ltd., Version 1.171.27p5 beta (release 01-04-2005 *CrysAlis171.NET*).
- [17] *CrysAlis RED*, Oxford Diffraction Ltd., Version 1.171.27p5 beta (release 01-04-2005 *CrysAlis171.NET*).
- [18] G. M. Sheldrick, *SHELXL-97, Program for the Refinement of Crystal Structures*. University of Göttingen, Germany, **1997**.
- [19] L. Farrugia, *J. Appl. Crystallogr.* **1999**, 32, 837.
- [20] A. L. Spek, *Platon, A Multipurpose Crystallographic Tool*, Utrecht University, Utrecht, The Netherlands, **1999**.
- [21] *Crystallographic data for the structure(s) have been deposited with the Cambridge Crystallographic Data Centre. Copies of the data can be obtained free of charge on application to The Director, CCDC, 12 Union Road, Cambridge CB2 1EZ, UK (Fax: int.code (1223)336-033; e-mail for inquiry: fileserv@ccdc.cam.ac.uk; e-mail for deposition: deposit-@ccdc.cam.ac.uk).*
- [22] T. Altenburg, Thomas M. Klapötke, A. Penger, J. Stierstorfer, *Z. Anorg. Allg. Chem.* **2010**, 636, 463.
- [23] G. W. T. M. J. Frisch, H. B. Schlegel, G. E. Scuseria, , J. R. C. M. A. Robb, J. A. Montgomery, Jr., T. Vreven, , J. C. B. K. N. Kudin, J. M. Millam, S. S. Iyengar, J. Tomasi, , B. M. V. Barone, M. Cossi, G. Scalmani, N. Rega, , H. N. G. A. Petersson, M. Hada, M. Ehara, K. Toyota, , J. H. R. Fukuda, M. Ishida, T. Nakajima, Y. Honda, O. Kitao, , M. K. H. Nakai, X. Li, J. E. Knox, H. P. Hratchian, J. B. Cross, , C. A. V. Bakken, J. Jaramillo, R. Gomperts, R. E. Stratmann, , A. J. A. O. Yazyev, R. Cammi, C. Pomelli, J. W. Ochterski, , K. M. P. Y. Ayala, G. A. Voth, P. Salvador, J. J. Dannenberg, , S. D. V. G. Zakrzewski, A. D. Daniels, M. C. Strain, , D. K. M. O. Farkas, A. D. Rabuck, K. Raghavachari, , J. V. O. J. B. Foresman, Q. Cui, A. G. Baboul, S. Clifford, , B. B. S. J. Cioslowski, G. Liu, A. Liashenko, P. Piskorz, , R. L. M. I. Komaromi, D. J. Fox, T. Keith, M. A. Al-Laham, , A. N. C. Y. Peng, M. Challacombe, P. M. W. Gill, , W. C. B. Johnson, M. W. Wong, C. Gonzalez, and J. A. Pople, *Gaussian 03, Revision D.01*, Gaussian Inc., Wallingford, CT, **2004**.

- [24] a) H. D. B. Jenkins, H. K. Roobottom, J. Passmore, L. Glasser, *Inorg. Chem.* **1999**, 38, 3609; b) H. D. B. Jenkins, D. Tudela, L. Glasser, *Inorg. Chem.* **2002**, 41, 2364.

5. NITROGEN-RICH BIS-1,2,4-TRIAZOLES –A COMPARATIVE STUDY OF STRUCTURAL AND ENERGETIC PROPERTIES

As published in: *Chemistry – A European Journal* **2012**, 18(52), 16742–16753.



ABSTRACT:

In this contribution the synthesis and full structural and spectroscopic characterization of five bis-1,2,4-triazoles in combination with different energetic moieties like amino, nitro, nitrimino, azido and dinitromethylene groups is presented. The main goal is a comparative study on the influence of those energetic moieties on structural and energetic properties. A complete characterization including IR and Raman as well as multinuclear NMR spectroscopy of all compounds is presented. Additionally, X-ray crystallographic measurements were performed and deliver insight into structural characteristics as well as inter- and intramolecular interactions. The standard enthalpies of formation were calculated for all compounds at the CBS-4M level of theory, the detonation parameters were calculated using the EXPLO5.05 program. Additionally, the impact as well as friction sensitivities and sensitivity against electrostatic discharge were determined. The potential application of the synthesized compounds as energetic material will be studied and evaluated using the experimentally obtained values for the thermal decomposition, the sensitivity data, as well as the calculated performance characteristics.

INTRODUCTION

The synthesis of energetic materials that combine high performance and low sensitivities has attracted worldwide research groups over the last decades.^[1] Nitrogen-rich heterocycles are promising compounds that fulfill many requirements in the challenging field of energetic materials research.^[1f, 2] A prominent family of novel high-energy-density materials (HEDMs) are azole-based compounds, since they are generally highly endothermic with high densities and low sensitivities towards outer stimuli. Owing to the

high positive heats of formation resulting from the large number of N–N and C–N bonds^[3] and the high level of environmental compatibility, those compounds have been studied in our group over the last couple of years with growing interest. Especially 1,2,4-triazoles show a perfect balance between thermal stability and high positive heats of formation, required for applications as prospective HEDMs.

Many energetic compounds that combine the 1,2,4-triazole backbone with energetic moieties have been synthesized over the last decades. Examples for these kind of molecules are 5-amino-3-nitro-1,2,4-triazole (ANTA),^[4] 2-azido-5-nitramino-1,2,4-triazole^[5] or trinitromethyl-substituted 1,2,4-triazoles^[6]. Bridged compounds like 5,5'-dinitro-3,3'-azo-1,2,4-triazole (DNAT)^[7] or the analogue nitrimino-compound (DNAAT)^[8] have already been investigated and show remarkably high decomposition temperatures and excellent energetic properties.

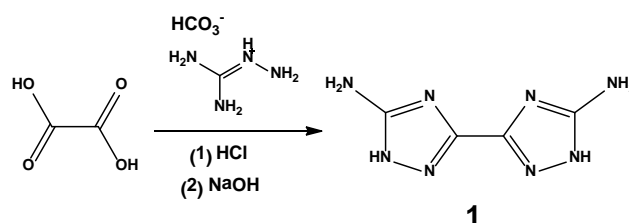
Bis-1,2,4-triazoles connected via C–C bond are expected to show similar energetic properties in comparison to azo-bridged 1,2,4-triazole compounds and with regard to the outstanding properties of 5,5'-bistetrazoles^[9]. Different synthetic pathways towards 5,5'-dinitrimino-3,3'-bis-1,2,4-triazole have been intensively investigated by Russian scientists^[10], the sensitivities (time to explosion delay, impact sensitivity) were first investigated by Astachov *et al.*^[11]. Shreeve and Charlesworth determined the energetic properties of the nitrogen-rich salts and the crystal structure of the neutral compound.^[12] 3,3'-Dinitro-5,5'-bis-1,2,4-triazole has been mentioned in literature before, but only characterized by means of ultraviolet absorption and infrared spectroscopy.^[13]

The focus of this contribution is on the full structural and spectroscopic characterization of five different bis-1,2,4-triazoles carrying energetic moieties like amino, nitro, nitramino, azido and dinitromethyl groups. We present a comparative study on the influence of those energetic moieties on structural and energetic properties. The potential application of the synthesized compounds as energetic material will be studied and evaluated using the experimentally obtained values for the thermal decomposition, the sensitivity data, as well as the calculated performance characteristics.

RESULTS AND DISCUSSION

SYNTHESIS

The starting material 3,3'-diamino-5,5'-bis(1*H*-1,2,4-triazole) (DABT, **1**) was first synthesized with a moderate yield of 56% by Shreve and Charlesworth.^[14] We developed a straightforward synthetic procedure yielding DABT as elemental analysis pure compound in yields of up to 70%. The modified procedure starts with the reaction of oxalic acid and aminoguanidinium bicarbonate in concentrated hydrochloric acid at 70 °C, followed by isolation of the intermediate product by filtration. While heating under reflux in basic media, the molecule undergoes cyclization which leads to the formation of DABT (Scheme 1).

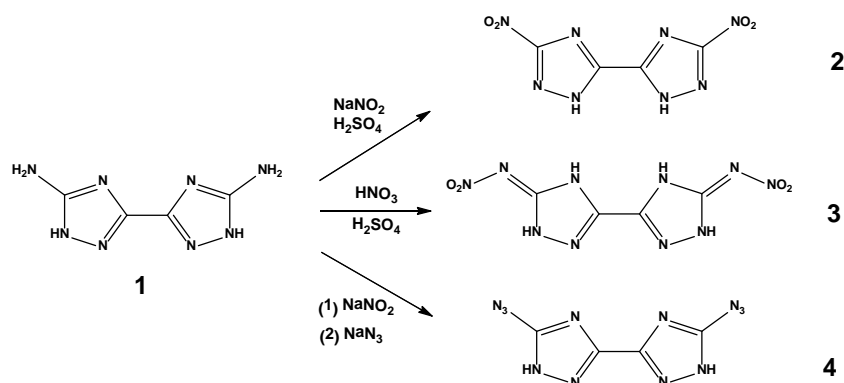


Scheme 1: Synthesis of DABT (**1**).

As shown in Scheme 2, oxidation of DABT was achieved by the well known Sandmeyer reaction via diazotization in sulfuric acid and subsequent reaction with sodium nitrite.^[15] The formation of 3,3'-dinitro-5,5'-bis(1*H*-1,2,4-triazole) (DNBT, **2**) was first mentioned by russian scientists with a low yield of 31%.^[13b] We were able to optimize the process by adding a suspension of DABT in 20% sulfuric acid to a solution of sodium nitrite in water at 40 °C, which leads to a remarkable increase of the yield up to 82%.

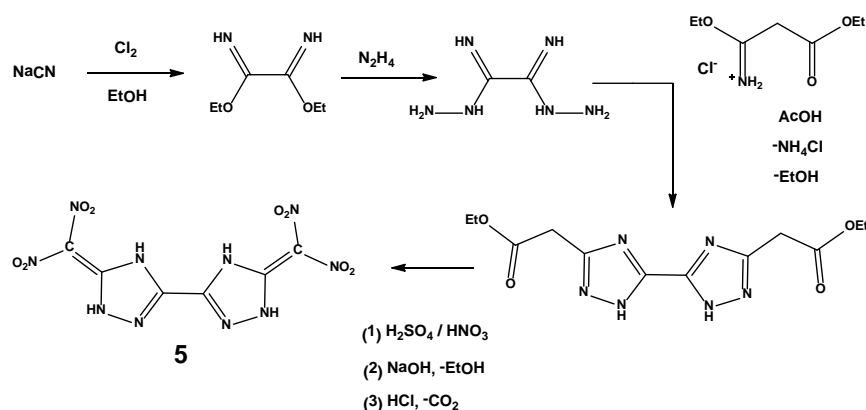
The nitrimino compound (**3**) was first synthesized by Metelkina *et al.* using oxalic acid dihydrazide and 2-nitroguanidine,^[10a] using 1-amino-2-nitroguanidine with oxalic acid^[10b] or 1-methyl-2-nitro-1-nitrosoguanidine and oxalic acid dihydrazide^[10c]. We followed the most efficient method first mentioned by Astachov *et al.*^[11] starting from the amino compound **1**. The nitration was optimized using concentrated sulfuric and nitric acid in a ratio of 3:1 resulting in a yield of 77%.

The azido compound (**4**) was synthesized via diazotization in sulfuric acid and subsequent reaction with an excess of sodium azide. After recrystallisation from water, compound **4** can be isolated as insensitive dihydrate.



Scheme 2: Synthesis of energetic bis-1,2,4-triazole derivatives **2–4** based on DABT (**1**).

The synthesis of the dinitromethyl-bis1,2,4-triazole (**5**, DNMBT) was achieved via a completely different synthetic pathway (Scheme 3). The chlorination of sodium cyanide in ethanol and subsequent reaction with hydrazine leads to the formation of the oxalimidohydrazide.^[16] This intermediate product was reacted with the commercially available 3-ethoxy-3-iminopropionic acid ethyl ester hydrochloride to form the 3,3'-(diethyl acetate)-5,5'-bis-1,2,4-triazole. Introduction of the NO_2 -moieties was accomplished by nitration with nitric acid in a mixture of sulfuric acid and oleum (1:1). The ethyl ester hydrolyses rapidly while stirring the nitrated intermediate product in basic media and subsequent acidification with concentrated hydrochloric acid leads to the release of CO_2 and the formation of 3,3'- dinitromethyl-5,5'-bis-1,2,4-triazole (**5**).



Scheme 3: Synthetic pathway towards DNMBT (**5**).

All nitrogen-rich bis-1,2,4-triazoles (**1–5**) were fully characterized by IR and Raman as well as multinuclear NMR spectroscopy, mass spectrometry and differential scanning calorimetry. Additional X-ray crystallographic measurements deliver insight into inter- and intramolecular interactions.

CRYSTAL STRUCTURES:

Single crystal X-ray measurements were accomplished for compounds **1**, **2**, **4** and **5** and are discussed in detail. The crystal structure of the nitrimino compound **3** has already been described in literature.^[12] All compounds could only be recrystallized from water resulting in the formation of the dihydrate as crystalline species, only compound **2** could be obtained water free.

Detailed examination of the crystal structures of all compounds, no difference is observed for the 1,2,4-triazole system in comparison to other triazole ring systems.^[7, 17] The bond lengths within the 1,2,4-triazole ring in the molecular structures are all in between the length of formal C–N and N–N single and double bonds (C–N: 1.47 Å, 1.22 Å; N–N: 1.48 Å, 1.20 Å).^[18]

Due to the very low solubility in any solvent, crystals of 5,5'-diamino-3,3'-bis-(1*H*-1,2,4-triazole) (**1**) could only be obtained by recrystallisation from DMSO. Compound **1** crystallizes as DMSO adduct in the monoclinic space group *P*2₁/*c* with a cell volume of 750.55(14) Å³ and two molecular moieties in the unit cell, the crystal structure together with the labeling scheme is displayed in Figure 1.

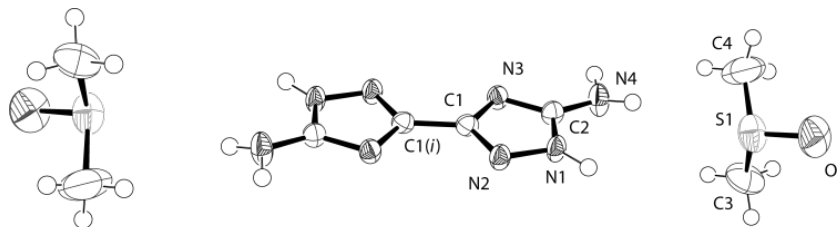


Figure 1: Crystal structure of DABT (**1**), only one orientation of disordered DMSO molecules is shown; Thermal ellipsoids are set to 50 % probability, symmetry: (i) 2-*x*, -*y*, 1-*z*.

As expected, the bis-triazole moiety shows a completely planar assembly. In relation to the planar 1,2,4-triazole ring, the protons of the amine groups are twisted out of the plane by only 26.1°. The angles surrounding the nitrogen N4 are larger than expected for a sp³-atom in the range of 116(1)° (C2–N4–H5a) to 118(1)° (C2–N4–H5b), which could be a reason for the low nucleophilicity observed in reactions with compound **1**.

It is remarkable to note that all nitrogen atoms of the 1,2,4-triazole ring as well as the amine group participate in hydrogen bonds. All contacts are short with a D⋯A length of 2.890(2) Å and 3.055(2) Å, but only the hydrogen bond N1–H1⋯N3 is strongly directed with a D–H⋯A angle of 170.8(17)° (Table 1).

Table 1: Hydrogen bonds present in **1**.

D–H···A	d (D–H) [Å]	d (H···A) [Å]	d (D–H···A) [Å]	< (D–H···A) [°]
N1–H1···N3 ⁱ	0.881(18)	2.017(19)	2.890(2)	170.8(17)
N4–H5a···N2 ⁱⁱ	0.867(19)	2.25(2)	3.055(2)	154.9(18)

Symmetry Operators: (i) $x, 3/2-y, 1/2+z$, (ii) $-x, 1/2+y, 1/2-z$.

All hydrogen bond lengths lie well within the sum of van der Waals radii ($r_w(\text{N}) + r_w(\text{N}) = 3.20 \text{ Å}$)^[18a], resulting in a strong network of hydrogen bonds in the *bc*-plane (Figure 2). The DMSO molecules do not participate in hydrogen bonds within this plane, but connect the layers via interaction with the free hydrogen atom of the amine groups.

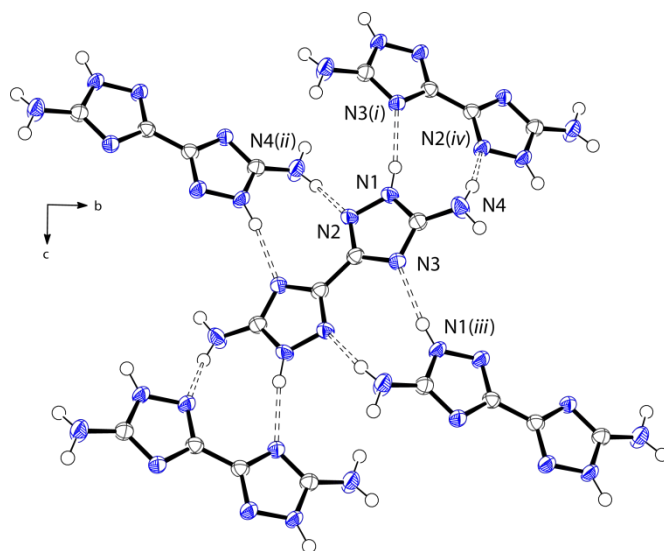


Figure 2: Hydrogen bonding within the crystal structure of DABT (**1**), DMSO molecules are omitted for clarity since they do not participate in hydrogen bonds in the *bc*-plane; Thermal ellipsoids are set to 50 % probability; symmetry: (i) $x, 1/2-y, -1/2+z$, (ii) $2-x, -1/2+y, 1/2-z$, (iii) $x, 1/2-y, 1/2+z$, (iv) $2-x, 1/2+y, 1/2-z$.

3,3'-Dinitro-5,5'-bis-(1*H*-1,2,4-triazole) (**2**) crystallizes in the monoclinic space group $P2_1/n$ with a cell volume of $394.73(8) \text{ Å}^3$ and one molecular moiety in the unit cell. The calculated density at 173 K is 1.902 g cm^{-3} and hence well above the density of the dihydrate (1.764 g cm^{-3})^[17c]. Again, the molecule shows a completely planar assembly with a torsion angle of the nitro group towards the triazole ring of $2.9(2)^\circ$. The formula unit of **1** together with the atom labeling is presented in Figure 3.

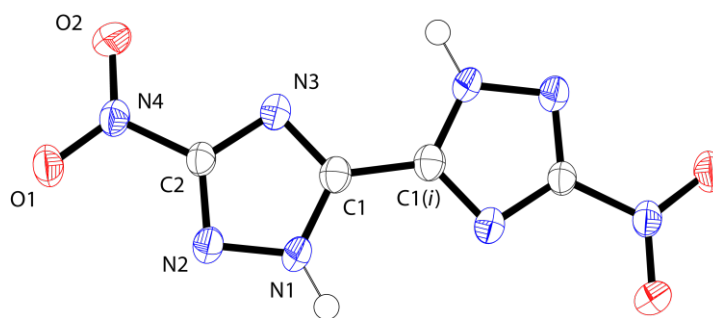


Figure 3: Crystal structure of **2**. Thermal ellipsoids are set to 50 % probability. Symmetry operators: (i) $-x$, $1-y$, $2-z$.

In contrast to compound **1**, the structure is build up by only one individual hydrogen bond $N_1-H_1\cdots O_1$. The $D-H\cdots A$ angle is close to 180° with $171.9(2)^\circ$ and the $D\cdots A$ length is shorter than the sum of van der Waals radii ($r_w(O) + r_w(N) = 3.07 \text{ \AA}$)^[18a] with $2.902(2) \text{ \AA}$ (Figure 4a). In contrast to compound **1**, the nitrogen atoms N2 and N3 do not participate as acceptor in any hydrogen bond. As shown in Figure 4, the crystal structure of **3** consists of infinite zig-zag rows along the b -axis including an angle of 60.5° . The layers are stacked above each other with a layer distance of $d = 2.96 \text{ \AA}$. The layers are connected by two short contacts, $N_2\cdots N_4(ii)$ and $C_1\cdots O_1(iii)$ (symmetry operators: (ii) $3/2-x, 1/2+y, 1/2-z$; (iii) $3/2-x, -1/2+y, 1/2-z$). Both contacts are shorter than the sum of van der Waals radii^[18a], with $N_2\cdots N_4$ being the shortest ($2.922(2) \text{ \AA}$) and $C_1\cdots O_1$ being the longest ($3.051(2) \text{ \AA}$). The stacking of the layers is displayed in Figure 4b together with the distance d between the layers.

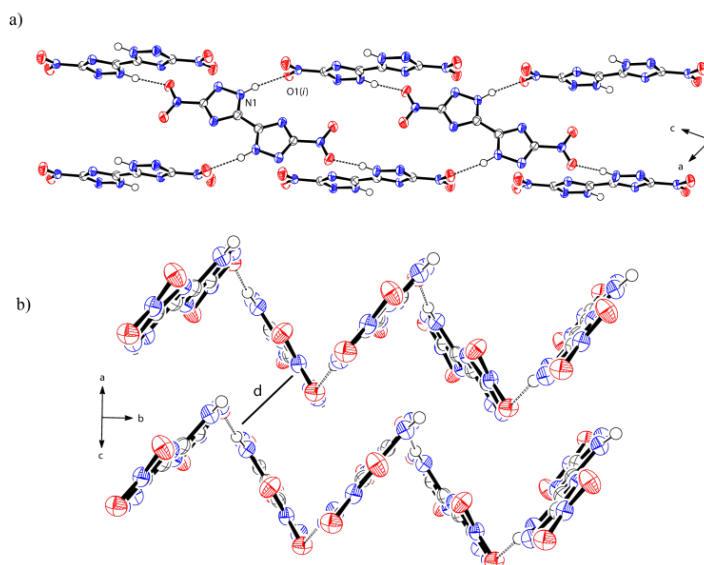


Figure 4: a) Hydrogen bonding scheme in the crystal structure of **2**. b) Wave-like arrangement of the infinite rows in the crystal structure of **2** (layer distance $d = 2.96 \text{ \AA}$). Thermal ellipsoids are set to 50 % probability. Symmetry Operators: (i) $1/2+x$, $1/2-y$, $1/2+z$.

The azido-compound **4** crystallizes in the triclinic space group $P\bar{1}$ with a cell volume of $256.34(9) \text{ \AA}^3$ and one molecular moiety in the unit cell, the calculated density for the dihydrate is 1.646 g cm^{-3} . As shown in Figure 5, the proton is located at the nitrogen atom N1 next to the azido group and not next to the C–C bond as it is the case for the nitro-compound **2**. The three nitrogen atoms of the azido group exhibit a slightly bent arrangement with a $\text{N}_4\text{--N}_5\text{--N}_6$ angle of $172.34(17)^\circ$. Both azido moieties are assembled parallel and point in the opposite direction.

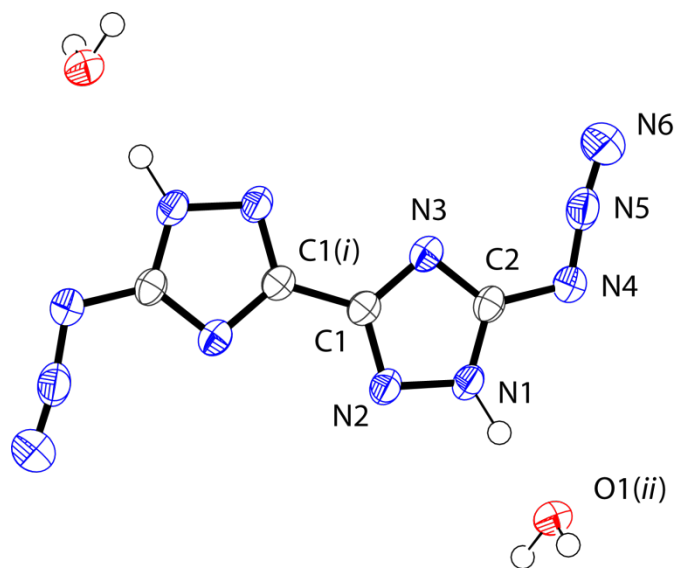


Figure 5: Crystal structure of **4**. Thermal ellipsoids are set to 50 % probability. Symmetry operators: (i) $1-x, 1-y, 2-z$, (ii) $-x, 1-y, 1-z$.

The crystal structure of compound **4** is build up by two individual hydrogen bonds including the nitrogen atoms N1 and N2 as well as two water molecules (Figure 6). Two molecules of **4** form pairs via the strong hydrogen bond $\text{N}_1\text{--H}_1\cdots\text{O}_1(\text{i})$. As shown in Table 2, the $\text{D--H}\cdots\text{A}$ angle is close to 180° with $174(2)^\circ$ and the $\text{D}\cdots\text{A}$ length is considerably shorter than the sum of van der Waals radii ($r_w(\text{O}) + r_w(\text{N}) = 3.07 \text{ \AA}$)^[18a]

Table 2: Hydrogen bonds present in **4**.

$\text{D--H}\cdots\text{A}$	$d(\text{D--H}) [\text{\AA}]$	$d(\text{H}\cdots\text{A}) [\text{\AA}]$	$d(\text{D--H}\cdots\text{A}) [\text{\AA}]$	$\angle(\text{D--H}\cdots\text{A}) [^\circ]$
$\text{N1--H1}\cdots\text{O1}^{\text{i}}$	0.98(2)	1.70(2)	2.676(2)	174(2)
$\text{O1--H1b}\cdots\text{N2}^{\text{ii}}$	0.92(2)	1.98(2)	2.892(2)	174(2)

Symmetry Operators: (i) $x, 1+y, z$, (ii) $2-x, 1-y, -z$.

The individual pairs are assembled coplanar which results in the formation of a layered structure within the *bc*-plane. The azido moieties do not participate in any hydrogen bond but are connected via a short contact $N_6 \cdots N_6(i)$ with a distance of 3.067(2) Å (symmetry code: (i) 1-*x*, -*y*, 1-*z*).

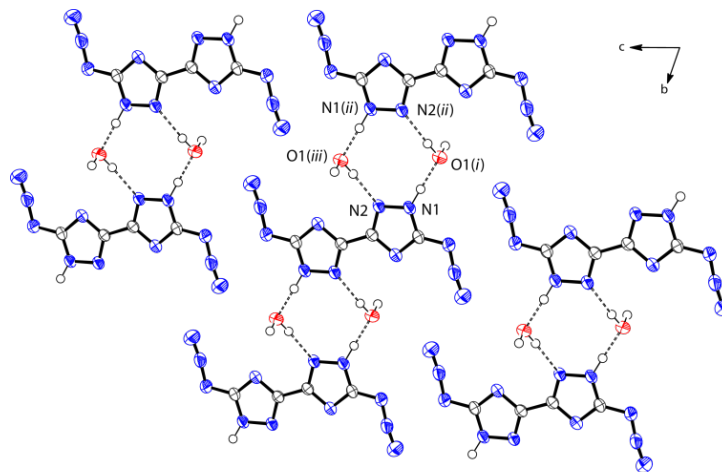


Figure 6: Hydrogen bonding scheme in the crystal structure of **4**. Thermal ellipsoids are set to 50 % probability. Symmetry Operators: (i) -*x*, 1-*y*, 1-*z*, (ii) -*x*, -*y*, 2-*z*, (iii) *x*, -1+*y*, 1+*z*.

3,3'-Dinitromethyl-5,5'-bis-1,2,4-triazole crystallizes as dihydrate in the monoclinic spacegroup $P2_1/c$, the formula unit of **5** together with the atom labeling is presented in Figure 7. In comparison to all other bis-1,2,4-triazoles, the density of compound **5** is remarkably high with 1.951 g cm⁻³.

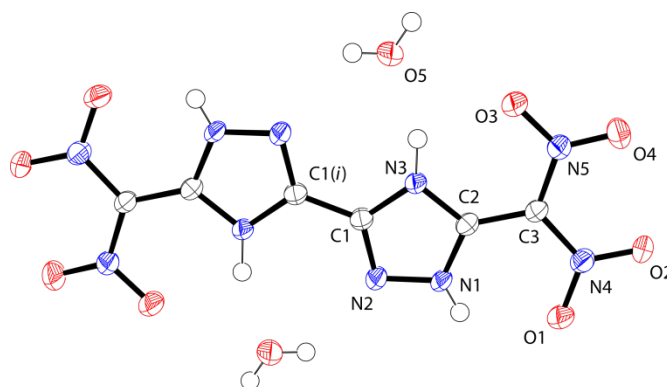


Figure 7: Crystal structure of **5**. Thermal ellipsoids are set to 50 % probability. Symmetry operators: (i) 1-*x*, 1-*y*, -*z*.

In contrast to the previously described 3,3'-bis(dinitro-methyl)-5,5'-azo-1*H*-1,2,4-triazole^[19], the proton of the dinitromethyl moiety is not located at the carbon atom C3 but at the nitrogen atom N3 within the triazole ring. This leads to a completely planar assembly typical for sp² carbon atoms and a C2–C3 distance in the range of a C–C double

bond (1.440(2) Å)^[18a]. For comparison, the C–C bond in the similar 5-dinitromethylene-4,5-dihydro-1*H*-tetrazole is 1.418(2) Å.^[20] The nitro groups are twisted out of the triazole plane by only 6.5(2) ° (O₁–N₄–C₃–C₂) and 0.9(2) ° (O₃–N₅–C₃–C₂), respectively. The planar assembly is encouraged by the formation of two intramolecular hydrogen bonds N₁–H₁···O₁ and N₃–H₃···O₃. Both interactions show rather small D–H···A angles of 117.9(16) ° and 113(2) ° but considerably short D–H···A distances of 2.558(2) Å and 2.603(2) Å. The hydrogen bonds within the crystal structure of compound **5** are summarized in Table 3.

Table 3: Hydrogen bonds present in **5**.

D–H···A	d (D–H) [Å]	d (H···A) [Å]	d (D–H···A) [Å]	< (D–H···A) [°]
N1–H1···O1	0.79(2)	2.090(18)	2.558(2)	117.9(16)
N1–H1···O2 ⁱ	0.79(2)	2.11(2)	2.839(2)	152.6(18)
N3–H3···O3	0.92(3)	2.10(3)	2.603(2)	113(2)
N3–H3···O5 ⁱⁱ	0.92(3)	1.83(3)	2.711(2)	160(2)
O5–H5b···O3 ⁱⁱⁱ	0.80(3)	2.09(3)	2.883(2)	173(3)

Symmetry Operators: (i) $-x, 1/2+y, 1/2-z$, (ii) $1-x, 1-y, -z$, (iii) $-1+x, 1+y, z$.

In addition to the intramolecular hydrogen bonds, three intermolecular interactions including the crystal water as well as the oxygen atoms O2 and O3 of the nitro groups could be observed. Both nitrogen atoms N1 and N3 are involved as donor atoms in further hydrogen bonds N₁–H₁···O₂ and N₃–H₃···O₅, resulting in strong interactions with surrounding molecules (Figure 8).

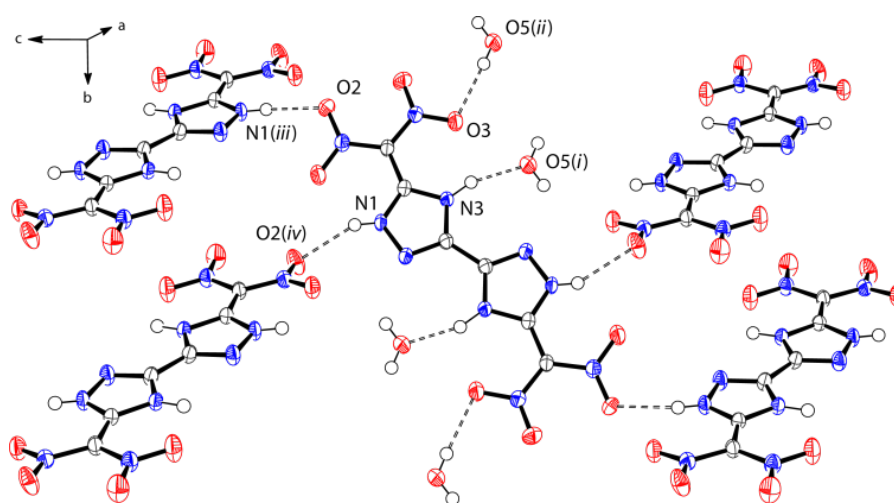


Figure 8: Surrounding and hydrogen bonds of a DNMBT molecule in the crystal structure of **5**. Thermal ellipsoids are set to 50 % probability. Symmetry Operators: (i) $1-x, 1-y, -z$; (ii) $1+x, -1+y, z$; (iii) $-x, -1/2+y, 1/2-z$, (iv) $-x, 1/2+y, 1/2-z$.

SPECTROSCOPIC DATA

Vibrational spectroscopy

IR and Raman spectra of all compounds were recorded and the frequencies were assigned according to literature.^[21] The Raman spectrum of compound **1** is dominated by the deformation mode of the amino groups at 1579 cm^{-1} . The valence stretching mode of the N–H bond is observed in the range of 3116 cm^{-1} to 3107 cm^{-1} . The nitro groups of compounds **2** and **5** are observed with both, their symmetric and asymmetric stretching modes. The vibrational frequencies for the asymmetric stretching mode of the nitro group are observed in the range of 1550 cm^{-1} (**2**) to 1568 cm^{-1} (**5**). The symmetric stretching modes are located at lower energy at 1410 cm^{-1} (**2**) and 1403 cm^{-1} (**5**). The signals of the nitrmino moiety of compound **3** can be observed at 1565 cm^{-1} (ν_{asym}) and 1298 cm^{-1} (ν_{sym}). The valence stretching mode of the N–H bond of the 1,2,4-triazole ring can be observed for all compounds in the range of 3154 cm^{-1} (**3**) to 3190 cm^{-1} (**2**). In addition, as for any heterocyclic compound, many combined stretching and deformation as well as torsion stretching modes can be observed in the fingerprint region between 1500 cm^{-1} and 600 cm^{-1} .^[21b] As shown in Figure 9, the Raman as well as IR spectrum of the azido compound **4** exhibits two signals for the individual asymmetric stretching modes of the azide groups in the expected range.^[21c] The bands for the different ‘in-phase’ and ‘out-of-phase’ stretching vibrations can be observed at 2171 cm^{-1} and 2142 cm^{-1} in the Raman spectrum and at 2156 cm^{-1} and 2137 cm^{-1} in the IR spectrum.

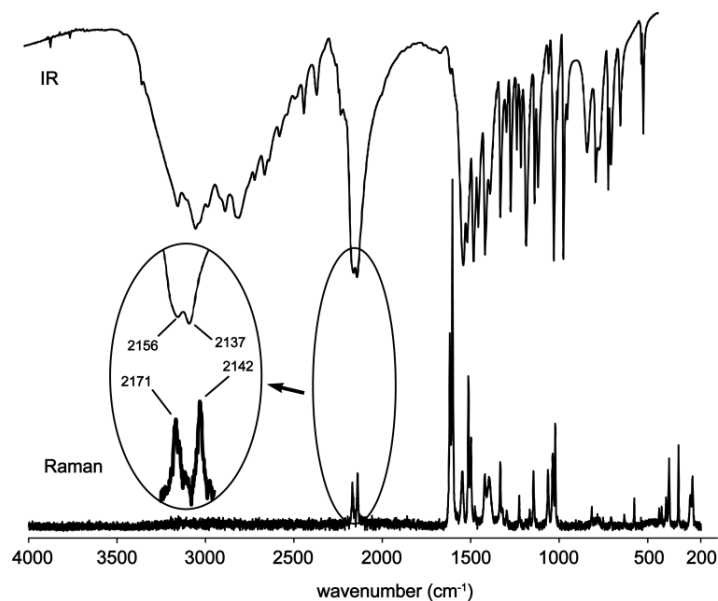


Figure 9: Comparison of the IR and Raman spectra of **4**. The individual stretching modes for the azide groups are expanded in the ellipse.

Multinuclear NMR spectroscopy

All compounds were investigated using ^1H , ^{13}C and ^{14}N NMR spectroscopy. Additional $^{13}\text{C}\{^1\text{H}\}$ and ^1H NMR spectra of compound **5** were recorded at elevated temperatures to give insight into the equilibrium between both possible isomers and will be discussed in the following paragraph. Due to insufficient solubility of compounds **1**, **3** and **5** in DMSO or any other solvent, ^{15}N NMR spectra could only be obtained for compounds **2** and **4**.

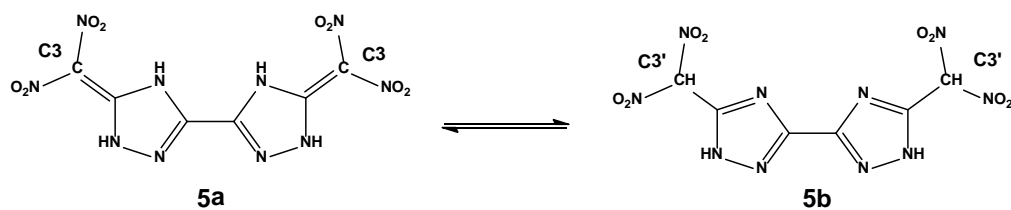
All compounds show two signals for the 1,2,4-triazole carbon atoms in the expected range.^[7-8] One singlet for the bridging carbon atom can be found at chemical shifts of 142.1(**3**) to 149.3 ppm (**1**). The signal of the carbon atom connected to the energetic moieties is shifted in all cases to lower field and is observed in the range of 151.1 (**5**) to 162.7 ppm (**2**). In the $^{14}\text{N}\{^1\text{H}\}$ NMR spectra, the nitro group of compounds **2**, **3** and **5** can be identified by a broad singlet at -21 (**3**) to -26 ppm (**2**). The azido moiety in compound **4** can be observed as a broad singlet at -145 ppm in the ^{14}N NMR spectrum, well resolved resonances could only be observed in the ^{15}N NMR spectrum (as discussed below). The NMR signals of all compounds are summarized in Table 4.

Table 4: NMR signals of compounds **2**, **3a–f** in DMSO- d_6 .

compound	δ [ppm]		
	$^{13}\text{C}\{^1\text{H}\}$	$^{14}\text{N}\{^1\text{H}\}$	^1H
1	157.3, 149.3	/	6.46
2	162.7, 145.6	-26	9.68
3	153.1, 142.1	-21	5.19
4	157.7, 145.9	-145	14.86
5	151.1 149.3*	-23	13.45, 8.91, 3.90

* recorded at 60 °C, $\text{C}(\text{NO}_2)_2$: 124.3 (**5a**), 106.5 (**5b**)

As mentioned before, the existence of different isomers of compound **5** (see Scheme 4) could be demonstrated by recording $^{13}\text{C}\{^1\text{H}\}$ and ^1H NMR spectra at elevated temperatures. Additionally, quantum chemical calculations at the B3LYP/aug-cc-pVDZ level of theory were performed.



Scheme 4: Equilibrium between the two isomers **5a** and **5b**.

Since isomer **5a** is obtained in the solid state (as discussed in the previous chapter), in this case a sp^2 carbon atom (C3) is the thermodynamically most stable configuration. However, the signals of both isomers could be observed in both the $^{13}\text{C}\{^1\text{H}\}$ and ^1H NMR spectrum at room temperature, indicating a small energy difference between both isomers.

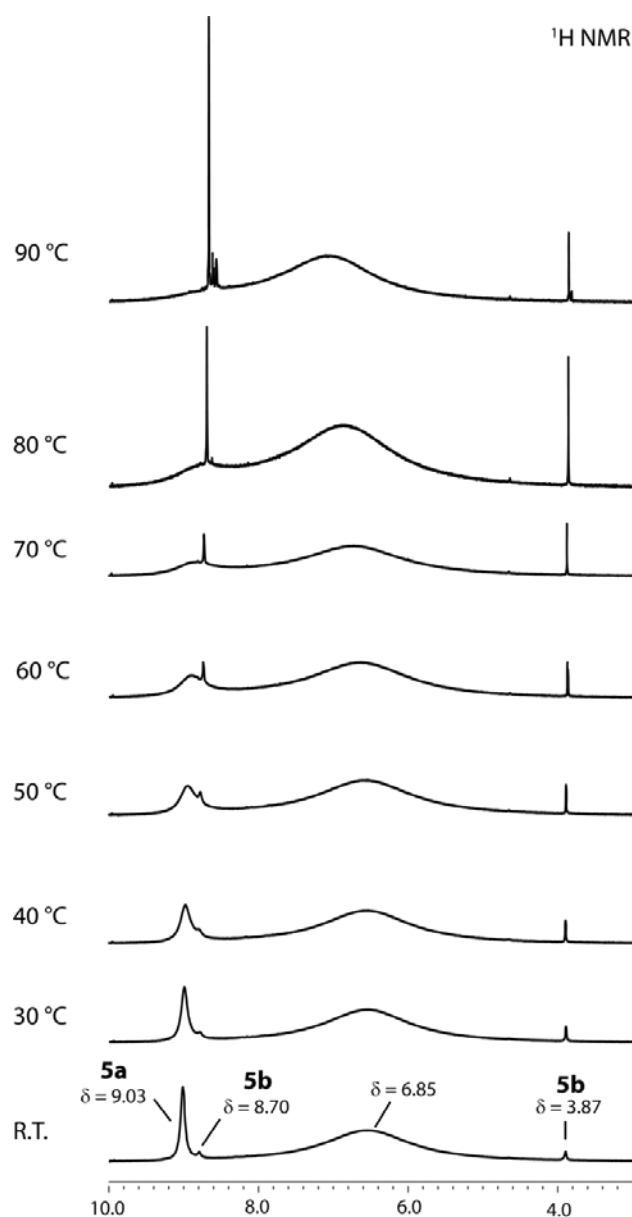


Figure 10: Comparison of ^1H NMR spectra of DNMBT (**5**) at room temperature and at elevated temperatures in $\text{DMSO}-d_6$; x-axis represents the chemical shift δ in ppm.

Of course there is another possible isomer in which one ring is a 1,2,4-triazole and the other a 1,2,4-triazoline. This isomer could not be detected in any spectra at any temperature. Apparently this transition state is not an energetic minimum and is therefore not part of the further discussion. Figure 10 shows a comparison of the experimentally obtained proton NMR spectra at different temperatures. At room temperature, isomer **5a** is the dominant species resulting in a broad signal for both protons at 9.03 ppm (for comparison: protons of the similar 5-dinitromethylene-4,5-dihydro-1*H*-tetrazole appear at 11.09 ppm).^[20] The signals of the bis-1,2,4-triazoline isomer (**5b**) can also be obtained at room temperature at 8.70 ppm ($N_{\text{triazole}}-H$) and 3.87 ppm ($C_{\text{sp}^3}-H$). Owing to the fact that compound **5** is very acidic and was used as dihydrate (as obtained after recrystallisation), the constant signal at 6.85 ppm was assigned to the protons of the water molecules.

With raising temperature, the signal of isomer **5a** decreases and the two signals of isomer **5b** gain intensity. The conversion is completed at about 90 °C, the signal of **5a** has disappeared completely. Simultaneously, the compound starts to decompose, resulting in small signals in the range of 8.60 ppm. As shown in Figure 11, the signals of the 1,2,4-triazole carbon atoms in the $^{13}\text{C}\{^1\text{H}\}$ NMR spectrum at room temperature interfere with each other resulting in a broad multiplet in the range of 150.0 ppm. The sp^2 carbon atom of isomer **5a** (C3) appears at 124.3 ppm, the sp^3 carbon atom of isomer **5b** (C3') could be found at 106.5 ppm. For comparison, similar sp^2 carbon atoms appear at 124.9 ppm (3,3'-bis(dinitromethylen)-5,5'-azo-1*H*-1,2,4-triazole)^[19] and at 121.5 ppm (5-dinitromethylene-4,5-dihydro-1*H*-tetrazole)^[20].

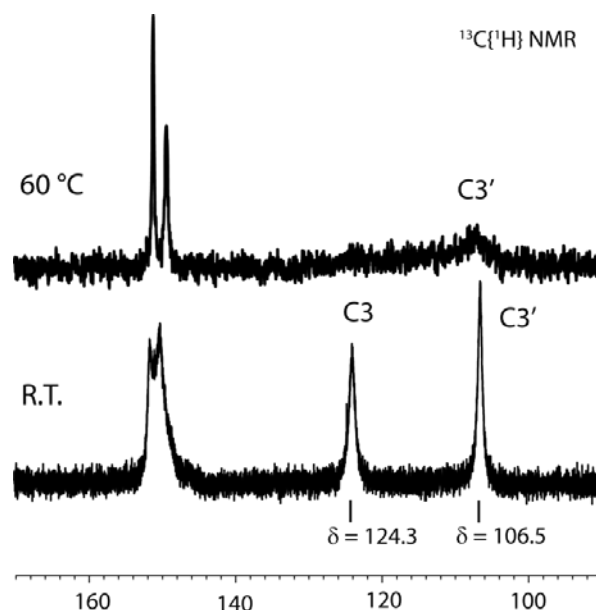


Figure 11: Comparison of ^{13}C NMR spectra of DNMBT (**5**) at room temperature and at elevated temperatures in $\text{DMSO}-d_6$; x-axis represents the chemical shift δ in ppm.

At 60 °C, only the signals of isomer **5b** could be observed. The triazole carbon atoms now show two well resolved resonances at 151.1 and 149.3 ppm, the sp^3 carbon atom C3' can be found at the identical chemical shift of 106.5 ppm (in comparison to R.T. measurement) as a broad singlet. Quantum chemical calculations at the B3LYP/aug-cc-pVDZ level of theory reveal an energy difference between both isomers of 30.4 kJ mol⁻¹ (Table 5). The calculated values go well with the experimentally obtained ¹H NMR spectra, especially with the exclusive appearance of isomer **5b** in the NMR spectrum above 90 °C.

Table 5: Calculations on Isomers of DNMBT (**5**) at the B3LYP/aug-cc-pVDZ level of theory

	Isomer A	Isomer B
point group	C_{2h}	C_1
$-E$ [Hartree]	1380.136812	1380.125222
E_{rel} [kcal mol ⁻¹]	0.0	+7.3
E_{rel} [kJ mol ⁻¹]	0.0	+30.4

The calculated optimized gas-phase structure of isomer **5a** is in good agreement with the experimentally obtained crystal structure of compound **5** (Figure 12). The planar assembly of the dinitromethylene moiety is the thermodynamically most stable configuration. In addition, the carbon atom C3' of isomer **5b** shows the expected tetrahedral coordination as it is the case for the sp^3 carbon atoms in the similar bis(dinitromethylen)-5,5'-azo-1*H*-1,2,4-triazole.^[19]

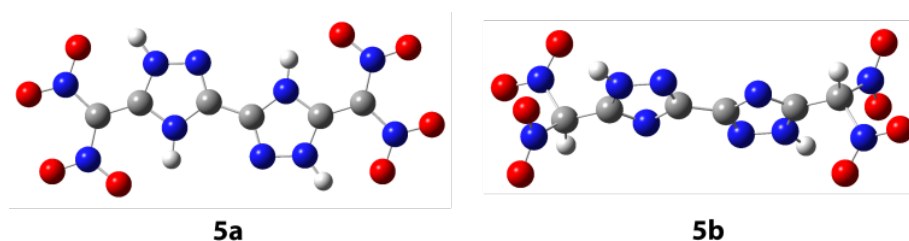


Figure 12: Comparison of calculated gas-phase structures of both isomers **5a** and **5b**.

Due to insufficient solubility, ¹⁵N NMR spectra could only be obtained for compounds **2** and **4**. Four well resolved resonances are observed in the ¹⁵N NMR spectrum for the four nitrogen atoms of the dinitro-compound **2** (Figure 13). The signals were assigned by comparison to literature values.^[21a, 22] The signals of the nitrogen atoms N1 and N2 of the diazido compound (**4**) appear in the same range as for compound **2**, but are rather broad

in comparison to the sharp signals of **2**. The three signal of the azido moiety are well resolved and can be found in the expected range with N4 being shifted to highest field with a chemical shift of -295.2 ppm.

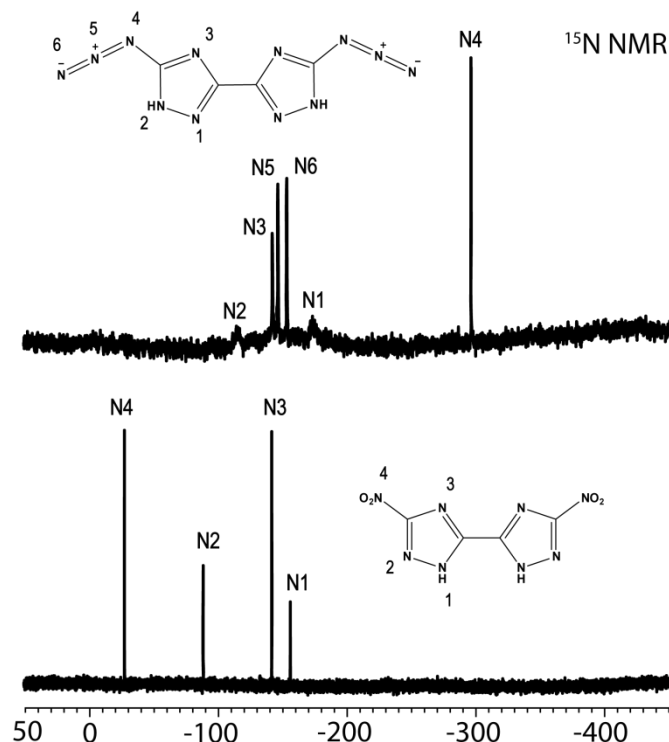


Figure 13: ^{15}N NMR spectra of 5,5'-diazido-3,3'-bis-1H-1,2,4-triazole (**4**, top) and 3,3'-dinitro-5,5'-bis-1H-1,2,4-triazole (**2**, bottom) recorded in DMSO-d_6 ; x-axis represents the chemical shift δ in ppm.

THEORETICAL CALCULATIONS, PERFORMANCE CHARACTERISTICS AND STABILITIES

All calculations regarding energies of formation were carried out using the Gaussian G09W Version 7.0 program package.^[23] Since very detailed descriptions of the calculation process have been published earlier^[8] and can be found in specialized books,^[1b] only a short summary of computational methods will be given. The enthalpies (H) and Gibbs free energies (G) were calculated using the complete basis set method (CBS) of Petersson *et al.* in order to obtain very accurate energies. In this contribution, we used the modified CBS-4M method with M referring to the use of minimal population localization, which is a re-parameterized version of the original CBS-4 computational method and also includes additional empirical calculations.^[24] The enthalpies of formation for the gas phase species were computed according to the atomization energy method, using NIST^[25] values as standardized values for the atoms standard heats of formation ($\Delta_f H^0$) according to equation 1.^[26]

$$\Delta_f H^0_{(\text{g, Molecule, 298})} = H_{(\text{Molecule})} - \sum H^0_{(\text{Atoms})} + \sum \Delta_f H^0_{(\text{Atoms, NIST})} \quad (1)$$

The solid state enthalpy of formation for neutral compounds is estimated from the computational results using Troutons rule,^[27] where T_m was taken equal to the decomposition temperatures.

$$\Delta H_m = \Delta_f H^0_{(\text{g, Molecule, 298})} - \Delta H_{\text{sub}} = \Delta_f H^0_{(\text{g, Molecule, 298})} - (188 [\text{J mol}^{-1} \text{K}^{-1}] * T_m) \quad (2)$$

The solid state enthalpies of formation for the ionic compounds are derived from the calculation of the corresponding lattice energies (U_L) and lattice enthalpies (H_L), calculated from the corresponding molecular volumes, using the equations provided by Jenkins et al.^[28] The derived molar standard enthalpies of formation for the solid state (ΔH_m) were used to calculate the solid state energies of formation (ΔU_m) according to equation three, with Δn being the change of moles of gaseous components.^[1b]

$$\Delta U_m = \Delta H_m - \Delta n RT \quad (3)$$

The calculated standard energies of formation were used to perform predictions of the detonation parameters with the program package Explo5, Version 5.05.^[29] The program is based on the chemical equilibrium, steady state model of detonation. It uses Becker-Kistiakowsky-Wilsons equation of state (BKW EOS) for gaseous detonation products together with Cowan-Ficketts equation of state for solid carbon.^[30] The calculation of the equilibrium composition of the detonation products is performed by applying modified White, Johnson and Dantzig's free energy minimization technique. The program was designed to enable calculations of detonation parameter at the Chapman-Jouguet point. The BKW equation as implemented in the Explo5.5 program was used with the BKW-G set of parameters ($\alpha, \beta, \kappa, \theta$) given below equation (4), in which X_i is the mol fraction of the i -th gaseous detonation product while k_i is the molar co-volume of the i -th gaseous detonation product.^[29-30]

$$pV / RT = 1 + x e^{\beta x} \quad \text{with} \quad x = (\kappa \sum X_i k_i) / [V(T + \theta)]^\alpha \quad (4)$$

$$\alpha = 0.5, \beta = 0.096, \kappa = 17.56, \theta = 4950$$

The results of the detonation runs, together with the calculated energies of formation and the corresponding sensitivities, are compiled in Table 6.

Table 6: Physico-chemical properties of compounds **2–5** in comparison to hexogen (RDX).

	DNBT (2)	DNABT (3)	DAzBT (4)	DNMBT (5)	RDX ^[n]
Formula	C ₄ H ₂ N ₈ O ₄	C ₄ H ₄ N ₁₀ O ₄	C ₄ H ₂ N ₁₂	C ₆ H ₄ N ₁₀ O ₈	C ₃ H ₆ N ₆ O ₆
Molecular Mass [g mol ⁻¹]	226.1	256.1	218.2	344.2	222.1
Impact sensitivity [J] ^a	10	3	3	20	7
Friction sensitivity [N] ^b	360	108	48	360	120
ESD–test [J]	0.1	0.5	0.04	0.2	--
N [%] ^c	49.45	54.68	77.05	40.70	37.8
Q [%] ^d	–35.4	–37.5	–66.0	–27.9	–21.6
T _{dec.} [°C] ^e	251	194	201	121	210
ρ [g cm ⁻³] ^f	1.90	1.80	1.70	1.95	1.80
Δ _f H _m ^o [kJ mol ⁻¹] ^g	285	405	971	298	70
Δ _f U ^o [kJ kg ⁻¹] ^h	1338	1667	4532	946	417
EXPLO5 values:					
V5.05					
–Δ _E U ^o [kJ kg ⁻¹] ⁱ	4888	4973	4639	4977	6125
T _E [K] ^j	3890	3814	3670	3862	4236
p _{C-J} [kbar] ^k	320	300	250	341	349
V _{Det.}					
[m s ⁻¹] ^l	8413	8355	7944	8499	8748
Gas vol. [L kg ⁻¹] ^m	642	670	653	641	739

^[a] BAM drop hammer; ^[b] BAM friction tester; ^[c] Nitrogen content; ^[d] Oxygen balance; ^[e] Temperature of decomposition by DSC (β = 5 °C, Onset values); ^[f] derived from X-ray structure; ^[g] Molar enthalpy of formation; ^[h] Energy of formation; ^[i] Energy of Explosion; ^[j] Explosion temperature; ^[k] Detonation pressure; ^[l] Detonation velocity; ^[m] Assuming only gaseous products; ^[n] values based on Ref. ^[31] and the EXPLO5.5 database; *Density values of **3**, **4** and **5** are based on X-ray densities of dihydrate species and additional pycnometer measurements of anhydrous compounds.

As shown in Table 6, physico-chemical properties were calculated for the energetic compounds **2–5**. For the starting material 3,3'-diamino-5,5'-bis(1*H*-1,2,4-triazole) (DABT, **1**), only the sensitivities and the decomposition temperature was determined. Compound **1** is insensitive towards friction and impact and shows no decomposition below 450 °C.

Compound **2** as well shows a remarkably high thermal stability of 251 °C together with an insensitivity towards friction and a moderate sensitivity towards impact (10 J). The beneficial detonation parameters of DNBT with $v_{\text{det}} = 8413 \text{ m s}^{-1}$ mainly stem from the

high positive heat of formation (285 kJ mol^{-1}) and the remarkably high density of 1.902 g cm^{-3} (X-ray measurement).

As it is characteristically for nitramino- and nitrimino-1,2,4-triazoles,^[8, 32] the nitrimino compound **3** is very sensitive towards impact (3 J) and sensitive towards friction (108 N). As expected, the decomposition temperature (194°C) is lower in comparison to the Nitro-derivative (**2**). However, the decomposition temperature was found to be repeatably higher in comparison to the value determined by Shreeve and coworkers (165°C ^[12] at a heating rate of $10^\circ\text{C min}^{-1}$). The calculated detonation parameters are well below the commonly used explosive RDX and in the same range compared to compound **2**.

The azido-compound (**4**) is the most sensitive compound with a friction sensitivity of 48 N, an impact sensitivity of 3 J and a sensitivity towards electrical discharge of 40 mJ. The compound can therefore be classified as primary explosive and shows outstanding energetic properties for this class of energetic materials.

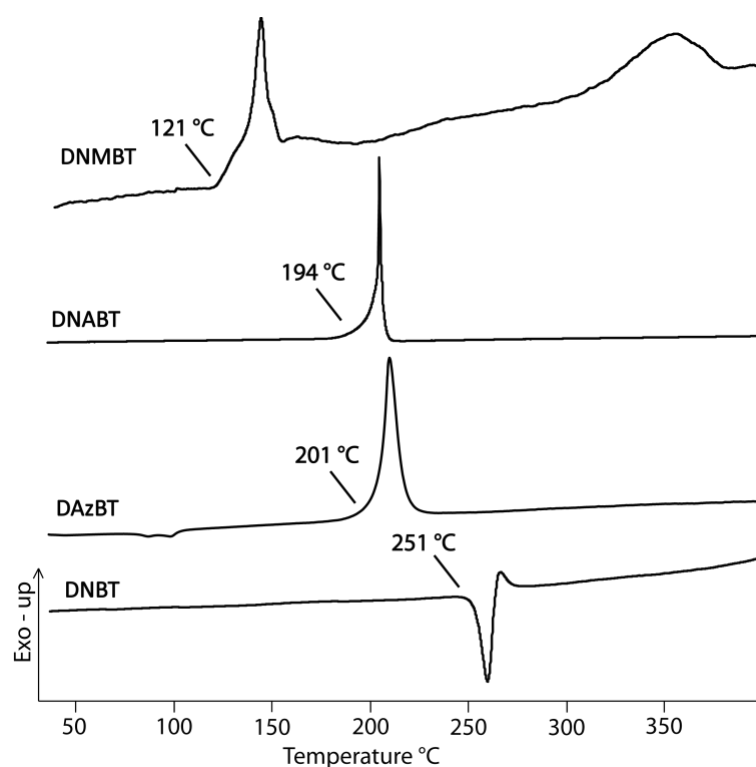


Figure 14: DSC plots of DNBT (**2**), DAzBT (**4**), DNABT (**3**) and DNMBT (**5**) in order of decreasing decomposition temperature (onset). DSC plots were recorded with a heating rate of 5°C min^{-1} .

Compound **5** shows the best performance of all compounds with a detonation velocity of 8499 m s^{-1} , a detonation pressure of 341 kbar and oxygen balance of -27.9% , which is in the range of RDX. Unfortunately, the introduction of the dinitromethyl group leads to a decrease of the decomposition temperature to 121°C in comparison to the nitro-

compound **2** (251 °C). 3,3'-Dinitromethyl-5,5'-bistriazole could therefore only be of interest for ionic derivatives in combination with nitrogen-rich cations, since deprotonation increases the thermal stability as it is known for the previously described 3,3'-bis(dinitro-methyl)-5,5'-azo-1*H*-1,2,4-triazole.^[19] The thermal stabilities of all compounds are illustrated in Figure 14.

CONCLUSION

The starting material DABT (**1**) was synthesized following a modified literature known procedure^[14] resulting in an increase of the yield from 56% up to 70%. The optimization of the reaction conditions for the formation of 3,3'-dinitro-5,5'-bis(1*H*-1,2,4-triazole)^[13] (DNBT, **2**) and 5,5'-dinitrimino-3,3'-bis(1*H*-1,2,4-triazole)^[12] (DNABT, **3**) resulted in excellent yields and high purities. The previously unknown syntheses of 3,3'-diazido-5,5'-bis(1*H*-1,2,4-triazole) (DAZBT, **4**) as well as 3,3'-dinitromethyl-5,5'-bis(1*H*-1,2,4-triazole) (DNMBT, **5**) are presented and reveal synthetic pathways towards numerous novel energetic 1,2,4-triazole derivatives. All compounds have been fully characterized by means of vibrational and multinuclear NMR spectroscopy, mass spectrometry and differential scanning calorimetry. Single crystal X-ray measurements were accomplished for compounds **1**, **2**, **4** and **5** and deliver insight into structural characteristics as well as inter- and intramolecular interactions.

Regarding the stability values and energetic parameters, compound **2** shows the highest thermal stability of 251 °C together with an insensitivity towards friction and a moderate sensitivity towards impact (10 J). As expected, the nitrimino compound (**3**) as well as the azido compound (**4**) are the most sensitive derivatives with an impact sensitivity of 3 J and friction sensitivities of 108 N (**3**) and 48 N (**4**) and can therefore be classified as primary explosive. The introduction of the dinitromethyl group in compound **5** leads to the best detonation parameters with a detonation velocity of 8499 m s⁻¹, a detonation pressure of 341 kbar and an oxygen balance of -27.9%. Unfortunately, the thermal stability is decreased to 121 °C, which limits the potential applications to ionic derivatives in combination with nitrogen-rich cations. In summary, compounds **2**, **3** and **5** are able to compete with commonly used TNT, however, the performance data for RDX are not reached. Those three compounds can be considered as nitrogen-rich starting materials for new energetic ionic derivatives in combination with nitrogen-rich cations, as it has already been shown by Shreeve and coworkers.^[12] Since nitrogen-rich salts of

energetic compounds tend to be more stable compared to the uncharged compounds and often show performance characteristics in the range of modern secondary explosives, those ionic derivatives could find application as high-nitrogen energetic materials.

EXPERIMENTAL SECTION

Caution: Although all presented bis-1,2,4-triazoles are rather stable against outer stimuli, proper safety precautions should be taken, when handling the dry materials. Especially derivatives of 3,3'-Diazido-5,5'-bis(1H-1,2,4-triazole) (DAzBT, **2**) are energetic primary materials and tend to explode under the influence of impact or friction. Lab personnel and the equipment should be properly grounded and protective equipment like earthed shoes, leather coat, Kevlar[®] gloves, ear protection and face shield is recommended for the handling of any energetic material.

General. All chemical reagents and solvents were obtained from Sigma-Aldrich Inc. or Acros Organics (analytical grade) and were used as supplied without further purification. ¹H, ¹³C{¹H}, ¹⁴N{¹H} and ¹⁵N NMR spectra were recorded on a JEOL Eclipse 400 instrument in DMSO-*d*₆ at 25 °C. The chemical shifts are given relative to tetramethylsilane (¹H, ¹³C) or nitro methane (¹⁴N, ¹⁵N) as external standards and coupling constants are given in Hertz (Hz). Infrared (IR) spectra were recorded on a Perkin-Elmer Spectrum BX FT-IR instrument equipped with an ATR unit at 25 °C. Transmittance values are qualitatively described as “very strong” (vs), “strong” (s), “medium” (m), “weak” (w) and “very weak” (vw). Raman spectra were recorded on a Bruker RAM II spectrometer equipped with a Nd:YAG laser (200 mW) operating at 1064 nm and a reflection angle of 180°. The intensities are reported as percentages of the most intense peak and are given in parentheses. Elemental analyses (CHNO) were performed with a Netzsch Simultaneous Thermal Analyzer STA 429. Melting and decomposition points were determined by differential scanning calorimetry (Linseis PT 10 DSC, calibrated with standard pure indium and zinc). Measurements were performed at a heating rate of 5 °C min⁻¹ in closed aluminum sample pans with a 1 µm hole in the lid for gas release to avoid an unsafe increase in pressure under a nitrogen flow of 20 mL min⁻¹ with an empty identical aluminum sample pan as a reference.

For initial safety testing, the impact and friction sensitivities as well as the electrostatic sensitivities were determined. The impact sensitivity tests were carried out according to STANAG 4489,^[33] modified according to WIWEB instruction 4-5.1.02^[34] using a

BAM^[35] drop hammer. The friction sensitivity tests were carried out according to STANAG 4487^[36] and modified according to WIWEB instruction 4-5.1.03^[37] using the BAM^[35] friction tester. The electrostatic sensitivity tests were accomplished according to STANAG 4490^[38] using an electric spark testing device ESD 2010EN (OZM Research) operating with the “Winspark 1.15 software package”.

Crystallographic measurements. The single crystal X-ray diffraction data of **1**, **2**, **4** and **5** were collected using an Oxford Xcalibur3 diffractometer equipped with a Spellman generator (voltage 50 kV, current 40 mA) and a Kappa CCD detector. The data collection was undertaken using the CrysAlis CCD software^[39] while the data reduction was performed with the CrysAlis Red software^[40]. Crystals of compound **3c** were investigated using a Bruker-Nonius Kappa CCD diffractometer equipped with a rotating molybdenum anode and Montel-graded multilayered X-ray optics. The structures were solved with Sir-92^[41] or Shelxs-97^[42] and refined with Shelxl-97^[43] implemented in the program package WinGX^[44] and finally checked using Platon^[45]. CCDC 887530 (**1**), 864398 (**2**), 887531 (**4**), 887532 (**5**) contains the supplementary crystallographic data for this paper. These data can be obtained free of charge from The Cambridge Crystallographic Data Centre via www.ccdc.cam.ac.uk/data_request/cif.

3,3'-Diamino-5,5'-bis(1H-1,2,4-triazole) (DABT, 1)

Hydrochloric acid (60 mL) was added to a stirred mixture of oxalic acid (20.0 g, 159 mmol) and aminoguanidinium bicarbonate (45.4 g, 332 mmol). The reaction was stirred at 70 °C for one hour and the precipitate was collected by filtration. The colorless solid was dissolved in water (240 mL) and alkalized with sodium hydroxide to pH = 14. The reaction mixture was refluxed for one hour and subsequently acidified with acetic acid to pH = 4. The resulting precipitate was collected by filtration, washed with water (appr. 200 mL) and dried in air to yield 3,3'-diamino-5,5'-bis(1,2,4-1*H*-triazole) (**4**) (18.6 g, 112 mmol, 70%) as a colorless solid. ¹H nmr (DMSO-*d*₆): δ = 6.46 (s, 2H, NH₂) ppm. ¹³C nmr (DMSO-*d*₆): δ = 157.3, 149.3 ppm. IR: ν (cm⁻¹) (rel. int.) = 3325(m), 3116(m), 2863(m), 2784(m), 1706(s), 1668(s), 1654(s), 1618(m), 1606(m), 1484(m), 1457(m), 1267(m), 1104(vs), 1061(s), 987(w), 956(w), 769(w), 721(s). Raman (200 mW): ν (cm⁻¹) (rel. int.) = 1636(62), 1614(100), 1591(67), 1575(57), 1495(13), 1439(21), 1432(21), 1361(9), 1152(24), 1143(23), 1059(23), 1042(34), 1022(22), 980(27), 772(18), 554(7), 413(11), 328(12), 249(16). **Elemental analysis** (C₄H₆N₁₀):

calc.: C 28.92, H 3.64, N 67.44; found: C 28.72, H 3.58, N 66.11. **Mass spectrometry:** m/z (DEI+): 166.1 [$C_4H_7N_8^+$].

3,3'-Dinitro-5,5'-bis(1H-1,2,4-triazole) (DNBT, 2)

A solution of 3,3'-diamino-5,5'-bis(1H-1,2,4-triazole) (**4**) (11.9 g, 72 mmol) in 20% sulfuric acid (140 mL) was added drop wise to a solution of sodium nitrite (10 eq., 98.8 g, 1.4 mol) in water (140 mL) at 40 °C. The mixture was stirred at 50 °C for 1 h. After cooling down to room temperature the mixture was acidified with sulfuric acid (20%) until no evolution of nitrogen dioxide could be observed. The precipitate was collected by filtration and dissolved in boiling water. The hot solution was filtrated and allowed to cool to room temperature. Collection of the pale green precipitate affords 3,3'-dinitro-5,5'-bis(1H-1,2,4-triazole) dihydrate (15.5 g, 59 mmol, 82%) as a crystalline solid.

1H nmr (DMSO- d_6): δ = 9.68 (s, 2H, H_{Triazole}) ppm; **^{13}C nmr** (DMSO- d_6): δ = 162.7, 145.6 ppm; **^{14}N nmr** (DMSO- d_6): δ = -26 (-NO₂) ppm; **^{15}N nmr** (DMSO- d_6): δ = -27.8 (N4), -88.8 (N2), -141.7 (N3), -156.1 (N1) ppm. **IR:** ν (cm⁻¹) (rel. int.) = 3599(m), 3499(m), 3052(w), 2849(w), 2747(w), 2670(m), 2621(m), 2574(m), 2530(m), 2488(m), 2419(m), 1844(w), 1609(m), 1532(vs), 1466(w), 1416(vs), 1314(vs), 1245(m), 1183(m), 1024(m), 953(s), 837(s), 690(w), 690(w). **Raman** (200 mW): ν (cm⁻¹) (rel. int.) = 3192(3), 1641(100), 1546(28), 1519(5), 1485(75), 1468(43), 1458(95), 1413(18), 1393(97), 1365(6), 1362(6), 1345(13), 1325(27), 1306(35), 1172(58), 1062(67), 1015(31), 855(4), 774(8), 744(5), 619(4), 511(4), 452(5), 452(5), 399(9), 297(9), 203(6). **Elemental analysis** (C₄H₂N₈O₄): calc.: C 21.25, H 0.89, N 49.56; found: C 21.44, H 0.95, N 49.19. **Mass spectrometry:** m/z (FAB-): 225.1 [C₄HN₈O₄⁻]. **Sensitivities** (grain size: <100 μ m): friction: 360 N, impact: 10 J, ESD: 0.1 J; **DSC** (onset, 5 °C min⁻¹): T_{Dec.}: 251 °C.

3,3'-Dinitrimino-5,5'-bis(1H-1,2,4-triazole) (DNABT, 3)

Synthesized according to modified literature known procedure:^[12]

Nitric acid (100%, 3.0 mL) was added slowly to a solution of 3,3'-diamino-5,5'-bis(1H-1,2,4-triazole) (**1**) (1.0 g, 6.0 mmol) in concentrated sulfuric acid (9.0 mL) at 0 °C. The mixture was allowed to warm to room temperature and stirred for one hour. The clear solution was poured on ice, the precipitate was collected by filtration and recrystallized

from boiling water to yield 3,3'-Dinitrimino-5,5'-bis(1H-1,2,4-triazole) dihydrate (1.35 g, 4.6 mmol, 77 %) as yellow crystalline solid.

¹H nmr (DMSO-*d*₆): δ = 5.52 (s, 2H, *H*_{Triazole}) ppm; **¹³C nmr** (DMSO-*d*₆): δ = 153.1, 142.1 ppm; **¹⁴N nmr** (DMSO-*d*₆): δ = -21 (-NO₂) ppm. **IR**: ν (cm⁻¹) (rel. int.) = 3165(m), 3154(m), 1565(vs), 1508(s), 1463(s), 1446(s), 1380(m), 1298(vs), 1229(vs), 1140(m), 1085(m), 1054(s), 989(m), 947(s), 849(m), 778(s), 766(s), 751(s), 708(vs). **Raman** (200 mW): ν (cm⁻¹) (rel. int.) = 1655(100), 1592(60), 1568(81), 1527(14), 1288(2), 1224(7), 1123(26), 1072(2), 1019(25), 992(35), 851(11), 764(26), 691(2), 558(6), 520(2), 440(2), 417(3), 407(3), 226(6). **Elemental analysis** (C₄H₂N₈O₄): calc.: C 16.44, H 2.76, N 47.94; found: C 16.73, H 2.69, N 47.73. **Sensitivities** (water free compound, grain size: <100 μm): friction: 108 N, impact: 3 J, ESD: 0.5 J; **DSC** (onset, 5 °C min⁻¹): T_{Dec}: 194 °C.

3,3'-Diazido-5,5'-bis(1H-1,2,4-triazole) (DAzBT, **4**)

A solution of sodium nitrite (3 eq., 0.37 g, 5.4 mol) in water (2.0 mL) was added dropwise to a suspension of 3,3'-diamino-5,5'-bis(1H-1,2,4-triazole) (**1**) (0.3 g, 1.8 mmol) in 20% sulfuric acid (20 mL) at 0 °C. The mixture was allowed to warm to room temperature and subsequently stirred at 40 °C for 1 h. After cooling down to room temperature, a solution of sodium azide (5 eq., 5.9 g, 9.0 mmol) in water (2.0 mL) was added dropwise. (DANGER: EVOLUTION OF HN₃!). The suspension was stirred over night at room temperature to remove the excess of sodium azide and extracted with ethyl acetate (3×20 mL). The solvent was evaporated and the resulting solid recrystallized from water. Collection of the colorless precipitate affords 3,3'-diazido-5,5'-bis(1H-1,2,4-triazole) dihydrate (0.25 g, 1.0 mmol, 56%) as a crystalline needles.

¹H nmr (DMSO-*d*₆): δ = 14.86 (s, 2H, *H*_{Triazole}) ppm; **¹³C nmr** (DMSO-*d*₆): δ = 157.7, 145.9 (C-N₃) ppm; **¹⁴N nmr** (DMSO-*d*₆): δ = -145 (-N₃) ppm; **¹⁵N nmr** (DMSO-*d*₆): δ = -115.3 (N₂), -141.9 (N₃), -146.2 (N₅), -153.0 (N₆), -173.2 (N₁), -295.2 (N₄) ppm. **IR**: ν (cm⁻¹) (rel. int.) = 3141(s), 3042(s), 2876(s), 2710(s), 2655(s), 2630(m), 2571(m), 2435(m), 2362(m), 2240(m), 2228(m), 2156(vs), 2138(vs), 2137(vs), 1541(vs), 1518(s), 1483(vs), 1457(s), 1420(vs), 1418(vs), 1391(s), 1333(s), 1299(m), 1299(m), 1275(s), 1241(m), 1218(m), 1188(s), 1142(s), 1122(s), 1033(vs), 1014(m), 980(vs), 958(m), 846(m), 799(s), 780(m), 729(s), 714(m), 661(m), 532(m). **Raman** (200 mW): ν (cm⁻¹) (rel. int.) = 2171(14), 2142(17), 1620(56), 1605(100), 1551(17), 1551(16), 1549(17),

1548(17), 1547(17), 1515(44), 1503(24), 1501(26), 1500(27), 1423(16), 1422(16), 1421(15), 1399(15), 1335(20), 1298(5), 1228(10), 1168(6), 1148(17), 1147(17), 1147(17), 1066(16), 1065(17), 1039(22), 1038(22), 1024(31), 817(7), 705(3), 629(3), 577(9), 436(6), 423(7), 397(9), 380(21), 326(24), 262(9), 247(16). **Elemental analysis** ($\text{C}_4\text{H}_6\text{N}_{12}\text{O}_2$): calc.: C 18.90, H 2.38, N 66.13; found: C 19.41, H 2.14, N 65.75. **Mass spectrometry**: m/z (DEI+): 218.1 [$\text{C}_4\text{H}_2\text{N}_{12}^+$]. **Sensitivities** (grain size: <100 μm): friction: 48 N, impact: 3 J, ESD: 0.04 J; **DSC** (onset, 5 $^\circ\text{C min}^{-1}$): $T_{\text{Dec.}}$: 202 $^\circ\text{C}$.

3,3'-Dinitromethyl-5,5'-bis(1,2H-1,2,4-triazole) (DNMBT, 5)

Precursors synthesized according to ^[16a] and ^[16b]

3,3'-diethyl-acetate-5,5'-bis(1H-1,2,4-triazole) (0.5 g, 1.62 mmol) was dissolved in sulfuric acid (conc., 6 mL) and cooled to 0 $^\circ$ C. Subsequently, nitric acid (conc., 4 mL) and oleum (60% SO_3 , 2 mL) were added slowly, the mixture was allowed to warm to room temperature and stirred at for 2h. The mixture was poured on ice, alkalized with sodium hydroxide and stirred until all solids were dissolved. The solution was acidified with sulfuric acid (conc.) until pH = 1. The precipitate was isolated by filtration and recrystallized from water. 3,3'-Dinitromethyl-5,5'-bis(1-H-1,2,4-triazole) (DNMBT, 7) was obtained as a yellow solid (0.27g, 0.79mmol, 49%).

^1H nmr (DMSO- d_6 , 60 $^\circ\text{C}$): δ = 8.94 (NH), 3.91 (s, CH) ppm; **^{13}C nmr** (DMSO- d_6 , 60 $^\circ\text{C}$): δ = 151.1, 149.3, 106.5 (C-C) ppm, **^{14}N nmr** (DMSO- d_6 , 60 $^\circ\text{C}$): δ = -23 (NO_2); **IR**: ν (cm^{-1}) (rel. int.) = 3544(m), 3467(m), 3319(m), 2360(vw), 2094(vw), 1643(w), 1511(s), 1484(m), 1467(m), 1436(s), 1388(m), 1364(m), 1300(m), 1286(m), 1271(s), 1200(vs), 1146(m), 1128(s), 1085(vs), 987(vs), 976(vs), 832(s), 779(w), 779(w), 745(s), 722(s), 666(m). **Raman** (200 mW): ν (cm^{-1}) (rel. int.) = 1646(78), 1575(75), 1559(100), 1517(20), 1490(4), 1473(3), 1419(3), 1403(10), 1341(55), 1320(30), 1302(24), 1226(59), 1213(43), 1163(15), 1101(4), 1025(4), 967(46), 834(16), 783(10), 753(2), 699(3), 475(7), 435(4), 435(4), 379(2), 326(3), 209(4). **Mass spectrometry**: m/z (FAB-): 343 [M-H]. **Sensitivities**: (grain size: <100 μm): friction: 360 N, impact: >20 J, ESD: 0.2 J; **DSC** (onset, 5 $^\circ\text{C min}^{-1}$): $T_{\text{Dec.}}$: 130 $^\circ\text{C}$.

REFERENCES

- [1] a) T. M. Klapötke, *Chemistry of high-energy materials*, De Gruyter, Berlin, **2011**;
b) T. M. Klapötke, *Chemie der hochenergetischen Materialien*, de Gruyter, Berlin, **2009**; c) P. F. Pagoria, G. S. Lee, A. R. Mitchell, R. D. Schmidt, *Thermochimica Acta* **2002**, 384, 187-204; d) R. P. Singh, R. D. Verma, D. T. Meshri, J. n. M. Shreeve, *Angew. Chem., Int. Ed.* **2006**, 45, 3584-3601; e) C. M. Sabate, T. M. Klapoetke, *New Trends in Research of Energetic Materials, Proceedings of the Seminar, 12th, Pardubice, Czech Republic, Apr. 1-3*, **2009**, 172-194; f) S. Yang, S. Xu, H. Huang, W. Zhang, X. Zhang, *Huaxue Jinzhan* **2008**, 20, 526-537; g) M. B. Talawar, R. Sivabalan, T. Mukundan, H. Muthurajan, A. K. Sikder, B. R. Gandhe, A. S. Rao, *J. Hazard. Mater.* **2009**, 161, 589-607.
- [2] a) T. M. Klapoetke, J. Stierstorfer, A. U. Wallek, *Chem. Mater.* **2008**, 20, 4519-4530; b) T. M. Klapoetke, C. M. Sabate, *Chem. Mater.* **2008**, 20, 3629-3637; c) D. E. Chavez, M. A. Hiskey, D. L. Naud, *Prop. Explos. Pyrot.* **2004**, 29, 209-215; d) Y. Huang, H. Gao, B. Twamley, J. M. Shreeve, *Eur. J. Inorg. Chem.* **2008**, 2560-2568; e) H. Gao, J. M. Shreeve, *Chem. Rev.* **2011**, 111, 7377-7436.
- [3] T. M. Klapötke, in *Structure and bonding* (Ed.: D. M. P. Mingos), Springer-Verlag, Berlin Heidelberg **2007**.
- [4] K. Y. Lee, C. B. Storm, M. A. Hiskey, M. D. Coburn, *J. Energ. Mater.* **1991**, 9, 415-428.
- [5] K. Wang, D. A. Parrish, J. M. Shreeve, *Chem-Eur. J.* **2011**, 17, 14485-14492.
- [6] V. Thottempudi, H. Gao, J. M. Shreeve, *J. Am. Chem. Soc.* **2011**, 133, 6464-6471.
- [7] D. L. Naud, M. A. Hiskey, H. H. Harry, *J. Energ. Mater.* **2003**, 21, 57-62.
- [8] A. Dippold, T. M. Klapötke, F. A. Martin, *Z. Anorg. Allg. Chem.* **2011**, 637, 1181-1193.
- [9] Y. Guo, G.-H. Tao, Z. Zeng, H. Gao, D. A. Parrish, J. M. Shreeve, *Chem-Eur. J.* **2010**, 16, 3753-3762.
- [10] a) E. L. Metelkina, T. A. Novikova, S. N. Berdonosova, D. Y. Berdonosov, V. S. Grineva, *Russ. J. Org. Chem.* **2004**, 40, 1412-1414; b) E. L. Metelkina, T. A. Novikova, S. N. Berdonosova, D. Y. Berdonosov, *Russ. J. Org. Chem.* **2005**, 41, 440-443; c) E. Metelkina, T. Novikova, *Russ. J. Org. Chem.* **2004**, 40, 1737-1743.
- [11] a) A. M. Astachov, V. A. Revenko, L. A. Kruglyakova, E. S. Buka, in *New Trends in Research of Energetic Materials, Proceedings of the Seminar, 10th, Pardubice*,

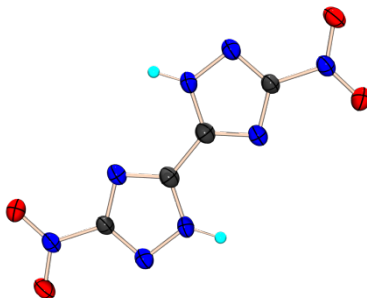
- Czech Republic, Apr. 25-27, 2007*, University of Pardubice, pp. 505-511; b) A. M. Astachov, V. A. Revenko, E. S. Buka, in *New Trends in Research of Energetic Materials, Proceedings of the Seminar, 12th, Pardubice, Czech Republic, Apr. 1-3, 2009*, University of Pardubice, pp. 396-404.
- [12] R. Wang, H. Xu, Y. Guo, R. Sa, J. n. M. Shreeve, *J. Am. Chem. Soc.* **2010**, *132*, 11904-11905.
- [13] a) Y. V. Serov, M. S. Pevzner, T. P. Kofman, I. V. Tselinskii, *Russ. J. Org. Chem.* **1990**, *26*, 773-777; b) L. I. Bagal, M. S. Pevzner, A. N. Frolov, N. I. Sheludyakova, *Chem. Heterocyc. Comp.* **1970**, *6*, 240-244.
- [14] R. N. Shreve, R. K. Charlesworth, *US2744116*, Purdue Research Foundation, **1956**.
- [15] J. P. Agrawal, *Organic Chemistry of Explosives*, John Wiley and Sons, Ltd, **2007**.
- [16] a) C. D. Bryan, A. W. Cordes, J. D. Goddard, R. C. Haddon, R. G. Hicks, C. D. MacKinnon, R. C. Mawhinney, R. T. Oakley, T. T. M. Palstra, A. S. Perel, *J. Am. Chem. Soc.* **1996**, *118*, 330-338; b) V. V. Kiseleva, A. A. Gakh, A. A. Fainzil'berg, *Izv. Akad. Nauk SSSR, Ser. Khim.* **1990**, 2075-2084.
- [17] a) D. E. Chavez, B. C. Tappan, B. A. Mason, D. Parrish, *Prop. Explos. Pyrot.* **2009**, *34*, 475-479; b) T. P. Kofman, *Russ. J. Org. Chem.* **2002**, *38*, 1231-1243; c) E. V. Nikitina, G. L. Starova, O. V. Frank-Kamenetskaya, M. S. Pevzner, *Kristallografiya* **1982**, *27*, 485-488.
- [18] a) A. F. Hollemann, E. Wiberg, N. Wiberg, *Lehrbuch der anorganischen Chemie*, de Gruyter, New York, **2007**; b) F. H. Allen, O. Kennard, D. G. Watson, L. Brammer, A. G. Orpen, R. Taylor, *J. Chem. Soc., Perkin Trans. 2* **1987**, S1-S19.
- [19] A. A. Dippold, T. M. Klapoetke, *Z. Anorg. Allg. Chem.* **2011**, *637*, 1453-1457.
- [20] T. M. Klapötke, F. X. Steemann, *Prop. Explos. Pyrot.* **2010**, *35*, 114-129.
- [21] a) M. Hesse, *Spektroskopische Methoden in der organischen Chemie*, 7th ed., Thieme Verlag, Stuttgart, **2005**; b) F. Billes, H. Endredi, G. Keresztury, *Theochem* **2000**, *530*, 183-200; c) E. Lieber, C. N. R. Rao, T. S. Chao, C. W. W. Hoffman, *Anal. Chem.* **1957**, *29*, 916-918.
- [22] H. H. Licht, H. Ritter, H. R. Bircher, P. Bigler, *Magn. Reson. Chem.* **1998**, *36*, 343-350.
- [23] M. J. Frisch, G. W. Trucks, H. B. Schlegel, G. E. Scuseria, M. A. Robb, J. R. Cheeseman, G. Scalmani, V. Barone, B. Mennucci, G. A. Petersson, H. Nakatsuji, M. Caricato, X. Li, H. P. Hratchian, A. F. Izmaylov, J. Bloino, G. Zheng, J. L.

- Sonnenberg, M. Hada, M. Ehara, K. Toyota, R. Fukuda, J. Hasegawa, M. Ishida, T. Nakajima, Y. Honda, O. Kitao, H. Nakai, T. Vreven, J. A. J. Montgomery, J. E. Peralta, F. Ogliaro, M. Bearpark, J. J. Heyd, E. Brothers, K. N. Kudin, V. N. Staroverov, R. Kobayashi, J. Normand, K. Raghavachari, A. Rendell, J. C. Burant, S. S. Iyengar, J. Tomasi, M. Cossi, N. Rega, J. M. Millam, M. Klene, J. E. Knox, J. B. Cross, V. Bakken, C. Adamo, J. Jaramillo, R. Gomperts, R. E. Stratmann, O. Yazyev, A. J. Austin, R. Cammi, C. Pomelli, J. W. Ochterski, R. L. Martin, K. Morokuma, V. G. Zakrzewski, G. A. Voth, P. Salvador, J. J. Dannenberg, S. Dapprich, A. D. Daniels, Ö. Farkas, J. B. Foresman, J. V. Ortiz, J. Cioslowski, D. J. Fox, Wallingford CT 2009.
- [24] a) J. A. Montgomery, Jr., M. J. Frisch, J. W. Ochterski, G. A. Petersson, *J. Chem. Phys.* **2000**, *112*, 6532-6542; b) J. W. Ochterski, G. A. Petersson, J. A. Montgomery, Jr., *J. Chem. Phys.* **1996**, *104*, 2598-2619.
- [25] P. J. Lindstrom, W. G. Mallard, NIST Chemistry Webbook, NIST Standard Reference 69, June 2005, National Institute of Standards and technology, Gaithersburg MD, <http://webbook.nist.gov>
- [26] a) E. F. C. Byrd, B. M. Rice, *J. Phys. Chem. A* **2006**, *110*, 1005-1013; b) B. M. Rice, J. J. Hare, *J. Phys. Chem. A* **2002**, *106*, 1770-1783; c) B. M. Rice, S. V. Pai, J. Hare, *Combust. Flame* **1999**, *118*, 445-458.
- [27] a) F. Trouton, *Philos. Mag.* **1884**, *18*, 54-57; b) M. S. Westwell, M. S. Searle, D. J. Wales, D. H. Williams, *J. Am. Chem. Soc.* **1995**, *117*, 5013-5015.
- [28] a) H. D. B. Jenkins, D. Tudela, L. Glasser, *Inorg. Chem.* **2002**, *41*, 2364-2367; b) H. D. B. Jenkins, H. K. Roobottom, J. Passmore, L. Glasser, *Inorg. Chem.* **1999**, *38*, 3609-3620.
- [29] M. Sućeska, *EXPLO5.5 program, Zagreb, Croatia*, **2010**.
- [30] a) M. Sućeska, *Materials Science Forum* **2004**, 465-466, 325-330; b) M. Suceška, *Prop. Explos. Pyrot.* **1999**, *24*, 280-285; c) M. Suceška, *Prop. Explos. Pyrot.* **1991**, *16*, 197-202.
- [31] R. Meyer, J. Köhler, A. Homburg, *Explosives*, Sixth ed., Wiley-VCH Verlag GmbH & Co. KGaA, Weinheim, **2007**.
- [32] a) A. A. Dippold, T. M. Klapötke, F. A. Martin, S. Wiedbrauk, *Eur. J. Inorg. Chem.* **2012**, *10*, 2429-2443; b) A. Dippold, T. M. Klapoetke, M. Feller, in *New Trends in Research of Energetic Materials, Proceedings of the Seminar, 14th*,

- Pardubice, Czech Republic, Apr. 13-15, 2011*, University of Pardubice, Institute of Energetic Materials, pp. 550-560.
- [33] *NATO standardization agreement (STANAG) on explosives and impact tests, no.4489, 1st ed., Sept. 17, 1999.*
- [34] *WIWEB-Standardarbeitsanweisung 4-5.1.02, Ermittlung der Explosionsgefährlichkeit, hier: der Schlagempfindlichkeit mit dem Fallhammer, Nov. 08, 2002.*
- [35] <http://www.bam.de>.
- [36] *NATO standardization agreement (STANAG) on explosives, friction tests, no.4487, 1st ed., Aug. 22, 2002.*
- [37] *WIWEB-Standardarbeitsanweisung 4-5.1.03, Ermittlung der Explosionsgefährlichkeit, hier: der Reibempfindlichkeit mit dem Reibeapparat, Nov. 08, 2002.*
- [38] *NATO standardization agreement (STANAG) on explosives, electrostatic discharge sensitivity tests, no.4490, 1st ed., Feb. 19, 2001.*
- [39] *CrysAlis CCD, Oxford Diffraction Ltd., Version 1.171.27p5 beta (release 01-04-2005 CrysAlis171.NET).*
- [40] *CrysAlis RED, Oxford Diffraction Ltd., Version 1.171.27p5 beta (release 01-04-2005 CrysAlis171 .NET).*
- [41] A. Altomare, G. Cascarano, C. Giacovazzo, A. Guagliardi, *J. Appl. Crystallogr.* **1993**, 26, 343-350.
- [42] G. M. Sheldrick, *SHELXS-97, Crystal structure solution, Version 97-1, Institut Anorg. Chemie, University of Göttingen, Germany, 1990.*
- [43] G. M. Sheldrick, *SHELXL-97, Program for the Refinement of Crystal Structures. University of Göttingen, Germany, 1997.*
- [44] L. Farrugia, *J. Appl. Crystallogr.* **1999**, 32, 837-838.
- [45] A. L. Spek, *Platon, A Multipurpose Crystallographic Tool, Utrecht University, Utrecht, The Netherlands, 1999.*

6. INSENSITIVE NITROGEN-RICH ENERGETIC COMPOUNDS BASED ON THE 3,3'-DINITRO-5,5'-BIS-1,2,4-TRIAZOLATE ANION

As published in: *European Journal of Inorganic Chemistry* **2012**, 21, 3474–3484.



ABSTRACT:

In this contribution the improvements achieved in the synthesis of the thermally stable energetic heterocycle 3,3'-dinitro-5,5'-bis-1H-1,2,4-triazole (DNBT) are described. The main goal was the synthesis of at least equally stable but more powerful energetic compounds based on the DNBT^{2-} anion in combination with nitrogen-rich cations. A complete structural and spectroscopic characterization including IR and Raman as well as multinuclear NMR spectroscopy of the uncharged compound is presented. Additionally, X-ray crystallographic measurements of DNBT were performed revealing a very high density of 1.903 g cm^{-3} . In order to increase both performance and stability, high nitrogen-rich salts of DNBT using the ammonium, hydroxylammonium, hydrazinium, guanidinium, aminoguanidinium and triaminoguanidinium cations were prepared and fully characterized by means of vibrational and multinuclear NMR spectroscopy, DSC measurements and X-ray diffraction measurements. The standard enthalpies of formation were calculated for selected compounds at the CBS-4M level of theory, the detonation parameters were calculated using the EXPLO5.05 program. Additionally, the impact as well as friction sensitivities and sensitivity against electrostatic discharge were determined.

INTRODUCTION

The synthesis of energetic materials has attracted research groups worldwide over the last decades.^[1] Nitrogen-rich compounds which mainly generate environmentally friendly molecular nitrogen as end-product of propulsion or explosion are in the focus of energetic materials research across the globe.^[1f, 2] Those modern heterocyclic energetic compounds derive their energy not only from the oxidation of their backbone but additionally from ring or cage strain. Due to the high positive heats of formation resulting from the large number of N–N and C–N bonds^[3] and the high level of environmental compatibility, those compounds have been studied in our group over the last couple of years with growing interest.

A prominent family of novel energetic materials are azole-based compounds, since they are generally highly endothermic with high densities and low sensitivities towards outer stimuli. Especially triazoles show a perfect balance between thermal stability and high positive heats of formation, required for applications as prospective HEDMs. Even though the heats of formation are larger for tetrazoles ($\Delta H_f^0 = + 237.2 \text{ kJ mol}^{-1}$)^[4] as well as 1,2,3-triazoles ($\Delta H_f^0 = + 272 \text{ kJ mol}^{-1}$),^[5a] 1,2,4-triazoles ($\Delta H_f^0 = + 109 \text{ kJ mol}^{-1}$)^[5b] are better suited for the development of energetic materials, since they have less catenated nitrogen atoms in one chain, which generally makes them more stable to outer stimuli.

Many energetic compounds that combine the triazole backbone with energetic moieties such as nitro groups have been synthesized over the last decades. Examples for these kind of molecules are 5-amino-3-nitro-1,2,4-triazole (ANTA),^[6] 3-nitro-5-triazolone (NTO)^[7] or also azo bridged compounds like 5,5'-dinitro-3,3'-azo-1,2,4-triazole (DNAT).^[8] The thermal stability of these materials is remarkably high with decomposition taking place well above 200 °C together with low sensitivity values. Especially the anionic species in combination with nitrogen-rich cations show excellent properties as future high explosives.^[9] In general, deprotonation of triazole species positively influences the thermal stability as well the sensitivity. In addition, the nitrogen content and the performance is increased by introduction of nitrogen-rich cations.

3,3'-Dinitro-5,5'-bis-1,2,4-triazole as well as its ammonium and guanidinium salt have been mentioned in literature before, but only characterized by means of ultraviolet absorption^[10] and infrared spectroscopy^[11] (DNBT) or investigated towards the use in gas-generating propellants (ammonium and guanidinium salt).^[12] All compounds

presented in this contribution have not been characterized structurally or in terms of their energetic properties.

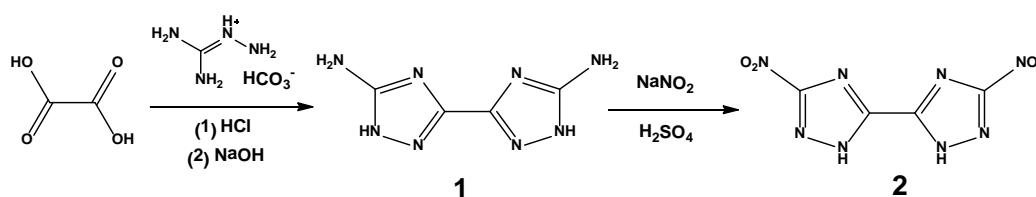
The focus of this study is on the full structural and spectroscopic characterization of the title compound 3,3'-dinitro-5,5'-bis-1,2,4-triazole as well as the formation and complete characterization of nitrogen-rich salts using ammonium, hydrazinium, hydroxylammonium, guanidinium, aminoguanidinium, and triaminoguanidinium as counterions. The potential application of the synthesized compounds as energetic materials will be studied and evaluated using the experimentally obtained values for thermal decomposition as well as sensitivity data together with calculated performance characteristics.

RESULTS AND DISCUSSION

SYNTHESIS

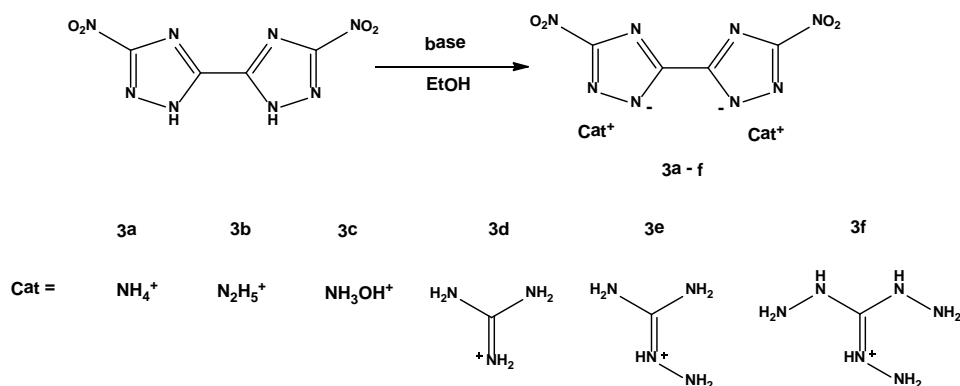
The starting material 3,3'-diamino-5,5'-bis(1*H*-1,2,4-triazole) (DABT, **1**) was first synthesized with a moderate yield of 56% by Shreve *et al.* using oxalic acid and aminoguanidine hydrochloride in water.^[13] We developed a straightforward synthetic procedure yielding DABT as elemental analysis pure compound in yields of up to 70%. The modified procedure starts with reacting oxalic acid with aminoguanidinium bicarbonate in concentrated hydrochloric acid at 70 °C, followed by isolation of the intermediate product by filtration. While heating under reflux in basic media, the molecule undergoes cyclization which leads to the formation of DABT (Scheme 1).

Oxidation of DABT was achieved by the well known Sandmeyer reaction via diazotization in sulfuric acid and subsequent reaction with sodium nitrite.^[14] The formation of 3,3'-dinitro-5,5'-bis(1*H*-1,2,4-triazole) (DNBT, **2**) was first mentioned by Russian scientists^[11] with a low yield of 31%. We were able to optimize the process by adding a suspension of DABT in 20% sulfuric acid to a solution of sodium nitrite in water at 40 °C, which leads to a remarkable increase of the yield up to 82%.



Scheme 1: Synthesis of DNBT (**2**).

The formation of the nitrogen-rich salts (**3a–f**) is straightforward. An ethanolic solution of the compound **2** was prepared and two equivalents of the corresponding nitrogen-rich bases were added (Scheme 2). Due to the high solubility of DNBt and the low solubility of compounds **3a–f** in ethanol, all ionic compounds could be isolated in excellent yields and high purity.



Scheme 2: Synthetic pathway towards the formation of nitrogen-rich salts of **2** using the corresponding bases.

All energetic compounds were fully characterized by IR and Raman as well as multinuclear NMR spectroscopy, mass spectrometry and differential scanning calorimetry. Selected compounds were additionally characterized by low temperature single crystal X-ray spectroscopy.

MOLECULAR STRUCTURES

Single crystal X-ray diffraction studies were undertaken for compounds **2**, **3a**, **3c**, **3e** and **3f**. All compounds were recrystallized from water as colorless plates or blocks, respectively. Selected crystallographic data of all compounds are compiled in Table S1 (Supporting information).

During the course of this study we only were able to obtain water free crystal structures of compound **2** as well as the nitrogen-rich salts salt **3c** and **3f**. Even though we used different solvents and crystallization methods only crystals too small for measurement (**3b,d**) or structures including crystal water (**3a,e**) were obtained. Selected bond lengths, bond angles and torsion angles of compounds **2**, **3a**, **3c**, **3e** and **3f** are compiled in Table S2 (Supporting information).

While having a closer look at the crystal structure of the uncharged compound, no difference is observed for the 1,2,4-triazole system in comparison to other triazole ring systems.^[8, 9b, 15] The bond lengths within the triazole ring in the molecular structure of **2**

are all in between the length of formal C–N and N–N single and double bonds (C–N: 1.47 Å, 1.22 Å; N–N: 1.48 Å, 1.20 Å).^[16] 3,3'-Dinitro-5,5'-bis-(1*H*-1,2,4-triazole) (**2**) crystallizes in the monoclinic space group $P2_1/n$ with a cell volume of 394.73(8) Å³ and two molecular moieties in the unit cell. The calculated density at 173 K is 1.902 g cm⁻³ and hence well above the density of the dihydrate (1.764 g cm⁻³)^[15b]. As expected, the molecule shows a completely planar assembly with a torsion angle of the nitro group towards the triazole ring of 2.9(2)°. The formula unit of **1** together with the atom labeling is presented in Figure 1.

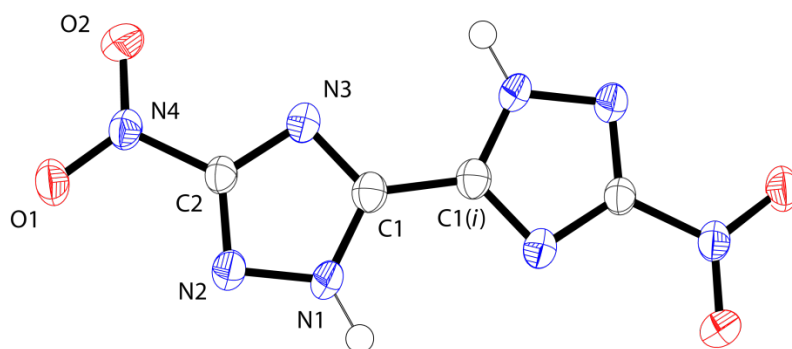


Figure 1: Crystal structure of **2**. Thermal ellipsoids are set to 50 % probability. Symmetry operators: (i) $-x$, $1-y$, $2-z$.

The structure is build up by only one individual hydrogen bond $N_1-H_1\cdots O_1$. The D–H \cdots A angle is close to 180° with 171.9(2)° and the D \cdots A length is shorter than the sum of van der Waals radii ($r_w(O) + r_w(N) = 3.07$ Å)^[16a] with 2.902(2) Å (Figure 2a). The nitrogen atoms of the triazole ring do not participate as acceptor in any hydrogen bond. As shown in Figure 2, the crystal structure of **3** consists of infinite zig-zag rows along the *b*-axis including an angle of 60.5°. The layers are stacked above each other with a layer distance of $d = 2.96$ Å. The layers are connected by two short contacts, $N_2\cdots N_4(ii)$ and $C1\cdots O_1(iii)$ (symmetry operators: (ii) $3/2-x, 1/2+y, 1/2-z$; (iii) $3/2-x, -1/2+y, 1/2-z$). Both contacts are shorter than the sum of van der Waals radii^[16a], with $N_2\cdots N_4$ being the shortest (2.922(2) Å) and $C1\cdots O_1$ being the longest (3.051(2) Å). The stacking of the layers is displayed in Figure 2b together with the distance *d* between the layers.

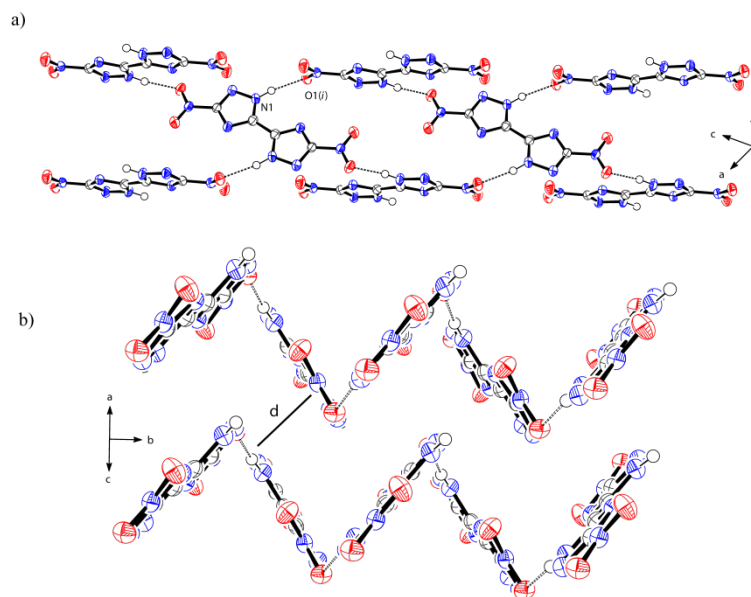


Figure 2: a) Hydrogen bonding scheme in the crystal structure of **2**. b) Wave-like arrangement of the infinite rows in the crystal structure of **2** (layer distance $d = 2.96 \text{ \AA}$). Thermal ellipsoids are set to 50 % probability. Symmetry Operators: (i) $\frac{1}{2}+x, \frac{1}{2}-y, \frac{1}{2}+z$.

In the case of the nitrogen-rich salts, only the crystal structures of compounds **3c** and **3f** will be discussed in detail. Illustrations as well as crystallographic details of the structures obtained for compounds **3a** and **3e** are collected in the Supporting Information.

Hydroxylammonium 3,3'-dinitro-bis-(1,2,4-triazolate) **3c** crystallizes in the monoclinic spacegroup $P2_1/c$ with two molecular moieties in the unit cell and a density of 1.836 g cm^{-3} . An illustration of the formula unit is shown in Figure S2 in the supporting information. As shown in Figure 3, each DNBT^{2-} anion within the crystal structure is surrounded by six hydroxylammonium cations via strong hydrogen bonds towards the nitrogen atoms of the triazole ring and the oxygen O2 of the nitro group (Table 1). It is remarkable to note that all nitrogen atoms of the triazole ring act as acceptor for hydrogen bonds, which is merely possible due to the surrounding hydroxylammonium cations. All three contacts are short with a $\text{D}\cdots\text{A}$ length of $2.706(2) \text{ \AA}$, $2.862(3) \text{ \AA}$ and $2.880(3) \text{ \AA}$, but only the hydrogen bonds $\text{O3-H3}\cdots\text{N1(i)}$ and the $\text{N5-H5a}\cdots\text{N2}$ are strongly directed with $\text{D-H}\cdots\text{A}$ angles of $172(3)^\circ$ and $173(3)^\circ$. In addition, the oxygen atom O2 acts as an acceptor in the moderately strong hydrogen bond $\text{N5-H5b}\cdots\text{O2(ii)}$ which shows a $\text{D}\cdots\text{A}$ length of $2.965(3) \text{ \AA}$ and a relatively small $\text{D-H}\cdots\text{A}$ angle of $164(3)^\circ$. Due to this strong network of hydrogen bonds with O1 being the only potential hydrogen bond acceptor

which does not participate in any short contact or other electrostatic interaction, the compound shows a remarkable high density of 1.836 g cm^{-3} .

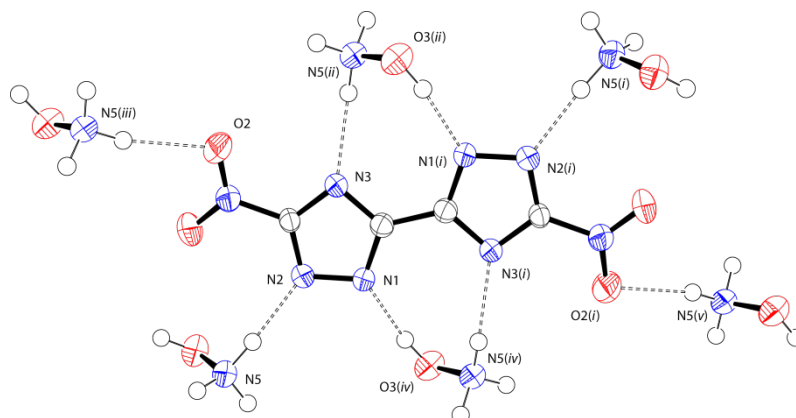


Figure 3: Surrounding of the DNBT^{2-} anion in the crystal structure of **3c**, hydrogen bonds towards hydroxylammonium cations are marked as dotted lines. Thermal ellipsoids are set to 50 % probability. Symmetry operators: (i) $1-x, 1-y, -z$; (ii) $1-x, \frac{1}{2}+y, \frac{1}{2}-z$; (iii) $1+x, \frac{1}{2}-y, \frac{1}{2}+z$; (iv) $x, \frac{1}{2}-y, -1/2+z$; (v) $-x, \frac{1}{2}+y, -1/2-z$.

The surrounding of the DNBT^{2-} anions with hydroxylammonium cations leads to the formation of layers in the bc -plane (Figure 4). The hydroxylammonium cations build up infinite rows along the a -axis and therefore connect the layers via strong hydrogen bonds. This structure of stacked layers is supported by a short contact $\text{O1}\cdots\text{O2}$ with a contact distance of $3.030(3) \text{ \AA}$.

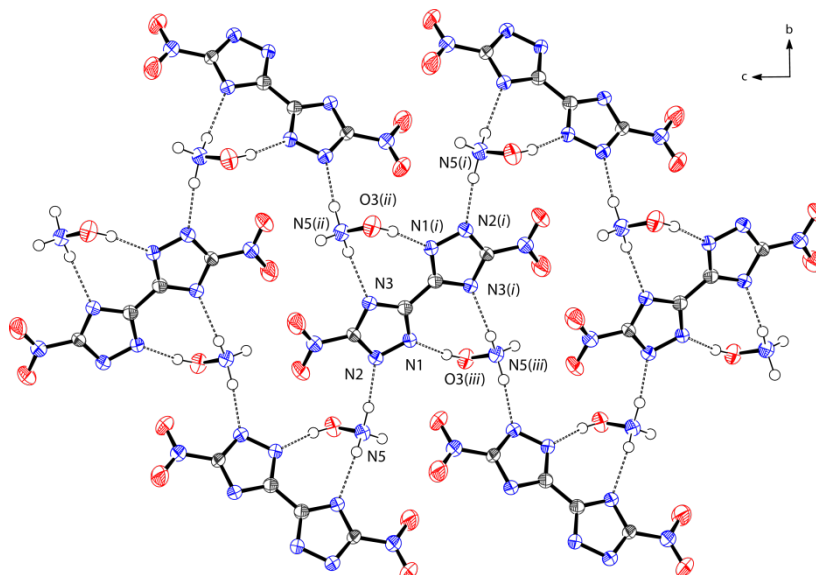


Figure 4: Hydrogen bonding scheme in the crystal structure of **3c** forming layers within the bc -plane. Thermal ellipsoids are set to 50 % probability. Symmetry operators: (i) $1-x, 1-y, -z$; (ii) $1-x, \frac{1}{2}+y, \frac{1}{2}-z$; (iii) $x, \frac{1}{2}-y, -1/2+z$.

Table 1: Hydrogen bonds present in **3c**.

D–H···A	d (D–H) [Å]	d (H···A) [Å]	d (D–H···A) [Å]	< (D–H···A) [°]
O3–H3···N1 ⁱ	0.90(4)	1.81(4)	2.706(2)	172(3)
N5–H5a···N2	1.00(4)	1.87(4)	2.862(3)	173(3)
N5–H5c···N3 ^{iv}	0.90(3)	2.04(3)	2.880(3)	157(3)
N5–H5b···O2 ⁱⁱ	0.92(3)	2.07(3)	2.965(3)	164(3)
N5–H5c···O3 ⁱⁱⁱ	0.90(3)	2.55(3)	3.018(2)	113(2)

Symmetry Operators: (i) $x, 1/2-y, 1/2+z$; (ii) $-1+x, 1/2-y, -1/2+z$; (iii) $1+x, y, z$; (iv) $1-x, -1/2+y, 1/2-z$.

The triaminoguanidinium salt (**3f**) crystallizes in the triclinic space group $P\bar{1}$ with a density of 1.664 g cm^{-3} and one formula unit in the unit cell. The molecular structure together with the labeling scheme is presented in Figure 5.

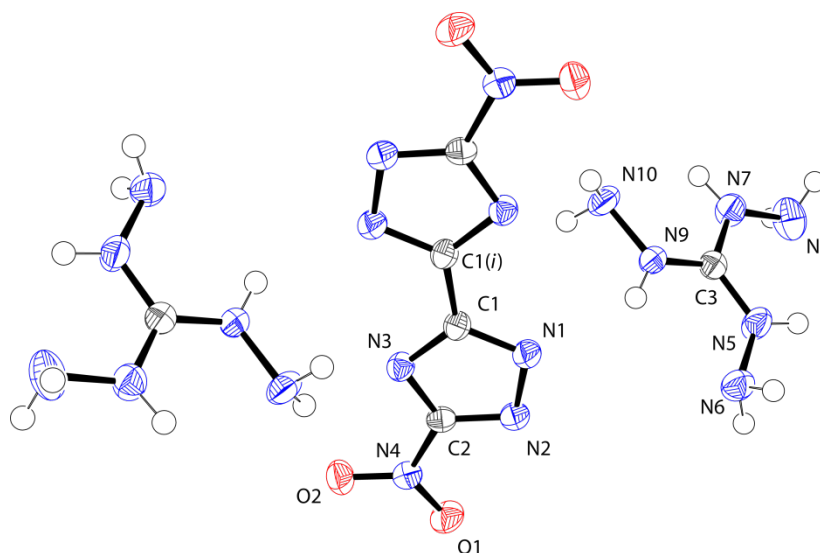


Figure 5: Crystal structure of **3f**. Thermal ellipsoids are set to 50 % probability. Symmetry operators: (i) $1-x, 1-y, -z$.

As expected for ionic compounds, the structure is build up by strong hydrogen bonds including both cations and anions. The structural main motive are the infinite rows of DNBT^{2-} anions along the b -axis. The layers of DNBT^{2-} anions are stacked with a distance of 3.307 Å and connected via hydrogen bonds towards the TAG molecules (Figure 6).

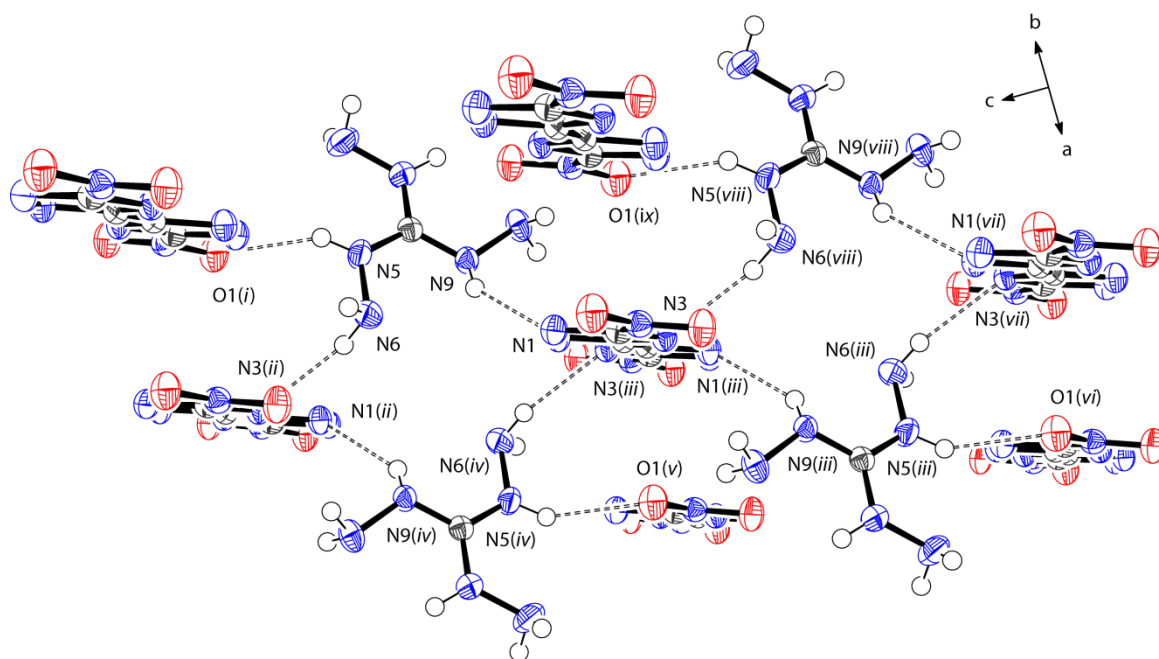


Figure 6: Hydrogen bonding scheme within the crystal structure of **3f**, displaying the connection of the infinite rows of DNBT anions by TAG cations. Thermal ellipsoids are set to 50 % probability. Symmetry operators: (i) $1-x, 2-y, 1-z$; (ii) $x, y, 1+z$; (iii) $1-x, 1-y, -z$; (iv) $1-x, 1-y, 1-z$; (v) $x, 1+y, z$; (vi) $x, -1+y, -1+z$; (vii) $1-x, 1-y, -1-z$; (viii) $x, y, -1+z$; (ix) $1-x, 2-y, -z$.

All hydrogen bond lengths lie well within the sum of van der Waals radii ($r_w(\text{O}) + r_w(\text{N}) = 3.07 \text{ \AA}$, $r_w(\text{N}) + r_w(\text{N}) = 3.20 \text{ \AA}$)^[16a] with $3.0443(16) \text{ \AA}$ ($\text{N5-H5a}\cdots\text{O1(i)}$), $3.0652(17) \text{ \AA}$ ($\text{N6-H6a}\cdots\text{N3(ii)}$) and $2.9147(17) \text{ \AA}$ ($\text{N9-H9}\cdots\text{N1}$) but are not strongly directed with angles of $147.0(14)^\circ$, $158.3(14)^\circ$ and $143.4(15)^\circ$, respectively.

Table 2: Hydrogen bonds present in **3f**.

D-H \cdots A	d (D-H) [\AA]	d (H \cdots A) [\AA]	d (D-H \cdots A) [\AA]	$\angle(\text{D-H}\cdots\text{A}) [^\circ]$
N5-H5a \cdots O1 ⁱ	0.851(16)	2.295(16)	3.0443(16)	147.0(14)
N6-H6a \cdots N3 ⁱⁱ	0.890(16)	2.221(16)	3.0652(17)	158.3(14)
N9-H9 \cdots N1	0.800(15)	2.233(15)	2.9147(17)	143.4(15)

Symmetry operators: (i) $1-x, 2-y, 1-z$; (ii) $x, y, 1+z$.

SPECTROSCOPIC DATA

Vibrational spectroscopy

IR and Raman spectra of all compounds were recorded and the frequencies were assigned according to literature.^[17] The Raman spectrum of compound **1** is dominated by the deformation mode of the amino groups at 1579 cm^{-1} . The valence stretching mode of the N–H bond is observed at 3116 cm^{-1} (IR) and 3107 cm^{-1} (Raman). After oxidation of the amino groups, the deformation modes of the amine group disappear. Instead, the nitro groups of compound **2** are observed with both, their symmetric and asymmetric stretching modes. The vibrational frequencies for the ν_{as} stretching mode of the nitro group are observed at 1551 cm^{-1} (IR) and 1546 cm^{-1} (Raman), the ν_{s} stretching modes are located at lower energy at 1410 cm^{-1} (IR) and 1393 cm^{-1} (Raman). The valence stretching mode of the N–H bond still can be observed at 3189 cm^{-1} (IR) and 3191 cm^{-1} (Raman). In addition, as for any heterocyclic compound, many combined stretching and deformation as well as torsion stretching modes can be observed in the fingerprint region between 1200 cm^{-1} and 600 cm^{-1} .^[17b]

The nitrogen-rich salts of **2** show absorption bands in the region between 3100 cm^{-1} and 3500 cm^{-1} as expected for N–H valence stretching modes of the cations (ammonium, hydrazinium and guanidines). The ν_{as} stretching modes of the nitro group are shifted to higher energy when compared to **2** and are observed between 1582 cm^{-1} and 1562 cm^{-1} in the Raman spectrum and between 1521 cm^{-1} and 1508 cm^{-1} in the IR spectrum, respectively. The symmetric stretching modes of the nitro group are in the same range as for the uncharged compound and can be found at $1410\text{--}1380\text{ cm}^{-1}$ (IR) and $1407\text{--}1383\text{ cm}^{-1}$ (Raman).

The combined stretching and deformation modes as well as torsion modes for the triazole ring are again observed between 1200 cm^{-1} and 600 cm^{-1} for the nitrogen-rich salts.

Multinuclear NMR spectroscopy

All compounds were investigated using ^1H , ^{13}C and ^{14}N NMR spectroscopy. Additionally, ^{15}N NMR spectra were recorded for compounds **2** and **3e**. The two signals of the uncharged compounds **1** and **2** differ only slightly in the $^{13}\text{C}\{^1\text{H}\}$ NMR spectrum. Both compounds show two signals in the expected range.^[8, 9c] One singlet for the bridging

carbon atom at 149.3 ppm for DABT (**1**) and at 145.6 ppm for DNBT (**2**). The oxidation of the amino group leads to a shift of the other carbon atom signal towards lower field from 157.3 ppm (**1**) to 162.7 ppm for compound **2**. The proton located at the triazole ring can be observed for DNBT and is located at a chemical shift of 9.68 ppm. In the $^{14}\text{N}\{^1\text{H}\}$ NMR spectra, the nitro group of compound **2** can be identified by a broad singlet at –26 ppm. The NMR signals of all compounds are summarized in Table 3.

Table 3: NMR signals of compounds **2**, **3a–f**.

compound	DNBT ^{2-*}		cation	
	$^{13}\text{C}\{^1\text{H}\}$	$^{14}\text{N}\{^1\text{H}\}$	^1H	$^{14}\text{N}\{^1\text{H}\}$
2	162.7, 145.6	–26	/	/
3a	165.5, 157.4	–18	7.16	–359
3b	165.0, 156.5	–22	7.24	–359
3c	165.1, 155.5	–14	5.52	/
				$^{13}\text{C}\{^1\text{H}\}$
3d	165.2, 156.6	–23	7.57	158.2
3e	165.4, 157.1	–17	7.60, 4.73	157.8
3f	165.6, 157.8	–16	7.61, 4.56	159.0

* DNBT in the case of **2**

As described in previous publications for triazole compounds,^[9b, 18] the deprotonation of DNBT with nitrogen-rich bases shifts the signals in the $^{13}\text{C}\{^1\text{H}\}$ NMR spectra to lower field. The carbon atom connecting both triazole rings can be found in the range of 155.5–157.4 ppm, the carbon atom connected to the nitro group is located in the range of 165.1–165.6 ppm. A trend for the shift of the nitro group signal in the $^{14}\text{N}\{^1\text{H}\}$ NMR spectra could not be observed, all signals could be found at chemical shifts of –18 to –23 ppm. The $^{14}\text{N}\{^1\text{H}\}$ NMR spectra of **3a** and **3b** additionally show the signal of the corresponding cation at –359 ppm. The signals of all nitrogen-rich cations in the ^1H NMR spectrum could be found in the expected range and assigned according to similar ionic compounds bases on triazolate anions.^[9c]

Four well resolved resonances are observed in the ^{15}N NMR spectra for the four nitrogen atoms of both compounds **2** and **3f** (Figure 12). In addition, the two signal of the triaminoguanidinium cation could be observed for compound **3f**. The signals were assigned by comparison to literature values.^[17a, 19]

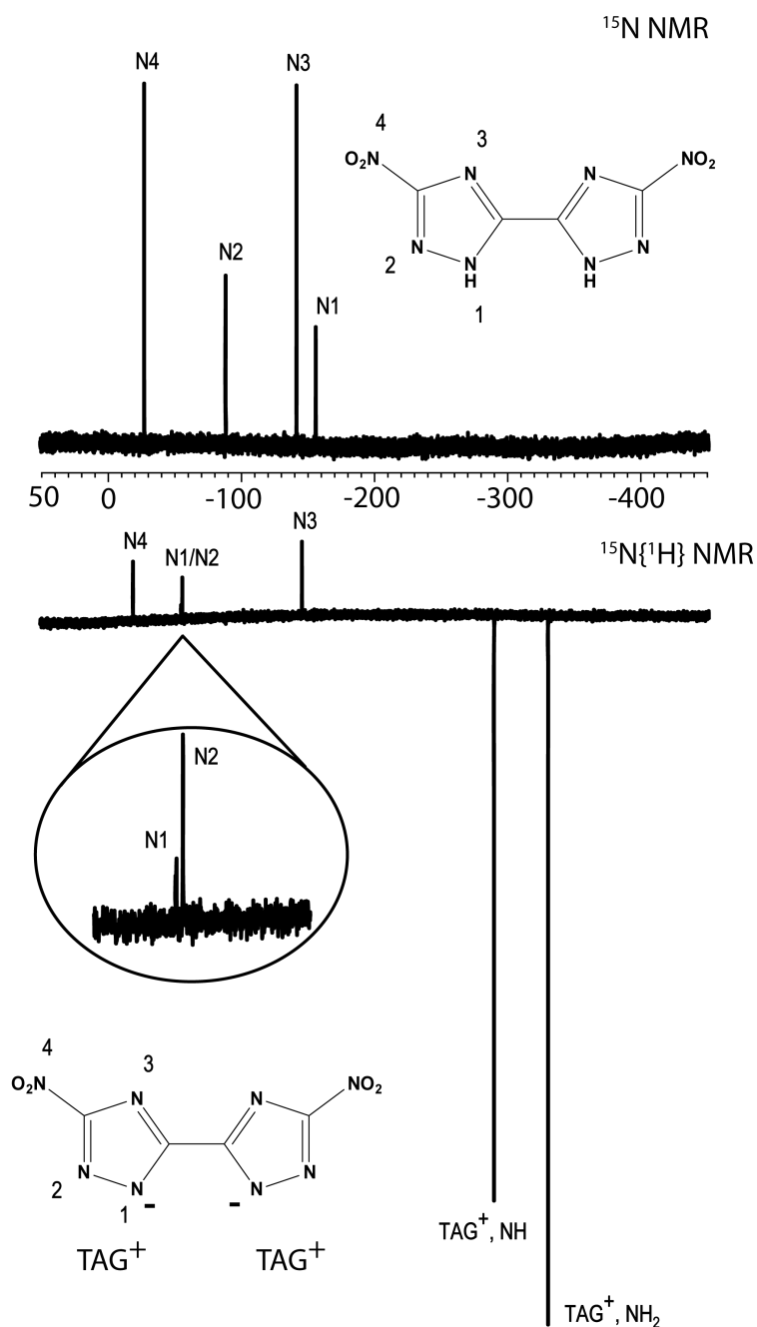


Figure 7: ^{15}N NMR spectra of 3,3'-dinitro-5,5'-bis-1H-1,2,4-triazole (**2**, top) and bis(triaminoguanidinium)-3,3'-dinitro-5,5'-bis-1H-1,2,4-triazolate (**3e**, bottom); x-axis represents the chemical shift δ in ppm.

As expected, the nitrogen atoms N1, N2 and N4 are shifted to lower field upon deprotonation. The largest effect can be observed for the nitrogen atom N1, which can now be found at a chemical shift of -55.3 ppm (-156.1 ppm for **2**).

THEORETICAL CALCULATIONS, PERFORMANCE CHARACTERISTICS AND STABILITIES

All calculations regarding energies of formation were carried out using the Gaussian G09W Version 7.0 program package.^[20] Since very detailed descriptions of the calculation process have been published earlier^[9c] and can be found in specialized books,^[1b] only a short summary of computational methods will be given. The enthalpies (H) and Gibbs free energies (G) were calculated using the complete basis set method (CBS) of Petersson et al. in order to obtain very accurate energies. In this contribution, we used the modified CBS-4M method with M referring to the use of minimal population localization, which is a re-parameterized version of the original CBS-4 computational method and also includes additional empirical calculations.^[21] The enthalpies of formation for the gas phase species were computed according to the atomization energy method, using NIST^[22] values as standardized values for the atoms standard heats of formation ($\Delta_f H^0$) according to equation 1.^[23]

$$\Delta_f H^0_{(g, \text{Molecule}, 298)} = H_{(\text{Molecule})} - \sum H^0_{(\text{Atoms})} + \sum \Delta_f H^0_{(\text{Atoms}, \text{NIST})} \quad (1)$$

The solid state enthalpy of formation for uncharged compounds is estimated from the computational results using Troutons rule,^[24] where T_m was taken equal to the decomposition temperatures.

$$\Delta H_m = \Delta_f H^0_{(g, \text{Molecule}, 298)} - \Delta H_{\text{sub}} = \Delta_f H^0_{(g, \text{Molecule}, 298)} - (188 [\text{J mol}^{-1} \text{K}^{-1}] * T_m) \quad (2)$$

The solid state enthalpies of formation for the ionic compounds are derived from the calculation of the corresponding lattice energies (U_L) and lattice enthalpies (H_L), calculated from the corresponding molecular volumes, using the equations provided by Jenkins et al.^[25] The derived molar standard enthalpies of formation for the solid state (ΔH_m) were used to calculate the solid state energies of formation (ΔU_m) according to equation three, with Δn being the change of moles of gaseous components.^[1b]

$$\Delta U_m = \Delta H_m - \Delta n RT \quad (3)$$

The calculated standard energies of formation were used to perform predictions of the detonation parameters with the program package Explo5, Version 5.05.^[26] The program is based on the chemical equilibrium, steady state model of detonation. It uses Becker-Kistiakowsky-Wilsons equation of state (BKW EOS) for gaseous detonation products together with Cowan-Ficketts equation of state for solid carbon.^[27] The calculation of the equilibrium composition of the detonation products is performed by applying modified White, Johnson and Dantzig's free energy minimization technique. The program was designed to enable calculations of detonation parameter at the Chapman-Jouguet point. The BKW equation as implemented in the Explo5 program was used with the BKW-G set of parameters (α , β , κ , θ) as stated below the equation, with X_i being the mol fraction of the i -th gaseous detonation product while k_i is the molar co-volume of the i -th gaseous detonation product.^[26-27]

$$pV/RT = 1 + xe^{\beta x} \quad \text{with} \quad x = (\kappa \sum X_i k_i) / [V(T + \theta)]^\alpha \quad (4)$$

$$\alpha = 0.5, \beta = 0.096, \kappa = 17.56, \theta = 4950$$

The results of the detonation runs, together with the calculated energies of formation and the corresponding sensitivities, are compiled in Table 4.

Compound **2** already shows a remarkably high thermal stability of 251 °C together with an insensitivity towards friction and a moderate sensitivity towards impact (10 J). In comparison, the 3,3'-dinitrimino-5,5'-bis-1*H*-1,2,4-triazole recently published by Shreeve *et al.* decomposes at 165 °C.^[29] The beneficial detonation parameters of DNBT with $v_{\text{det}} = 8413 \text{ m s}^{-1}$ are mainly based on the highly positive heat of formation (285 kJ mol⁻¹) and the remarkably high density of 1.902 g cm⁻³ (X-ray measurement).

Table 4: Physico-chemical properties of compounds **2**, **3a–f** in comparison to hexogen (RDX).

	2	3a	3b	3c	3d	3e	3f	RDXⁿ
Formula	C ₄ H ₂ N ₈ O ₄	C ₄ H ₈ N ₁₀ O ₄	C ₄ H ₁₀ N 12O ₄	C ₄ H ₈ N ₁ 0O ₆	C ₆ H ₁₂ N 14O ₄	C ₆ H ₁₄ N 16O ₄	C ₆ H ₁₈ N 20O ₄	C ₃ H ₆ N ₆ O ₆
M [g mol ⁻¹]	226.1	261.0	290.2	292.1	344.2	374.2	434.3	222.1
IS [J] ^a	10	40	15	40	40	40	40	7
FS [N] ^b	360	360	360	360	360	360	360	120
ESD–test [J]	0.1	0.5	0.15	0.5	0.75	1.0	0.5	--
N [%] ^c	49.45	53.84	57.92	47.94	56.96	59.88	64.50	37.8
Q [%] ^d	–35.4	–49.2	–49.6	–49.2	–65.1	–64.1	–62.6	–21.6
T _{dec.} [°C] ^e	251	252	237	204	335	253	201	210
ρ [g cm ⁻³] ^f	1.902	1.7*	1.7*	1.836	1.7*	1.7*	1.664	1.80
Δ _f H _m ^o [kJ mol ⁻¹] ^g	285	109	412	189	125	355	828	70
Δ _f U ^o [kJ kg ⁻¹] ^h	1338	522	1530	617	470	1060	2027	417
EXPLO5 (V5.05) values:								
–Δ _E U ^o [kJ kg ⁻¹] ⁱ	4888	4176	4914	4277	3419	3839	4538	6125
T _E [K] ^j	3890	3121	3399	3111	2596	2782	3045	4236
p _{C-J} [kbar] ^k	320	248	281	299	225	248	271	349
V _{Det.} [m s ⁻¹] ^l	8413	7938	8400	8477	7699	8020	8365	8748
Gas vol. [L kg ⁻¹] ^m	642	771	798	771	760	780	811	739

^[a] BAM drop hammer; ^[b] BAM friction tester; ^[c] Nitrogen content; ^[d] Oxygen balance; ^[e] Temperature of decomposition by DSC ($\beta = 5$ °C, Onset values); ^[f] derived from X-ray structure; ^[g] Molar enthalpy of formation; ^[h] Energy of formation; ^[i] Energy of Explosion; ^[j] Explosion temperature; ^[k] Detonation pressure; ^[l] Detonation velocity; ^[m] Assuming only gaseous products; ^[n] values based on Ref. ^[28] and the EXPLO5.4 database; *Density values of **3a**, **3b**, **3d** and **3e** based on pycnometer measurements and compared to trends in the row of triazolate salts.^[9c]

Since salts of energetic compounds tend to be more stable as the uncharged compound, the nitrogen-rich salts of DNBT are expected to show an improved stability. The decomposition temperatures of the ammonium salt (**3a**) and aminoguanidinium salt (**3e**) are in the range of the uncharged compound, the decomposition temperature of the guanidium compound (**3d**) is even higher (335 °C). As shown in Figure 8, the decomposition temperature decreases in the row of compounds **3a–c** with the ammonium salt (**3a**) showing the highest value of 252 °C and the hydroxylammonium salt (**3c**) showing a decomposition onset at 204 °C. The same trend can be observed for the series of guanidinium derivatives (**3d–f**). The guanidinium salt (**3d**) shows the highest decomposition temperature with 335 °C, followed by the aminoguanidinium salt (**3e**) (253 °C) and the triaminoguanidinium salt (**3f**) with a decomposition onset at 201 °C.

Nearly all compounds are insensitive towards friction, impact and electrostatic discharge, only the hydrazinium salt is moderately sensitive towards impact (15 J). The nitrogen-rich salts of DNBT all exhibit highly positive heats and energies of formation in the range of the similar nitrimino compound.^[29] The detonation velocities were calculated in the range of 7699 m s^{-1} (**3d**) to 8477 m s^{-1} (**3b**). The best performances were calculated for the hydrazinium salt (**3f**) with a detonation velocity of 8400 m s^{-1} and the hydroxylammonium salt (**3c**) with a detonation velocity of 8477 m s^{-1} , which is around 4% lower than the performance of RDX.

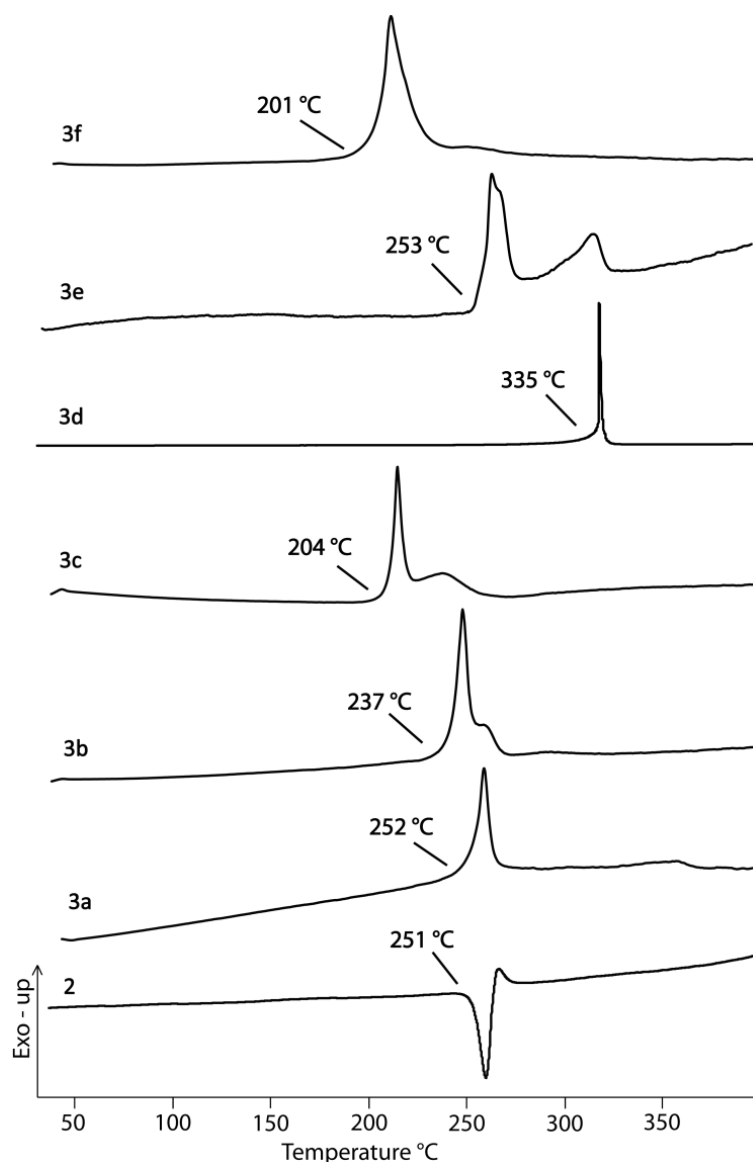


Figure 8: DSC plots of DNBT (**2**), $(\text{NH}_4^+)_2\text{DNBT}^{2-}$ (**3a**), $(\text{N}_2\text{H}_5^+)_2\text{DNBT}^{2-}$ (**3b**), $(\text{NH}_3\text{OH}^+)_2\text{DNBT}^{2-}$ (**3c**), $(\text{G}^+)_2\text{DNBT}^{2-}$ (**3d**), $(\text{AG}^+)_2\text{DNBT}^{2-}$ (**3e**) and $(\text{TAG}^+)_2\text{DNBT}^{2-}$ (**3f**). DSC plots were recorded with a heating rate of $5 \text{ }^\circ\text{C min}^{-1}$.

Since the focus of this study was the evaluation of potential replacements for commonly used secondary explosive, only three compounds show suitable values regarding the detonation parameters, sensitivities and thermal stability. The best compounds suitable for replacing RDX would be the triaminoguanidinium as well as the hydroxylammonium salt, taking into account the performance values and sensitivities. Compound **3c** displays the best performance with a calculated detonation velocity of 8477 m s^{-1} , a detonation pressure of 299 kbar and a decomposition temperature of 204°C . The triaminoguanidinium compound exhibits energetic properties in the same range with 8365 m s^{-1} , a detonation pressure of 271 kbar and a decomposition temperature of 201°C . In addition, both compounds are in contrast to RDX insensitive towards friction and impact.

The performance characteristics of the hydrazinium compound (**3b**) would be even better in comparison to **3f** with a calculated detonation velocity of 8400 m s^{-1} and a detonation pressure of 281 kbar. Unfortunately, the compound is sensitive towards impact (15 J). Although the guanidinium salt **3d** shows lower performance values ($v_{\text{det}} = 7699 \text{ m s}^{-1}$, $p_{\text{C-J}} = 225 \text{ kbar}$) than **3c** and **3f**, it displays an excellent decomposition temperature of 335°C together with an insensitivity towards friction and impact and could therefore be a potential replacement for HNS. Even though all compounds are not able to perform better than RDX by calculations they can probably find use in certain applications for civilian use or as burn rate modifiers in military applications.

CONCLUSION

The starting material DABT (**1**) was synthesized following a modified literature known procedure^[13] resulting in an increase of the yield from 56% up to 70%. The optimization of the reaction conditions for the oxidation of the amino compound to 3,3'-dinitro-5,5'-bis(1*H*-1,2,4-triazole) (DNBT, **2**)^[11] resulted in an improvement of the yield from 31% up to 82%. Compound **2** can therefore be considered as low cost starting material for new energetic materials and has been fully characterized by means of vibrational and multinuclear NMR spectroscopy, mass spectrometry and differential scanning calorimetry. The uncharged compound **2** shows a thermal stability of 251°C together with an insensitivity towards friction and a moderate sensitivity towards impact (10 J). Due to the calculated positive heat of formation (285 kJ mol^{-1}), the detonation parameters ($v_{\text{det}} = 8413 \text{ m s}^{-1}$) are well in the range of RDX.

Energetic ionic compounds were synthesized from **2** using nitrogen-rich cations, all reactions were carried out using the free bases or their corresponding carbonates. All energetic, ionic compounds (**3a–f**) were characterized with the same techniques as described for the uncharged compounds. Crystal structures could be obtained from selected compounds and were discussed in detail for compounds **2**, **3c** and **3f**. All ionic compounds reveal positive heats of formation in the range of 109 kJ mol⁻¹ (**3a**) to 828 kJ mol⁻¹ (**3f**). The most interesting compounds regarding the energetic properties are the hydroxylammonium and triaminoguanidinium compound (**3c** and **3f**) as well as the hydrazinium salt (**3b**). All of these compounds exhibit decomposition temperatures of above 200 °C and performance values in the range of RDX (8477 m s⁻¹ (**3c**), 8365 m s⁻¹ (**3f**)). Worth mentioning is the guanidinium salt (**3d**) with a remarkable high decomposition temperature of 335 °C and an insensitivity against friction and impact. Those compounds could find application since they are easy to obtain, safe to handle and show performance characteristics in the range of modern secondary explosives.^[2e]

EXPERIMENTAL PART

Caution: Although all presented nitroazoles are rather stable against outer stimuli, proper safety precautions should be taken, when handling the dry materials. All derivatives of DNBT are energetic materials and tend to explode under the influence of heat, impact or friction. Lab personnel and the equipment should be properly grounded and protective equipment like earthed shoes, leather coat, Kevlar[®] gloves, ear protection and face shield is recommended.

General. All chemical reagents and solvents were obtained from Sigma-Aldrich Inc. or Acros Organics (analytical grade) and were used as supplied without further purification. ¹H, ¹³C{¹H}, ¹⁴N{¹H} and ¹⁵N NMR spectra were recorded on a JEOL Eclipse 400 instrument in DMSO-*d*₆ at 25 °C. The chemical shifts are given relative to tetramethylsilane (¹H, ¹³C) or nitro methane (¹⁴N, ¹⁵N) as external standards and coupling constants are given in Hertz (Hz). Infrared (IR) spectra were recorded on a Perkin-Elmer Spectrum BX FT-IR instrument equipped with an ATR unit at 25 °C. Transmittance values are qualitatively described as “very strong” (vs), “strong” (s), “medium” (m), “weak” (w) and “very weak” (vw). Raman spectra were recorded on a Bruker RAM II spectrometer equipped with a Nd:YAG laser (200 mW) operating at 1064 nm and a reflection angle of 180°. The intensities are reported as percentages of the most intense

peak and are given in parentheses. Elemental analyses (CHNO) were performed with a Netzsch Simultaneous Thermal Analyzer STA 429. Melting and decomposition points were determined by differential scanning calorimetry (Linseis PT 10 DSC, calibrated with standard pure indium and zinc). Measurements were performed at a heating rate of $5\text{ }^{\circ}\text{C min}^{-1}$ in closed aluminum sample pans with a $1\text{ }\mu\text{m}$ hole in the lid for gas release to avoid an unsafe increase in pressure under a nitrogen flow of 20 mL min^{-1} with an empty identical aluminum sample pan as a reference.

For initial safety testing, the impact and friction sensitivities as well as the electrostatic sensitivities were determined. The impact sensitivity tests were carried out according to STANAG 4489,^[30] modified according to WIWEB instruction 4-5.1.02^[31] using a BAM^[32] drop hammer. The friction sensitivity tests were carried out according to STANAG 4487^[33] and modified according to WIWEB instruction 4-5.1.03^[34] using the BAM^[32] friction tester. The electrostatic sensitivity tests were accomplished according to STANAG 4490^[35] using an electric spark testing device ESD 2010EN (OZM Research) operating with the “Winspark 1.15 software package”.

Crystallographic measurements. The single crystal X-ray diffraction data of **2**, **3a**, **3e**, **3f** were collected using an Oxford Xcalibur3 diffractometer equipped with a Spellman generator (voltage 50 kV, current 40 mA) and a KappaCCD detector. The data collection was undertaken using the CrysAlis CCD software^[36] while the data reduction was performed with the CrysAlis Red software^[37]. Crystals of compound **3c** were investigated using a Bruker-Nonius Kappa CCD diffractometer equipped with a rotating molybdenum anode and Montel-graded multilayered X-ray optics. The structures were solved with Sir-92^[38] or Shelxs-97^[39] and refined with Shelxl-97^[40] implemented in the program package WinGX^[41] and finally checked using Platon^[42]. Further information regarding the crystal-structure determination were deposited with the Cambridge Crystallographic Data Centre^[43] as supplementary publication Nos. 864398 (**2**), 864400 (**3a**), 864399 (**3c**), 864397 (**3e**), 864401 (**3f**).

3,3'-Diamino-5,5'-bis(1H-1,2,4-triazole) (DABT, 1)

According to a modified literature procedure^[13], hydrochloric acid (60 mL) was added to a stirred mixture of oxalic acid (20.0 g, 159 mmol) and aminoguanidinium bicarbonate (45.4 g, 332 mmol). The reaction was stirred at $70\text{ }^{\circ}\text{C}$ for one hour and the precipitate was collected by filtration. The colorless solid was dissolved in water (240 mL) and alkalized with sodium hydroxide to $\text{pH} = 14$. The reaction mixture was refluxed for one hour and

subsequently acidified with acetic acid to pH = 4. The resulting precipitate was collected by filtration, washed with water (appr. 200 mL) and dried in air to yield 3,3'-diamino-5,5'-bis(1,2,4-1*H*-triazole) (**1**) (18.6 g, 112 mmol, 70%) as a colorless solid.

¹H nmr (DMSO-*d*₆): δ = 6.46 (s, 2H, NH₂) ppm. **¹³C nmr** (DMSO-*d*₆): δ = 157.3, 149.3 ppm. **IR**: ν (cm⁻¹) (rel. int.) = 3325(m), 3116(m), 2863(m), 2784(m), 1706(s), 1668(s), 1654(s), 1618(m), 1606(m), 1484(m), 1457(m), 1267(m), 1104(vs), 1061(s), 987(w), 956(w), 769(w), 721(s). **Raman** (200 mW): ν (cm⁻¹) (rel. int.) = 1636(62), 1614(100), 1591(67), 1575(57), 1495(13), 1439(21), 1432(21), 1361(9), 1152(24), 1143(23), 1059(23), 1042(34), 1022(22), 980(27), 772(18), 554(7), 413(11), 328(12), 249(16). **Elemental analysis** (C₄H₆N₁₀): calc.: C 28.92, H 3.64, N 67.44; found: C 28.72, H 3.58, N 66.11. **Mass spectrometry**: m/z (DEI+): 166.1 [C₄H₇N₈⁺].

3,3'-Dinitro-5,5'-bis(1*H*-1,2,4-triazole) (DNBT, **2**)

A solution of 3,3'-diamino-5,5'-bis(1*H*-1,2,4-triazole) (**1**) (11.9 g, 72 mmol) in 20% sulfuric acid (140 mL) was added drop wise to a solution of sodium nitrite (10 eq., 98.8 g, 1.4 mol) in water (140 mL) at 40 °C. The mixture was stirred at 50 °C for 1 h. After cooling down to room temperature the mixture was acidified with sulfuric acid (20%) until no evolution of nitrogen dioxide could be observed. The precipitate was collected by filtration and dissolved in boiling water. The hot solution was filtrated and allowed to cool to room temperature. Collection of the pale green precipitate affords 3,3'-dinitro-5,5'-bis(1*H*-1,2,4-triazole) dihydrate (15.5 g, 59 mmol, 82%) as a crystalline solid.

¹H nmr (DMSO-*d*₆): δ = 9.68 (s, 2H, H_{Triazole}) ppm; **¹³C nmr** (DMSO-*d*₆): δ = 162.7, 145.6 ppm; **¹⁴N nmr** (DMSO-*d*₆): δ = -26 (-NO₂) ppm; **¹⁵N nmr** (DMSO-*d*₆): δ = -27.8 (N4), -88.8 (N2), -141.7 (N3), -156.1 (N1) ppm. **IR**: ν (cm⁻¹) (rel. int.) = 3599(m), 3499(m), 3052(w), 2849(w), 2747(w), 2670(m), 2621(m), 2574(m), 2530(m), 2488(m), 2419(m), 1844(w), 1609(m), 1532(vs), 1466(w), 1416(vs), 1314(vs), 1245(m), 1183(m), 1024(m), 953(s), 837(s), 690(w), 690(w). **Raman** (200 mW): ν (cm⁻¹) (rel. int.) = 3192(3), 1641(100), 1546(28), 1519(5), 1485(75), 1468(43), 1458(95), 1413(18), 1393(97), 1365(6), 1362(6), 1345(13), 1325(27), 1306(35), 1172(58), 1062(67), 1015(31), 855(4), 774(8), 744(5), 619(4), 511(4), 452(5), 452(5), 399(9), 297(9), 203(6). **Elemental analysis** (C₄H₂N₈O₄): calc.: C 21.25, H 0.89, N 49.56; found: C 21.44, H 0.95, N 49.19. **Mass spectrometry**: m/z (FAB-): 225.1 [C₄HN₈O₄⁻]. **Sensitivities**

(grain size: <100 μm): friction: 360 N, impact: 10 J, ESD: 0.1 J; **DSC** (onset, 5 $^{\circ}\text{C min}^{-1}$): $T_{\text{Dec.}}$: 251 $^{\circ}\text{C}$.

Ammonium 3,3'-dinitro-5,5'-bis(1H-1,2,4-triazolate) (3a)

3,3'-dinitro-5,5'-bis(1H-1,2,4-triazole) (**9**) (250 mg, 1.1 mmol) was dissolved in ethanol (50 mL). Ammonia was passed through the solution for 5 min. Collection of the precipitate by filtration affords ammonium 3,3'-dinitro-5,5'-bis(1H-1,2,4-triazolate) (**3a**) (374 mg, 1.0 mmol, 91%) as a yellow solid.

^1H nmr (DMSO- d_6): δ = 7.16 (s, 8H, NH_4^+) ppm; **^{13}C nmr** (DMSO- d_6): δ = 165.4, 159.1 (CH_7N_4^+), 157.1 ppm; **^{14}N nmr** (DMSO- d_6): δ = -18 (- NO_2), -359 (NH_4^+) ppm; **^{15}N nmr** (DMSO- d_6): δ = -20.0 (N4), -58.6 (N1), -59.2 (N2), -147.3 (N3), -358.5 (NH_4^+) ppm. **IR**: ν (cm^{-1}) (rel. int.) = 3265(m), 2999(m), 2890(m), 2852(m), 2786(m), 1704(w), 1671(m), 1521(s), 1457(s), 1438(s), 1408(s), 1390(vs), 1306(s), 1244(s), 1090(s), 1036(m), 984(m), 841(s), 714(m), 661(m). **Raman** (200 mW): ν (cm^{-1}) (rel. int.) = 1572(58), 1555(7), 1541(1), 1523(7), 1480(10), 1472(24), 1427(3), 1405(39), 1399(51), 1352(45), 1314(1), 1300(3), 1109(76), 1101(100), 1072(6), 1032(9), 850(13), 779(2), 765(2), 521(1), 472(2), 420(2), 298(2), 298(2), 206(2). **Elemental analysis** ($\text{C}_4\text{H}_8\text{N}_{10}\text{O}_4$): calc.: C 18.47, H 3.10, N 53.84; found: C 18.79, H 3.04, N 53.28. **Mass spectrometry**: m/z (FAB $^+$): 18 [NH_4^+]. m/z (FAB $^-$): 225.1 [$\text{C}_4\text{HN}_8\text{O}_4^-$]. **Sensitivities** (grain size: <100 μm): friction: 360 N, impact: 40 J, ESD: 0.5 J; **DSC** (onset, 5 $^{\circ}\text{C min}^{-1}$): $T_{\text{Dec.}}$: 252 $^{\circ}\text{C}$.

Hydrazinium 3,3'-dinitro-5,5'-bis(1H-1,2,4-triazolate) (3b)

3,3'-Dinitro-5,5'-bis(1H-1,2,4-triazole) (**2**) (250 mg, 1.1 mmol) was dissolved in ethanol (50 mL) followed by addition of hydrazine hydrate (0.11 mL, 2.2 mmol). Collection of the precipitate by filtration affords hydrazinium 3,3'-dinitro-5,5'-bis(1H-1,2,4-triazolate) (263 mg, 0.9 mmol, 83%) (**3b**) as a yellow solid.

^1H nmr (DMSO- d_6): δ = 7.24 (s, N_2H_5^+) ppm; **^{13}C nmr** (DMSO- d_6): δ = 165.0, 156.5 ppm; **^{14}N nmr** (DMSO- d_6): δ = -22 (- NO_2), -359 (N_2H_5^+) ppm; **IR**: ν (cm^{-1}) (rel. int.) = 3346(w), 3258(w), 2648(m), 1642(w), 1586(w), 1509(s), 1455(vs), 1392(vs), 1306(s), 1263(s), 1135(m), 1110(s), 1104(s), 1043(m), 990(m), 968(s), 836(vs), 709(m), 652(m). **Raman** (200 mW): ν (cm^{-1}) (rel. int.) = 1575(30), 1554(3), 1525(4), 1516(5), 1485(16), 1400(61), 1355(44), 1305(4), 1113(100), 1032(6), 970(2), 845(12), 778(2), 765(3), 473(2), 408(2), 293(1), 210(4). **Elemental analysis** ($\text{C}_4\text{H}_{10}\text{N}_{12}\text{O}_4$): calc.: C 16.56, H 3.47, N 57.92; found: C 16.89, H 3.44, N 57.28. **Mass spectrometry**: n.d. **Sensitivities**

(grain size: <100 μm): friction: 360 N, impact: 15 J, ESD: 0.15 J; **DSC** (onset, 5 $^{\circ}\text{C min}^{-1}$): $T_{\text{Dec.}}$: 237 $^{\circ}\text{C}$.

Hydroxylammonium 3,3'-dinitro-5,5'-bis(1H-1,2,4-triazolate) (3c)

3,3'-Dinitro-5,5'-bis(1H-1,2,4-triazole) (**2**) (250 mg, 1.1 mmol) was dissolved in ethanol (50 mL) followed by addition of hydroxylamine (50% in H_2O , 145 mg, 2.2 mmol). The mixture was refluxed for 30 min and allowed to cool to room temperature. Collection of the precipitate by filtration affords hydroxylammonium 3,3'-dinitro-5,5'-bis(1H-1,2,4-triazolate) (**3c**) (273 mg, 0.9 mmol, 93%) as a yellow solid.

^1H nmr (DMSO-d_6): δ = 5.52 (s, NH_3OH^+) ppm; **^{13}C nmr** (DMSO-d_6): δ = 165.1, 155.5 ppm; **^{14}N nmr** (DMSO-d_6): δ = -14 ($-\text{NO}_2$) ppm; **^{15}N nmr** (DMSO-d_6): δ = -22.5 (N4), -64.0 (N1), -75.3 (N2), -155.8 (N3), -296.9 (NH_4OH^+). **IR**: ν (cm^{-1}) (rel. int.) = 3174(w), 2915(w), 2668(w), 2510(w), 1614(w), 1537(w), 1508(m), 1483(w), 1473(w), 1454(s), 1401(vs), 1310(s), 1266(m), 1248(m), 1218(w), 1119(s), 1050(w), 998(m), 843(s), 801(m), 766(w), 710(w), 656(w), 656(w). **Raman** (200 mW): ν (cm^{-1}) (rel. int.) = 1582(37), 1526(5), 1480(14), 1408(58), 1363(43), 1311(2), 1117(100), 1041(5), 1003(3), 851(7). **Elemental analysis** ($\text{C}_4\text{H}_8\text{N}_{10}\text{O}_6$): calc.: C 16.44, H 2.76, N 47.94; found: C 17.03, H 2.74, N 47.90. **Mass spectrometry**: m/z (FAB+): 126.1 [$\text{Matrix}+\text{NH}_3\text{O}^+$]; m/z (FAB-): 224.9 [$\text{C}_4\text{HN}_8\text{O}_4^-$]. **Sensitivities** (grain size: <100 μm): friction: 360 N, impact: 40 J, ESD: 0.5 J; **DSC** (onset, 5 $^{\circ}\text{C min}^{-1}$): $T_{\text{Dec.}}$: 204 $^{\circ}\text{C}$.

Guanidinium 3,3'-dinitro-5,5'-bis(1H-1,2,4-triazolate) (3d)

3,3'-Dinitro-5,5'-bis(1H-1,2,4-triazole) (**2**) (250 mg, 1.1 mmol) was dissolved in ethanol (50 mL) followed by addition of guanidinium carbonate (198 mg, 1.1 mmol). The mixture was refluxed for half an hour, the precipitate was collected by filtration affording guanidinium 3,3'-dinitro-5,5'-bis(1H-1,2,4-triazolate) (**3d**) (331 mg, 1.0 mmol, 87%) as a yellow solid.

^1H nmr (DMSO-d_6): δ = 7.57 (s, 12H, CH_6N_3^+) ppm; **^{13}C nmr** (DMSO-d_6): δ = 165.2, 158.2 (CH_6N_3^+), 156.6 ppm; **^{14}N nmr** (DMSO-d_6): δ = -23 ($-\text{NO}_2$) ppm; **IR**: ν (cm^{-1}) (rel. int.) = 3467(m), 3357(w), 3143(m), 1663(s), 1560(w), 1510(s), 1447(s), 1387(vs), 1302(s), 1246(m), 1105(s), 1036(w), 990(w), 843(s), 716(m), 689(w), 655(w). **Raman** (200 mW): ν (cm^{-1}) (rel. int.) = 1568(44), 1554(8), 1540(3), 1525(5), 1516(7), 1470(25), 1401(56), 1389(43), 1348(71), 1298(4), 1099(100), 1088(77), 1065(14), 1060(20), 1029(12), 1008(28), 849(16), 778(2), 764(3), 536(7), 472(5), 419(3), 207(3). **Elemental**

analysis ($\text{C}_6\text{H}_{12}\text{N}_{14}\text{O}_4$): calc.: C 20.93, H 3.51, N 56.96; found: C 19.88, H 4.95, N 47.06. **Mass spectrometry**: m/z (FAB+): 60.1 [CH_6N_3^+]. m/z (FAB-): 225 [$\text{C}_4\text{HN}_8\text{O}_4^-$]. **Sensitivities** (grain size: <100 μm): friction: 360 N, impact: 40 J, ESD: 0.75 J; **DSC** (onset, 5 $^\circ\text{C min}^{-1}$): $T_{\text{Dec.}}$: 335 $^\circ\text{C}$

Aminoguanidinium 3,3'-dinitro-5,5'-bis(1H-1,2,4-triazolate) (3e)

3,3'-Dinitro-5,5'-bis(1H-1,2,4-triazole) (**2**) (250 mg, 1.1 mmol) was dissolved in ethanol (50 mL) followed by addition of aminoguanidinium bicarbonate (299 mg, 2.2 mmol). The mixture was refluxed for 30 min and allowed to cool to room temperature. Collection of the precipitate by filtration affords aminoguanidinium 3,3'-dinitro-5,5'-bis(1H-1,2,4-triazolate) (**3e**) (374 mg, 1.0 mmol, 91%) as a yellow solid.

^1H nmr (DMSO- d_6): δ = 9.38 (s, 2H, AG^+), 7.60 (s, 4H, CH_7N_4^+), 4.73 (s, 8H, CH_7N_4^+) ppm; **^{13}C nmr** (DMSO- d_6): δ = 165.4, 159.1 (CH_7N_4^+), 157.1 ppm; **^{14}N nmr** (DMSO- d_6): δ = -17 (- NO_2) ppm; **IR**: ν (cm^{-1}) (rel. int.) = 3265(m), 2999(m), 2890(m), 2852(m), 2786(m), 1704(w), 1671(m), 1521(s), 1457(s), 1438(s), 1408(s), 1390(vs), 1306(s), 1244(s), 1090(s), 1036(m), 984(m), 841(s), 714(m), 661(m). **Raman** (200 mW): ν (cm^{-1}) (rel. int.) = 1572(58), 1555(7), 1541(1), 1523(7), 1480(10), 1472(24), 1427(3), 1405(39), 1399(51), 1352(45), 1314(1), 1300(3), 1109(76), 1101(100), 1072(6), 1032(9), 850(13), 779(2), 765(2), 521(1), 472(2), 420(2), 298(2), 298(2), 206(2). **Elemental analysis** ($\text{C}_6\text{H}_{14}\text{N}_{16}\text{O}_4$): calc.: C 19.25, H 3.77, N 59.88; found: C 18.17, H 3.81, N 46.95. **Mass spectrometry**: m/z (FAB+): 75.1 [CH_7N_3^+]. m/z (FAB-): 225.1 [$\text{C}_4\text{HN}_8\text{O}_4^-$]. **Sensitivities** (grain size: <100 μm): friction: 360 N, impact: 40 J, ESD: 1.0 J; **DSC** (onset, 5 $^\circ\text{C min}^{-1}$): $T_{\text{Dec.}}$: 253 $^\circ\text{C}$.

Triaminoguanidinium 3,3'-dinitro-5,5'-bis(1,2,4-1H-triazolate) (3f)

3,3'-Dinitro-5,5'-bis(1H-1,2,4-triazole) (**2**) (250 mg, 1.1 mmol) was dissolved in ethanol (50 mL) followed by addition of triaminoguanidine (230 mg, 2.2 mmol). The mixture was refluxed for 30 min and allowed to cool to room temperature. Collection of the precipitate by filtration affords triaminoguanidinium 3,3'-dinitro-5,5'-bis(1H-1,2,4-triazolate) (**3f**) (292 mg, 0.7 mmol, 61%) as a yellow solid.

^1H nmr (DMSO- d_6): δ = 8.69 (s, 3H, CH_9N_6^+), 4.56 (s, 6H, TAG^+) ppm; **^{13}C nmr** (DMSO- d_6): δ = 165.6, 159.0 (CH_9N_6^+), 157.8 ppm; **^{14}N nmr** (DMSO- d_6): δ = -16 (- NO_2) ppm; **^{15}N nmr** (DMSO- d_6): δ = -19.4 (N4), -55.3 (N1), -56.3 (N2), -145.7 (N3), -289.4 (CH_9N_6^+ , NH), -329.8 (CH_9N_6^+ , NH_2) ppm. **IR**: ν (cm^{-1}) (rel. int.) = 3343(m),

3308(s), 3184(m), 1671(vs), 1585(m), 1520(s), 1446(s), 1380(s), 1347(m), 1295(s), 1236(s), 1194(m), 1132(s), 1088(s), 1034(s), 978(vs), 962(s), 838(s), 739(w), 714(m). **Raman** (200 mW): ν (cm^{-1}) (rel. int.) = 1573(10), 1563(49), 1555(31), 1542(4), 1514(16), 1461(26), 1384(67), 1340(41), 1293(4), 1083(100), 1018(6), 990(2), 894(2), 841(2), 765(2), 464(3), 412(2). **Elemental analysis** ($\text{C}_6\text{H}_{18}\text{N}_{20}\text{O}_4$): calc.: C 16.59, H 4.18, N 64.50; found: C 17.58, H 3.98, N 63.30. **Mass spectrometry**: m/z (FAB+): 105.1 [CH_9N_6^+]. m/z (FAB-): 225.1 [$\text{C}_4\text{HN}_8\text{O}_4^-$]. **Sensitivities** (grain size: $<100\text{ }\mu\text{m}$): friction: 360 N, impact: 40 J, ESD: 0.5 J; **DSC** (onset, $5\text{ }^\circ\text{C min}^{-1}$): T_{Dec} : $201\text{ }^\circ\text{C}$.

REFERENCES

- [1] a) T. M. Klapötke, *Chemistry of high-energy materials*, De Gruyter, Berlin, **2011**;
 b) T. M. Klapötke, *Chemie der hochenergetischen Materialien*, de Gruyter, Berlin, **2009**; c) P. F. Pagoria, G. S. Lee, A. R. Mitchell, R. D. Schmidt, *Thermochimica Acta* **2002**, 384, 187-204; d) R. P. Singh, R. D. Verma, D. T. Meshri, J. M. Shreeve, *Angew. Chem. Int. Ed.* **2006**, 45, 3584-3601; e) C. M. Sabate, T. M. Klapötke, *New Trends in Research of Energetic Materials, Proceedings of the Seminar, 12th, Pardubice, Czech Republic, Apr. 1-3*, **2009**, 172-194; f) S. Yang, S. Xu, H. Huang, W. Zhang, X. Zhang, *Huaxue Jinzhan* **2008**, 20, 526-537; g) M. B. Talawar, R. Sivabalan, T. Mukundan, H. Muthurajan, A. K. Sikder, B. R. Gandhe, A. S. Rao, *J. Hazard. Mater.* **2009**, 161, 589-607.
- [2] a) T. M. Klapötke, J. Stierstorfer, A. U. Wallek, *Chem. Mater.* **2008**, 20, 4519-4530; b) T. M. Klapötke, C. M. Sabate, *Chem. Mater.* **2008**, 20, 3629-3637; c) D. E. Chavez, M. A. Hiskey, D. L. Naud, *Prop. Explos. Pyrot.* **2004**, 29, 209-215; d) Y. Huang, H. Gao, B. Twamley, J. M. Shreeve, *Eur. J. Inorg. Chem.* **2008**, 2560-2568; e) H. Gao, J. M. Shreeve, *Chem. Rev.* **2011**, 111, 7377-7436.
- [3] T. M. Klapötke, in *Structure and bonding* (Ed.: D. M. P. Mingos), Springer-Verlag, Berlin Heidelberg **2007**.
- [4] V. A. Ostrovskii, M. S. Pevzner, T. P. Kofman, I. V. Tselinskii, *Targets Heterocyclic systems* **1999**, 3, 467-526.
- [5] a) J. B. Pedley, *Thermodynamic Research Center Data Series, Vol. 1*, College Station, **1994**. b) P. Jiminez, M. V. Roux, C. J. Turrion, *J. Chem. Thermodyn.* **1989**, 21, 759-764.
- [6] K. Y. Lee, C. B. Storm, M. A. Hiskey, M. D. Coburn, *J. Energ. Mater.* **1991**, 9, 415-428.
- [7] a) S. L. Collignon, R. E. Farncomb, K. L. Wagaman, *US 861 H 19901204*, **1990**
 b) J. Schmidt, H. Gehlen, *Z. Chem.* **1965**, 5, 304.
- [8] D. L. Naud, M. A. Hiskey, H. H. Harry, *J. Energ. Mater.* **2003**, 21, 57-62.
- [9] a) L. Y. Lee, M. M. Stinecipher, **1993**, US 450,788; b) D. E. Chavez, B. C. Tappan, B. A. Mason, D. Parrish, *Prop. Explos. Pyrot.* **2009**, 34, 475-479; c) A. Dippold, Thomas M. Klapötke, Franz A. Martin, *Z. Anorg. Allg. Chem.* **2011**, 637, 1181-1193.

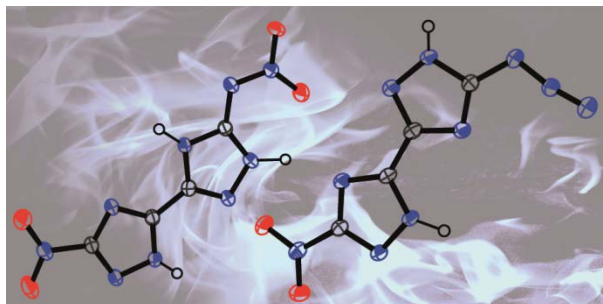
- [10] Y. V. Serov, M. S. Pevzner, T. P. Kofman, I. V. Tselinskii, *J. Org. Chem. USSR (English Translation)* **1990**, 26, 773-777.
- [11] L. I. Bagal, M. S. Pevzner, A. N. Frolov, N. I. Sheludyakova, *Chem. Heterocyc. Comp.* **1970**, 6, 240-244.
- [12] a) G. K. Williams, S. P. Burns, I. B. Mishra, Automotive Systems Laboratory, Inc., USA . **2005**; b) C. G. Miller, G. K. Williams, Automotive Systems Laboratory, Inc., USA . **2006**.
- [13] R. N. Shreve, R. K. Charlesworth, Purdue Research Foundation . **1956**, US 2,744,116.
- [14] J. P. Agrawal, *Organic Chemistry of Explosives*, John Wiley and Sons, Ltd, **2007**.
- [15] a) T. P. Kofman, *Russ. J. Org. Chem.* **2002**, 38, 1231-1243; b) E. V. Nikitina, G. L. Starova, O. V. Frank-Kamenetskaya, M. S. Pevzner, *Kristallografiya* **1982**, 27, 485-488.
- [16] a) A. F. Hollemann, E. Wiberg, N. Wiberg, *Lehrbuch der anorganischen Chemie*, de Gruyter, New York, **2007**; b) F. H. Allen, O. Kennard, D. G. Watson, L. Brammer, A. G. Orpen, R. Taylor, *J. Chem. Soc., Perkin Trans. 2* **1987**, S1-S19.
- [17] a) M. Hesse, *Spektroskopische Methoden in der organischen Chemie*, 7th ed., Thieme Verlag, Stuttgart, **2005**; b) F. Billes, H. Endredi, G. Keresztury, *Theochem* **2000**, 530, 183-200.
- [18] A. A. Dippold, M. Feller, T. M. Klapötke, *Cent. Eur. J. Energ. Mat.* **2011**, 8, 261 - 278.
- [19] H. H. Licht, H. Ritter, H. R. Bircher, P. Bigler, *Magn. Reson. Chem.* **1998**, 36, 343-350.
- [20] M. J. Frisch, G. W. Trucks, H. B. Schlegel, G. E. Scuseria, M. A. Robb, J. R. Cheeseman, G. Scalmani, V. Barone, B. Mennucci, G. A. Petersson, H. Nakatsuji, M. Caricato, X. Li, H. P. Hratchian, A. F. Izmaylov, J. Bloino, G. Zheng, J. L. Sonnenberg, M. Hada, M. Ehara, K. Toyota, R. Fukuda, J. Hasegawa, M. Ishida, T. Nakajima, Y. Honda, O. Kitao, H. Nakai, T. Vreven, J. A. J. Montgomery, J. E. Peralta, F. Ogliaro, M. Bearpark, J. J. Heyd, E. Brothers, K. N. Kudin, V. N. Staroverov, R. Kobayashi, J. Normand, K. Raghavachari, A. Rendell, J. C. Burant, S. S. Iyengar, J. Tomasi, M. Cossi, N. Rega, J. M. Millam, M. Klene, J. E. Knox, J. B. Cross, V. Bakken, C. Adamo, J. Jaramillo, R. Gomperts, R. E. Stratmann, O. Yazyev, A. J. Austin, R. Cammi, C. Pomelli, J. W. Ochterski, R. L. Martin, K. Morokuma, V. G. Zakrzewski, G. A. Voth, P. Salvador, J. J. Dannenberg, S.

- Dapprich, A. D. Daniels, Ö. Farkas, J. B. Foresman, J. V. Ortiz, J. Cioslowski, D. J. Fox, *Wallingford CT*, **2009**.
- [21] a) J. A. Montgomery, Jr., M. J. Frisch, J. W. Ochterski, G. A. Petersson, *J. Chem. Phys.* **2000**, *112*, 6532-6542; b) J. W. Ochterski, G. A. Petersson, J. A. Montgomery, Jr., *J. Chem. Phys.* **1996**, *104*, 2598-2619.
- [22] P. J. Lindstrom, W. G. Mallard, NIST Chemistry Webbook, NIST Standard Reference 69, June 2005, National Institute of Standards and technology, Gaithersburg MD, <http://webbook.nist.gov>
- [23] a) E. F. C. Byrd, B. M. Rice, *J. Phys. Chem. A* **2006**, *110*, 1005-1013; b) B. M. Rice, J. J. Hare, *J. Phys. Chem. A* **2002**, *106*, 1770-1783; c) B. M. Rice, S. V. Pai, J. Hare, *Combust. Flame* **1999**, *118*, 445-458.
- [24] a) F. Trouton, *Philos. Mag.* **1884**, *18*, 54-57; b) M. S. Westwell, M. S. Searle, D. J. Wales, D. H. Williams, *J. Am. Chem. Soc.* **1995**, *117*(18), 5013-5015.
- [25] a) H. D. B. Jenkins, D. Tudela, L. Glasser, *Inorg. Chem.* **2002**, *41*, 2364-2367; b) H. D. B. Jenkins, H. K. Roobottom, J. Passmore, L. Glasser, *Inorg. Chem.* **1999**, *38*, 3609-3620.
- [26] M. Sućeska, *EXPLO5.5 program, Zagreb, Croatia*, **2010**.
- [27] a) M. Sućeska, *Materials Science Forum* **2004**, 465-466, 325-330; b) M. Suceška, *Prop. Explos. Pyrot.* **1999**, *24*, 280-285; c) M. Suceška, *Prop. Explos. Pyrot.* **1991**, *16*, 197-202.
- [28] R. Meyer, J. Köhler, A. Homburg, *Explosives*, Sixth ed., Wiley-VCH Verlag GmbH & Co. KGaA, Weinheim, **2007**.
- [29] R. Wang, H. Xu, Y. Guo, R. Sa, J. M. Shreeve, *J. Am. Chem. Soc.* **2010**, *132*, 11904-11905.
- [30] *NATO standardization agreement (STANAG) on explosives and impact tests, no.4489, 1st ed., Sept. 17, 1999*.
- [31] *WIWEB-Standardarbeitsanweisung 4-5.1.02, Ermittlung der Explosionsgefährlichkeit, hier: der Schlagempfindlichkeit mit dem Fallhammer, Nov. 08, 2002*.
- [32] <http://www.bam.de>.
- [33] *NATO standardization agreement (STANAG) on explosives, friction tests, no.4487, 1st ed., Aug. 22, 2002*.

- [34] *WIWEB-Standardarbeitsanweisung 4-5.1.03, Ermittlung der Explosionsgefährlichkeit, hier: der Reibempfindlichkeit mit dem Reibeapparat, Nov. 08, 2002.*
- [35] *NATO standardization agreement (STANAG) on explosives, electrostatic discharge sensitivity tests, no.4490, 1st ed., Feb. 19, 2001.*
- [36] *CrysAlis CCD, Oxford Diffraction Ltd., Version 1.171.27p5 beta (release 01-04-2005 CrysAlis171.NET).*
- [37] *CrysAlis RED, Oxford Diffraction Ltd., Version 1.171.27p5 beta (release 01-04-2005 CrysAlis171 .NET).*
- [38] A. Altomare, G. Casciarano, C. Giacovazzo, A. Guagliardi, *J. Appl. Crystallogr.* **1993**, 26, 343-350.
- [39] G. M. Sheldrick, *SHELXS-97, Crystal structure solution, Version 97-1, Institut Anorg. Chemie, University of Göttingen, Germany, 1990.*
- [40] G. M. Sheldrick, *SHELXL-97, Program for the Refinement of Crystal Structures. University of Göttingen, Germany, 1997.*
- [41] L. Farrugia, *J. Appl. Crystallogr.* **1999**, 32, 837-838.
- [42] A. L. Spek, *Platon, A Multipurpose Crystallographic Tool, Utrecht University, Utrecht, The Netherlands, 1999.*
- [43] *Crystallographic data for the structure(s) have been deposited with the Cambridge Crystallographic Data Centre. Copies of the data can be obtained free of charge on application to The Director, CCDC, 12 Union Road, Cambridge CB2 1EZ, UK (Fax: int.code (1223)336-033; e-mail for inquiry: fileserv@ccdc.cam.ac.uk; e-mail for deposition: deposit-@ccdc.cam.ac.uk).*

7. ASYMMETRICALLY SUBSTITUTED 5,5'-BISTRIAZOLES – NITROGEN-RICH MATERIALS WITH VARIOUS ENERGETIC FUNCTIONALITIES

As published in: *Dalton Transactions* **2013**, 42, 11136–11145.



ABSTRACT:

In this contribution the synthesis and full structural and spectroscopic characterization of three asymmetrically substituted bis-1,2,4-triazoles, along with different energetic moieties like amino, nitro, nitrimino and azido moieties is presented. Additionally, selected nitrogen-rich ionic derivatives have been prepared and characterized. This comparative study on the influence of these energetic moieties on structural and energetic properties contains a complete characterization including IR, Raman and multinuclear NMR spectroscopy. Single crystal X-ray crystallographic measurements were performed and deliver insight into structural characteristics as well as inter- and intramolecular interactions. The standard enthalpies of formation were calculated for all compounds at the CBS-4M level of theory, revealing highly positive heats of formation for all compounds. The detonation parameters were calculated using the EXPLO5 program and compared to the common secondary explosive RDX as well as recently published symmetric bistriazoles. As expected, the measured sensitivities to mechanical stimuli and decomposition temperatures strongly depend on the energetic moiety of the triazole ring. All compounds were characterized in terms of sensitivities (impact, friction, electrostatic) and thermal stabilities, the ionic derivatives were found to be thermally stable, insensitive compounds

INTRODUCTION

In the past, the chemistry of explosives has been largely guided by intuition, experience and testing. Nowadays, a better understanding of the basic principles and relationships which are necessary to predict the properties of an energetic material lead to a more rational design of novel compounds with tailored properties. The academic research mainly focuses on the work with energetic systems to determine factors affecting stability and performance and to bring new strategies into the design of energetic materials.

The main challenge is the desired combination of a large energy content with a maximum possible chemical stability to ensure safe synthesis and handling. Modern heterocyclic energetic compounds derive their energy not only from the oxidation of their carbon backbone, but additionally from ring or cage strain, high-nitrogen content and high heats of formation.¹⁻⁶ Nitrogen-rich heterocycles are promising compounds that fulfill many requirements in the challenging field of energetic materials research.^{5, 7-11} A prominent family of novel high-energy-density materials (HEDMs) are azole-based compounds, since they are generally highly endothermic with high densities and low sensitivities towards outer stimuli. Owing to the high positive heats of formation resulting from the large number of N–N and C–N bonds¹² and the high level of environmental compatibility, triazole and tetrazole compounds have been studied over the last couple of years with growing interest.

Many energetic compounds that combine the triazole backbone with energetic moieties have been synthesized over the last decades. Examples for these kind of molecules are 5-amino-3-nitro-1,2,4-triazole (ANTA),¹³ 2-azido-5-nitramino-1,2,4-triazole¹⁴ or trinitromethyl-substituted triazoles¹⁵. Bridged compounds like 5,5'-dinitro-3,3'-azo-1,2,4-triazole (DNAT)¹⁶ or the analogue nitrimino-compound (DNAAT)¹⁷ have already been investigated and show remarkably high decomposition temperatures and excellent energetic properties. Recently investigated symmetrically substituted bistriazoles connected via C–C bond show promising properties as energetic materials.¹⁸⁻²⁷

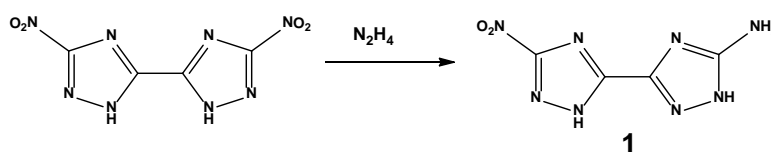
The focus of this contribution is on the full structural and spectroscopic characterization of three different asymmetrically substituted bis-1,2,4-triazoles along with energetic moieties like amino, nitro, nitramino and azido groups. We present a comparative study on the influence of those energetic moieties on structural and energetic properties in comparison to literature known symmetric 5-5'-bistriazoles. The potential application of the synthesized compounds as energetic material will be studied and evaluated using the

experimentally obtained values for the thermal decomposition, the sensitivity data, as well as the calculated performance characteristics.

RESULTS AND DISCUSSION

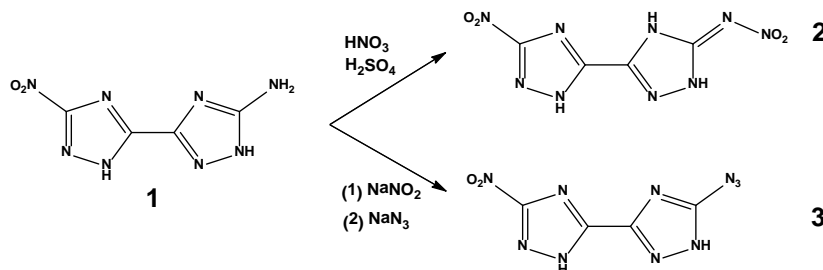
SYNTHESIS

3,3'-Diamino-5,5'-bis(1*H*-1,2,4-triazole) and 3,3'-dinitro-5,5'-bis(1*H*-1,2,4-triazole) were synthesized according to literature.²⁷ The synthesis is based on the reaction of oxalic acid and aminoguanidinium bicarbonate in concentrated hydrochloric acid and subsequent cyclisation in basic media. Oxidation of 3,3'-diamino-5,5'-bis(1*H*-1,2,4-triazole) was accomplished by the well known Sandmeyer reaction via diazotization in sulfuric acid and subsequent reaction with sodium nitrite. As shown in Scheme 1, one nitro group of 3,3'-dinitro-5,5'-bis(1*H*-1,2,4-triazole) was successfully reduced to 5-(5-amino-1*H*-1,2,4-triazol-3-yl)-3-nitro-1*H*-1,2,4-triazole (**1**), similar to the selective reduction of the mono-heterocycle 3,5-dinitro-1*H*-1,2,4-triazole.¹³



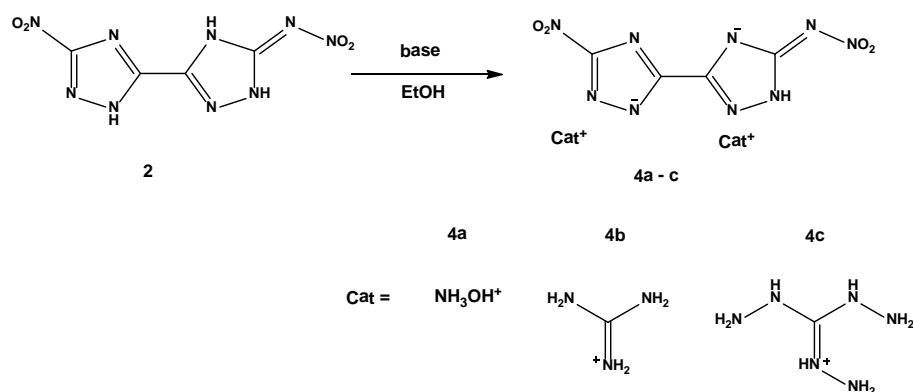
Scheme 1 Synthesis of 5-(5-amino-1*H*-1,2,4-triazol-3-yl)-3-nitro-1*H*-1,2,4-triazole (ANBT, **1**)

The amine group of 5-(5-amino-1*H*-1,2,4-triazol-3-yl)-3-nitro-1*H*-1,2,4-triazole (**1**) was further converted to a nitrimino and an azido moiety (Scheme 2). The treatment of **1** with a mixture of sulfuric acid/nitric acid (6:1) leads to the formation of 5-(5-nitrimino-1,3*H*-1,2,4-triazol-3-yl)-3-nitro-1*H*-1,2,4-triazole (NNBT, **2**). The azido compound 5-(5-azido-1*H*-1,2,4-triazol-3-yl)-3-nitro-1*H*-1,2,4-triazole (AzNBT, **3**) was synthesized via diazotization in sulfuric acid and subsequent reaction with an excess of sodium azide.



Scheme 2 Synthesis of 5-(5-nitrimino-1,3*H*-1,2,4-triazol-3-yl)-3-nitro-1*H*-1,2,4-triazole (NNBT, **2**) and 5-(5-azido-1*H*-1,2,4-triazol-3-yl)-3-nitro-1*H*-1,2,4-triazole (AzNBT, **3**).

Additionally, selected nitrogen-rich ionic derivatives based on compound **2** have been prepared in order to increase both performance and stability. The formation of the nitrogen-rich salts (**4a–c**) is straightforward. An ethanolic solution of compound **2** was prepared and two equivalents of the corresponding nitrogen-rich bases were added (Scheme 3). Due to the high solubility of compound **2** and the low solubility of compounds **4a–c** in ethanol, all ionic compounds could be isolated in excellent yields and high purity.



Scheme 3: Synthetic pathway towards the formation of nitrogen-rich salts of **2** using the corresponding bases.

All energetic compounds were fully characterized by IR and Raman as well as multinuclear NMR spectroscopy, mass spectrometry and differential scanning calorimetry. Selected compounds were additionally characterized by low temperature single crystal X-ray diffractometry.

VIBRATIONAL SPECTROSCOPY

IR and Raman spectra of all compounds were recorded and the frequencies were assigned according to literature.^{28, 29}

The Raman spectrum of compound **1** is dominated by the deformation mode of the amino groups at 1629 cm^{-1} . The valence stretching mode of the N–H bond is observed in the range of $3224\text{--}3402\text{ cm}^{-1}$. The vibrational frequencies for the asymmetric stretching mode of the nitro group are observed at 1397 cm^{-1} (IR) and 1434 cm^{-1} (Raman). The symmetric stretching modes are located at lower energy at 1308 cm^{-1} (IR) and 1396 cm^{-1} (Raman). After nitration of the amino group, the deformation modes of the amine group disappear. Instead, the asymmetric valence stretching mode of the nitrimino moiety of compound **2** can be observed at 1581 cm^{-1} . In the case of compound **3**, a signal for the

asymmetric stretching modes of the azide group can be observed at 2160 cm^{-1} in the Raman spectrum and at 2143 cm^{-1} in the IR spectrum. The vibrational frequencies for the ν_{as} stretching mode of the nitro group are as well observed at 1540 cm^{-1} (IR) and 1505 cm^{-1} (Raman), the ν_{s} stretching modes are located at 1393 cm^{-1} (IR) and 1389 cm^{-1} (Raman).

The nitrogen-rich salts **4a–c** show additional absorption bands in the region between 3100 cm^{-1} and 3500 cm^{-1} as expected for N–H valence stretching modes of the cations (hydroxylammonium and guanidine derivatives).

MULTINUCLEAR NMR SPECTROSCOPY

All compounds were investigated using ^1H , ^{13}C and ^{14}N NMR spectroscopy. Additionally, ^{15}N NMR spectra were recorded for compounds **1–3**. All compounds show four signals in the ^{13}C NMR spectrum for the 1,2,4-triazole carbon atoms in the expected range. One singlet for the bridging carbon atom can be found at chemical shifts of 142.9 (**2**) to 150.6 ppm (**1**). The signal of the carbon atom connected to the variable energetic moieties is shifted in all cases to lower field in comparison to compound **1** (153.1 (**2**) to 155.5 ppm (**3**)), the signal for the carbon atom connected to the nitro group remains almost constant in all cases similar to the symmetric 3,3'-dinitro-5,5'-bis(1*H*-1,2,4-triazole).²⁷

In the ^{14}N NMR spectra, the nitro group of compounds **1–3** can be identified by a broad singlet at -23 (**1,2**) to -30 ppm (**3**). The azido moiety in compound **3** can be observed as a broad singlet at -146 ppm in the ^{14}N NMR spectrum. Well resolved resonances could only be observed in the ^{15}N NMR spectrum (as discussed below). The NMR signals of all compounds are summarized in Table 1.

Table 1: NMR signals of compounds **2**, **3a–f** in DMSO- d_6 .

	δ [ppm]				
	$^{13}\text{C}\{^1\text{H}\}$			$^{14}\text{N}\{^1\text{H}\}$	^1H
	C-NO ₂	C-X ^[a]	C-C		
1	163.5	158.3	150.6, 149.1	−23	6.41
2	163.1	153.1	146.6, 142.9	−23	12.39
3	163.0	155.5	147.3, 146.8	−30, −146	6.11

[a] X = NH₂ (**1**), =N-NO₂ (**2**), N₃ (**3**).

The deprotonation of compound **2** with nitrogen-rich bases shifts the signals in the $^{13}\text{C}\{^1\text{H}\}$ NMR spectra to lower field. The carbon atom connected to the nitro group is located in the range of 164.1–165.6 ppm, whereas the carbon atom connected to the nitrimino moiety can be found at 157.3–159.2 ppm. The nitro group signal in the $^{14}\text{N}\{^1\text{H}\}$ NMR spectra could be observed for all ionic compounds at -17 ppm. The $^{14}\text{N}\{^1\text{H}\}$ NMR spectra of **3b–c** additionally show the signal of the corresponding cation at -359 ppm.

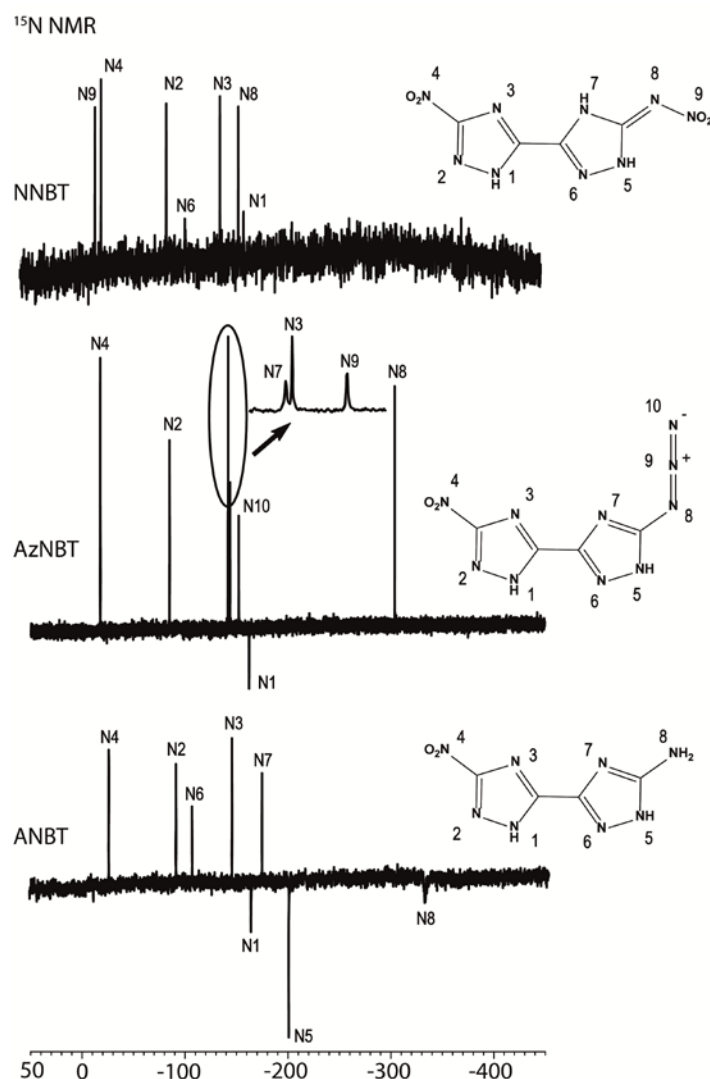


Fig. 1 ^{15}N NMR spectra of 5-(5-nitrimino-1,3H-1,2,4-triazol-3-yl)-3-nitro-1H-1,2,4-triazole (**2**, top), 5-(5-azido-1H-1,2,4-triazol-3-yl)-3-nitro-1H-1,2,4-triazole (**3**, middle) and 5-(5-amino-1H-1,2,4-triazol-3-yl)-3-nitro-1H-1,2,4-triazole (**1**, bottom) recorded in $\text{DMSO}-d_6$; x-axis represents the chemical shift δ in ppm.

The assignments in the ^{15}N NMR spectra are based on the comparison with the symmetric bistriazoles²⁷ and additional theoretical calculations using Gaussian 09 (MPW1PW91/aug-cc-pVDZ).³⁰ In all cases, four well resolved resonances are observed

in the ^{15}N NMR spectrum for the four nitrogen atoms of the nitrotriazole moiety in the expected range (Figure 1). In the case of compound **1**, the signals of the aminotriazole moiety are located at -106.5 ppm (N6), -173.8 ppm (N7), -199.7 ppm (N5) and -330.9 ppm (N8). The two signals of the nitrogen atoms N5 and N6 in the spectrum of compound **3** could not be observed, as it is often the case for 5-azidotriazoles due to a fast proton exchange.³¹ All other signals of the azido-triazole moiety could be observed in the same range compared to 3,3'-diazido-5,5'-bis(1*H*-1,2,4-triazole).²⁷ The three signal of the azido moiety are well resolved and can be found in the expected range with N4 being shifted to highest field with a chemical shift of -295.4 ppm. Compound **2** exhibits only the signals of the nitrogen atoms N6 (-108.4 ppm) and N8 (-159.7 ppm) of the triazole ring as well as the additional nitro group (N9, -22.1 ppm). Similar to compound **3**, the signals for N5 and N7 are not visible

SINGLE CRYSTAL X-RAY STRUCTURE ANALYSIS

Single crystal X-ray diffraction studies were undertaken for compounds **2** and **3**, both compounds were recrystallized from water to obtain crystals suitable for X-Ray analysis. In the following, the structural characteristics of these compounds will be discussed in detail in comparison to the recently published symmetric bistriazoles.²⁷

5-(5-nitrimino-1,3*H*-1,2,4-triazol-3-yl)-3-nitro-1*H*-1,2,4-triazole (**2**) crystallizes as tetrahydrate in the triclinic space group *P*-1 with a cell volume of $629.3(2) \text{ \AA}^3$ and two molecular moieties in the unit cell. The calculated density at 173 K is 1.653 g cm^{-3} and hence well below the corresponding symmetric dinitro- (1.902 \AA^3)²⁷ and dinitrimino (1.772 \AA^3)²³ compound. As expected, the bistriazole moiety shows a completely planar assembly due to the electron delocalization in the molecule, the nitrimino moiety is pointing towards the nitrogen atom N5 and participates in an intramolecular hydrogen bond N5–H5...O3 with a D...A length of $2.619(3) \text{ \AA}$ and a D–H...A angle of $103(2)^\circ$. The asymmetric unit of compound **2** together with the atom labeling is presented in Figure 2.

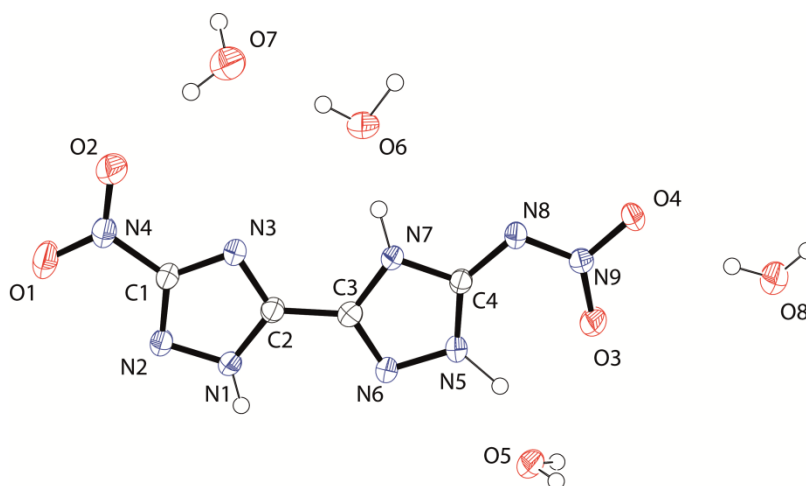


Fig. 2 Asymmetric unit within the crystal structure of **2**. Thermal ellipsoids are set to 50 % probability; Selected bond lengths [Å]: N7 C4 1.360(3), N7 C3 1.364(3), N7 H7 0.97(4), O4 N9 1.273(3), N3 C2 1.320(3), N3 C1 1.350(3), N2 C1 1.313(3), N2 N1 1.348(3), N1 C2 1.347(3), N1 H1 0.85(3), N8 N9 1.324(3), N8 C4 1.356(3), N9 O3 1.232(3), N6 C3 1.300(3), N6 N5 1.378(3), C4 N5 1.333(3), C2 C3 1.452(4), O2 N4 1.228(3), N5 H5 1.10(3), C1 N4 1.441(4), O1 N4 1.234(3).

The structure is build up by several intermolecular hydrogen bonds towards the surrounding water molecules. As shown in Figure 3, the dominating structures are infinite chains along the *b*-axis. The chains are connected by water molecules to a two dimensional network in the *bc*-plane, the layers are stacked above each other along the *a*-axis. The two dimensional network built up by strong hydrogen bonds is displayed in Figure 3.

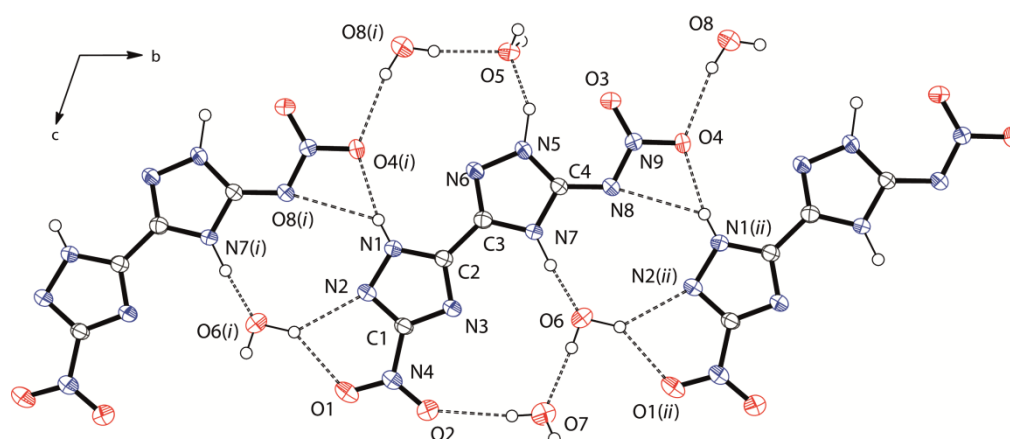


Fig. 3 Hydrogen bonding scheme in the crystal structure of **2** forming chains along the *b*-axis. Thermal ellipsoids are set to 50 % probability. Symmetry operators: (i) $x, -1+y, z$; (ii) $x, 1+y, z$.

Table 2: Hydrogen bonds present in the crystal structure of **2**.

D–H...A	d (D–H) [Å]	d (H...A) [Å]	d (D–H...A) [Å]	< (D–H...A) [°]
N1–H1...O4 ⁱ	0.86(3)	1.94(4)	2.786(3)	168(3)
N1–H1...O8 ⁱ	0.86(3)	2.54(4)	3.189(4)	134(3)
N5–H5...O5 ⁱ	1.10(4)	1.62(4)	2.647(3)	152(3)
N7–H7...O6	0.98(4)	1.61(4)	2.583(3)	174(3)
O5–H5a...O7	0.84(4)	2.07(4)	2.835(4)	151(4)
O5–H5b...O8	0.88(5)	1.95(5)	2.807(3)	167(5)
O6–H6a...O7	0.84(2)	1.91(2)	2.746(3)	176(3)
O6–H6b...O1 ⁱⁱ	1.02(3)	2.10(3)	2.988(4)	144(2)
O6–H6b...N2 ⁱⁱ	1.02(3)	2.17(3)	3.008(4)	138(2)
O7–H7a...O8 ⁱⁱⁱ	0.84(6)	1.96(6)	2.785(3)	167(6)
O7–H7b...O2	0.84(3)	2.23(3)	3.036(4)	160(5)
O8–H8a...O4	0.84(3)	2.11(3)	2.942(3)	169(4)
O8 ⁱ –H8b...O5	0.85(6)	1.97(6)	2.809(4)	167(6)

Symmetry Operators: (i) $x, -1+y, z$; (ii) $x, 1+y, z$, (iii) $1-x, 1-y, -z$.

The azido-compound **3** also crystallizes in the triclinic space group $P\bar{1}$ with a cell volume of 1013.55(18) Å³ and two molecular moieties in the asymmetric unit, the calculated density for the dihydrate is 1.692 g cm⁻³. As shown in Figure 4, the proton is located at the nitrogen atom N5 next to the azido group and not next to the C–C bond as it is the case for the nitrotriazole. Both heterocycles are now twisted by 180° around the C2–C3 bond, the three nitrogen atoms of the azido group exhibit a slightly bent arrangement with a N₈–N₉–N₁₀ angle of 170.4(3)°.

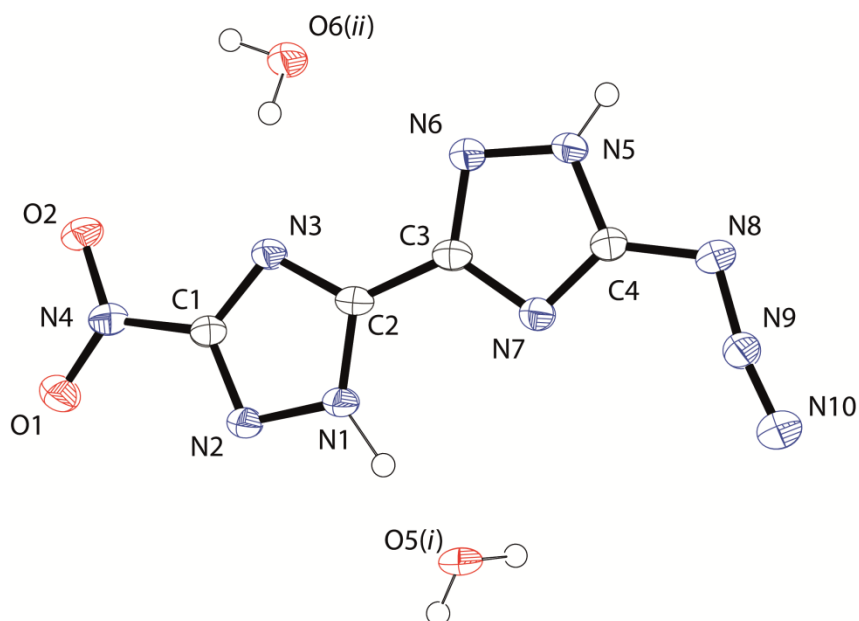


Fig. 4 Crystal structure of **3**. Thermal ellipsoids are set to 50 % probability; Symmetry operators: (i) $1-x, 1-y, -z$; (ii) $-x, 1-y, 1-z$; Selected bond lengths [\AA]: O1 N4 1.220(3), O2 N4 1.238(3), N1 C2 1.350(4), N1 N2 1.356(3), N1 H1 1.01(3), N2 C1 1.325(4), N3 C1 1.335(4), N3 C2 1.339(4), N4 C1 1.451(4), N5 C4 1.353(4), N5 N6 1.354(4), N5 H5 0.84(4), N6 C3 1.332(4), N7 C4 1.313(4), N7 C3 1.368(4), N8 N9 1.255(4), N8 C4 1.398(4), N9 N10 1.129(3), C2 C3 1.451(4).

The crystal structure of compound **3** is build up by the formation of pairs via the strong hydrogen bond including oxygen atoms O5 and O7 of the water molecules. As shown in Table 3, the D–H \cdots A angle is close to 180° and the D \cdots A length is considerably shorter than the sum of van der Waals radii ($r_w(\text{O}) + r_w(\text{N}) = 3.07 \text{ \AA}$).³²

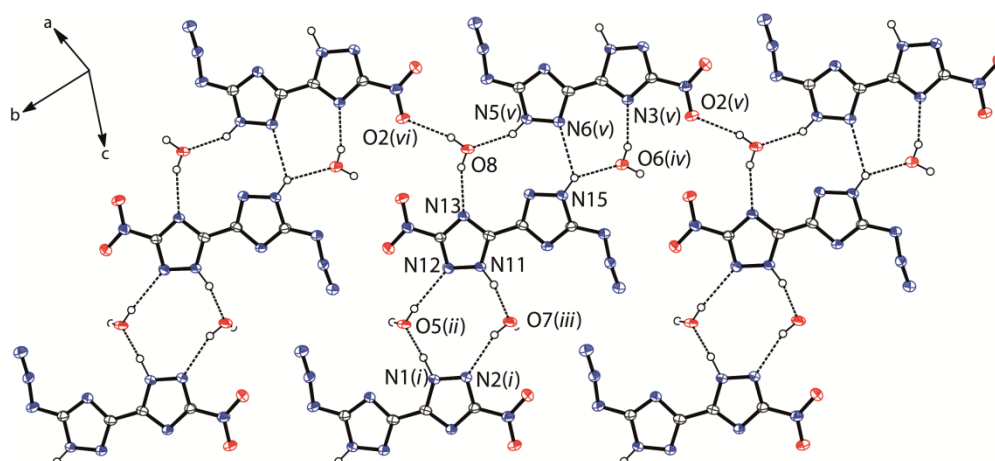


Fig. 5 Hydrogen bonding scheme in the crystal structure of **3**; Thermal ellipsoids are set to 50 % probability. Symmetry operators: (i) $x, y, 1+z$; (ii) $1-x, 1-y, 1-z$, (iii) $-x, 1-y, 1-z$, (iv) $-x, -y, 1-z$, (v) $x, -1+y, z$, (vi) $1+x, y, z$.

The pairs of AzNBT molecules are further connected to a two dimensional network by several hydrogen bonds towards surrounding water molecules (Table 3). The azido moieties do not participate in any hydrogen bond but are connected via a short contact $N_{10}\cdots N_{20}$ (distance $d = 3.011(4)$ Å) towards each other and towards the oxygen atom O3 of nitro group ($N_{20}\cdots O_3$, distance $d = 2.903(3)$ Å).

Table 3: Hydrogen bonds present in the crystal structure of **3**.

D–H \cdots A	d (D–H) [Å]	d (H \cdots A) [Å]	d (D–H \cdots A) [Å]	< (D–H \cdots A) [°]
N1 ⁱ –H1 \cdots O5 ⁱⁱ	1.01(4)	1.62(4)	2.631(3)	175(3)
N5 ^v –H5 \cdots O8 ⁱ	0.85(4)	2.08(3)	2.842(3)	149(3)
N11–H11 \cdots O7 ⁱⁱⁱ	0.94(4)	1.70(4)	2.627(4)	166(3)
N15–H15 \cdots N6 ^v	0.89(4)	2.41(4)	3.048(4)	129(3)
N15–H15 \cdots O6 ^{iv}	0.89(4)	2.21(4)	2.906(3)	135(3)
O5 ⁱⁱ –H5b \cdots N12	0.78(5)	2.27(5)	3.025(3)	165(5)
O6 ^{iv} –H6a \cdots N3 ^v	0.83(4)	2.07(4)	2.871(3)	163(4)
O7 ⁱⁱⁱ –H7a \cdots N2 ⁱ	0.85(4)	2.12(3)	2.945(3)	162(3)
O8–H8a \cdots N13	0.81(5)	2.03(5)	2.796(3)	157(4)

Symmetry Operators: (i) $x, y, 1+z$; (ii) $1-x, 1-y, 1-z$, (iii) $-x, 1-y, 1-z$, (iv) $-x, -y, 1-z$, (v) $x, -1+y, z$, (vi) $1+x, y, .z$

PHYSICOCHEMICAL PROPERTIES: HEATS OF FORMATION, DETONATION PARAMETERS AND THERMAL STABILITIES

The heats of formation of **1–3** and **4a–c** have been calculated on the CBS-4M level of theory using the atomization energy method and utilizing experimental data (for further details and results refer to the Supporting Information). All compounds show highly endothermic enthalpies of formation with 267 kJ mol^{-1} (**1**), 360 kJ mol^{-1} (**2**) and 635 kJ mol^{-1} (**3**), all by far outperforming RDX (85 kJ mol^{-1}). The enthalpies of the ionic derivatives **4a** and **4b** are in the same range (243 kJ mol^{-1} (**4a**), 129 kJ mol^{-1} (**4b**)), the very high nitrogen content of compound **4c** (65.5%) leads to the highest value of 834 kJ mol^{-1} . To estimate the detonation performances of the prepared compounds selected key parameters were calculated with EXPLO5 (version 5.05)³³ and compared to RDX. The calculated detonation parameters using experimentally determined densities (gas pycnometry at 25°C with dried compounds) and heats of formation are summarized in Table 4.

The starting material 5-(5-amino-1*H*-1,2,4-triazol-3-yl)-3-nitro-1*H*-1,2,4-triazole (**1**) is insensitive towards friction and impact and shows a decomposition temperature of 255 °C similar to the precursor 3,3'-dinitro-5,5'-bis(1*H*-1,2,4-triazole) (251 °C).²⁷ As shown in Figure 6, the introduction of energetic moieties dramatically decreases the thermal stability to 150 °C (**2**) and 181 °C (**3**). In comparison to the symmetric bistriazole compounds, the decomposition temperatures of all compounds are significantly lower, emphasizing the unique stability of bistriazoles.

The sensitivities towards impact (8 J) were found to be in the range of RDX, surprisingly higher in comparison to the symmetric nitrimino- and azido-triazoles. The same trend could be observed for the friction sensitivity, which was found to be very low (360 N). Again, the symmetrically substituted bistriazoles are far more sensitive. Both compounds **2** and **3** show lower detonation velocities and pressures than RDX, although all have higher heats of formation and comparable densities. The calculated detonation velocities of both compounds (7925 ms⁻¹ (**2**), 7823 ms⁻¹ (**3**)) are in the same range and well below the commonly used explosive RDX. In contrast to compound **2**, the ionic derivatives **4a–c** are insensitive towards friction and impact, only the hydroxylammonium salt is slightly sensitive towards impact (15 J).

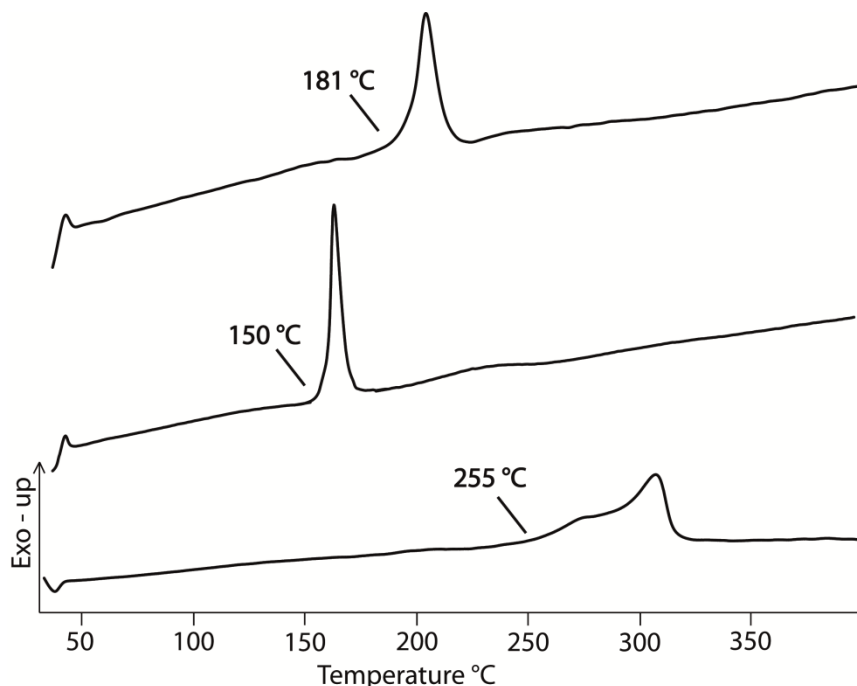


Fig. 6 DSC plots of ANBT (**1**), NNBT (**2**) and AzNBT (**3**); DSC plots were recorded with a heating rate of 5 °C min⁻¹.

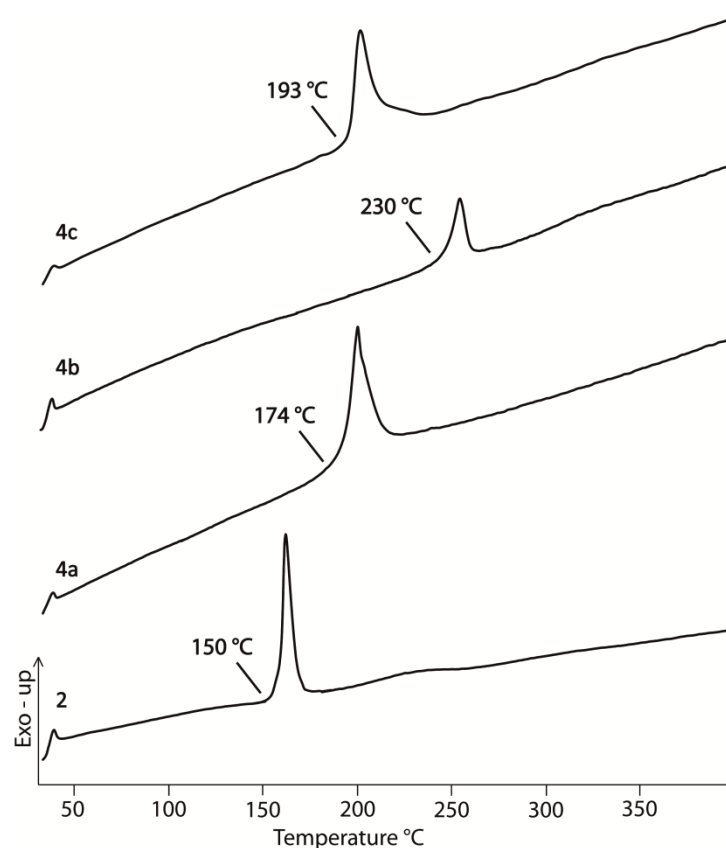


Fig. 7 DSC plots of NNBT (**2**) and ionic derivatives **4a–c**; DSC plots were recorded with a heating rate of $5\text{ }^{\circ}\text{C min}^{-1}$.

As expected, the combination with nitrogen-rich cations increases both thermal stability and performance (Figure 7). The ionic derivatives show higher decomposition temperatures ($174\text{ }^{\circ}\text{C}$ (**4a**), $230\text{ }^{\circ}\text{C}$ (**4b**), $193\text{ }^{\circ}\text{C}$ (**4c**)) and enhanced detonation parameters. The detonation velocities were calculated in the range of 7611 m s^{-1} (**4b**) to 8707 m s^{-1} (**4c**). The best performances were calculated for the triaminoguanidinium salt (**4c**) with a detonation velocity of 8707 m s^{-1} and the hydroxylammonium salt (**3a**) with a detonation velocity of 8706 m s^{-1} , which is in the same range compared to RDX. Taking into account the high nitrogen content (50.2% (**4a**), 58.5% (**4b**), 65.5% (**4c**)), those compounds could be of interest as secondary explosive or burn rate modifiers

Table 4: Physico-chemical properties of compounds **1–3** and **4a–c** in comparison to hexogen (RDX).

	(1)	(2)	(3)	(4a)	(4b)	(4c)	RDX ^[n]
Formula	C ₄ H ₄ N ₈ O ₂	C ₄ H ₃ N ₉ O ₄	C ₄ H ₂ N ₁₀ O ₂	C ₄ H ₉ N ₁₁ O ₆	C ₆ H ₁₃ N ₁₅ O ₄	C ₆ H ₁₉ N ₂₁ O ₄	C ₃ H ₆ N ₆ O ₆
M [g mol ⁻¹]	196.1	241.1	222.1	307.2	359.3	449.4	222.1
IS [J] ^a	40	8	8	15	40	40	7
FS [N] ^b	360	360	360	360	360	360	120
ESD [J]	1.5	0.5	0.3	0.25	0.5	0.35	--
N [%] ^c	57.1	45.5	63.1	50.2	58.5	65.5	37.8
Ω [%] ^d	-65.3	-36.4	-50.4	-33.8	-64.5	-62.3	-21.6
T _{dec.} [°C] ^e	255	150	181	174	230	193	210
ρ [g cm ⁻³] ^f	1.61	1.70	1.68	1.80	1.75	1.75	1.80
Δ _f H _m ^o [kJ mol ⁻¹] ^g	267	360	635	243	129	834	85
Δ _f U ^o [kJ kg ⁻¹] ^h	1451	1577	2934	896	469	1976	417
EXPLO5 (V5.05) values:							
-Δ _E U ^o [kJ kg ⁻¹] ⁱ	3853	4965	4798	5287	3332	4432	6125
T _E [K] ^j	3061	3967	3880	3699	2542	2971	4236
p _{C-J} [kbar] ^k	194	261	246	326	242	303	349
V _{Det.} [m s ⁻¹] ^l	7216	7925	7823	8706	7911	8707	8748
Gas vol.[L kg ⁻¹] ^m	684	678	663	778	770	817	739

^[a] BAM drop hammer; ^[b] BAM friction tester; ^[c] Nitrogen content; ^[d] Oxygen balance; ^[e] Temperature of decomposition by DSC ($\beta = 5$ °C, Onset values); ^[f] Density values derived from gas-pycnometer measurements of anhydrous compounds at 25 °C; ^[g] Molar enthalpy of formation; ^[h] Energy of formation; ^[i] Energy of Explosion; ^[j] Explosion temperature; ^[k] Detonation pressure; ^[l] Detonation velocity; ^[m] Assuming only gaseous products; ^[n] values based on Ref. ³⁴ and the EXPLO5.5 database.

CONCLUSIONS

The starting material 3,3'-dinitro-5,5'-bis(1*H*-1,2,4-triazole) was successfully reduced to 5-(5-amino-1*H*-1,2,4-triazol-3-yl)-3-nitro-1*H*-1,2,4-triazole (**1**). The amine group of **1** was further converted to energetic moieties (nitrimino (**2**) and azido(**3**)), which leads to the previously unknown asymmetric energetic bistriazole compounds. All compounds have been fully characterized by means of vibrational and multinuclear NMR spectroscopy, mass spectrometry and differential scanning calorimetry. Single crystal X-ray measurements were accomplished for compounds **2** and **3** and deliver insight into structural characteristics as well as inter- and intramolecular interactions. Regarding the stability values and energetic parameters, the nitrimino compound (**2**) and the azido

compound (**3**) are sensitive towards impact sensitivity (8 J) but insensitive towards friction (360 N). With detonation velocities below 8000 ms^{-1} , compounds **2** and **3** are able to compete with commonly used TNT, however, the performance data for RDX are not reached. Energetic ionic compounds were synthesized from **2** using nitrogen-rich cations, all reactions were carried out using the free bases or their corresponding carbonates. All energetic, ionic compounds (**4a–c**) were characterized with the same techniques as described for the uncharged compounds. All ionic compounds reveal positive heats of formation in the range of 129 kJ mol^{-1} (**4b**) to 834 kJ mol^{-1} (**4c**). The most interesting compounds regarding the energetic properties are the hydroxylammonium and triaminoguanidinium compound (**4a** and **4c**). Those compounds exhibit decomposition temperatures above 200°C and performance values in the range of RDX (8706 m s^{-1} (**4a**) and 8707 m s^{-1} (**4c**)).

EXPERIMENTAL SECTION

Caution: Due to the fact that energetic triazole compounds are to some extent unstable against outer stimuli, proper safety precautions should be taken when handling the materials. Especially dry samples are able to explode under the influence of impact or friction. Lab personnel and the equipment should be properly grounded and protective equipment like earthed shoes, leather coat, Kevlar® gloves, ear protection and face shield is recommended for the handling of any energetic material.

General. All chemical reagents and solvents were obtained from Sigma-Aldrich Inc. or Acros Organics (analytical grade) and were used as supplied without further purification. ^1H , $^{13}\text{C}\{1\text{H}\}$, $^{14}\text{N}\{1\text{H}\}$ and ^{15}N NMR spectra were recorded on a JEOL Eclipse 400 instrument in $\text{DMSO-}d_6$ at 25°C . The chemical shifts are given relative to tetramethylsilane (^1H , ^{13}C) or nitro methane (^{14}N , ^{15}N) as external standards and coupling constants are given in Hertz (Hz). Infrared (IR) spectra were recorded on a Perkin-Elmer Spectrum BX FT-IR instrument equipped with an ATR unit at 25°C . Transmittance values are qualitatively described as “very strong” (vs), “strong” (s), “medium” (m), “weak” (w) and “very weak” (vw). Raman spectra were recorded on a Bruker RAM II spectrometer equipped with a Nd:YAG laser (200 mW) operating at 1064 nm and a reflection angle of 180° . The intensities are reported as percentages of the most intense peak and are given in parentheses. Elemental analyses (CHNO) were performed with a Netzsch Simultaneous Thermal Analyzer STA 429 (The N microanalysis values are all

lower than the calculated values. This is common with high N compounds and cannot be avoided). Melting and decomposition points were determined by differential scanning calorimetry (Linseis PT 10 DSC, calibrated with standard pure indium and zinc). Measurements were performed at a heating rate of 5 °C min⁻¹ in closed aluminum sample pans with a 1 µm hole in the lid for gas release to avoid an unsafe increase in pressure under a nitrogen flow of 20 mL min⁻¹ with an empty identical aluminum sample pan as a reference.

For initial safety testing, the impact and friction sensitivities as well as the electrostatic sensitivities were determined. The impact sensitivity tests were carried out according to STANAG 4489³⁵, modified according to WIWeB instruction 4-5.1.02³⁶ using a BAM³⁷ drop hammer. The friction sensitivity tests were carried out according to STANAG 4487³⁸ and modified according to WIWeB instruction 4-5.1.03³⁹ using the BAM friction tester. The electrostatic sensitivity tests were accomplished according to STANAG 4490⁴⁰ using an electric spark testing device ESD 2010 EN (OZM Research).

The single-crystal X-ray diffraction data of **2** and **3** were collected using an Oxford Xcalibur3 diffractometer equipped with a Spellman generator (voltage 50 kV, current 40 mA), Enhance molybdenum K α radiation source (λ = 71.073 pm), Oxford Cryosystems Cryostream cooling unit, four circle kappa platform and a Sapphire CCD detector. Data collection and reduction were performed with CrysAlisPro.⁴¹ The structures were solved with SIR97⁴², refined with full-matrix least-square procedures using SHELXL-97⁴³, and checked with PLATON⁴⁴, all integrated into the WinGX software suite⁴⁵. The finalized CIF files were checked with checkCIF.⁴⁶ Intra- and intermolecular contacts were analyzed with Mercury.⁴⁷ CCDC 935564 (**2**) and 935565 (**3**), contain the supplementary crystallographic data for this paper. These data can be obtained free of charge from the Cambridge Crystallographic Data Centre via www.ccdc.cam.ac.uk/data_request/cif.

3,3'-Diamino-5,5'-bis(1*H*-1,2,4-triazole) and 3,3'-dinitro-5,5'-bis(1*H*-1,2,4-triazole) were synthesized according to literature.²⁷

*5-(5-amino-1*H*-1,2,4-triazol-3-yl)-3-nitro-1*H*-1,2,4-triazole (ANBT, **1**)*

3,3'-Dinitro-5,5'-bis(1*H*-1,2,4-triazole) dihydrate (13.0 g, 49.6 mmol) was suspended in hydrazine (50wt% in water, 105 mL) and stirred at 80 °C for 16 h. 50 % hydrochloric acid (500 mL) was added to the mixture resulting in a color change from red to colorless. The solution was extracted with ethyl acetate to remove unreacted 3,3'-dinitro-5,5'-

bis(1*H*-1,2,4-triazole) (regained after evaporation of the solvent: 4.1 g, 18 mmol). The aqueous phase was brought to pH = 3 by adding a saturated solution of sodium acetate. The occurring precipitate was collected by filtration and resuspended in 0.25 M hydrochloric acid (400 mL). Filtration and washing with water, ethanol and diethyl ether yielded 5-(5-amino-1*H*-1,2,4-triazol-3-yl)-3-nitro-1*H*-1,2,4-triazole (4.00 g, 20.4 mmol, 41%) as a colorless solid.

¹H NMR (DMSO-*d*₆): δ = 6.41 (s, 2H, -NH₂) ppm; **¹³C NMR** (DMSO-*d*₆): δ = 163.5, 158.3, 150.6, 149.1 ppm; **¹⁴N NMR** (DMSO-*d*₆): δ = -23 (-NO₂) ppm. **IR**: ν (cm⁻¹) (rel. int.) = 3578(w), 3402(m), 3320(m), 3224(m), 3155(m), 2922(w), 2709(m), 2584(m), 1699(vs), 1660(m), 1550(s), 1533(m), 1522(s), 1476(m), 1463(m), 1446(m), 1430(m), 1397(s), 1333(m), 1308(s), 1241(w), 1183(w), 1123(m), 1123(m), 1079(w), 1067(m), 1023(w), 978(s), 890(m), 838(vs), 751(w), 713(m), 654(w). **Raman** (200 mW): ν (cm⁻¹) (rel. int.) = 1709(4), 1660(7), 1629(79), 1549(8), 1530(10), 1471(8), 1434(36), 1420(32), 1396(100), 1334(54), 1311(14), 1252(3), 1180(3), 1124(89), 1093(9), 1072(13), 1036(22), 952(4), 843(14), 770(6), 754(7), 747(5), 591(2), 591(2), 497(3), 400(9), 332(6), 318(7), 299(3), 243(4), 222(9). **Elemental analysis** (C₄H₄N₈O₂): calc.: C 24.50, H 2.06, N 57.13; found: C 24.20, H 2.39, N 55.02. **Mass spectrometry**: *m/z* (DEI⁺) 196.1 [M⁺].

*5-(5-nitrimino-1,3*H*-1,2,4-triazol-3-yl)-3-nitro-1*H*-1,2,4-triazole (NNBT, 2)*

5-(5-amino-1*H*-1,2,4-triazol-3-yl)-3-nitro-1*H*-1,2,4-triazole (2.4 g, 12 mmol) was dissolved in concentrated sulfuric acid (24 mL) and cooled to 0 °C. Concentrated nitric acid (4.8 mL) was added dropwise and the mixture was stirred at room temperature for 1 h. The solution was poured on ice and the resulting precipitate collected by filtration. 5-(5-nitrimino-1,3*H*-1,2,4-triazol-3-yl)-3-nitro-1*H*-1,2,4-triazole (2.7 g, 11 mmol, 92%) was yielded as a colorless solid.

¹H NMR (DMSO-*d*₆): δ = 12.39 ppm; **¹³C NMR** (DMSO-*d*₆): δ = 163.1, 153.1, 146.6, 142.9 ppm; **¹⁴N NMR** (DMSO-*d*₆): δ = -23 ppm. **IR**: ν (cm⁻¹) (rel. Int.) = 3564(w), 3461(w), 3295(w), 2715(w), 1651(w), 1581(s), 1558(m), 1554(m), 1524(w), 1462(s), 1408(m), 1383(m), 1350(m), 1312(vs), 1264(s), 1220(m), 1159(w), 1119(w), 1096(w), 1037(w), 1001(vw), 951(vs), 879(m), 879(m), 842(m), 774(w), 756(w), 751(w), 735(w), 709(s). **Raman** (200 mW): ν (cm⁻¹) (rel. Int.) = 1652(77), 1610(8), 1581(100), 1561(20), 1523(24), 1502(40), 1457(12), 1430(18), 1385(10), 1353(6), 1318(15), 1224(3), 1161(6), 1122(22), 1099(3), 1016(23), 1004(27), 854(6), 844(4), 775(2), 759(20), 662(1), 596(1),

596(1), 550(1), 501(2), 469(1), 422(4), 252(5), 229(2). **Elemental analysis** ($\text{C}_4\text{H}_3\text{N}_9\text{O}_4$): calc.: C 19.92, H 1.25, N 52.28; found: C 22.26, H 1.60, N 50.20. **Mass spectrometry**: m/z (FAB⁻) 240.3 [$\text{C}_4\text{H}_2\text{N}_9\text{O}_4^-$]. **Sensitivities** (grain size: <100 μm): friction: 360 N; impact: 8 J; ESD: 0.5 J. **DSC** (onset 5 $^\circ\text{Cmin}^{-1}$): T_{Dec} : 150 $^\circ\text{C}$.

5-(5-azido-1H-1,2,4-triazol-3-yl)-3-nitro-1H-1,2,4-triazole (AzNBT, 3)

3-Amino-3'-nitro-5,5'-bis(1H-1,2,4-triazole) (1.04 g, 5.30 mmol) was dissolved in 20% sulfuric acid (60 mL) and cooled to -5 $^\circ\text{C}$. Sodium nitrite (0.37 g, 5.37 mmol) was dissolved in water (20 mL) and added dropwise. The solution was stirred for 3 h at room temperature. Sodium azide (1.72 g, 26.5 mmol, 5 eq) was dissolved in water (10 mL) and added dropwise (**Danger**: Evolution of HN_3 !). After stirring over night, the solution was extracted with ethyl acetate and the combined organic phases dried over magnesium sulfate. The solvent was removed in vacuum yielding 3-azido-3'-nitro-5,5'-bis(1H-1,2,4-triazole) dihydrate (0.89 g, 3.99 mmol, 75%) as colorless solid.

^1H NMR (DMSO- d_6): δ = 6.11 (s, 2H, $\text{H}_{\text{Triazole}}$) ppm; **^{13}C NMR** (DMSO- d_6): δ = 163.0, 155.5, 147.3, 146.8 ppm; **^{14}N NMR** (DMSO- d_6): δ = -30 ($-\text{NO}_2$), -146 ($-\text{N}_3$) ppm. **IR**: ν (cm^{-1}) (rel. Int.) = 3231(w), 3150(w), 3044(w), 2944(w), 2830(w), 2221(vw), 2143(s), 2139(s), 1614(w), 1541(vs), 1496(m), 1466(m), 1443(m), 1411(s), 1393(s), 1307(vs), 1190(m), 1048(m), 1031(m), 968(m), 836(s), 800(m), 707(m), 707(m). **Raman** (200 mW): ν (cm^{-1}) (rel. Int.) = 2160(11), 1617(100), 1548(33), 1505(55), 1452(5), 1417(46), 1389(52), 1331(3), 1319(9), 1294(2), 1266(3), 1179(20), 1120(4), 1066(3), 1048(3), 1033(8), 1020(19), 841(5), 804(3), 764(6), 717(1), 550(2), 500(1), 500(1), 414(3), 391(13), 318(5), 210(4). **Elemental analysis** ($\text{C}_4\text{H}_2\text{N}_{10}\text{O}_2$): calc.: C 21.63, H 0.91, N 63.06; found: C 21.74, H 1.06, N 61.47; **Mass spectrometry**: m/z (DEI⁺) 222.0 [$\text{C}_4\text{H}_2\text{N}_{10}\text{O}_2^+$]. **Sensitivities** (grain size: <100 μm): friction: 360 N; impact: 8 J; ESD: 0.3 J. **DSC** (onset 5 $^\circ\text{Cmin}^{-1}$): T_{Dec} : 181 $^\circ\text{C}$.

Dihydroxylammonium 5-(5-nitrimino-1H-1,2,4-triazolate-3-yl)-3-nitro-1,2,4-triazolate (4a)

5-(5-nitrimino-1,3H-1,2,4-triazol-3-yl)-3-nitro-1H-1,2,4-triazole (526 mg, 2.18 mmol) was dissolved in ethanol (50 mL) and hydroxylamine (50% in H_2O , 0.27 mL, 4.36 mmol, 2.2 eq) was added. The resulting precipitate was collected by filtration and yielded hydroxylammonium 5-(5-nitrimino-1,2,4-triazol-3-yl)-3-nitro-1H-1,2,4-triazolate (540 mg, 1.76 mmol, 81%) as a colorless solid.

¹H NMR (DMSO-d₆): δ = 12.85, 8.69, 4.57 ppm; **¹³C NMR** (DMSO-d₆): δ = 165.7, 159.2, 157.4, 156.9 ppm; **¹⁴N NMR** (DMSO-d₆): δ = -17 ppm. **IR**: ν (cm⁻¹) (rel. Int.) = 3579(w), 3013(w), 2711(m), 1611(w), 1521(m), 1480(w), 1451(s), 1405(m), 1344(m), 1327(m), 1307(m), 1284(s), 1255(vs), 1209(m), 1138(m), 1123(m), 1107(s), 1017(w), 1003(w), 986(s), 867(m), 842(s), 800(w), 800(w), 773(w), 765(m), 749(w), 726(m), 685(vw), 655(vw). **Raman** (200 mW): ν (cm⁻¹) (rel. Int.) = 1587(100), 1531(33), 1482(18), 1465(18), 1458(17), 1442(10), 1412(65), 1388(35), 1340(25), 1311(9), 1289(11), 1141(44), 1125(47), 1071(6), 1042(11), 1019(28), 1006(14), 989(11), 871(5), 846(14), 775(2), 765(4), 751(12), 751(12), 728(3), 687(2), 603(2), 437(4), 258(2), 211(3). **Elemental analysis** (C₄H₉N₁₁O₆): calc.: C 15.64, H 2.95, N 50.16; found: C 15.39, H 3.22, N 47.61. **Mass spectrometry**: *m/z* (FAB⁺) 34 [NH₃OH⁺] *m/z* (FAB⁻) 240.1 [C₄H₂N₉O₄⁻]. **Sensitivities** (grain size: <100 μm): friction: 360 N; impact: 15 J; ESD: 0.25 J. **DSC** (onset 5 °Cmin⁻¹): T_{Dec}: 174 °C.

Diguanidinium 5-(5-nitrimino-1H-1,2,4-triazolate-3-yl)-3-nitro-1,2,4-triazolate (4b)

5-(5-nitrimino-1,3H-1,2,4-triazol-3-yl)-3-nitro-1H-1,2,4-triazole (508 mg, 2.11 mmol) was dissolved in ethanol (50 mL). Guanidinium bicarbonate (380 mg, 2.11 mmol, 1 eq) was dissolved in water and added to the solution. The mixture was refluxed for 30 min. The formed precipitate was collected by filtration and yielded guanidinium 5-(5-nitrimino-1,2,4-triazol-3-yl)-3-nitro-1H-1,2,4-triazolate (655 mg, 1.82 mmol, 86%) as a yellow solid.

¹H NMR (DMSO-d₆): δ = 13.20, 7.38 ppm; **¹³C NMR** (DMSO-d₆): δ = 165.3, 158.1 (G⁺), 157.3, 156.0, 152.9 ppm; **¹⁴N NMR** (DMSO-d₆): δ = -17 ppm. **IR**: ν (cm⁻¹) (rel. Int.) = 3604(vw), 3442(m), 3436(m), 3430(m), 3427(m), 3421(m), 3347(w), 3151(m), 3146(m), 1680(s), 1668(s), 1665(s), 1643(s), 1576(w), 1524(m), 1509(m), 1479(m), 1443(s), 1394(s), 1387(s), 1359(vs), 1313(s), 1283(vs), 1283(vs), 1259(m), 1143(w), 1090(s), 1014(w), 983(m), 869(w), 843(m), 774(w), 761(m), 745(w), 726(m), 678(w), 662(w). **Raman** (200 mW): ν (cm⁻¹) (rel. Int.) = 1574(100), 1551(9), 1521(24), 1484(41), 1447(3), 1396(65), 1382(50), 1313(11), 1298(13), 1287(6), 1259(3), 1146(21), 1096(64), 1035(14), 1015(41), 985(2), 870(4), 844(14), 764(3), 747(7), 681(1), 604(1), 538(7), 538(7), 533(7), 432(5), 420(6), 310(1), 253(2). **Elemental analysis** (C₆H₁₃N₁₅O₄): calc.: C 20.06, H 3.65, N 58.48; found: C 19.88, H 3.99, N 54.95. **Mass spectrometry**: *m/z*

(FAB⁺) 60 [CH₆N₃⁺] *m/z* (FAB⁻) 240.1 [C₄H₂N₉O₄⁻]. **Sensitivities** (grain size: <100 μm): friction: 360 N; impact: 40 J; ESD: 0.5 J. **DSC** (onset 5 °Cmin⁻¹): T_{Dec}: 230 °C.

Di(triaminoguanidinium) 5-(5-nitrimino-1H-1,2,4-triazolate-3-yl)-3-nitro-1,2,4-triazolate (4c)

Triaminoguanidine (419 mg, 4.02 mmol, 2 eq) was added to a solution of 5-(5-nitrimino-1,3H-1,2,4-triazol-3-yl)-3-nitro-1H-1,2,4-triazole (485 mg, 2.01 mmol) in ethanol (50 mL). Filtration of the precipitate yielded triaminoguanidinium 5-(5-nitrimino-1,2,4-triazol-3-yl)-3-nitro-1H-1,2,4-triazolate (762 mg, 1.70 mmol, 85%) as a yellow solid.

¹H NMR (DMSO-d₆): δ = 9.71 ppm; **¹³C NMR** (DMSO-d₆): δ = 164.9, 157.8, 154.8, 151.4 ppm; **¹⁴N NMR** (DMSO-d₆): δ = -17 ppm. **IR**: ν (cm⁻¹) (rel. Int.) = 3440(w), 3360(m), 3356(m), 3326(m), 3187(m), 1688(vs), 1522(s), 1480(m), 1440(s), 1396(vs), 1376(s), 1352(vs), 1305(m), 1297(m), 1279(s), 1227(w), 1212(m), 1139(m), 1083(m), 1073(m), 1039(m), 1022(m), 979(s), 979(s), 857(w), 839(m), 775(w), 762(w), 704(m), 660(m). **Raman** (200 mW): ν (cm⁻¹) (rel. Int.) = 3225(4), 1686(2), 1655(2), 1575(100), 1554(13), 1516(22), 1479(32), 1385(60), 1358(19), 1325(9), 1307(13), 1279(14), 1256(4), 1133(13), 1085(73), 1024(11), 1008(28), 887(7), 861(5), 840(12), 750(6), 420(8), 262(3), 262(3). **Elemental analysis** (C₆H₁₉N₂₁O₄): calc.: C 16.11, H 4.26, N 65.46; found: C 16.11, H 4.48, N 62.55. **Mass spectrometry**: *m/z* (FAB⁺) 105 [CH₉N₆⁺] *m/z* (FAB⁻) 240.2 [C₄H₂N₉O₄⁻]. **Sensitivities** (grain size: <100 μm): friction: 360 N; impact: 40 J; ESD: 0.35 J. **DSC** (onset 5 °Cmin⁻¹): T_{Dec}: 193 °C.

REFERENCES

1. T. M. Klapötke, *Chemistry of high-energy materials*, de Gruyter, Berlin, **2012**.
2. P. F. Pagoria, G. S. Lee, A. R. Mitchell and R. D. Schmidt, *Thermochimica Acta*, 2002, **384**, 187-204.
3. R. P. Singh, R. D. Verma, D. T. Meshri and J. M. Shreeve, *Angew. Chem., Int. Ed.*, 2006, **45**, 3584-3601.
4. C. M. Sabate and T. M. Klapötke, *New Trends in Research of Energetic Materials, Proceedings of the Seminar, 12th, Pardubice, Czech Republic, Apr. 1-3, 2009*, 2009, 172-194.

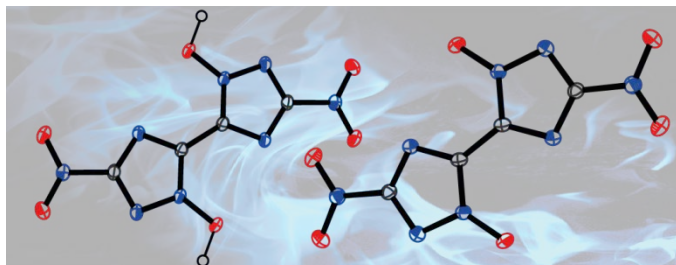
5. S. Yang, S. Xu, H. Huang, W. Zhang and X. Zhang, *Prog. Chem.*, 2008, **20**, 526-537.
6. M. B. Talawar, R. Sivabalan, T. Mukundan, H. Muthurajan, A. K. Sikder, B. R. Gandhe and A. S. Rao, *J. Hazard. Mater.*, 2009, **161**, 589-607.
7. T. M. Klapötke, J. Stierstorfer and A. U. Wallek, *Chemistry of Materials*, 2008, **20**, 4519-4530.
8. T. M. Klapötke and C. M. Sabate, *Chemistry of Materials*, 2008, **20**, 3629-3637.
9. D. E. Chavez, M. A. Hiskey and D. L. Naud, *Prop. Explos. Pyrot.*, 2004, **29**, 209-215.
10. Y. Huang, H. Gao, B. Twamley and J. M. Shreeve, *Eur. J. Inorg. Chem.*, 2008, 2560-2568.
11. H. Gao and J. M. Shreeve, *Chem. Rev.*, 2011, **111**, 7377-7436.
12. T. M. Klapötke, ed., *High energy density materials*, Springer-Verlag, Berlin Heidelberg 2007.
13. K. Y. Lee, C. B. Storm, M. A. Hiskey and M. D. Coburn, *J. Energ. Mater.*, 1991, **9**, 415-428.
14. K. Wang, D. A. Parrish and J. M. Shreeve, *Chem-Eur. J.*, 2011, **17**, 14485-14492.
15. V. Thottempudi, H. Gao and J. M. Shreeve, *J. Am. Chem. Soc.*, 2011, **133**, 6464-6471.
16. D. L. Naud, M. A. Hiskey and H. H. Harry, *J. Energ. Mater.*, 2003, **21**, 57-62.
17. A. Dippold, T. M. Klapötke and F. A. Martin, *Z. Anorg. Allg. Chem.*, 2011, **637**, 1181-1193.
18. E. L. Metelkina, T. A. Novikova, S. N. Berdonosova, D. Y. Berdonosov and V. S. Grineva, *Russ. J. Org. Chem.*, 2004, **40**, 1412-1414.
19. E. L. Metelkina, T. A. Novikova, S. N. Berdonosova and D. Y. Berdonosov, *Russ. J. Org. Chem.*, 2005, **41**, 440-443.
20. E. Metelkina and T. Novikova, *Russ. J. Org. Chem.*, 2004, **40**, 1737-1743.
21. A. M. Astachov, V. A. Revenko, L. A. Kruglyakova and E. S. Buka, in: *New Trends in Research of Energetic Materials, Proceedings of the 10th Seminar, University of Pardubice, Czech Republic*, 2007.
22. A. M. Astachov, V. A. Revenko and E. S. Buka, in: *New Trends in Research of Energetic Materials, Proceedings of the 12th Seminar, University of Pardubice, Czech Republic*, 2009.

23. R. Wang, H. Xu, Y. Guo, R. Sa and J. M. Shreeve, *J. Am. Chem. Soc.*, 2010, **132**, 11904-11905.
24. Y. V. Serov, M. S. Pevzner, T. P. Kofman and I. V. Tselinskii, *Russ. J. Org. Chem.*, 1990, **26**, 773-777.
25. L. I. Bagal, M. S. Pevzner, A. N. Frolov and N. I. Sheludyakova, *Chem. Heterocyc. Comp.*, 1970, **6**, 240-244.
26. A. A. Dippold, T. M. Klapötke and N. Winter, *Eur. J. Inorg. Chem.* **2012**, 3474-3484.
27. A. A. Dippold and T. M. Klapötke, *Chem-Eur. J.*, 2012, **18**, 16742-16753.
28. M. Hesse, *Spektroskopische Methoden in der organischen Chemie*, Thieme Verlag, Stuttgart, 2005.
29. F. Billes, H. Endrédi and G. Keresztury, *Journal of Molecular Structure: THEOCHEM*, 2000, **530**, 183-200.
30. M. J. Frisch, G. W. Trucks, H. B. Schlegel, G. E. Scuseria, M. A. Robb, J. R. Cheeseman, G. Scalmani, V. Barone, B. Mennucci, G. A. Petersson, H. Nakatsuji, M. Caricato, X. Li, H. P. Hratchian, A. F. Izmaylov, J. Bloino, G. Zheng, J. L. Sonnenberg, M. Hada, M. Ehara, K. Toyota, R. Fukuda, J. Hasegawa, M. Ishida, T. Nakajima, Y. Honda, O. Kitao, H. Nakai, T. Vreven, J. A. J. Montgomery, J. E. Peralta, F. Ogliaro, M. Bearpark, J. J. Heyd, E. Brothers, K. N. Kudin, V. N. Staroverov, R. Kobayashi, J. Normand, K. Raghavachari, A. Rendell, J. C. Burant, S. S. Iyengar, J. Tomasi, M. Cossi, N. Rega, J. M. Millam, M. Klene, J. E. Knox, J. B. Cross, V. Bakken, C. Adamo, J. Jaramillo, R. Gomperts, R. E. Stratmann, O. Yazyev, A. J. Austin, R. Cammi, C. Pomelli, J. W. Ochterski, R. L. Martin, K. Morokuma, V. G. Zakrzewski, G. A. Voth, P. Salvador, J. J. Dannenberg, S. Dapprich, A. D. Daniels, Ö. Farkas, J. B. Foresman, J. V. Ortiz, J. Cioslowski and D. J. Fox, Wallingford CT 2009.
31. A. A. Dippold and T. M. Klapötke, *Chem-Asian J.*, 2013, *in press*, DOI: asia.201300063.
32. A. Bondi, *J. Phys. Chem.*, 1964, **68**, 441-451.
33. M. Sućeska, *EXPLO5.5 program*, Zagreb, Croatia, 2010.
34. R. Meyer, J. Köhler and A. Homburg, *Explosives*, Wiley-VCH Verlag GmbH & Co. KGaA, Weinheim, 2007.
35. *NATO standardization agreement (STANAG) on explosives and impact tests*, no.4489, 1st ed., Sept. 17, 1999.

36. WIWEB-Standardarbeitsanweisung 4-5.1.02, Ermittlung der Explosionsgefährlichkeit, hier: der Schlagempfindlichkeit mit dem Fallhammer, Nov. 08, 2002.
37. Bundesanstalt für Materialforschung, <http://www.bam.de>.
38. NATO standardization agreement (STANAG) on explosives, friction tests, no.4487, 1st ed., Aug. 22, 2002.
39. WIWEB-Standardarbeitsanweisung 4-5.1.03, Ermittlung der Explosionsgefährlichkeit, hier: der Reibempfindlichkeit mit dem Reibeapparat, Nov. 08, 2002.
40. NATO standardization agreement (STANAG) on explosives, electrostatic discharge sensitivity tests, no.4490, 1st ed., Feb. 19, 2001.
41. CrysAlisPro 1.171.36.21, Agilent Technologies, 2012.
42. A. Altomare, G. Cascarano, C. Giacovazzo, A. Guagliardi, *J. Appl. Crystallogr.* **1993**, 26, 343-350.
43. G. M. Sheldrick, *SHELXL-97, Program for the Refinement of Crystal Structures*. University of Göttingen, Germany, 1997.
44. A. L. Spek, *Platon, A Multipurpose Crystallographic Tool*, Utrecht University, Utrecht, The Netherlands, 2012.
45. L. J. Farrugia, *J. Appl. Crystallogr.*, 1999, **32**, 837-838.
46. <http://journals.iucr.org/services/cif/checkcif.html>.
47. C. F. Macrae, P. Edgington, P. McCabe, E. Pidcock, G. P. Shields, R. Taylor, M. Towler and J. van de Streek, *J. Appl. Crystallogr.*, 2006, **39**, 565

8. A STUDY OF DINITRO-BIS-1,2,4-TRIAZOLE-1,1'-DIOL AND DERIVATIVES – DESIGN OF HIGH PERFORMANCE INSENSITIVE ENERGETIC MATERIALS BY THE INTRODUCTION OF N-OXIDES

As published in: *Journal of the American Chemical Society* **2013**, 135, 9931-9938.



ABSTRACT:

In this contribution we report on the synthesis and full structural as well as spectroscopic characterization of 3,3'-dinitro-5,5'-bis-1,2,4-triazole-1,1'-diol and nitrogen-rich salts thereof. The first synthesis and characterization of an energetic 1-hydroxy-bistriazole in excellent yields and high purity is presented. This simple and straightforward method of N-Oxide introduction in triazole compounds using commercially available Oxone® improves the energetic properties and reveals a straightforward synthetic pathway towards novel energetic 1,2,4-triazole derivatives. X-ray crystallographic measurements were performed and deliver insight into structural characteristics and strong intermolecular interactions. The standard enthalpies of formation were calculated for all compounds at the CBS-4M level of theory, revealing highly positive heats of formation for all compounds. The energetic properties of all compounds (detonation velocity, pressure, etc.) were calculated using the EXPLO5.05 program, the ionic derivatives show superior performance in comparison to the corresponding compounds bearing no *N*-oxide. All substances were characterized in terms of sensitivities (impact, friction, electrostatic) and thermal stabilities, the ionic derivatives were found to be high thermally stable, insensitive compounds that are exceedingly powerful but safe to handle and prepare.

INTRODUCTION

The chemistry of explosives, their development and application are as old as 220 years BC, when blackpowder was discovered accidentally by the Chinese. Nowadays, not only the application for military purposes is studied, but the utilization of energetic materials for civilian use in mining, construction, demolition and safety equipment such as airbags, signal flares and fire extinguishing systems is extensively studied.^{1,2} The academic research mainly focuses on the work with novel energetic systems to determine factors affecting stability and performance and to bring new strategies into the design of energetic materials. The main challenge is the desired combination of a large energy content with a maximum possible chemical stability to ensure safe synthesis and handling. Several strategies for the design of energetic materials that combine the increasing demand for high performing materials with high thermal and mechanical stabilities have been developed by numerous research groups over the last decades.²⁻⁷

Traditional energetic materials are based on the oldest strategy in energetic materials design: the presence of fuel and oxidizer in the same molecule. Modern heterocyclic energetic compounds derive their energy not only from the oxidation of their carbon backbone but additionally from ring or cage strain, high-nitrogen content and high heats of formation. Intense research is focused on the tailoring of new energetic molecules with performances and stability superior to that of RDX (1,3,5-trinitro-1,3,5-triazinane). Unfortunately, the synthesis of modern explosives with high performance like HMX (1,3,5,7-tetranitro-1,3,5,7-tetrazocane) or CL-20 (2,4,6,8,10,12-hexanitro-2,4,6,8,10,12hexazaiso-wurtzitane) is often expensive and includes multiple steps which makes the industrial scale-up and practical use infeasible. Additionally, in many cases high performance and low sensitivity to mechanical stimuli appears to be mutually exclusive. Materials with sufficiently large energy content are often too sensitive to find practical use and many energetic materials with adequate stability do not possess the performance requirements.

Nitrogen-rich heterocycles are promising compounds that fulfill many requirements in the challenging field of energetic materials research.^{6,8-12} A prominent family of novel high-energy-density materials (HEDMs) are azole-based compounds, since they are generally highly endothermic with high densities and low sensitivities towards outer stimuli. Owing to the high positive heats of formation resulting from the large number of N–N and C–N bonds¹³ and the high level of environmental compatibility, triazole and tetrazole

compounds have been studied over the last couple of years with growing interest. Numerous compounds with promising properties as energetic materials arose from the C–C connection of those heterocycles to 5,5'-bistetrazoles¹⁴⁻¹⁸ and 5,5'-bistriazoles¹⁹⁻²⁷.

A further way of azole functionalization is the oxidation of the heterocycle to its corresponding N-hydroxy compound. The introduction of N-oxides is a recently reintroduced method using oxidizing agents like trifluoroperacetic acid,²⁸ potassium peroxomonosulfate (Oxone®),²⁹ or hypofluorous acid.³⁰ The additional oxygen atom generally leads to increased energetic properties due to a higher density and an even greater energy output.^{29,31-34} The oxidation of tetrazole compounds has been successfully accomplished recently, resulting in high performance explosives with low sensitivities.^{34,35}

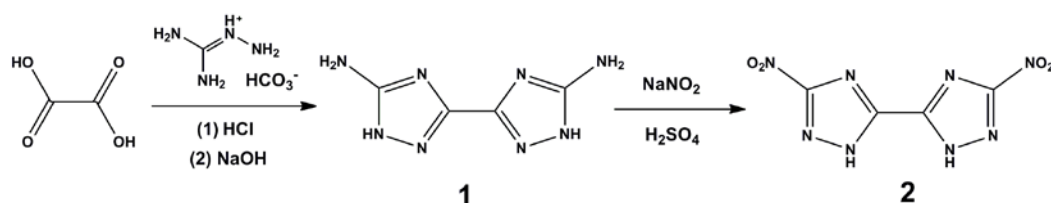
Only few examples of the oxidation of 1,2,4-triazoles to 1-hydroxy-1,2,4-triazoles using H₂O₂/phthalic anhydride,³⁶ 3-chloro-benzenecarboxoperoxoic acid³⁷ or hypofluorous acid³⁸ resulting in low yields and different isomers are known in literature. The focus of this contribution is on the synthesis of the previously unknown 3,3'-dinitro-5,5'-bis(1,2,4-triazole)-1,1'-diol as well as ionic derivatives thereof. We report on a simple and straightforward method of N-Oxide introduction in triazole compounds to improve energetic performance. The compounds were characterized using infrared and Raman as well as multinuclear NMR spectroscopy. Additionally, X-ray crystallographic measurements were performed and deliver insight into structural characteristics as well as intermolecular interactions. The potential application of the synthesized compounds as energetic materials were studied and evaluated using the experimentally obtained values for the thermal decomposition, the sensitivity data, as well as the calculated performance characteristics..

RESULTS AND DISCUSSION

SYNTHESIS

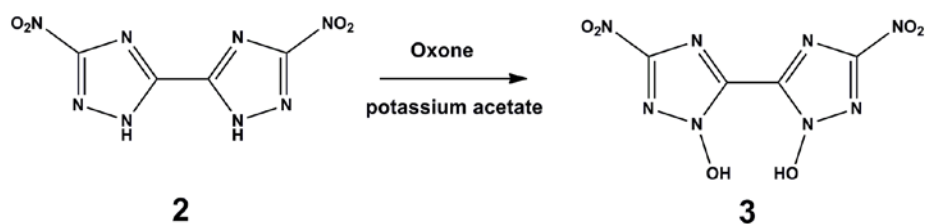
3,3'-Diamino-5,5'-bis(1*H*-1,2,4-triazole) (**1**) and 3,3'-dinitro-5,5'-bis(1*H*-1,2,4-triazole) (**2**) were synthesized according to literature.³⁹ The synthesis is based on the reaction of oxalic acid and aminoguanidinium bicarbonate in concentrated hydrochloric acid and subsequent cyclisation in basic media. Oxidation of DABT was accomplished by the well

known Sandmeyer reaction via diazotization in sulfuric acid and subsequent reaction with sodium nitrite (Scheme 1).



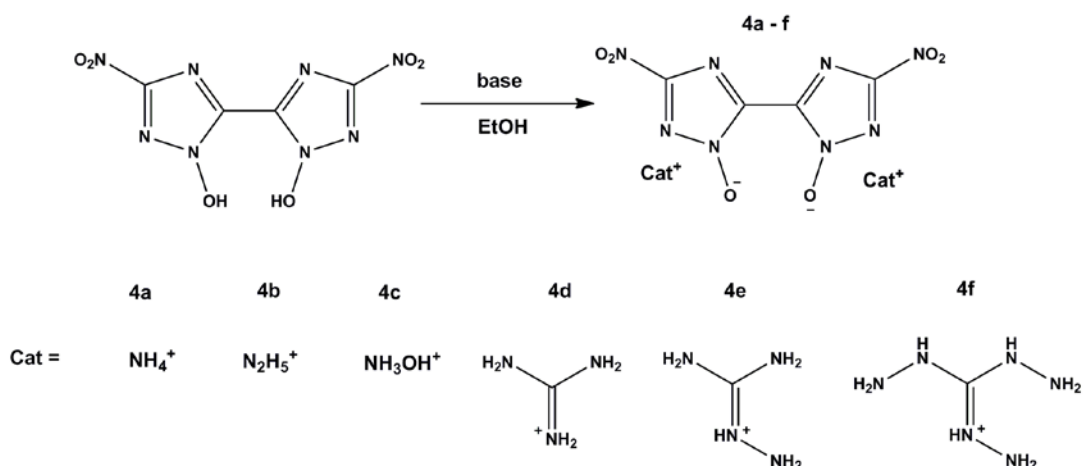
Scheme 1. Synthesis of 3,3'-dinitro-5,5'-bis-1*H*-1,2,4-triazole.

3,3'-Dinitro-5,5'-bis(1*H*-1,2,4-triazole) was successfully oxidized in an buffered aqueous solution of Oxone® at 40 °C similar to the recently published oxidation of 5-nitro- and 5-azidotetrazole.^{35,40} (Scheme 2). Best results were obtained with a portionwise addition of Oxone® and a carefully adjusted pH of 4–5, which leads to the selective oxidation to 3,3'-dinitro-5,5'-bis-1,2,4-triazole-1,1'-diol. The simple and straightforward method of N-Oxide introduction in triazole compounds is based on the unique properties of Oxone® like suitable oxidation potential, moderate costs, simple handling and sufficient long time stability. Other oxidation agents like organic peracids, perborates, hydrogen peroxide or hyperfluoric acid are either more expensive or involve a larger effort regarding the whole process.



Scheme 2. Synthesis of 3,3'-dinitro-5,5'-bis-1,2,4-triazole-1,1'-diol.

The formation of the nitrogen-rich salts (**4a–f**) is straightforward. An ethanolic solution of the compound **3** was prepared and two equivalents of the corresponding nitrogen-rich base were added (Scheme 3). Due to the high solubility of DNBTO and the low solubility of compounds **4a–f** in ethanol, all ionic derivatives could be isolated in excellent yields and high purity.



Scheme 3. Synthesis of ionic derivatives based on the 3,3'-dinitro-5,5'-bis-1,2,4-triazole-1,1'-diolate anion.

All compounds were fully characterized by IR and Raman as well as multinuclear NMR spectroscopy, mass spectrometry and differential scanning calorimetry. Selected compounds were additionally characterized by low temperature single crystal X-ray spectroscopy.

MULTINUCLEAR NMR SPECTROSCOPY

All compounds were investigated using ^1H , ^{13}C and ^{14}N NMR spectroscopy. Additionally, ^{15}N NMR spectra were recorded for compounds **3** and **4c**. The two signals of the compounds **2** and **3** differ only slightly in the $^{13}\text{C}\{^1\text{H}\}$ NMR spectrum. One signal for the bridging carbon atom can be observed at 145.6 ppm for DNBTO (**2**) and at 134.4 ppm for DNBTO (**3**). The oxidation of the triazole ring leads to a shift of the carbon atom (C- NO_2) signal towards higher field from 162.7 ppm (**2**) to 154.9 ppm for compound **3**. In the $^{14}\text{N}\{^1\text{H}\}$ NMR spectra, the nitro group of compound **3** can be identified by a broad singlet at -27 ppm.

The deprotonation of DNBTO with nitrogen-rich bases shifts the signals in the $^{13}\text{C}\{^1\text{H}\}$ NMR spectra to higher field. The carbon atom connecting both triazole rings can be found in the range of 132.7–133.2 ppm, the one connected to the nitro group is located in the range of 150.7–152.3 ppm. A trend for the shift of the nitro group signal in the $^{14}\text{N}\{^1\text{H}\}$ NMR spectra could not be observed, all signals appeared at chemical shifts of -20 to -33 ppm. The $^{14}\text{N}\{^1\text{H}\}$ NMR spectra of **4a** and **4b** additionally show the signal of the corresponding cation at -359 ppm. The signals of all nitrogen-rich cations in the ^1H NMR spectrum could be observed in the expected range.^{27,41}

Four well resolved resonances are detected in the ^{15}N NMR spectra for the four nitrogen atoms of both compounds **3** and **4c** (Figure 1). In addition, the signal of the hydroxylammonium cation could be observed for compound **4c** at -298.7 ppm. The assignments were based on comparison with theoretical calculations using Gaussian 09 (MPW1PW91/aug-cc-pVDZ).⁴² The signals mostly remain unchanged upon oxidation of the triazole ring in comparison to compound **2**.³⁹ Only the nitrogen atom N1, which is directly connected to the hydroxyl group is shifted towards higher field (-156.1 ppm (**2**), -121.5 ppm (**3**)). As expected, the nitrogen atoms N1 and N2 are shifted to lower field upon deprotonation in compound **4c**. The largest effect can be observed for the nitrogen atom N1, which can now be found at a chemical shift of -95.9 ppm (-121.5 ppm for **3**).

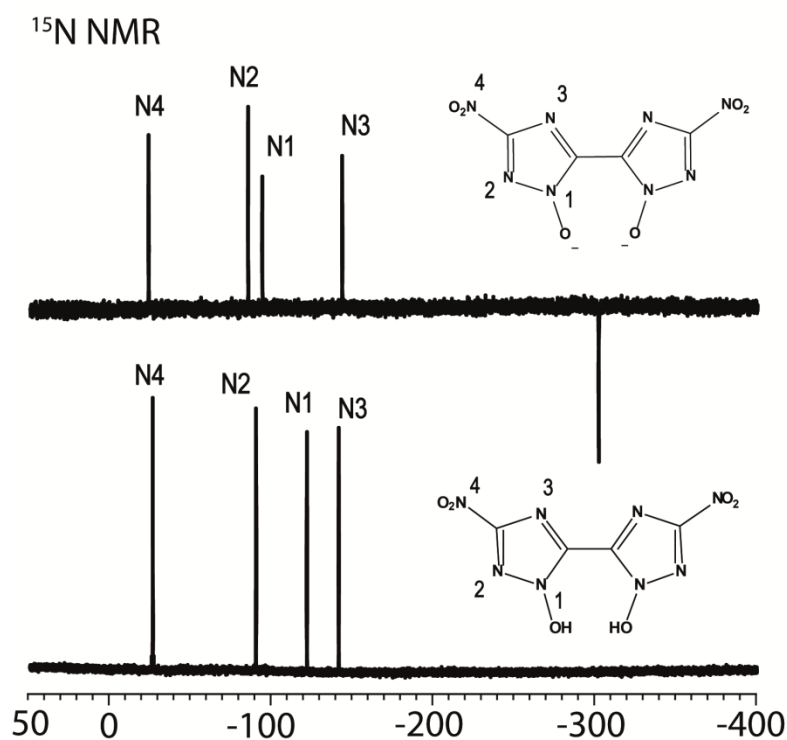


Figure 1: ^{15}N NMR spectra of compounds **3** and **4c** in DMSO-d_6 ; x-axis represents the chemical shift δ in ppm.

SINGLE CRYSTAL X-RAY STRUCTURE ANALYSIS

Single crystal X-ray diffraction studies were accomplished for compounds **3** and **4a–f** at 173 K. All compounds were recrystallized from water and show high crystal densities (1.862 g cm^{-3} (**3** $\times 2 \text{ H}_2\text{O}$), 1.696 g cm^{-3} (**4a** $\times 2 \text{ H}_2\text{O}$), 1.841 g cm^{-3} (**4b**), 1.952 g cm^{-3} (**4c**), 1.788 g cm^{-3} (**4d**), 1.764 g cm^{-3} (**4e**), 1.730 g cm^{-3} (**4f** $\times 2 \text{ H}_2\text{O}$)). In the following, the structural properties of compounds **3** and **4c** will be discussed in detail to point out the

structural characteristics of N-oxides in comparison to the parent compounds without hydroxy group. Selected crystallographic data of all compounds **4a–f** are compiled in Table S1 (Supporting information). A comparison of selected bond length and bond angles of compounds **4a–f** with the values obtained for corresponding compounds bearing no N-oxide²⁷ is given in Table S3 in the supporting information.

The bond lengths of both bistriazolate anions (with and without N-oxide) are comparable within the limits of error in contrast to their bond angles. The average C₁–N₁–N₂ angle of the N-oxide anions has an average value of 110.0° as compared to an average value of 106.1° for the N-oxide free 3,3'-dinitro-5,5'-bis-1,2,4-triazolate anion. Both neighboring angles N₁–C₁–N₃ (109.8°) and N₁–N₂–C₂ (100.8°) are smaller in comparison to the average value of the triazolate anions (113.7° and 103.6°).

This difference is not observed in the case of the corresponding free acids **2** and **3**. Both compounds show comparable values for bond length and bond angles, the C₁–N₁–N₂ angle is only slightly elongated from 110.2° (**2**) to 112.1° (**3**) due to the introduction of the N-hydroxy group.

The most striking difference between the N-oxide containing compounds and their parent relatives is observed in their extended structures. Each of the compounds **4a–f** has a higher crystal density (about 0.1 g cm⁻³) compared to the corresponding N-oxide free compound as a consequence of the N-oxide being involved in multiple intermolecular bonding interactions as exemplified in the case of **4c**.

Hydroxylammonium 3,3'-dinitro-bis-(1,2,4-triazole)-1,1'-diolate **4c** crystallizes in the monoclinic spacegroup *P*2₁/*c* with two molecular moieties in the unit cell. The calculated density at 173 K is 1.952 g cm⁻³, which is notably higher than the corresponding hydroxylammonium salt of compound **2** (1.836 g cm⁻³).²⁷ The remarkably high densities can be rationalized in terms of intermolecular interactions, as shown exemplarily for compound **4c** in the following. Each DNBTO²⁻ anion within the crystal structure of **4c** is surrounded by six hydroxylammonium cations via strong hydrogen bonds towards the nitrogen atoms of the triazole (N2, N3) ring and the oxygen O3 of the N-oxide (Figure 2). It is remarkable to note that all accessible hydrogen bond acceptors in the triazole-N-oxide moiety are connected to the surrounding hydroxylammonium cations. All three contacts are well within the sum of van der Waals radii ($r_w(\text{O}) + r_w(\text{N}) = 3.07 \text{ \AA}$, $r_w(\text{N}) + r_w(\text{N}) = 3.20 \text{ \AA}$)⁴³ with a D⋯A length of 2.575(2) Å, 3.144(2) Å and 2.874(2) Å (Table 1). The strong network is supported by several short contacts of the nitro group (O1, O2) with the nitrogen N5 of the cations (dashed lines in Figure 3). The O1⋯N5ⁱⁱ and

O2...N5^{iv} contact distance are in the range of 2.834(2) Å to 3.069(2) Å. Additionally, one of the oxygen atoms (O2) of the nitro group is involved in an interaction with the π -electrons of the overlying triazole ring, which leads to a stacking along the *b*-axis.

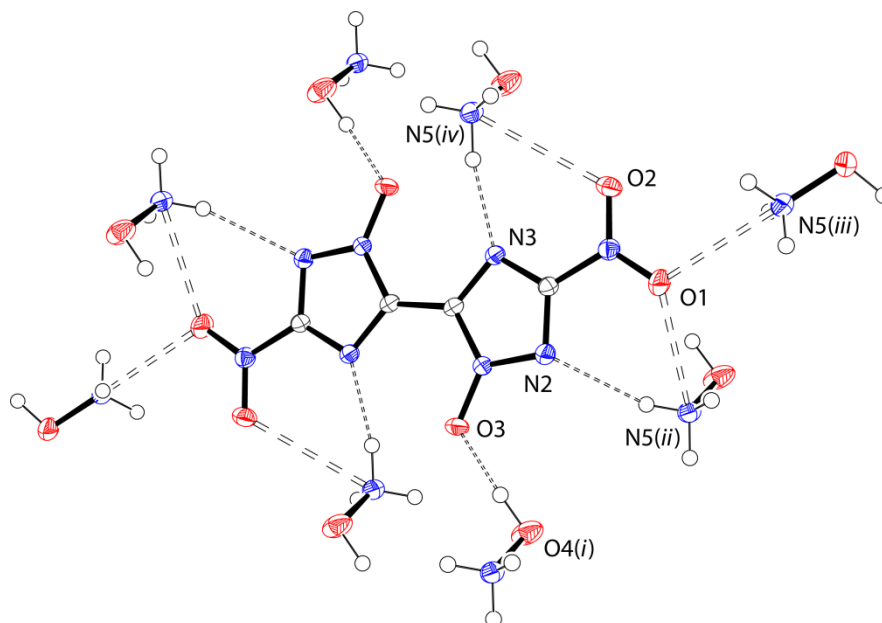


Figure 2: Surrounding of the DNBTO²⁻ anion in the crystal structure of **4c**, hydrogen bonds towards hydroxylammonium cations are marked as dotted lines, short contacts as dashed lines. Thermal ellipsoids are set to 50 % probability. Symmetry operators: (i) 1+x, y, z; (ii) 1+x, -1+y, z; (iii) 1-x, -1.5+y, 1/2-z; (iv) x, -1+y, z.

Table 1: Hydrogen bonds present in **4c**.

D-H...A	d (D-H) [Å]	d (H...A) [Å]	d (D-H...A) [Å]	< (D-H...A) [°]
O4 ⁱ -H4...O3	0.92(2)	1.65(2)	2.575(2)	176(2)
N5 ⁱⁱ -H5c...N2	0.86(2)	2.33(2)	3.144(2)	159(2)
N5 ^{iv} -H5b...N3	0.93(2)	1.96(2)	2.874(2)	169(2)

Symmetry Operators: (i) 1+x, y, z; (ii) 1+x, -1+y, z; (iii) 1-x, -1.5+y, 1/2-z; (iv) x, -1+y, z.

The structure of the free acid **3** (dihydrate) at 100 K has monoclinic symmetry ($P2_1/c$) with two molecular moieties in the unit cell. The calculated density is 1.883 g cm⁻³ which is again notably above the density of the dihydrate of compound **2** (1.764 g cm⁻³).⁴⁴ As expected the N1-O3 bond is elongated from 1.30 Å (average value for compounds **4a-f**) to 1.349(2) Å by protonation. The structure is also dominated by several intermolecular interactions such as strong hydrogen bonds (Table 2) and an

interaction of the oxygen atom O1 of the nitro group with the π -electrons of the triazole ring (Figure 3).

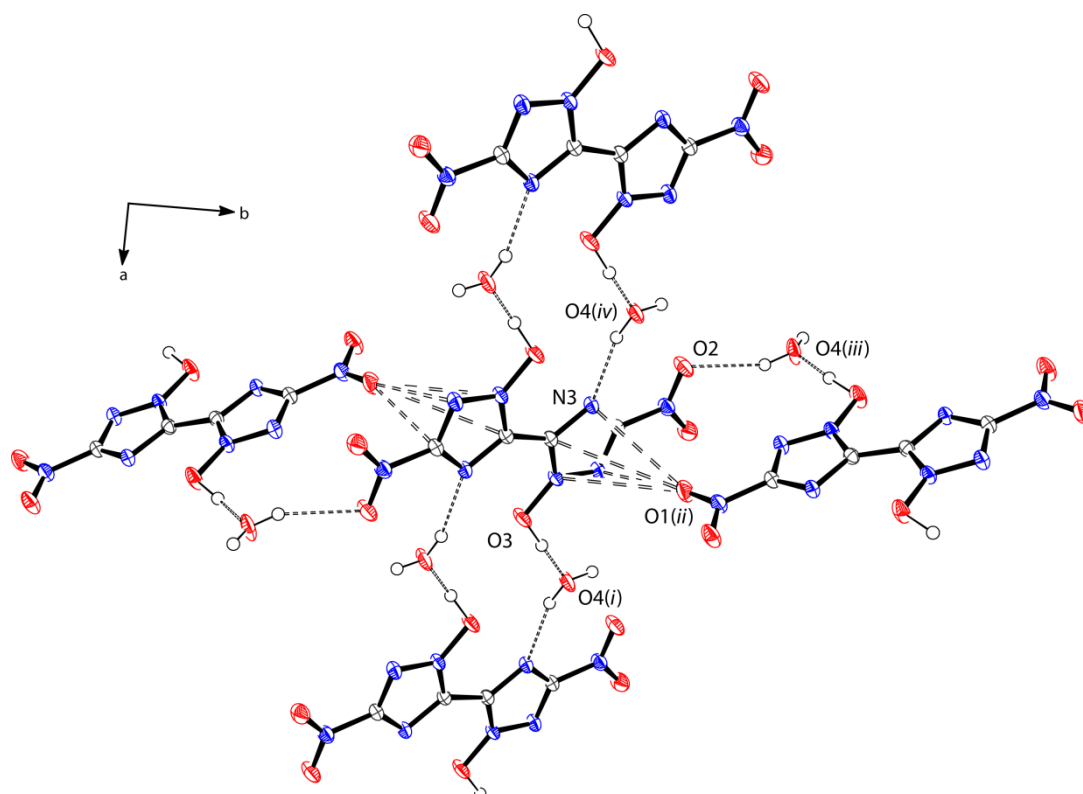


Figure 3: Intermolecular interactions in the crystal structure of **3** (view along c -axis), hydrogen bonds are marked as dotted lines, dashed lines indicate the interaction between the oxygen atom O1 of the nitro group and the π -electrons of the triazole (contact distance: 3.041(1) Å [O1ⁱⁱ...Cg(π_{ring})]). Thermal ellipsoids are set to 50 % probability. Symmetry operators: (i) $-x, 1-y, 1-z$; (ii) $x, 0.5-y, 0.5+z$; (iii) $x, 0.5-y, 0.5+z$; (iv) $-1-x, -y, 1-z$.

Table 2: Hydrogen bonds present in **3**.

D-H...A	d (D-H) [Å]	d (H...A) [Å]	d (D-H...A) [Å]	< (D-H...A) [°]
O3-H3...O4 ⁱ	1.10(2)	1.34(2)	2.439(9)	174(2)
O4 ⁱⁱⁱ -H42...O2	0.83(3)	2.26(3)	2.949(7)	141(2)
O4 ^{iv} -H41...N3	0.91(3)	2.00(3)	2.890(11)	164(2)

Symmetry Operators: (i) $-x, 1-y, 1-z$; (ii) $x, 0.5-y, 0.5+z$; (iii) $x, 0.5-y, 0.5+z$; (iv) $-1-x, -y, 1-z$.

PHYSICOCHEMICAL PROPERTIES: HEATS OF FORMATION, DETONATION PARAMETERS AND THERMAL STABILITIES

The heats of formation of **3** and **4a–4f** and RDX have been calculated using the atomization energy method and utilizing experimental data (for further details and results refer to the Supporting Information). All compounds show highly endothermic enthalpies of formation in the range from 98 kJ mol⁻¹ (**4d**) to 812 kJ mol⁻¹ (**4f**). The enthalpy of formation for compound **3** (290 kJ mol⁻¹) is similar in comparison to the starting material **2** (285 kJ mol⁻¹).²⁷ To estimate the detonation performances of the prepared compounds selected key parameters were calculated with EXPLO5 (version 5.05),⁴⁵ and compared to RDX. The calculated detonation parameters using experimentally determined densities (gas pycnometry at 25 °C, all compounds were dried before the measurements at 110 °C to remove moisture and crystal water) and above mentioned heats of formation are summarized in Table 3.

The N-hydroxy compound **3** shows the same sensitivities towards impact and friction and a lower decomposition temperature of 191 °C compared to the starting compound **2** (251 °C),²⁷ as it is expected for N-hydroxy azoles.^{34,35} Since salts of energetic compounds tend to be more stable in comparison to the non-ionic parent compound, the nitrogen-rich salts of DNBTO are expected to show an improved stability.

The decomposition temperatures of all ionic compounds are higher than that of compound **3** in the range from 207 °C (**4f**) to 329 °C (**4d**) and similar to the ones of the ionic derivatives of compound **2**.²⁷ The thermal stability decreases in the row of compounds **4a–c** with the ammonium salt (**4a**) showing the highest value of 257 °C and the hydroxylammonium salt (**4c**) having a decomposition onset at 217 °C. The same trend can be observed for the series of guanidinium derivatives (**4d–f**). The guanidinium salt (**4d**) shows the highest decomposition temperature with 329 °C, followed by the aminoguanidinium salt (**4e**) (246 °C) and the triaminoguanidinium salt (**4f**) with a decomposition onset at 207 °C. In addition, compounds **4a–f** are mostly insensitive towards friction and impact, merely the hydrazinium compound **4b** is sensitive towards outer stimuli (15 J, 324 N).

The detonation velocities were calculated to lie within the range of 8102 m s⁻¹ (**4d**) to 9087 m s⁻¹ (**4c**). In comparison to the ionic derivatives of compound **2**,²⁷ a marked performance increase is seen. The detonation velocities increase in the range from 400 ms⁻¹ to 600 ms⁻¹. The introduction of the *N*-Oxide also positively influences other

detonation parameters like the detonation pressure or the energy of explosion, which are also a remarkably increased.

Table 4: Physico-chemical properties of compounds **1–3** and **4a–c** in comparison to hexogen (RDX).

	(3)	(4a)	(4b)	(4c)	(4d)	(4e)	(4f)	RDX ^[n]
Formula	C ₄ H ₂ N ₈ O ₆	C ₄ H ₈ N ₁₀ O ₆	C ₄ H ₁₀ N ₁₂ O ₆	C ₄ H ₈ N ₁₀ O ₈	C ₆ H ₁₂ N ₁₄ O ₆	C ₄ H ₁₄ N ₁₆ O ₆	C ₆ H ₁₈ N ₂₀ O ₆	C ₃ H ₆ N ₆ O ₆
M [g mol ⁻¹]	258.1	292.2	322.2	324.2	376.2	406.3	466.3	222.1
IS [J] ^a	10	>40	15	>40	>40	35	>40	7
FS [N] ^b	360	360	324	>360	>360	>360	>360	120
ESD [J]	0.40	0.80	0.15	0.50	0.80	0.24	0.20	--
N [%] ^c	43.4	47.9	52.2	43.2	52.1	55.2	60.0	37.8
Ω [%] ^d	-18.6	-32.9	-34.8	-19.7	-51.0	-51.2	-51.5	-21.6
T _{dec.} [°C] ^e	191	257	228	217	329	246	207	210
ρ [g cm ⁻³] ^f	1.92	1.76	1.80	1.90	1.75	1.72	1.78	1.80
Δ _f H _m ^o [kJ mol ⁻¹] ^g	290	104	413	213	98	339	812	70
Δ _f U ^o [kJ kg ⁻¹] ^h	1201	457	1391	756	366	944	1858	417
EXPLO5 (V5.05) values:								
-Δ _E U ^o [kJ kg ⁻¹] ⁱ	5786	4999	5654	5985	4161	4540	5106	6125
T _E [K] ^j	4529	3628	3842	4153	3060	3212	3372	4236
p _{C-J} [kbar] ^k	362	297	342	390	263	272	328	349
V _{Det.} [m s ⁻¹] ^l	8729	8388	8915	9087	8102	8268	8919	8748
Gas vol. [L kg ⁻¹] ^m	647	763	795	734	770	790	818	739

^[a] BAM drop hammer; ^[b] BAM friction tester; ^[c] Nitrogen content; ^[d] Oxygen balance; ^[e] Temperature of decomposition by DSC ($\beta = 5$ °C, Onset values); ^[f] density values are based on gas pycnometer measurements at 25 °C of anhydrous compounds, except **4c**: density derived from X-ray structure measurement at 25 °C; ^[g] Molar enthalpy of formation (for further details refer to the Supporting Information); ^[h] Energy of formation; ^[i] Energy of Explosion; ^[j] Explosion temperature; ^[k] Detonation pressure; ^[l] Detonation velocity; ^[m] Assuming only gaseous products; ^[n] values based on Ref. ⁴⁶ and the EXPLO5.05 database.

As potential replacements for commonly used secondary explosive, two compounds show the most suitable values regarding the detonation parameters, sensitivities and thermal stability. The best compounds competing with RDX are the triaminoguanidinium (**4f**) as

well as the hydroxylammonium salt (**4c**), taking into account the performance values and sensitivities. Compound **4c** displays the best performance with a calculated detonation velocity of 9087 ms^{-1} , a detonation pressure of 390 kbar and a decomposition temperature of 217°C . The triaminoguanidinium compound exhibits energetic properties in the same range with 8919 m s^{-1} , a detonation pressure of 328 kbar and a decomposition temperature of 207°C . Both compounds outperform RDX by calculations and show lower sensitivities along with a higher nitrogen content. Especially the hydroxylammonium salt **4c** exhibits sufficient performance requirements and adequate stability in order to find application.

Although lower performance values ($v_{\text{det}} = 8102 \text{ m s}^{-1}$, $p_{\text{C-J}} = 263 \text{ kbar}$) were calculated for the guanidinium salt **4d** in comparison to **4c** and **4f**, this compound displays an excellent decomposition temperature of 329°C together with an insensitivity towards friction and impact and could therefore be a potential replacement for hexanitrostilbene (HNS).

CONCLUSIONS

In this contribution we reported on the synthesis and full structural as well as spectroscopic characterization of 3,3'-dinitro-5,5'-bis-1,2,4-triazole-1,1'-diol and nitrogen-rich salts thereof. It is possible to oxidize 3,3'-dinitro-5,5'-bis-1*H*-1,2,4-triazole to the corresponding 1,1'-dihydroxy compound under mild, aqueous conditions in high yield. The ionic compounds **4a–f** were synthesized by reaction of the neutral compound **3** with the corresponding nitrogen rich bases. The simple and straightforward method of N-Oxide introduction in triazole compounds using commercially available Oxone® improves the energetic properties and reveals a new synthetic pathway towards novel energetic 1,2,4-triazole derivatives. All compounds were characterized using infrared and Raman as well as multinuclear NMR spectroscopy, X-ray crystallographic measurements were performed for the first time and deliver insight into structural characteristics and strong intermolecular interactions. The most striking difference between the N-oxide containing compounds **4a–f** and their parent relatives is a higher crystal density (about 0.1 g cm^{-3}) compared to the corresponding N-oxide free compounds as a consequence of the N-oxide being involved in multiple intermolecular bonding interactions as exemplified in the case of **4c**.

The standard enthalpies of formation were calculated for all compounds at the CBS-4M level of theory, revealing highly positive heats of formation in all cases. The energetic properties (detonation velocity, pressure, etc.) were calculated using the EXPLO5.05 program, all compounds show superior performance in comparison to the corresponding ones bearing no *N*-oxide. All compounds were characterized in terms of sensitivities (impact, friction, electrostatic) and thermal stabilities. In general, the deprotonation of 3,3'-dinitro-5,5'-bis-1*H*-1,2,4-triazole-1,1'-diol influences the thermal stability as well the sensitivity values positively. Decomposition temperatures range from 207 °C to 329 °C indicating the 3,3'-dinitro-5,5'-bis-1*H*-1,2,4-triazole-1,1'-dioxide anion has the ability to form thermally stable energetic materials with appropriate cation pairing. In addition, compounds **4a–f** are mostly insensitive towards friction and impact, merely the hydrazinium compound **4b** is sensitive towards outer stimuli (15 J, 324 N). In summary, the ionic derivatives were found to be high thermally stable, insensitive compounds that are highly powerful but safe to handle and prepare. The most promising compound for industrial scale-up and practical use is the hydroxylammonium salt **4c**, which shows a straightforward synthesis including only four cheap and facile steps. Especially the combination of an exceedingly high performance superior to RDX and insensitivity to mechanical stimuli highlights this compound as potential high explosive, which could find practical use as RDX replacement.

EXPERIMENTAL SECTION

Caution: Due to the fact that energetic triazole compounds are to some extent unstable against outer stimuli, proper safety precautions should be taken when handling the materials. Especially dry samples are able to explode under the influence of impact or friction. Lab personnel and the equipment should be properly grounded and protective equipment like grounded shoes, leather coat, Kevlar® gloves, ear protection and face shield is recommended for the handling of any energetic material.

General. All chemical reagents and solvents were obtained from Sigma-Aldrich Inc. or Acros Organics (analytical grade) and were used as supplied without further purification. ^1H , $^{13}\text{C}\{^1\text{H}\}$, $^{14}\text{N}\{^1\text{H}\}$ and ^{15}N NMR spectra were recorded on a JEOL Eclipse 400 instrument in $\text{DMSO-}d_6$ at 25 °C. The chemical shifts are given relative to tetramethylsilane (^1H , ^{13}C) or nitro methane (^{14}N , ^{15}N) as external standards and coupling constants are given in Hertz (Hz). Infrared (IR) spectra were recorded on a Perkin-Elmer

Spectrum BX FT-IR instrument equipped with an ATR unit at 25 °C. Transmittance values are qualitatively described as “very strong” (vs), “strong” (s), “medium” (m), “weak” (w) and “very weak” (vw). Raman spectra were recorded on a Bruker RAM II spectrometer equipped with a Nd:YAG laser (200 mW) operating at 1064 nm and a reflection angle of 180°. The intensities are reported as percentages of the most intense peak and are given in parentheses. Elemental analyses (CHNO) were performed with a Netzsch Simultaneous Thermal Analyzer STA 429. Melting and decomposition points were determined by differential scanning calorimetry (Linseis PT 10 DSC, calibrated with standard pure indium and zinc). Measurements were performed at a heating rate of 5 °C min⁻¹ in closed aluminum sample pans with a 1 µm hole in the lid for gas release to avoid an unsafe increase in pressure under a nitrogen flow of 20 mL min⁻¹ with an empty identical aluminum sample pan as a reference.

For initial safety testing, the impact and friction sensitivities as well as the electrostatic sensitivities were determined. The impact sensitivity tests were carried out according to STANAG 4489⁴⁷, modified according to WIWeB instruction 4-5.1.02⁴⁸ using a BAM⁴⁹ drop hammer. The friction sensitivity tests were carried out according to STANAG 4487⁵⁰ and modified according to WIWeB instruction 4-5.1.03⁵¹ using the BAM friction tester. The electrostatic sensitivity tests were accomplished according to STANAG 4490⁵² using an electric spark testing device ESD 2010 EN (OZM Research).

The single-crystal X-ray diffraction data of **3**, **4a–4c** were collected using an Oxford Xcalibur3 diffractometer equipped with a Spellman generator (voltage 50 kV, current 40 mA), Enhance molybdenum K α radiation source (λ = 71.073 pm), Oxford Cryosystems Cryostream cooling unit, four circle kappa platform and a Sapphire CCD detector. Data collection and reduction were performed with CrysAlisPro.⁵³ The structures were solved with SIR97⁵⁴, refined with SHELXL-97⁵⁵, and checked with PLATON⁵⁶, all integrated into the WinGX software suite⁵⁷. The finalized CIF files were checked with checkCIF.⁵⁸ Intra- and intermolecular contacts were analyzed with Mercury.⁵⁹ CCDC 934360 (**3**), 934361 (**4a**), 934362 (**4b**), 934363 (**4c**), 934364 (**4d**), 934365 (**4e**) and 934366 (**4f**) contain the supplementary crystallographic data for this paper. These data can be obtained free of charge from the Cambridge Crystallographic Data Centre via www.ccdc.cam.ac.uk/data_request/cif.

3,3'-Diamino-5,5'-bis(1H-1,2,4-triazole) (**1**) and 3,3'-Dinitro-5,5'-bis(1H-1,2,4-triazole) (**2**) were synthesized according to literature.³⁹

3,3'-Dinitro-5,5'-bis-1H-1,2,4-triazole-1,1'-diol (3)

3,3'-Dinitro-5,5'-bis(1H-1,2,4-triazole) (5.0 g, 19 mmol) was dissolved in a solution of water (125 mL) and potassium acetate (25.0 g, 0.25 mol) and heated to 40 °C. Oxone® (83.0 g, 0.27 mol) was added portion wise within 2 hours and the pH was meanwhile carefully adjusted to 4–5 by dropwise addition of potassium acetate (38.0 g, 0.38 mol) in water (50 mL). The mixture was subsequently stirred at 40 °C for 48 h. The solution was acidified with sulfuric acid (50 wt%, 150 mL) and extracted with ethyl acetate (4×100 mL). The combined organic phases were dried over magnesium sulfate and the solvent was evaporated in vacuum to yield **3** (4.0 g, 16 mmol, 81%) as a colorless solid.

¹H NMR (DMSO-*d*₆): δ (ppm) = 9.01 (s, 2H, OH) ppm; ¹³C NMR (DMSO-*d*₆): δ (ppm) = 154.9 (C-NO₂), 134.4 (C-C); ¹⁴N NMR (DMSO-*d*₆): δ (ppm) = -27 (NO₂); ¹⁵N NMR (DMSO-*d*₆): δ (ppm) = -28.4 (N4), -90.7 (N2), -121.5 (N1), -140.6 (N3); IR: ν (cm⁻¹) = 3502(m), 3462(s), 3346(s), 1628(m), 1550(vs), 1461(s), 1407(m), 1346(w), 1314(m), 1232(m), 1177(m), 1041(w), 1006(w), 872(w), 831(m), 803(m), 760(w), 753(w), 732(w), 669(w). Raman (200 mW): ν (cm⁻¹) = 1670(15), 1664(15), 1653(14), 1619(23), 1591(74), 1557(18), 1486(46), 1467(62), 1435(39), 1409(98), 1328(37), 1255(46), 1182(100), 1036(65), 779(10), 767(9), 717(5), 473(3), 458(9), 415(12), 290(4), 271(6), 214(3), 214(3); EA (C₄H₂N₈O₆): calcd: C 18.61, H 0.78, N 43.41; found: C 18.77, H 0.94, N 42.13 *m/z* (FAB⁻): 257.0 [C₄N₈O₆H⁻]. Sensitivities (grain size: <100 μm): BAM friction: 360 N, BAM impact: 10 J, ESD: 0.4 J; DSC (onset, 5 °C min⁻¹): T_{Dec.}: 191 °C.

Diammonium 3,3'-dinitro-5,5'-bis-1,2,4-triazole-1,1'-diolate (4a)

Ammonia (gaseous) was led through a solution of **3** (0.30 g, 1.2 mmol) in ethanol (50 mL) for one minute. The precipitate was collected by filtration to give **4a** (0.29 mg, 1.0 mmol, 83%) as orange powder.

¹H NMR (DMSO-*d*₆): δ (ppm) = 6.93 (s, 8H, NH₄⁺) ppm; ¹³C NMR (DMSO-*d*₆): δ (ppm) = 151.1 (C-NO₂), 132.8 (C-C); ¹⁴N NMR (DMSO-*d*₆): δ (ppm) = -26 (NO₂), -359 (NH₄⁺); IR: ν (cm⁻¹) = 3401(s), 3192(s), 2993(vs), 2877(s), 2132(w), 1680(w), 1640(w), 1530(m), 1445(vs), 1412(vs), 1394(vs), 1387(vs), 1354(s), 1299(s), 1186(s), 1103(vs), 1028(vs), 885(w), 835(m), 764(w), 754(w), 740(m), 680(w), 680(w). Raman (200 mW): ν (cm⁻¹) = 1589(56), 1546(4), 1463(25), 1432(3), 1363(100), 1306(36), 1243(15), 1191(3), 1141(50), 1106(10), 1089(6), 1027(42), 862(2), 782(5), 559(3), 461(2), 442(2). EA

(C₄H₈N₁₀O₄): calcd: C 16.44, H 2.76, N 47.94; found: C 16.04, H 2.99, N 45.61; *m/z* (FAB⁺): 18 [NH₄⁺]; *m/z* (FAB⁻): 257.0 [C₄N₈O₆H⁻]; Sensitivities (grain size: <100 μm): friction: 360 N, impact: 40 J, ESD: 0.8 J; DSC (onset, 5 °C min⁻¹): T_{Dec}: 297 °C.

Dihydrazinium 3,3'-dinitro-5,5'-bis-1,2,4-triazole-1,1-diolate (4b)

Compound **3** (0.30 g, 1.2 mmol) was dissolved in ethanol (50 mL) and hydrazine (50 wt% in water, 0.12 mL, 2.4 mmol) was added. The precipitate was collected by filtration to give **4b** (0.33 mg, 1.0 mmol, 86%) as orange powder.

¹H NMR (DMSO-*d*₆): δ (ppm) = 4.64 (s, 6H, N₂H₅⁺) ppm; ¹³C NMR (DMSO-*d*₆): δ (ppm) = 152.3 (C-NO₂), 133.2 (C-C); ¹⁴N NMR (DMSO-*d*₆): δ (ppm) = -22 (NO₂), -356 (N₂H₅⁺); IR: ν (cm⁻¹) (rel. int.) = 3350(w), 3293(w), 3065(w), 2932(m), 2799(m), 2718(m), 2644(m), 2529(w), 1640(w), 1617(w), 1585(w), 1551(m), 1514(m), 1463(m), 1386(s), 1356(s), 1297(s), 1173(s), 1115(s), 1093(vs), 1037(s), 1023(s), 965(vs), 965(vs), 838(s), 750(s), 680(s). Raman: 1591(15), 1466(9), 1447(4), 1408(3), 1376(100), 1315(15), 1249(14), 1130(10), 1113(22), 1031(15), 868(4), 560(2), 469(1), 453(2), 369(1), 309(4), 293(2), 207(1). EA (C₄H₁₀N₁₂O₆): calcd: C 14.91, H 3.13, N 52.17; found: C 15.25, H 2.97, N 51.94; *m/z* (ESI⁻) 257.0 [C₄N₈O₆H⁻]. Sensitivities: (grain size: <100 μm): friction: 324 N, impact: >15 J, ESD: 0.15 J; DSC (onset, 5 °C min⁻¹): T_{Dec}: 228 °C.

Dihydroxylammonium 3,3'-dinitro-5,5'-bis-1,2,4-triazole-1,1-diolate (4c)

Compound **3** (0.30 g, 1.2 mmol) was dissolved in ethanol (50 mL) and hydroxylamine (50 wt% in water, 0.12 mL, 2.4 mmol) was added. The precipitate was collected by filtration to give **4c** (0.36 g, 1.1 mmol, 93%) as orange powder.

¹H NMR (DMSO-*d*₆): δ (ppm) = 10.24 (s, 6H, NH₃OH⁺) ppm; ¹³C NMR (DMSO-*d*₆): δ (ppm) = 152.3 (C-NO₂), 133.3 (C-C); ¹⁴N NMR (DMSO-*d*₆): δ (ppm) = -29 (NO₂), -359 (NH₃OH⁺); ¹⁵N NMR (DMSO-*d*₆): δ (ppm) = -27.4 (N4), -87.4 (N2), -95.9 (N1), -144.0 (N3), -298.7 (NH₃OH⁺); IR: ν (cm⁻¹) = 3261(w), 2361(w), 2332(w), 1534(m), 1519(m), 1466(s), 1408(s), 1394(s), 1358(s), 1302(vs), 1171(s), 1035(vs), 1016(s), 837(s), 740(s), 679(m). Raman: ν (cm⁻¹) = 1601(52), 1465(16), 1437(4), 1363(100), 1317(64), 1247(10), 1143(72), 1035(49), 872(9), 790(3), 756(2), 721(2), 565(8), 463(7), 451(3), 343(3), 298(2). EA (C₄H₈N₁₀O₈): calcd: C 14.82, H 2.49, N 43.21; found: C 15.11, H 2.37, N 43.27; *m/z* (FAB⁺): 34.0 [NH₄O⁺]; *m/z* (FAB⁻): 256.9 [C₄N₈O₆H⁻].

Sensitivities: (grain size: <100 μm): friction: 360 N, impact: >40 J, ESD: 0.5 J; DSC (onset, 5 $^{\circ}\text{C min}^{-1}$): $T_{\text{Dec.}}$: 217 $^{\circ}\text{C}$.

Diguanidinium 3,3'-dinitro-5,5'-bis-1,2,4-triazole-1,1-diolate (4d)

Guanidinium carbonate (0.20 g, 1.2 mmol) was added to a solution of compound **3** (0.30 g, 1.2 mmol) in ethanol (50 mL). The mixture was refluxed at 60 $^{\circ}\text{C}$ for 30 min and the precipitate was collected by filtration to give **4d** (0.31 g, 0.84 mmol, 71%) as orange powder.

^1H NMR (DMSO- d_6): δ (ppm) = 7.06 (s, 6H, NH_2) ppm; ^{13}C NMR (DMSO- d_6): δ (ppm) = 158.1 (C- NH_2), 151.1 (C- NO_2), 132.9 (C-C); ^{14}N NMR (DMSO- d_6): δ (ppm) = -33 (NO_2); IR: ν (cm^{-1}) = 3464(m), 3423(m), 3335(m), 3262(m), 3204(m), 3135(m), 2790(m), 2703(m), 2491(w), 2363(m), 2339(m), 1653(vs), 1571(m), 1499(m), 1454(s), 1387(s), 1367(vs), 1299(s), 1151(s), 1043(s), 1028(s), 837(m), 756(s), 756(s), 733(m). Raman: ν (cm^{-1}) = 1588(41), 1502(3), 1455(6), 1431(4), 1369(100), 1314(35), 1245(21), 1136(42), 1029(40), 863(16), 562(2), 542(2), 517(2), 465(4), 449(6), 303(7), 284(5), 236(3). EA ($\text{C}_6\text{H}_{12}\text{N}_{14}\text{O}_6$): calc.: C 19.25, H 3.21, N 52.12; found: C 19.30, H 3.09, N 50.85; m/z (FAB $^+$): 60.1 [CH_6N_3^+]. m/z (FAB $^-$): 257.0 [$\text{C}_4\text{N}_8\text{O}_6\text{H}^-$]. Sensitivities: (grain size: <100 μm): friction: 360 N, impact: >40 J, ESD: 0.8 J; DSC (onset, 5 $^{\circ}\text{C min}^{-1}$): $T_{\text{Dec.}}$: 329 $^{\circ}\text{C}$.

Di(aminoguanidinium) 3,3'-dinitro-5,5'-bis-1,2,4-triazole-1,1-diolate (4e)

Guanidinium carbonate (0.32 g, 2.3 mmol) was added to a solution of compound **3** (0.30 g, 1.2 mmol) in ethanol (50 mL). The mixture was refluxed at 60 $^{\circ}\text{C}$ for 30 min and the precipitate was collected by filtration to give **4e** (0.39 g, 0.96 mmol, 83%) as orange powder.

^1H NMR (DMSO- d_6): δ (ppm) = 7.36 (s, 4H, NH_2), 5.56 (s, 1H, NH), 4.61 (s, 2H, NH_2) ppm; ^{13}C NMR (DMSO- d_6): δ (ppm) = 158.9 (C- NH_2), 150.9 (C- NO_2), 132.7 (C-C); ^{14}N NMR (DMSO- d_6): δ (ppm) = -22 (NO_2); IR: ν (cm^{-1}) = 3744(vw), 3449(m), 3413(m), 3372(m), 3345(m), 3183(m), 2700(w), 2496(w), 2370(w), 1675(m), 1647(s), 1627(m), 1520(s), 1464(s), 1380(s), 1355(s), 1298(vs), 1199(w), 1156(s), 1040(m), 1028(s), 920(s), 836(s), 836(s), 748(s), 690(w), 673(w). Raman: ν (cm^{-1}) = 1578(30), 1502(1), 1463(11), 1401(6), 1361(100), 1314(25), 1239(18), 1165(3), 1132(43), 1103(5), 1028(36), 922(6), 859(9), 847(2), 788(2), 559(2), 513(3), 463(5), 340(2), 289(2), 273(4), 236(1), 208(1), 208(1). EA ($\text{C}_6\text{H}_{14}\text{N}_{16}\text{O}_6$): calcd: C 17.74, H 3.47, N 55.16; found: C

18.14, H 3.89, N 51.73; m/z (FAB⁺): 75.0 [CH₇N₃⁺]; m/z (FAB⁻): 256.9 [C₄N₈O₆H⁻]. Sensitivities: (grain size: <100 μm): friction: 360 N, impact: 35 J, ESD: 0.24 J; DSC (onset, 5 °C min⁻¹): T_{Dec.}: 246 °C.

Di(triaminoguanidinium) 3,3'-dinitro-5,5'-bis-1,2,4-triazole-1,1-diolate (4f)

Triaminoguanidine (0.24 g, 2.3 mmol) was added to a solution of compound **3** (0.30 g, 1.2 mmol) in ethanol (50 mL). The mixture was stirred for 30 min and the precipitate was collected by filtration to give **4f** (0.42 g, 0.95 mmol, 79%) as orange powder.

¹H NMR (DMSO-*d*₆): δ (ppm) = 8.58 (s, 3H, NH), 4.46 (s, 6H, NH₂) ppm; ¹³C NMR (DMSO-*d*₆): δ (ppm) = 159.1 (C-NH₂), 150.7 (C-NO₂), 132.9 (C-C); ¹⁴N NMR (DMSO-*d*₆): δ (ppm) = -20 (NO₂); IR: ν (cm⁻¹) = 3743(vw), 3627(w), 3341(m), 3180(m), 2918(w), 2849(w), 2362(w), 1675(s), 1652(s), 1539(w), 1510(m), 1456(s), 1379(s), 1340(s), 1293(vs), 1190(w), 1129(vs), 1034(m), 1020(s), 989(m), 953(m), 921(s), 834(m), 834(m), 752(s), 693(w), 678(w). Raman: ν (cm⁻¹) = 3372(2), 1683(3), 1589(100), 1521(2), 1499(3), 1455(26), 1426(15), 1399(14), 1376(75), 1348(61), 1308(71), 1247(48), 1203(5), 1112(71), 1013(94), 860(28), 847(3), 791(3), 750(2), 555(8), 463(11), 305(3), 287(3), 287(3), 257(1), 226(2). EA (C₆H₁₈N₂₀O₆): calcd: C 15.45, H 3.89, N 60.07; found: C 15.32, H 3.96, N 57.12; m/z (FAB⁺): 105.1 [CH₉N₆⁺]; m/z (FAB⁻): 257.0 [C₄N₈O₆H⁻]. Sensitivities: (grain size: <100 μm): friction: 360 N, impact: 40 J, ESD: 0.2 J; DSC (onset, 5 °C min⁻¹): T_{Dec.}: 207° C.

REFERENCES

- (1) Badgujar, D. M.; Talawar, M. B.; Asthana, S. N.; Mahulikar, P. P. *J. Hazard. Mater.* **2008**, *151*, 289.
- (2) Klapötke, T. *Chemistry of high-energy materials*; 2. ed.; de Gruyter: Berlin, **2012**.
- (3) Pagoria, P. F.; Lee, G. S.; Mitchell, A. R.; Schmidt, R. D. *Thermochimica Acta* **2002**, *384*, 187.
- (4) Singh, R. P.; Verma, R. D.; Meshri, D. T.; Shreeve, J. M. *Angew. Chem., Int. Ed.* **2006**, *45*, 3584.
- (5) Sabate, C. M.; Klapötke, T. M. *New Trends in Research of Energetic Materials, Proceedings of the 12th Seminar, University of Pardubice, Czech Republic, Apr. 1-3*, **2009**, p.172.

- (6) Yang, S.; Xu, S.; Huang, H.; Zhang, W.; Zhang, X. *Prog. Chem.* **2008**, *20*, 526.
- (7) Talawar, M. B.; Sivabalan, R.; Mukundan, T.; Muthurajan, H.; Sikder, A. K.; Gandhe, B. R.; Rao, A. S. *J. Hazard. Mater.* **2009**, *161*, 589.
- (8) Klapötke, T. M.; Stierstorfer, J.; Wallek, A. U. *Chem. Mater.* **2008**, *20*, 4519.
- (9) Klapötke, T. M.; Sabate, C. M. *Chem. Mater.* **2008**, *20*, 3629.
- (10) Chavez, D. E.; Hiskey, M. A.; Naud, D. L. *Prop. Explos. Pyrot.* **2004**, *29*, 209.
- (11) Huang, Y.; Gao, H.; Twamley, B.; Shreeve, J. M. *Eur. J. Inorg. Chem.* **2008**, 2560.
- (12) Gao, H.; Shreeve, J. M. *Chem. Rev.* **2011**, *111*, 7377.
- (13) *High energy density materials*; Klapötke, T. M., Ed.; Springer-Verlag: Berlin Heidelberg **2007**.
- (14) Fischer, N.; Izsák, D.; Klapötke, T. M.; Rappenglück, S.; Stierstorfer, J. *Chem-Eur. J.* **2012**, *18*, 4051.
- (15) Fischer, N.; Klapötke, T. M.; Peters, K.; Rusan, M.; Stierstorfer, J. *Z. Anorg. Allg. Chem.* **2011**, 637, 1693.
- (16) Guo, Y.; Tao, G.-H.; Zeng, Z.; Gao, H.; Parrish, D. A.; Shreeve, J. n. M. *Chem-Eur. J.* **2010**, *16*, 3753.
- (17) Oliveri-Mandala, E.; Passalacqua, T. *Gazz. Chim. Ital.* **1914**, *43*, 465.
- (18) Chavez, D. E.; Hiskey, M. A.; Naud, D. L. *J. Pyrotech.* **1999**, 17.
- (19) Metelkina, E. L.; Novikova, T. A.; Berdonosova, S. N.; Berdonosov, D. Y.; Grineva, V. S. *Russ. J. Org. Chem.* **2004**, *40*, 1412.
- (20) Metelkina, E. L.; Novikova, T. A.; Berdonosova, S. N.; Berdonosov, D. Y. *Russ. J. Org. Chem.* **2005**, *41*, 440.
- (21) Metelkina, E.; Novikova, T. *Russ. J. Org. Chem.* **2004**, *40*, 1737.
- (22) Astachov, A. M.; Revenko, V. A.; Kruglyakova, L. A.; Buka, E. S. In *New Trends in Research of Energetic Materials, Proceedings of the 10th Seminar, University of Pardubice, Czech Republic, Apr. 25-27, 2007*, p.505.
- (23) Astachov, A. M.; Revenko, V. A.; Buka, E. S. In *New Trends in Research of Energetic Materials, Proceedings of the 12th Seminar, University of Pardubice, Czech Republic, Apr. 1-3, 2009*, p 396.
- (24) Wang, R.; Xu, H.; Guo, Y.; Sa, R.; Shreeve, J. M. *J. Am. Chem. Soc.* **2010**, *132*, 11904.
- (25) Serov, Y. V.; Pevzner, M. S.; Kofman, T. P.; Tselinskii, I. V. *Russ. J. Org. Chem.* **1990**, *26*, 773.

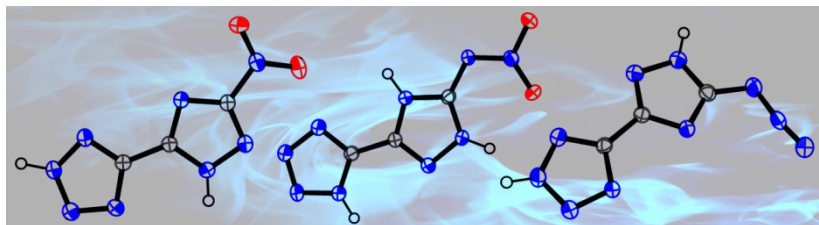
- (26) Bagal, L. I.; Pevzner, M. S.; Frolov, A. N.; Sheludyakova, N. I. *Chem. Heterocyc. Comp.* **1970**, 6, 240.
- (27) Dippold, A. A.; Klapötke, T. M.; Winter, N. *Eur. J. Inorg. Chem.* **2012**, 2012, 3474.
- (28) Rong, D.; Phillips, V. A.; Rubio, R. S.; Castro, M. A.; Wheelhouse, R. T. *Tetrahedron Lett.* **2008**, 49, 6933.
- (29) Klapötke, T. M.; Piercey, D. G.; Stierstorfer, J. *Chem-Eur. J.* **2011**, 17, 13068.
- (30) Harel, T.; Rozen, S. *J. Org. Chem.* **2010**, 75, 3141.
- (31) Molchanovaa, M. S.; Pivinaa, T. S.; Arnautovab, E. A.; Zefirovb, N. S. *J. Mol. Struct. THEOCHEM* **1999**, 465, 11.
- (32) Goebel, M.; Karaghiosoff, K.; Klapötke, T. M.; Piercey, D. G.; Stierstorfer, J. *J. Am. Chem. Soc.* **2010**, 132, 17216.
- (33) Singh, H.; Mukherjee, U.; Saini, R. S. *J. Energ. Mater.* **2012**, 30, 265.
- (34) Fischer, N.; Fischer, D.; Klapötke, T. M.; Piercey, D. G.; Stierstorfer, J. *J. Mater. Chem.* **2012**, 22, 20418.
- (35) Göbel, M.; Karaghiosoff, K.; Klapötke, T. M.; Piercey, D. G.; Stierstorfer, J. *J. Am. Chem. Soc.* **2010**, 132, 17216.
- (36) Neubauer, H.-J.; Kardoff, U.; Leyendecker, J.; Baus, U.; Künast, C.; Hofmeister, P.; Krieg, W.; Kristgen, R.; Reuther, W.; AG, B., Ed. 1992; Vol. US5120756.
- (37) Begtrup, M.; Vedso, P. *J. Chem. Soc. Perk. T. 1* **1995**, 0, 243.
- (38) Petrie, M. A.; Koolpe, G.; Malhotra, R.; Penwell P.; *SRI Project No. P18608 Final report* **2012**.
- (39) Dippold, A. A.; Klapötke, T. M. *Chem-Eur. J.* **2012**, 18, 16742.
- (40) Klapötke, T. M.; Piercey, D. G.; Stierstorfer, J. *Chem. Eur. J.* **2011**, 17, 13068.
- (41) Dippold, A. A.; Klapötke, T. M.; Martin, F. A.; Wiedbrauk, S. *Eur. J. Inorg. Chem.* **2012**, 2012, 2429.
- (42) Frisch, M. J.; Trucks, G. W.; Schlegel, H. B.; Scuseria, G. E.; Robb, M. A.; Cheeseman, J. R.; Scalmani, G.; Barone, V.; Mennucci, B.; Petersson, G. A.; Nakatsuji, H.; Caricato, M.; Li, X.; Hratchian, H. P.; Izmaylov, A. F.; Bloino, J.; Zheng, G.; Sonnenberg, J. L.; Hada, M.; Ehara, M.; Toyota, K.; Fukuda, R.; Hasegawa, J.; Ishida, M.; Nakajima, T.; Honda, Y.; Kitao, O.; Nakai, H.; Vreven, T.; Montgomery, J. A. J.; Peralta, J. E.; Ogliaro, F.; Bearpark, M.; Heyd, J. J.; Brothers, E.; Kudin, K. N.; Staroverov, V. N.; Kobayashi, R.; Normand, J.; Raghavachari, K.; Rendell, A.; Burant, J. C.; Iyengar, S. S.; Tomasi, J.; Cossi, M.;

- Rega, N.; Millam, J. M.; Klene, M.; Knox, J. E.; Cross, J. B.; Bakken, V.; Adamo, C.; Jaramillo, J.; Gomperts, R.; Stratmann, R. E.; Yazyev, O.; Austin, A. J.; Cammi, R.; Pomelli, C.; Ochterski, J. W.; Martin, R. L.; Morokuma, K.; Zakrzewski, V. G.; Voth, G. A.; Salvador, P.; Dannenberg, J. J.; Dapprich, S.; Daniels, A. D.; Farkas, Ö.; Foresman, J. B.; Ortiz, J. V.; Cioslowski, J.; Fox, D. J. Wallingford CT 2009.
- (43) Bondi, A. *J. Phys. Chem.* **1964**, 68, 441.
- (44) Nikitina, E. V.; Starova, G. L.; Frank-Kamenetskaya, O. V.; Pevzner, M. S. *Kristallografiya* **1982**, 27, 485.
- (45) Sućeska, M. *EXPLO5.5 program, Zagreb, Croatia*, 2010.
- (46) Meyer, R.; Köhler, J.; Homburg, A. *Explosives*; Sixth ed.; Wiley-VCH Verlag GmbH & Co. KGaA: Weinheim, 2007.
- (47) *NATO standardization agreement (STANAG) on explosives and impact tests, no.4489, 1st ed., Sept. 17, 1999.*
- (48) *WIWEB-Standardarbeitsanweisung 4-5.1.02, Ermittlung der Explosionsgefährlichkeit, hier: der Schlagempfindlichkeit mit dem Fallhammer, Nov. 08, 2002.*
- (49) *Bundesanstalt für Materialforschung, <http://www.bam.de>.*
- (50) *NATO standardization agreement (STANAG) on explosives, friction tests, no.4487, 1st ed., Aug. 22, 2002.*
- (51) *WIWEB-Standardarbeitsanweisung 4-5.1.03, Ermittlung der Explosionsgefährlichkeit, hier: der Reibempfindlichkeit mit dem Reibeapparat, Nov. 08, 2002.*
- (52) *NATO standardization agreement (STANAG) on explosives, electrostatic discharge sensitivity tests, no.4490, 1st ed., Feb. 19, 2001.*
- (53) *CrysAlisPro 1.171.36.21, Agilent Technologies, 2012.*
- (54) Altomare, A.; Cascarano, G.; Giacovazzo, C.; Guagliardi, A.; Moliterni, A. A. G.; Burla, M. C.; Poidori, G.; Camalli, M.; Spagne, R., *SIR-97, A program for crystal structure solution* **1997**.
- (55) Sheldrick, G. M. *SHELXL-97, Program for the Refinement of Crystal Structures. University of Göttingen, Germany*, 1997.
- (56) Spek, A. L. *Platon, A Multipurpose Crystallographic Tool, Utrecht University, Utrecht, The Netherlands*, 2012.
- (57) Farrugia, L. J. *J. Appl. Crystallogr.* **1999**, 32, 837.

- (58) <http://checkcif.iucr.org/>
- (59) Macrae, C. F.; Edgington, P.; McCabe, P.; Pidcock, E.; Shields, G. P.; Taylor, R.; Towler, M.; van de Streek, J. *J. Appl. Crystallogr.* **2006**, *39*, 565.

9. SYNTHESIS AND CHARACTERIZATION OF 5-(1,2,4-TRIAZOL-3-YL)TETRAZOLES WITH VARIOUS ENERGETIC FUNCTIONALITIES

As published in: Chemistry – An Asian Journal 2013, 8, 1463-1471.



ABSTRACT:

In this contribution the synthesis and full structural as well as spectroscopic characterization of three 5-(1,2,4-Triazol-3-yl)tetrazoles along with selected energetic moieties like nitro, nitrimino and azido groups are presented. The main goal is a comparative study on the influence of those variable energetic moieties on structural and energetic properties. A complete characterization including IR and Raman as well as multinuclear NMR spectroscopy of all compounds is presented. Additionally, X-ray crystallographic measurements were performed and deliver insight into structural characteristics as well as inter- and intramolecular interactions. The standard enthalpies of formation were calculated for all compounds at the CBS-4M level of theory, revealing high positive heats of formation for all compounds. The calculated detonation parameters (using the EXPLO5.05 program) are in the range of 8000 ms^{-1} (8097 ms^{-1} (**5**), 8020 ms^{-1} (**6**), 7874 ms^{-1} (**7**)). As expected, the measured impact and friction sensitivities as well as decomposition temperatures strongly depend on the energetic moiety of the triazole ring. The C–C connection of a triazole ring with its opportunity to introduce a large variety of energetic moieties and a tetrazole ring implying a large energy content leads to the selective synthesis of primary and secondary explosives.

INTRODUCTION

The design of energetic materials that combine high performance and low sensitivities has attracted worldwide research groups over the last decades.^[1] Intense research is focused on the tailoring of new energetic molecules with performances and stability similar to that of RDX (cyclotrimethylenetrinitramine) to replace this widely-used high explosive. Those traditional energetic materials are based on the oldest strategy in energetic materials design: the presence of fuel and oxidizer in the same molecule. Modern heterocyclic energetic compounds derive their energy not only from the oxidation of their carbon backbone but additionally from ring or cage strain, high-nitrogen content and high heats of formation. Nitrogen-rich compounds which mainly generate environmentally friendly molecular nitrogen as end-product of propulsion or explosion are in the focus of energetic materials research across the globe.^[1f, 2] Nitrogen-rich heterocycles are promising compounds that fulfill many requirements in the challenging field of energetic materials research.^[1f, 2] A prominent family of novel high-energy-density materials (HEDMs) are azole-based compounds, since they are generally highly endothermic with high densities and low sensitivities towards outer stimuli. Owing to the high positive heats of formation resulting from the large number of N–N and C–N bonds^[3] and the high level of environmental compatibility, those compounds have been studied in our group over the last couple of years with growing interest. Possessing high heats of formation and ring strain, triazoles and tetrazoles have been used for the preparation of high-performance primary^[4] and secondary explosives^[5]. Energetic materials based on those heterocycles show the desirable compromise in properties with high nitrogen contents on the one hand, and surprising kinetic and thermal stabilities due to aromaticity on the other. Many research has been done on the combination of those heterocycles to bistetrazoles^[6] and bistriazoles^[7], resulting in numerous compounds with outstanding properties as energetic materials. The connection via C–C bond of a triazole ring with its opportunity to introduce a large variety of energetic moieties such as nitro groups (R–NO₂),^[8] nitramines (R₂N–NO₂)^[9] or azides (R–N₃)^[10] and a tetrazole ring implying a large energy content leads to energetic materials with tunable properties.

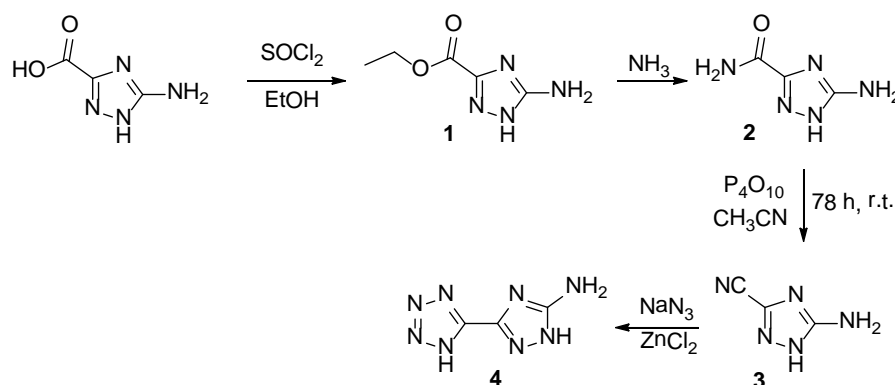
The focus of this contribution is on the full structural and spectroscopic characterization of three selected triazolyl-tetrazoles carrying energetic moieties like nitro, nitramino and azido groups. We present a comparative study on the influence of those energetic moieties on structural and energetic properties. The potential application of the

synthesized compounds as energetic material will be studied and evaluated using the experimentally obtained values for the thermal decomposition, the sensitivity data, as well as the calculated performance characteristics.

RESULTS AND DISCUSSION

SYNTHESIS

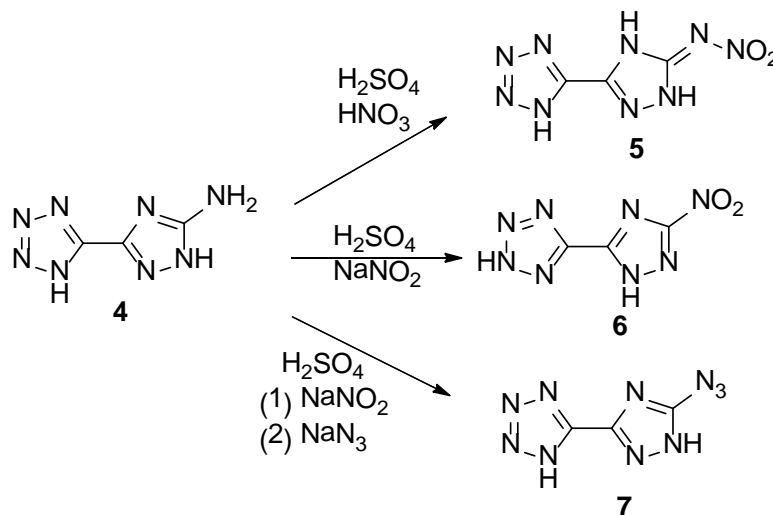
The synthesis of 5-amino-1*H*-1,2,4-triazole-3-carbonitrile (ATCN, **3**) starts with the in situ chlorination of the 5-amino-1*H*-1,2,4-triazole-3-carboxylic acid with thionyl chloride in ethanol and subsequent formation of the carboxylic acid ester (**1**). The intermediate product ethyl 5-amino-1*H*-1,2,4-triazole-3-carboxylate (**1**) is reacted with ammonia resulting in the formation of 5-amino-1*H*-1,2,4-triazole-3-carboxamide (**2**). 5-amino-1*H*-1,2,4-triazole-3-carbonitrile (**3**) is obtained by dehydration of the carboxamide using phosphorus pentoxide in acetonitrile. 5-(5-Amino-1,2,4-1*H*-triazol-3-yl)-1*H*-tetrazole (**4**) was synthesized on the basis of the procedure developed by Sharpless and coworkers, which has been widely used in the synthesis of tetrazole-5-yl-azole compounds.^[11] The [3+2] cycloaddition of sodium azide with the nitrile proceeds readily in water with zinc chloride as catalyst in excellent yields (Scheme 1). This modified synthesis leads to the previously unknown combination of a triazole ring with a tetrazole ring connected by a C–C bond.



Scheme 1: Synthesis of 5-(5-amino-1*H*-1,2,4-triazol-3-yl)-1*H*-tetrazole (**4**, ATT)

The starting material 5-(5-amino-1*H*-1,2,4-triazol-3-yl)- (**4**) was converted to energetic derivatives by introduction of nitro-, nitrimino- and azido-moieties (Scheme 2). The treatment of 5-(5-amino-1*H*-1,2,4-triazol-3-yl)-1*H*-tetrazole with a mixture of sulfuric acid/nitric acid (6:1) leads to 5-(5-nitrimino-1*H*-1,2,4-triazol-3-yl)-1*H*-tetrazole (NATT,

5). 5-(3-Nitro-1*H*-1,2,4-triazol-5-yl)-2*H*-tetrazole (NTT, **6**) was obtained by the well known Sandmeyer reaction via diazotization in sulfuric acid and subsequent reaction with the excess of sodium nitrite. The azido compound (AzTT, **7**) was as well synthesized via diazotization in sulfuric acid and subsequent reaction with an excess of sodium azide.



Scheme 2: Synthesis of 5-(5-nitrimino-1*H*-1,2,4-triazol-3-yl)-1*H*-tetrazole (**5**, NATT), 5-(3-nitro-1*H*-1,2,4-triazol-5-yl)-2*H*-tetrazole (**6**, NTT) and 5-(5-azido-1*H*-1,2,4-triazol-3-yl)tetrazole (**7**, AzTT).

SINGLE CRYSTAL X-RAY STRUCTURE ANALYSIS

Single crystal X-ray measurements were accomplished for compounds **3** and **5–7** and are discussed in detail. Due to the very low solubility of the amino compound **4**, this molecule could only be crystallized from 2*M* HCl as a chloride salt (see supporting information). All other compounds were recrystallized from water and obtained as hydrated species.

5-Amino-1*H*-1,2,4-triazole-3-carbonitrile (**3**) crystallizes in the monoclinic space group $P2_1/c$ with a cell volume of 462.88(10) Å³ and four formula units per unit cell. As expected, the molecule shows a complete planar assembly. In relation to the triazole ring, only the protons of the amine group are slightly twisted out of the plane by 29°. The C–C bond length between the nitrile and the triazole ring is as expected (1.438(3) Å) in comparison to literature known $\text{C}_{\text{sp}2}\text{--C}_{\text{sp}1}$ carbon atoms (1.44 Å).^[12] All nitrogen atoms participate in hydrogen bonds which leads to the formation of dimers via $\text{N1}\cdots\text{N2}$. Those dimers are connected by the nitrile group which acts as acceptor in the hydrogen bond

N1–H1···N5 (Figure 1). The resulting tetramers consist of four individual molecules and are connected with each other by hydrogen bonds summarized in Table 1.

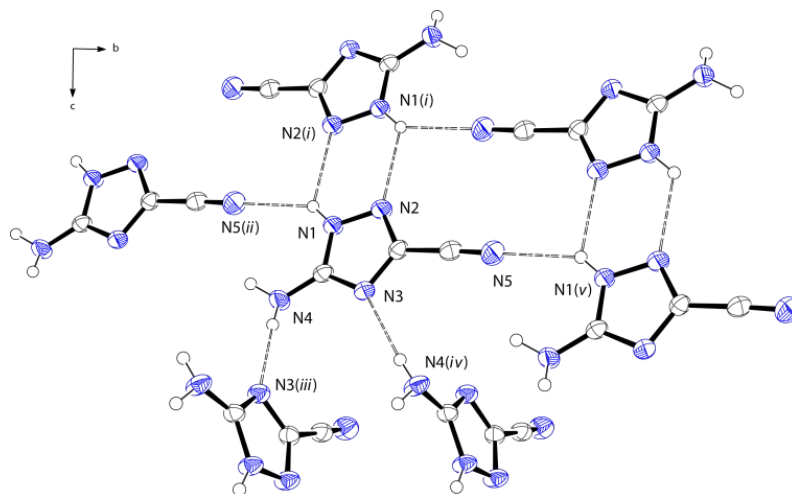


Figure 1: Hydrogen bonds within the crystal structure of **3**, thermal ellipsoids are set to 50 % probability, symmetry codes: (i) $1-x, 2-y, -z$; (ii) $1+x, -1+y, z$; (iii) $-x, -1/2+y, 1/2-z$; (iv) $-x, 1/2+y, 1/2-z$; (v) $-1+x, 1+y, z$.

Table 1: Hydrogen bonds present in the crystal structure of **3**.

D–H···A	$d(\text{D–H}) [\text{\AA}]$	$d(\text{H···A}) [\text{\AA}]$	$d(\text{D–H···A}) [\text{\AA}]$	$\angle(\text{D–H···A}) [^\circ]$
N1–H1···N5 ⁱⁱ	0.87(3)	2.26(3)	2.995(3)	142(2)
N1–H1···N2 ⁱ	0.87(3)	2.36(2)	2.952(2)	126(2)
N4–H4B···N3 ⁱⁱⁱ	0.84(3)	2.17(3)	3.007(3)	175.4(19)

Symmetry codes: (i) $1-x, 2-y, -z$; (ii) $1+x, -1+y, z$; (iii) $-x, -1/2+y, 1/2-z$.

The bond lengths and torsion angles within the azole ring of compounds **5–7** are all in the expected range in comparison to similar triazole and tetrazole compounds.^[6a, 8, 13] The bond lengths within the triazole and the tetrazole ring in the crystal structures are all in between the length of formal C–N and N–N single and double bonds (C–N: 1.47 Å, 1.22 Å; N–N: 1.48 Å, 1.20 Å).^[12, 14] The small torsion angle N3–C2–C3–N5 between the heterocycles indicates a completely planar ring, which together with the bond lengths leads to the assumption of an aromatic ring system. In the case of the nitrimino compound **5**, the torsion angle between the two heterocycles is 0.2(3)°. The protons at the triazole ring are located at the nitrogen atoms N1 and N3, therefore the compound can be classified as nitrimino-triazole. In addition, the intramolecular hydrogen bond N1–H1···O3 keeps the nitrimino moiety within the plane of the triazole ring due to the

formation of a six membered ring (Figure 2), which is often the case for nitrimino-triazoles.^[7f, 15] The D–H···A angle is only 107(2)°, but the D···A length is very short with 2.621(2) Å. 5-(5-nitrimino-1*H*-1,2,4-triazol-3-yl)-1*H*-tetrazole (NATT, **5**) crystallizes as trihydrate in the monoclinic space group $P2_1/c$ with a cell volume of 1031.09(15) Å³ and four molecular moieties in the unit cell. The molecular structure of **5** together with the atom labeling is presented in Figure 2.

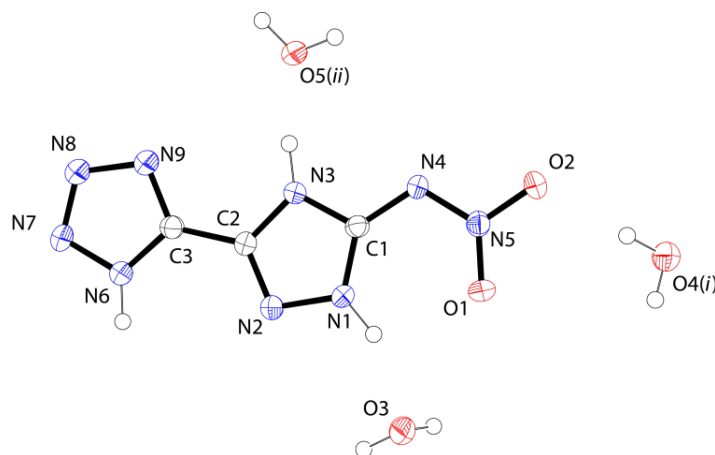


Figure 2: Molecular structure of 5-(5-nitrimino-1*H*-1,2,4-triazol-3-yl)-1*H*-tetrazole (NATT, **5**), thermal ellipsoids are set to 50 % probability, symmetry codes: (i) $-x, 1/2+y, 1/2-z$; (ii) $x, 1+y, z$.

NATT forms tetramers via a threefold hydrogen bond with the oxygen atom O5 acting both as acceptor and donor. Three further nitrogen atoms N1, N3 and N6 are involved as donor atoms in further hydrogen bonds (Table 2), resulting in strong interactions with surrounding molecules. The bifurcated hydrogen bond N6–H6···O2 and N6–H6···N4 connect the tetrazole ring to the nitrimino moiety (Figure 3).

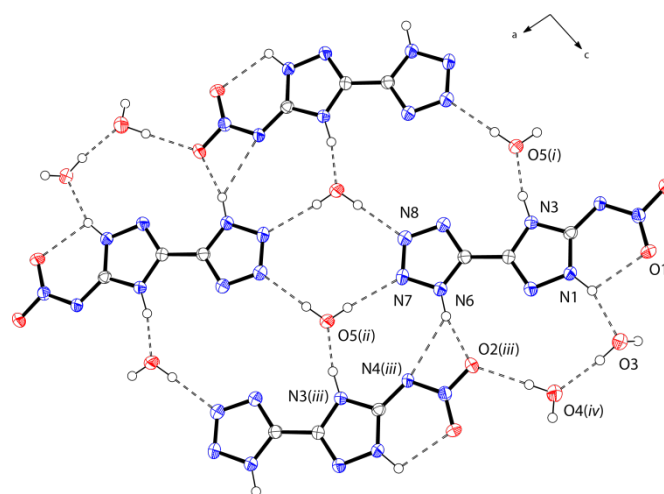


Figure 3: Hydrogen bonds within the crystal structure of **5**, thermal ellipsoids are set to 50 % probability, symmetry codes: (i) $x, 1+y, z$; (ii) $1+x, -1+y, z$; (iii) $1+x, y, z$; (iv) $1-x, -1/2+y, 1/2-z$.

Table 2: Hydrogen bonds present in the crystal structure of **5**.

D–H...A	d (D–H) [Å]	d (H...A) [Å]	d (D–H...A) [Å]	< (D–H...A) [°]
N1–H1...O1	0.92(2)	2.20(2)	2.621(2)	107(2)
N1–H1...O3	0.92(2)	1.89(2)	2.762(2)	157(2)
N3–H3...O5 ⁱ	0.94(2)	1.70(2)	2.625(2)	170(2)
O3–H3B... O4 ^{iv}	0.91(3)	1.87(3)	2.776(2)	172(2)
O4 ^{iv} –H4B...O2 ⁱⁱⁱ	0.89(3)	1.96(3)	2.843(2)	170(3)
O5 ⁱⁱ –H5A...N7	0.84(3)	2.10(3)	2.934(2)	173(2)
O5 ⁱⁱ –H5B...N8	0.86(2)	2.00(2)	2.853(2)	171(2)
N6–H6...O2 ⁱⁱⁱ	0.93(2)	1.85(2)	2.752(2)	165(2)
N6–H6...N4 ⁱⁱⁱ	0.93(2)	2.45(2)	3.187(2)	136(2)

Symmetry codes: (i) $1-x, 2-y, -z$; (ii) $1+x, -1+y, z$; (iii) $-x, -1/2+y, 1/2-z$.

Furthermore, 5-(3-nitro-1*H*-1,2,4-triazol-5-yl)-2*H*-tetrazole (NTT, **6**) crystallizes as dihydrate in the triclinic space group *P*-1 with a cell volume of 436.08(8) Å³ and two molecular moieties in the unit cell. Again, the molecule shows a nearly planar assembly with a torsion angle between the two heterocycles of 5.0(2)°. The nitro group is twisted out of the triazole plane by only 5.1(2)°. The proton is located at the nitrogen atom N1 next to the C–C bond and not next to the energetic moiety as it is the case for the nitrimino compound **5**. The formula unit of **6** together with the atom labeling is presented in Figure 4.

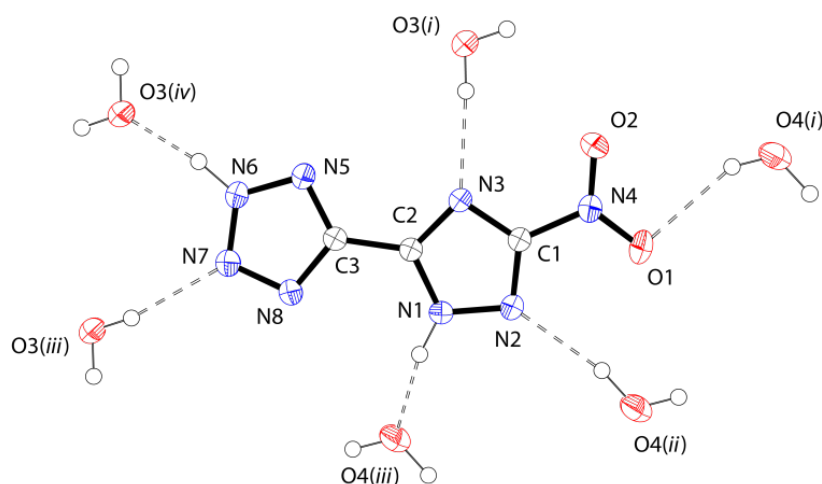


Figure 4: Molecular structure of 5-(3-nitro-1*H*-1,2,4-triazol-5-yl)-2*H*-tetrazole (NTT, **6**) and hydrogen bonds towards surrounding water molecules, thermal ellipsoids are set to 50 % probability, symmetry codes: (i) $1-x, 1-y, 1-z$; (ii) $1+x, y, z$; (iii) $1-x, -y, 1-z$; (iv) $-1+x, -1+y, 1+z$.

The crystal structure of **6** is build up by planes of NTT molecules that are kept together by several threefold hydrogen bonds with the water molecules (Figure 5a). In contrast to the crystal structure of compound **5**, there is no direct interaction between two NTT molecules. The Oxygen atoms O3 and O4 act both as donor and acceptor, all hydrogen bonds lengths lie well within the sum of van der Waals radii ($r_w(\text{N}) + r_w(\text{O}) = 3.07 \text{ \AA}$)^[14], resulting in a strong network of hydrogen bonds. The layers are stacked above each other with a layer distance of $d = 3.18 \text{ \AA}$. The layers are connected by two short contacts, $\text{C1}\cdots\text{O3}$ ($d(\text{C}\cdots\text{O}) = 3.02 \text{ \AA}$) and $\text{C1}\cdots\text{O4}$ ($d(\text{C}\cdots\text{O}) = 3.08 \text{ \AA}$). The stacking of the layers is displayed in Figure 5b together with the distance d between the layers.

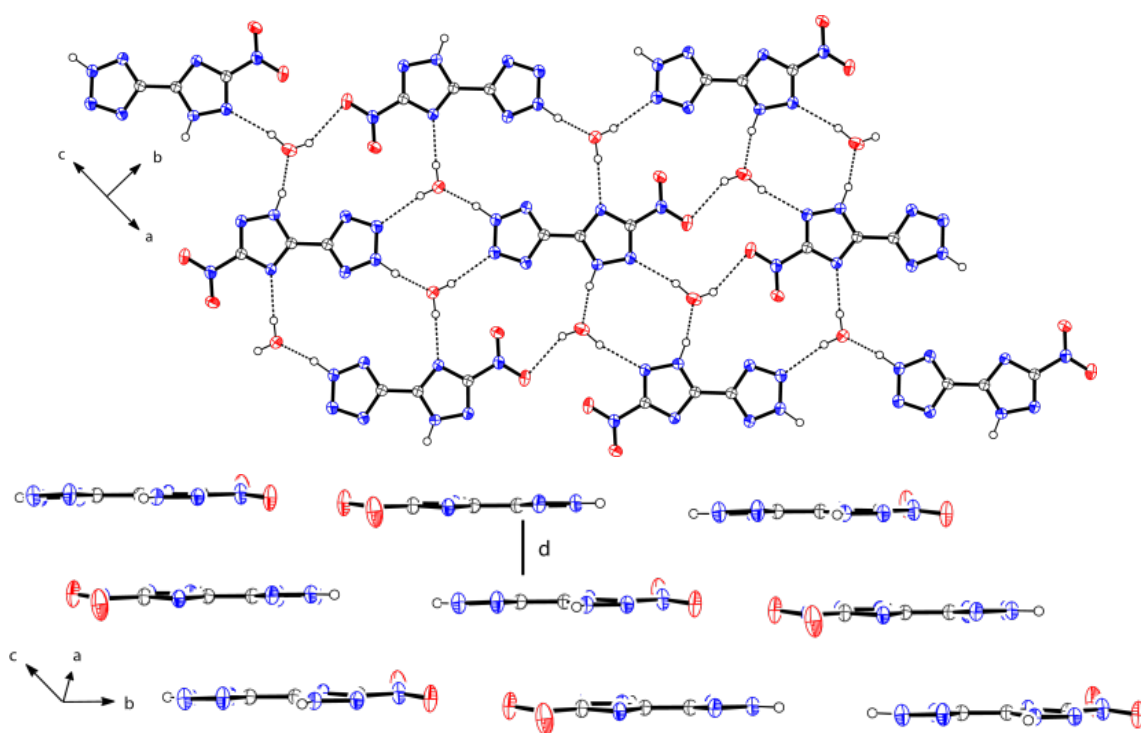


Figure 5: a) Formation of planes in the crystal structure of **6**; b) stacking of layers (layer distance $d = 3.18 \text{ \AA}$, water molecules are omitted for clarity). Thermal ellipsoids are set to 50 % probability.

Table 3: Hydrogen bonds present in **6**.

D–H...A	<i>d</i> (D–H) [Å]	<i>d</i> (H...A) [Å]	<i>d</i> (D–H...A) [Å]	< (D–H...A) [°]
N1–H1...O4 ⁱⁱⁱ	0.921(19)	1.781(19)	2.6895(18)	168.7(17)
O3 ⁱ –H3A... N3	0.89(3)	2.05(3)	2.9384(16)	174(2)
O3 ⁱ –H3B ...N7	0.83(3)	2.15(3)	2.9649(18)	166(2)
O4 ⁱ –H4A...O1	0.839(18)	2.266(19)	3.0274(18)	151(2)
O4 ⁱⁱ –H4B...N2	0.96(4)	2.10(4)	3.036(2)	167(3)
N6–H6...O3 ^{iv}	0.97(2)	1.70(2)	2.6566(18)	168.1(19)

Symmetry codes: (i) 1–*x*, 1–*y*, 1–*z*; (ii) 1+*x*, *y*, *z*; (iii) 1–*x*, –*y*, 1–*z*; (iv) –1+*x*, –1+*y*, 1+*z*.

Finally, the azido-compound **7** (AzTT) shows again a nearly planar assembly with a torsion angle between the two heterocycles of 1.3(3)°. The azido moiety is slightly bent with an angle of 172.1(2)° and nearly in plane with the triazole ring (torsion angle N5–N4–C1–N3: 3.0(3)°). 5-(5-Azido-1*H*-1,2,4-triazol-3-yl)tetrazole crystallizes as dihydrate in the orthorhombic space group *Fdd2* with a cell volume of 3545.1(2) Å³ and 16 molecular moieties in the unit cell. It is worth mentioning that the hydrogen atoms at the tetrazole ring are disordered, the hydrogen atoms are located one time at nitrogen atom N7 and the other at N9. This enables the formation of pairs of AzTT molecules via the hydrogen bond N7–H7...N7(*i*) as only intermolecular interaction with a short D...A length of 2.830(2) Å (Figure 6). In addition, the water molecules are as well disordered and therefore not shown in figure 6. They act both as donor and acceptor for several further hydrogen bonds which connect the pairs of AzTT molecules.

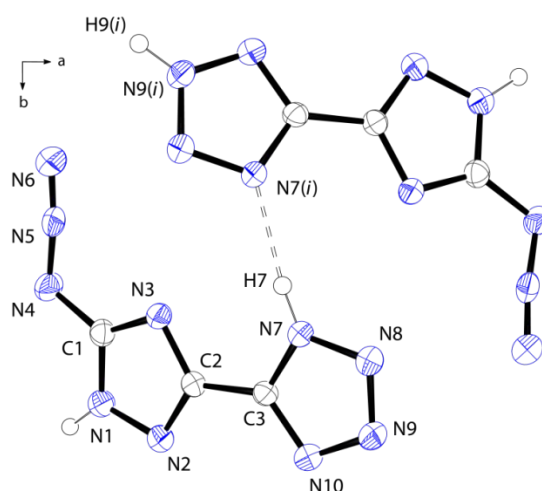


Figure 6: Molecular structure of 5-(5-azido-1*H*-1,2,4-triazol-3-yl)tetrazole (AzTT, **7**), disordered hydrogen atoms are located one time at nitrogen atom N7 and the other at N9, thermal ellipsoids are set to 50 % probability, symmetry codes: (i) 1–*x*, –*y*, *z*.

MULTINUCLEAR NMR SPECTROSCOPY

All compounds were investigated using ^1H , ^{13}C and ^{14}N NMR spectroscopy. Due to insufficient solubility of compound **5** in DMSO or any other solvent, ^{15}N NMR spectra could only be obtained for compounds **6** and **7**.

Compounds **4–7** show two signals for the triazole carbon atoms and one signal for the tetrazole carbon atom in the expected range.^[5c, 8] Two singlets for the carbon atoms of the C–C bridge can be found at chemical shifts of 141.8 ppm (**5**) to 150.2 ppm (**4**). The signal of the carbon atom connected to the energetic moieties is shifted in all cases to lower field and is observed in the range of 153.0 (**5**) to 162.9 ppm (**6**). In the $^{14}\text{N}\{^1\text{H}\}$ NMR spectra, the nitro group of compounds **5** and **6** can be identified by a singlet at –22 (**5**) to –26 ppm (**6**). The azido moiety in compound **7** can be observed as a broad singlet at –143 ppm in the ^{14}N NMR spectrum, well resolved resonances could only be observed in the ^{15}N NMR spectrum (as discussed below). The NMR signals of all compounds are summarized in Table 4.

Table 4: NMR signals of compounds **4–7** in DMSO- d_6 .

compound	δ [ppm]			
	$^{13}\text{C}\{^1\text{H}\}$	$^{13}\text{C}\{^1\text{H}\}$	$^{14}\text{N}\{^1\text{H}\}$	^1H
	C _{Triazole}	C _{Tetrazole}		
4	158.2, 150.2	148.2	–	6.50
5	153.0, 148.4	141.8	–22	11.52
6	162.9, 148.3	145.4	–26	14.44
7	155.5, 146.3	148.5	–143	11.83

Due to the insufficient solubility of compound **5**, ^{15}N NMR spectra could only be obtained for compounds **6** and **7**. Six well resolved resonances are observed in the ^{15}N NMR spectrum of the nitro-compound **6** (Figure 7). The signals were assigned by comparison to literature values of similar bistetrazole and bistriazole compounds.^[16] The signals of the triazole nitrogen atoms N1, N2 and N3 as well as the nitro group can be found in the expected range similar to the recently published 3,3'-dinitro-5,5'-bistriazole.^[16c] The nitrogen atoms N4 and N4' are equal and show a broad signal at –89.4 ppm, the nitrogen atoms N5 and N5' appear at a chemical shift of –19 ppm.

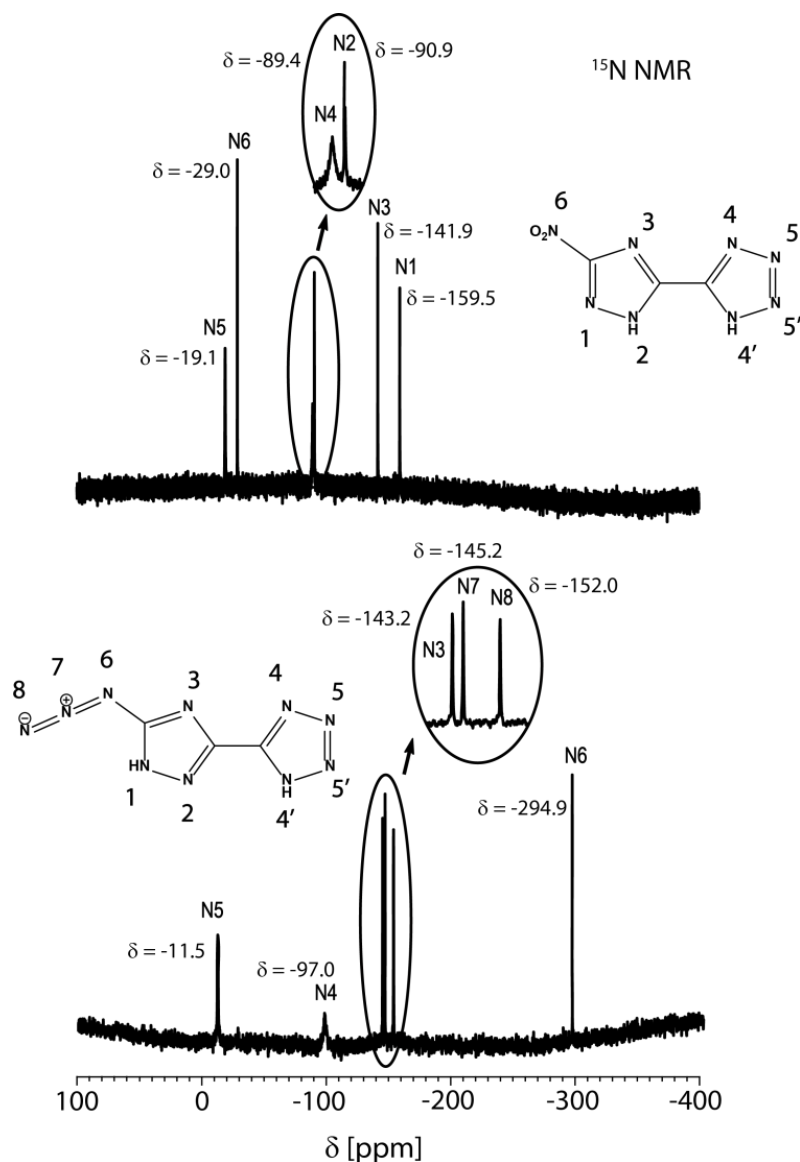


Figure 7: ¹⁵N NMR spectra of 5-(5-nitrimino-1,4H-1,2,4-triazol-3-yl)-1H-tetrazole (**5**), 5-(3-nitro-1H-1,2,4-triazol-5-yl)-2H-tetrazole (**6**) and 5-(5-azido-1H-1,2,4-triazol-3-yl) tetrazole (**7**) recorded in DMSO-*d*₆; *x*-axis represents the chemical shift δ in ppm.

The signals of the nitrogen atoms N3, N4 and N5 of the azido compound (**7**) can be observed in the same region in comparison to the nitro-compound (−143.2(N3), −97.0 (N4), −11.5 (N5)). The signals of the nitrogen atoms N1 and N2 of the azido compound (**7**) are not observable even with a saturated solution due to the high acidity of the proton and the resulting fast proton exchange. In the case of the similar 5,5'-diazido-3,3'-bistriazole^[16c], the nitrogen atoms N1 and N2 are as well hardly visible and appear as very broad signals. The three signal of the azido moiety are well resolved and can be found in the expected range with N6 being shifted to highest field with a chemical shift of −294.9 ppm.

THEORETICAL CALCULATIONS, PERFORMANCE CHARACTERISTICS AND STABILITIES

All calculations regarding energies of formation were carried out using the Gaussian 09 (revision C.01) program package.^[17] Since very detailed descriptions of the calculation process have been published earlier^[5c] and can be found in specialized books,^[1b] only a short summary of computational methods will be given. The enthalpies (H) and Gibbs free energies (G) were calculated using the modified complete basis set method (CBS-4M) of Petersson *et al.*^[18] in order to obtain very accurate energies. The enthalpies of formation for the gas phase species were computed according to the atomization energy method, using NIST^[19] values as standardized values for the atoms standard heats of formation ($\Delta_f H^\circ$) according to equation 1.^[20]

$$\Delta_f H^\circ_{(g, \text{Molecule}, 298)} = H_{(\text{Molecule})} - \sum H^\circ_{(\text{Atoms})} + \sum \Delta_f H^\circ_{(\text{Atoms}, \text{NIST})} \quad (1)$$

The solid state enthalpy of formation for neutral compounds is estimated from the computational results using Troutons rule,^[21] where T_m was taken equal to the decomposition temperatures.

$$\Delta_f H^\circ_{(s, M.)} = \Delta_f H^\circ_{(g, M.)} - \Delta_{\text{sub}} H = \Delta_f H^\circ_{(g, M.)} - (188 [\text{J mol}^{-1} \text{K}^{-1}] \times T_m [\text{K}]) \quad (2)$$

The solid state enthalpies of formation for the ionic compounds are derived from the calculation of the corresponding lattice energies (ΔU_L) and lattice enthalpies (ΔH_L), calculated from the corresponding molecular volumes, using the equations provided by Jenkins *et al.*^[22] The derived molar standard enthalpies of formation for the solid state (ΔH_m) were used to calculate the solid state energies of formation (ΔU_m) according to equation three, with Δn being the change of moles of gaseous components.^[1b]

$$\Delta U_m = \Delta H_m - \Delta n RT \quad (3)$$

The calculated standard energies of formation were used to perform predictions of the detonation parameters with the program package Explo5, Version 5.05.^[23] The program is based on the chemical equilibrium, steady state model of detonation. It uses Becker-Kistiakowsky-Wilsons equation of state (BKW EOS) for gaseous detonation products together with the Cowan-Ficketts equation of state for solid carbon.^[24] The calculation of

the equilibrium composition of the detonation products is performed by applying a modified free energy minimization technique of White, Johnson and Dantzig.^[24] The program was designed to enable calculations of detonation parameter at the Chapman-Jouguet point.

As shown in Table 5, physicochemical properties were calculated for the energetic compounds **5**–**7**. The starting material 5-(5-amino-1*H*-1,2,4-triazol-3-yl)-1*H*-tetrazole (**4**) is insensitive towards friction and impact and shows a very high decomposition temperature of 347 °C. As shown in Figure 8, the introduction of energetic moieties dramatically decreases the thermal stability to 215 °C (**5**), 211 °C (**6**) and 164 °C (**7**). The lowest thermal stability was obtained for the azido compound **7** with a decomposition onset at 164 °C. In comparison to the recently synthesized bistriazole compounds,^[5c, 13d] the decomposition temperatures of all compounds are significantly lower. The introduction of the tetrazole moiety obviously decreases the thermal stability and emphasizes the unique stability of bistriazoles.

As it is characteristically for nitramino- and nitrimino-triazoles,^[5c, 9, 26] the nitrimino compound **5** is very sensitive towards impact (<1 J) and sensitive towards friction (18 N), which is in the same range as the azido compound with a friction sensitivity of 20 N and an impact sensitivity of less than 1 J. Both compounds are in addition sensitive towards electrostatic discharge with values of 0.07 J (**5**) and 0.05 J (**7**).

The calculated detonation velocities of all compounds (8097 ms⁻¹ (**5**), 8020 ms⁻¹ (**6**) and 7874 ms⁻¹ (**7**)) are in the same range and well below the commonly used explosive RDX. In contrast to compounds **5** and **7**, the nitro compound **6** shows moderate sensitivities towards friction (288 N) and impact (25 J). 5-(3-Nitro-1,2,4-1*H*-triazol-5-yl)-2*H*-tetrazole (**6**) could therefore be of interest as secondary explosive or propellant ingredient especially as ionic derivative in combination with nitrogen-rich cations, since those generally increases both thermal stability and performance^[7i, 13a].

Table 5: Physicochemical properties of compounds **4–7** in comparison to hexogen (RDX).

	ATT	NATT	NTT	AzTT	RDX ^[n]
	(4)	(5)	(6)	(7)	
Formula	C ₃ H ₄ N ₈	C ₃ H ₃ N ₉ O ₂	C ₃ H ₂ N ₈ O ₂	C ₃ H ₂ N ₁₀	C ₃ H ₆ N ₆ O ₆
M [g mol ⁻¹]	152.1	197.1	182.1	178.1	222.1
IS [J] ^a	>40	<1	25	<1	7
FS [N] ^b	>360	18	288	20	120
ESD–test [J]	1.5	0.07	0.85	0.05	--
N [%] ^c	73.7	64.0	61.5	78.6	37.8
Ω [%] ^d	–84.1	–44.6	–43.9	–62.8	–21.6
T _{dec.} [°C] ^e	347	215	211	164	210
ρ [g cm ⁻³] ^f	1.61	1.71	1.73	1.66	1.80
Δ _f H _(g) ^o [kJ mol ⁻¹] ^g	511	577	519	859	176
Δ _f H _m ^o [kJ mol ⁻¹] ^h	394	485	428	777	70
Δ _f U ^o [kJ kg ⁻¹] ⁱ	2688	2549	2430	4444	417
EXPLO5 values: V5.05					
–Δ _E U ^o [kJ kg ⁻¹] ^j	3040	4804	4735	4578	6125
T _E [K] ^k	2452	3774	3810	3602	4236
p _{C-J} [kbar] ^l	187	266	265	241	349
V _{Det.} [m s ⁻¹] ^m	7193	8097	8020	7874	8748
Gas vol. [L kg ⁻¹] ⁿ	691	712	681	674	739

^[a] BAM drop hammer; ^[b] BAM friction tester; ^[c] Nitrogen content; ^[d] Oxygen balance; ^[e] Temperature of decomposition by DSC ($\beta = 5$ °C, Onset values); ^[f] Density values of **5–7** derived from gas-pycnometer measurements of anhydrous compounds at 25 °C; ^[g] Molar enthalpy of formation in the gas phase; ^[h] Molar enthalpy of formation; ^[i] Energy of formation; ^[j] Energy of Explosion; ^[k] Explosion temperature; ^[l] Detonation pressure; ^[m] Detonation velocity; ^[n] Assuming only gaseous products; ^[o] values based on Ref. ^[25] and the EXPLO5.5 database.

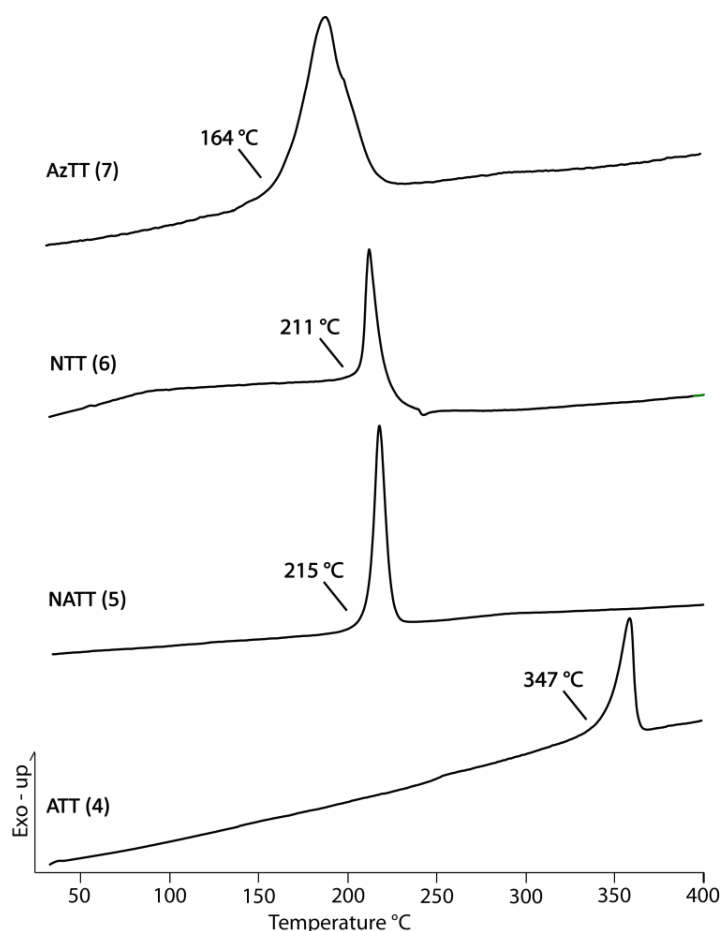


Figure 8: DSC plots of ATT (4), NATT (5), NTT (6) and AzTT (7). DSC plots were recorded with a heating rate of 5 °C min⁻¹.

CONCLUSION

The previously unknown syntheses of 5-amino-3-cyano-1*H*-1,2,4-triazole (ACT, **3**) is presented and reveals new synthetic pathways towards numerous novel energetic 1,2,4-triazole derivatives. 5-(3-Amino-1,2,4-1*H*-triazol-5-yl)-1*H*-tetrazole (**4**) was synthesized from compound **3** on the basis of the procedure developed by Sharpless and coworkers, which has been widely used in the synthesis of tetrazole-5-yl-azole compounds.^[11] The reaction of sodium azide with the nitrile proceeds readily in water with zinc chloride as catalyst in excellent yields. This modified synthesis leads to the previously unknown combination of a triazole ring with a tetrazole ring connected by C–C bond.

The starting material 5-(5-amino-1*H*-1,2,4-triazol-3-yl)-1*H*-tetrazole (**4**) was converted to energetic derivatives by introduction of nitro-, nitrimino- and azido-moieties. Those different energetic groups containing oxygen or nitrogen lead to variable energetic properties. All energetic compounds have been fully characterized by means of vibrational and multinuclear NMR spectroscopy, mass spectrometry and differential

scanning calorimetry. Single crystal X-ray measurements deliver insight into structural characteristics as well as inter- and intramolecular interactions.

Regarding the stability values and energetic parameters, compounds **5** and **6** show thermal stabilities (215 °C (**5**), 211 °C (**6**)) in the range of RDX. As expected, the nitrimino compound (**5**) as well as the azido compound (**7**) are the most sensitive derivatives with an impact sensitivity of less than 1 J and friction sensitivities of 18 N (**5**) and 20 N (**7**). In contrast, the nitro derivative shows moderate sensitivities towards friction (288 N) and impact (25 J) and could therefore be of interest as secondary explosive or propellant ingredient. In summary, compounds **5–7** are able to compete with commonly used TNT regarding their detonation parameters. However, the performance data for RDX are not reached. Compound **6** can be considered as nitrogen-rich starting material for energetic ionic derivatives. Due to the fact that nitrogen-rich salts of energetic compounds tend to be more stable compared to the uncharged compounds and often show performance characteristics in the range of modern secondary explosives,^[7i, 13a] those ionic derivatives could find application as high-nitrogen energetic materials. In general, the connection via C–C bond of a triazole ring with its opportunity to introduce a large variety of energetic moieties and a tetrazole ring implying a large energy content leads to the selective synthesis of primary and secondary explosives.

EXPERIMENTAL SECTION

Caution: Due to the fact that energetic triazole- and tetrazole compounds are to some extent rather instable against outer stimuli, proper safety precautions should be taken when handling the dry materials. Especially derivatives of azido- and nitrimino-triazoles are energetic primary materials and tend to explode under the influence of impact or friction. Lab personnel and the equipment should be properly grounded and protective equipment like earthed shoes, leather coat, Kevlar[®] gloves, ear protection and face shield is recommended for the handling of any energetic material.

General. All chemical reagents and solvents were obtained from Sigma-Aldrich Inc. or Acros Organics (analytical grade) and were used as supplied without further purification. ¹H, ¹³C{¹H}, ¹⁴N{¹H} and ¹⁵N NMR spectra were recorded on a JEOL Eclipse 400 instrument in DMSO-*d*₆ at 25 °C. The chemical shifts are given relative to tetramethylsilane (¹H, ¹³C) or nitromethane (¹⁴N, ¹⁵N) as external standards and coupling constants are given in Hertz (Hz). Infrared (IR) spectra were recorded on a Perkin-Elmer

Spectrum BX FT-IR instrument equipped with an ATR unit at 25 °C. Transmittance values are qualitatively described as “very strong” (vs), “strong” (s), “medium” (m), “weak” (w) and “very weak” (vw). Raman spectra were recorded on a Bruker RAM II spectrometer equipped with a Nd:YAG laser (200 mW) operating at 1064 nm and a reflection angle of 180°. The intensities are reported as percentages of the most intense peak and are given in parentheses. Elemental analyses (CHNO) were performed with an Elementar Vario EL. Melting and decomposition points were determined by differential scanning calorimetry (Linseis DSC-PT10, calibrated with standard pure indium and zinc). Measurements were performed at a heating rate of 5 °C min⁻¹ in closed aluminum sample pans with a 1 µm hole in the lid for gas release to avoid an unsafe increase in pressure under a nitrogen flow of 20 mL min⁻¹ with an empty identical aluminum sample pan as a reference.

For initial safety testing, the impact and friction sensitivities as well as the electrostatic sensitivities were determined. The impact sensitivity tests were carried out according to STANAG 4489,^[27] modified according to WIWEB instruction 4-5.1.02^[28] using a BAM^[29] drop hammer. The friction sensitivity tests were carried out according to STANAG 4487^[30] and modified according to WIWEB instruction 4-5.1.03^[31] using the BAM^[29] friction tester. The electrostatic sensitivity tests were accomplished according to STANAG 4490^[32] using an electric spark testing device ESD 2010 EN (OZM Research).

Crystallographic measurements. The single crystal X-ray diffraction data of **3–6** were collected using an Oxford Xcalibur3 diffractometer equipped with a Spellman generator (voltage 50 kV, current 40 mA) and a Kappa CCD detector. The data collection and reduction was undertaken using the CrysAlisPro software^[33]. Crystals of compound **7** were investigated using a Bruker D8-Quest diffractometer equipped with a IµS microfocus X-Ray source. The structures were solved with Sir92^[34] or Shelxs-97^[35] and refined with Shelxl-97^[35] implemented in the program package WinGX^[36] and finally checked using Platon^[37]. CCDC 906004 (**3**), 906005 (**4**·HCl), 906006 (**6**), 906007 (**5**) and 906008 (**7**) contains the supplementary crystallographic data for this paper. These data can be obtained free of charge from The Cambridge Crystallographic Data Centre via www.ccdc.cam.ac.uk/data_request/cif.

5-Amino-1H-1,2,4-triazole-3-carboxamide (2)

Thionyl chloride (18.7 mL, 258 mmol) was added dropwise to a suspension of 5-amino-1H-1,2,4-triazole-3-carboxylic acid (25.0 g, 195 mmol) in 260 mL of ethanol at 0 °C. Subsequently, the mixture was refluxed for 2 hours and the solvent evaporated in vacuum. A saturated solution of sodium acetate (200 mL) was added to the remaining highly viscous residue, the resulting precipitate was collected by filtration and washed with cold water. The obtained colorless solid was dissolved in concentrated aqueous ammonia (150 mL) and heated to 70 °C for 2 hours. The mixture was cooled to room temperature, acidified with concentrated acetic acid to pH = 4 and the resulting precipitate was collected by filtration to yield 5-amino-1H-1,2,4-triazole-3-carboxamide (17.5 g, 136 mmol, 70%) as a colorless solid.

¹H NMR (DMSO-*d*₆): δ = 12.5 (s, H_{triazole}), 7.42 (s, NH₂), 6.03 (s, NH₂) ppm; **¹³C NMR** (DMSO-*d*₆): δ = 161.9 (C=O), 158.4 (CNH₂), 154.1 (C_{Triazole}-CONH₂) ppm; **Raman** (200 mW): ν (cm⁻¹) (rel. int.) = 3354(8), 3338(8), 3255(7), 3166(9), 3140(17), 3135(18), 1676(15), 1651(9), 1573(73), 1522(100), 1425(29), 1358(5), 1316(21), 1139(23), 1109(19), 1068(79), 1014(72), 795(9), 788(12), 690(20), 574(6), 537(6), 433(42), 414(25), 361(5), 233(61). **Elemental analysis** (C₃H₅N₅O): calc.: C 28.35, H 3.96, N 55.10; found: C 28.64, H 3.76, N 55.03.

5-Amino-3-cyano-1H-1,2,4-triazole (3)

5-Amino-1H-1,2,4-triazole-3-carboxamide (5.0 g, 40 mmol) and phosphorus pentoxide (30 g, 105 mmol) was suspended in 1.0 L dry acetonitrile and the flask was sealed. After stirring for 72 hours at room temperature, the acetonitrile was evaporated in vacuum and the remaining solid dissolved in water (1.0 L). The resulting clear solution was extracted with ethyl acetate (3×200 mL), the combined organic layers were dried over magnesium sulfate and the solvent was removed in vacuum to yield 5-amino-3-cyano-1H-1,2,4-triazole as a colorless powder (3.1 g, 28 mmol, 70%).

¹H NMR (DMSO-*d*₆): δ = 12.9 (s, H_{triazole}), 6.49 (s, -NH₂) ppm; **¹³C NMR** (DMSO-*d*₆): δ = 157.9 (C-NH₂), 136.2 (C-CN), 114.2 (CN) ppm; **IR**: ν (cm⁻¹) (rel. int.) = 3430(m), 3284(m), 3156(m), 2260(m), 1624(s), 1583(s), 1561(s), 1541(m), 1485(s), 1429(m), 1359(m), 1306(s), 1127(m), 1101(m), 1051(m), 1017(s), 757(s), 728(s), 709(s), 704(s), 701(s), 696(s), 674(vs), 674(vs), 667(vs), 659(s). **Raman** (200 mW): ν (cm⁻¹) (rel. int.) = 3286(3), 2263(100), 2209(3), 1690(3), 1641(5), 1592(10), 1563(14), 1490(11), 1445(7),

1363(13), 1310(5), 1130(8), 1115(5), 1102(5), 1050(19), 1016(12), 978(7), 770(4), 681(2), 564(7), 491(6), 421(9), 414(9), 414(9), 239(2); **Elemental analysis** ($C_2H_3N_5$): calc.: C 33.03, H 2.77, N 64.20; found: C 33.11, H 2.82, N 62.47. **Mass spectrometry**: m/z (DEI+): 109.1 [$C_2H_3N_5^+$].

5-(5-Amino-1H-1,2,4-triazole-3-yl)-1H-tetrazole (4)

3-Amino-5-cyano-1H-1,2,4-triazole (2.61 g, 23.9 mmol), sodium azide (1.71 g, 26.3 mmol) and zinc chloride (4.0 g, 29.3 mmol) were suspended in 120 ml water and the reaction mixture was refluxed for 16 h. After cooling to room temperature, 20 ml of 2 M HCl solution were added to avoid precipitation of zinc hydroxide. The precipitate was collected by filtration, washed with water and dried in air to yield 5-(5-amino-1H-1,2,4-triazole-3-yl)-1H-tetrazole (**4**) (3.41 g, 22.4 mmol, 94%) as colorless solid.

1H NMR (DMSO- d_6): δ = 6.50 (s, $-NH_2$) ppm; **^{13}C NMR** (DMSO- d_6): δ = 158.2 ($C-NH_2$), 150.2, 148.2 ppm; **IR**: ν (cm^{-1}) (rel. int.) = 3381(m), 3327(m), 3214(w), 1645(vs), 1583(s), 1524(m), 1444(w), 1386(m), 1346(w), 1290(s), 1210(w), 1152(w), 1108(m), 1102(m), 1068(w), 1035(w), 988(w), 849(w), 738(w), 695(m), 661(w); **Raman** (200 mW): ν (cm^{-1}) (rel. int.) = 1640(14), 1618(100), 1550(2), 1445(4), 1388(5), 1288(4), 1211(18), 1153(4), 1118(7), 1076(5), 1035(5), 986(2), 776(4), 758(9), 530(3), 446(10), 413(5), 380(8), 297(4), 233(4), 203(6); **Elemental analysis** ($C_3H_4N_8$): calc.: C 23.69, H 2.65, N 73.66; found: C 24.01, H 2.66, N 71.95; **Mass spectrometry**: m/z (DEI+) = 152.1 [$(C_3H_4N_8)^+$]; **Sensitivities** (grain size < 100 μm): friction: 360 N, impact: 40 J, ESD: n.d.; **DSC** (onset, 5 $^{\circ}C\ min^{-1}$): $T_{dec.}$ = 347 $^{\circ}C$.

5-(5-Nitrimino-1,4H-1,2,4-triazol-3-yl)-1H-tetrazole (5)

Nitric acid (100%, 1.0 mL) was added slowly to a solution of **4** (0.5 g, 3.3 mmol) in concentrated sulfuric acid (6.0 mL) at 0 $^{\circ}C$. The mixture was allowed to warm to room temperature and stirred for one hour. The clear solution was poured on ice and the precipitate was collected by filtration to yield **5** (0.4 g, 2.4 mmol, 65 %) as colorless solid.

1H NMR (DMSO- d_6): δ = 7.81 (s, $H_{triazole/tetrazole}$) ppm; **^{13}C NMR** (DMSO- d_6): δ = 153.0 ($CNNO_2$), 148.4 ($C_{triazole}$), 141.8 ($C_{tetrazole}$) ppm; **^{14}N NMR** (DMSO- d_6): δ = -23 ppm; **IR**: ν (cm^{-1}) (rel. int.) = 3309(m), 1681(vs), 1650(m), 1628(m), 1376(s), 1257(m), 1194(m), 1121(m), 1091(s), 1054(m), 1035(m), 972(vs), 958(s), 910(s), 756(m), 745(m), 723(m); **Raman** (200 mW): ν (cm^{-1}) (rel. int.) = 1650(97), 1606(100), 1537(15), 1511(6),

1494(7), 1405(3), 1310(9), 1258(10), 1237(23), 1130(39), 1099(4), 1070(7), 1059(25), 995(18), 983(27), 865(10), 760(32), 752(6), 705(2), 663(2), 534(2), 500(3), 416(8), 416(8), 306(12), 228(11); **Elemental analysis** ($\text{C}_3\text{H}_3\text{N}_9\text{O}_3$): calc.: C 18.28, H 1.53, N 63.95; found: C 18.64, H 1.67, N 63.26; **Mass spectrometry**: m/z (DCI+) = 198.1 ($[\text{C}_3\text{H}_3\text{N}_9\text{O}_3]^+$); **Sensitivities** (grain size < 100 μm): friction: 20 N, impact: <1 J, ESD: 0.05 J; **DSC** (onset, 5 $^\circ\text{C min}^{-1}$): $T_{\text{dec.}}$ = 215 $^\circ\text{C}$.

5-(3-Nitro-1,2,4-1H-triazol-5-yl)-2H-tetrazole (**6**)

A suspension of **4** (0.5 g, 3.3 mmol) in 20% sulfuric acid (6.0 mL) was added drop wise to a solution of sodium nitrite (30 eq., 6.8 g, 98 mmol) in water (10 mL) at 40 $^\circ\text{C}$. The mixture was stirred at 50 $^\circ\text{C}$ for one hour. After cooling down to room temperature the mixture was acidified with sulfuric acid (20%) until no evolution of nitrogen dioxide could be observed. The reaction mixture was extracted with ethyl acetate, dried over magnesium sulfate and the solvent was evaporated to yield **6** (0.49 g, 2.7 mmol, 82 %) as colorless solid.

$^1\text{H NMR}$ ($\text{DMSO-}d_6$): δ = 7.32 (s, $\text{H}_{\text{triazole/tetrazole}}$) ppm; **$^{13}\text{C NMR}$** ($\text{DMSO-}d_6$): δ = 163.0 (CNO_2), 148.3 ($\text{C}_{\text{triazole}}$), 145.4 ($\text{C}_{\text{tetrazole}}$) ppm; **$^{14}\text{N NMR}$** ($\text{DMSO-}d_6$): δ = -26 ppm; **$^{15}\text{N NMR}$** ($\text{DMSO-}d_6$): δ = -19.1 (N6), -29.0 (N4), -89.4 (N5), -90.9 (N2), -141.9 (N3), -159.5 (N1) ppm; **IR**: ν (cm^{-1}) (rel. int.) = 3135(m), 3019(w), 2970(w), 2790(m), 2730(w), 2646(w), 1754(w), 1630(w), 1555(s), 1506(w), 1486(m), 1477(m), 1460(w), 1420(m), 1384(w), 1365(s), 1338(s), 1312(vs), 1241(m), 1174(s), 1129(s), 1075(m), 1034(m), 1034(m), 1023(m), 971(s), 899(s), 842(vs), 774(m), 767(m), 708(s), 692(m), 644(s), 622(w), 606(w); **Raman** (200 mW): ν (cm^{-1}) (rel. int.) = 1631(100), 1608(4), 1557(6), 1504(25), 1477(15), 1446(4), 1420(42), 1366(18), 1340(5), 1315(9), 1244(4), 1212(3), 1187(17), 1175(9), 1128(26), 1078(10), 1035(2), 1019(20), 970(5), 844(2), 776(2), 768(8), 468(5), 468(5), 395(10), 334(9), 261(2), 247(2), 236(4); **Elemental analysis** ($\text{C}_3\text{H}_2\text{N}_8\text{O}_2$): calc.: C 19.79, H 1.11, N 61.53; found: C 20.12, H 1.11, N 60.95; **Mass spectrometry**: m/z (DEI+) = 182.1 ($[\text{C}_3\text{H}_2\text{N}_8\text{O}_2]^+$). **Sensitivities** (grain size 100–500 μm): friction: 288 N, impact: 25 J, ESD: 0.85 J; **DSC** (onset, 5 $^\circ\text{C min}^{-1}$): $T_{\text{dec.}}$ = 211 $^\circ\text{C}$.

5-(5-Azido-1H-1,2,4-triazol-3-yl)tetrazole (**7**)

A solution of sodium nitrite (0.72 g, 10 mmol) in water (6.0 mL) was added dropwise to a suspension of **4** (1.1 g, 7.0 mmol) in sulfuric acid (25 wt%, 30 mL) at 0 $^\circ\text{C}$. The mixture

was allowed to warm to room temperature and subsequently stirred at 40 °C for 30 minutes. After cooling down to room temperature, a solution of sodium azide (5 eq., 2.3 g, 35 mmol) in water (10 mL) was added dropwise. (DANGER: EVOLUTION OF HN₃!). The suspension was stirred over night at room temperature to remove the excess of sodium azide and subsequently extracted with ethyl acetate (3×30 mL). The solvent was evaporated and **7** (0.8 g, 4.5 mmol, 64%) was obtained as a colorless solid.

¹H NMR (DMSO-*d*₆): δ = 11.83 (s, H_{triazole/tetrazole}) ppm; **¹³C NMR** (DMSO-*d*₆): δ = 155.5, 148.5, 146.3 ppm; **¹⁴N NMR** (DMSO-*d*₆): δ = -143 (N8) ppm; **¹⁵N NMR** (DMSO-*d*₆): δ = -11.5 (N5), -97.0 (N4), -143.2 (N3), -145.2 (N7), -152.0 (N8), -294.9 (N6) ppm; **IR**: ν (cm⁻¹) (rel. int.) = 3141(m), 3055(w), 2929(w), 2862(w), 2381(vw), 2233(vw), 2148(vs), 1754(w), 1625(m), 1559(s), 1544(s), 1493(m), 1484(s), 1412(m), 1392(s), 1322(w), 1265(s), 1194(s), 1140(w), 1081(m), 1054(m), 1043(s), 981(s), 981(s), 827(w), 819(w), 813(m), 811(m), 800(m), 790(m), 784(m), 775(m), 773(m), 769(m), 764(m), 759(m), 755(m), 753(m), 743(m), 738(m), 736(m), 727(s), 710(w), 696(s); **Raman** (200 mW): ν (cm⁻¹) (rel. int.) = 2148(7), 1627(100), 1560(8), 1485(16), 1441(4), 1415(8), 1268(8), 1243(4), 1196(3), 1143(10), 1084(2), 1062(6), 1043(13), 1012(1), 981(2), 801(1), 766(2), 559(3), 514(1), 412(4), 403(7), 358(5), 295(3), 295(3); **Elemental analysis** (C₃H₂N₁₀): calc.: C 20.23, H 1.13, N 78.64; found: C 21.09, H 1.10, N 75.83. **Mass spectrometry**: m/z (DEI+) = 178.1 ([C₃H₂N₁₀]⁺); **Sensitivities** (grain size < 100 μ m): friction: 20 N, impact: < 1 J, ESD: 0.05 J; **DSC** (onset, 5 °C min⁻¹): $T_{\text{dec.}}$ = 164 °C.

REFERENCES

- [1] a) T. M. Klapötke, *Chemistry of high-energy materials*, de Gruyter, Berlin **2011**; b) T. M. Klapötke, *Chemie der hochenergetischen Materialien*, de Gruyter, Berlin **2009**; c) P. F. Pagoria, G. S. Lee, A. R. Mitchell, R. D. Schmidt, *Thermochimica Acta* **2002**, 384, 187-204; d) R. P. Singh, R. D. Verma, D. T. Meshri, J. M. Shreeve, *Angew. Chem., Int. Ed.* **2006**, 45, 3584-3601; e) C. M. Sabate, T. M. Klapötke, *New Trends in Research of Energetic Materials*, Proceedings of the 12th Seminar, University of Pardubice, Czech Republic, **2009**, 172-194; f) S. Yang, S. Xu, H. Huang, W. Zhang, X. Zhang, *Huaxue Jinzhan* **2008**, 20, 526-537; g) M. B. Talawar, R. Sivabalan, T. Mukundan, H. Muthurajan, A. K. Sikder, B. R. Gandhe, A. S. Rao, *J. Hazard. Mater.* **2009**, 161, 589-607.

- [2] a) T. M. Klapötke, J. Stierstorfer, A. U. Wallek, *Chem. Mater.* **2008**, *20*, 4519-4530; b) T. M. Klapötke, C. M. Sabate, *Chem. Mater.* **2008**, *20*, 3629-3637; c) D. E. Chavez, M. A. Hiskey, D. L. Naud, *Prop. Explos. Pyrot.* **2004**, *29*, 209-215; d) Y. Huang, H. Gao, B. Twamley, J. M. Shreeve, *Eur. J. Inorg. Chem.* **2008**, 2560-2568; e) H. Gao, J. M. Shreeve, *Chem. Rev.* **2011**, *111*, 7377-7436.
- [3] T. M. Klapötke, in *Structure and bonding* (Ed.: D. M. P. Mingos), Springer-Verlag, Berlin Heidelberg **2007**.
- [4] M. H. V. Huynh, M. A. Hiskey, T. J. Meyer, M. Wetzler, *Proceedings of the National Academy of Sciences* **2006**, *103*, 5409-5412.
- [5] a) T. M. Klapötke, J. Stierstorfer, *Helvetica Chimica Acta* **2007**, *90*, 2132-2150; b) T. M. Klapötke, C. M. Sabate, J. Stierstorfer, *New J. Chem.* **2009**, *33*, 136-147; c) A. Dippold, Thomas M. Klapötke, Franz A. Martin, *Z. Anorg. Allg. Chem.* **2011**, 637, 1181-1193.
- [6] a) N. Fischer, D. Izsák, T. M. Klapötke, S. Rappenglück, J. Stierstorfer, *Chem. Eur. J.* **2012**, *18*, 4051-4062; b) N. Fischer, T. M. Klapötke, K. Peters, M. Rusan, J. Stierstorfer, *Z. Anorg. Allg. Chem.* **2011**, 637, 1693-1701; c) Y. Guo, G.-H. Tao, Z. Zeng, H. Gao, D. A. Parrish, J. M. Shreeve, *Chem. Eur. J.* **2010**, *16*, 3753-3762; d) E. Oliveri-Mandala, T. Passalacqua, *Gazz. Chim. Ital.* **1914**, *43*, 465-475; e) D. E. Chavez, M. A. Hiskey, D. L. Naud, *J. Pyrotech.* **1999**, 17-36.
- [7] a) E. L. Metelkina, T. A. Novikova, S. N. Berdonosova, D. Y. Berdonosov, V. S. Grineva, *Russ. J. Org. Chem.* **2004**, *40*, 1412-1414; b) E. L. Metelkina, T. A. Novikova, S. N. Berdonosova, D. Y. Berdonosov, *Russ. J. Org. Chem.* **2005**, *41*, 440-443; c) E. Metelkina, T. Novikova, *Russ. J. Org. Chem.* **2004**, *40*, 1737-1743; d) A. M. Astachov, V. A. Revenko, L. A. Kruglyakova, E. S. Buka, in *New Trends in Research of Energetic Materials*, Proceedings of the 10th Seminar, University of Pardubice, Czech Republic, **2007**, 505-511; e) A. M. Astachov, V. A. Revenko, E. S. Buka, in *New Trends in Research of Energetic Materials*, Proceedings of the 12th Seminar, University of Pardubice, Czech Republic, **2009**, 396-404; f) R. Wang, H. Xu, Y. Guo, R. Sa, J. M. Shreeve, *J. Am. Chem. Soc.* **2010**, *132*, 11904-11905; g) Y. V. Serov, M. S. Pevzner, T. P. Kofman, I. V. Tselinskii, *Russ. J. Org. Chem.* **1990**, *26*, 773-777; h) L. I. Bagal, M. S. Pevzner, A. N. Frolov, N. I. Sheludyakova, *Chem. Heterocyc. Comp.* **1970**, *6*, 240-244; i) A. A. Dippold, T. M. Klapötke, N. Winter, *Eur. J. Inorg. Chem.* **2012**, 2012, 3474-3484.
- [8] D. L. Naud, M. A. Hiskey, H. H. Harry, *J. Energ. Mater.* **2003**, *21*, 57-62.

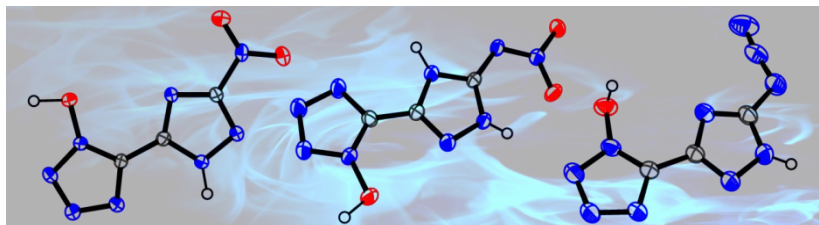
- [9] A. A. Dippold, T. M. Klapötke, F. A. Martin, S. Wiedbrauk, *Eur. J. Inorg. Chem.* **2012**, 10, 2429–2443.
- [10] P. Cardillo, M. Dellavedova, L. Gigante, A. Lunghi, C. Pasturenzi, E. Salatelli, P. Zanirato, *Europ. J. Inorg. Chem.* **2012**, 2012, 1195–1201.
- [11] a) Z. P. Demko, K. B. Sharpless, *J. Org. Chem.* **2001**, 66, 7945–7950; b) L. Liang, H. Huang, K. Wang, C. Bian, J. Song, L. Ling, F. Zhao, Z. Zhou, *J. Mater. Chem.* **2012**, 22, 21954–21964; c) H. Huang, Z. Zhou, L. Liang, J. Song, K. Wang, D. Cao, C. Bian, W. Sun, M. Xue, *Z. Anorg. Allg. Chem.* **2012**, 638, 392–400; d) T. Hiroaki, T. Toshiyuki, *PCT Int. Appl.* **2007**, WO 2007013323.
- [12] F. H. Allen, O. Kennard, D. G. Watson, L. Brammer, A. G. Orpen, R. Taylor, *J. Chem. Soc., Perkin Trans. 2* **1987**, S1–S19.
- [13] a) D. E. Chavez, B. C. Tappan, B. A. Mason, D. Parrish, *Prop. Explos. Pyrot.* **2009**, 34, 475–479; b) T. P. Kofman, *Russ. J. Org. Chem.* **2002**, 38, 1231–1243; c) E. V. Nikitina, G. L. Starova, O. V. Frank-Kamenetskaya, M. S. Pevzner, *Kristallografiya* **1982**, 27, 485–488; d) A. A. Dippold, T. M. Klapötke, *Chem-Eur. J.* **2012**, in press.
- [14] A. F. Hollemann, E. Wiberg, N. Wiberg, *Lehrbuch der anorganischen Chemie*, de Gruyter, New York, **2007**.
- [15] A. A. Dippold, T. M. Klapötke, F. A. Martin, S. Wiedbrauk, *Eur. J. Inorg. Chem.* **2012**, 2012, 2429–2443.
- [16] a) M. Hesse, *Spektroskopische Methoden in der organischen Chemie*, 7th ed., Thieme Verlag, Stuttgart, **2005**; b) H. H. Licht, H. Ritter, H. R. Bircher, P. Bigler, *Magn. Reson. Chem.* **1998**, 36, 343–350; c) A. A. Dippold, T. M. Klapötke, *Chem-Eur. J.* **2012**, 18, 16742–16753.
- [17] M. J. Frisch, G. W. Trucks, H. B. Schlegel, G. E. Scuseria, M. A. Robb, J. R. Cheeseman, G. Scalmani, V. Barone, B. Mennucci, G. A. Petersson, H. Nakatsuji, M. Caricato, X. Li, H. P. Hratchian, A. F. Izmaylov, J. Bloino, G. Zheng, J. L. Sonnenberg, M. Hada, M. Ehara, K. Toyota, R. Fukuda, J. Hasegawa, M. Ishida, T. Nakajima, Y. Honda, O. Kitao, H. Nakai, T. Vreven, J. A. J. Montgomery, J. E. Peralta, F. Ogliaro, M. Bearpark, J. J. Heyd, E. Brothers, K. N. Kudin, V. N. Staroverov, R. Kobayashi, J. Normand, K. Raghavachari, A. Rendell, J. C. Burant, S. S. Iyengar, J. Tomasi, M. Cossi, N. Rega, J. M. Millam, M. Klene, J. E. Knox, J. B. Cross, V. Bakken, C. Adamo, J. Jaramillo, R. Gomperts, R. E. Stratmann, O. Yazyev, A. J. Austin, R. Cammi, C. Pomelli, J. W. Ochterski, R. L. Martin, K. Morokuma, V. G. Zakrzewski, G. A. Voth, P. Salvador, J. J. Dannenberg, S. Dapprich, A. D.

- Daniels, Ö. Farkas, J. B. Foresman, J. V. Ortiz, J. Cioslowski, D. J. Fox, Wallingford **2009**.
- [18] a) J. A. Montgomery, Jr., M. J. Frisch, J. W. Ochterski, G. A. Petersson, *J. Chem. Phys.* **2000**, *112*, 6532-6542; b) J. W. Ochterski, G. A. Petersson, J. A. Montgomery, Jr., *J. Chem. Phys.* **1996**, *104*, 2598-2619.
- [19] P. J. Lindstrom, W. G. Mallard, NIST Chemistry Webbook, NIST Standard Reference 69, June 2005, National Institute of Standards and technology, Gaithersburg MD, <http://webbook.nist.gov>
- [20] a) E. F. C. Byrd, B. M. Rice, *J. Phys. Chem. A* **2006**, *110*, 1005-1013; b) B. M. Rice, J. J. Hare, *J. Phys. Chem. A* **2002**, *106*, 1770-1783; c) B. M. Rice, S. V. Pai, J. Hare, *Combust. Flame* **1999**, *118*, 445-458.
- [21] a) F. Trouton, *Philos. Mag.* **1884**, *18*, 54-57; b) M. S. Westwell, M. S. Searle, D. J. Wales, D. H. Williams, *J. Am. Chem. Soc.* **1995**, *117*, 5013-5015.
- [22] a) H. D. B. Jenkins, D. Tudela, L. Glasser, *Inorg. Chem.* **2002**, *41*, 2364-2367; b) H. D. B. Jenkins, H. K. Roobottom, J. Passmore, L. Glasser, *Inorg. Chem.* **1999**, *38*, 3609-3620.
- [23] M. Sućeska, *EXPLO5.05 program, Zagreb, Croatia*, **2010**.
- [24] a) M. Sućeska, *Materials Science Forum* **2004**, 465-466, 325-330; b) M. Suceka, *Prop. Explos. Pyrot.* **1999**, *24*, 280-285; c) M. Suceka, *Prop. Explos. Pyrot.* **1991**, *16*, 197-202.
- [25] R. Meyer, J. Köhler, A. Homburg, *Explosives*, Sixth ed., Wiley-VCH Verlag GmbH & Co. KGaA, Weinheim, **2007**.
- [26] A. Dippold, T. M. Klapötke, M. Feller, in *New Trends in Research of Energetic Materials*, Proceedings of the 14th Seminar, University of Pardubice, Czech Republic, **2011**, 550-560.
- [27] NATO standardization agreement (STANAG) on explosives and impact tests, no.4489, 1st ed., Sept. 17, **1999**.
- [28] WIWEB-Standardarbeitsanweisung 4-5.1.02, Ermittlung der Explosionsgefährlichkeit, hier: der Schlagempfindlichkeit mit dem Fallhammer, Nov. 08, **2002**.
- [29] <http://www.bam.de>.
- [30] NATO standardization agreement (STANAG) on explosives, friction tests, no.4487, 1st ed., Aug. 22, **2002**.

- [31] *WIWEB-Standardarbeitsanweisung 4-5.1.03, Ermittlung der Explosionsgefährlichkeit, hier: der Reibempfindlichkeit mit dem Reibeapparat*, Nov. 08, **2002**.
- [32] *NATO standardization agreement (STANAG) on explosives, electrostatic discharge sensitivity tests, no.4490, 1st ed., Feb. 19*, **2001**.
- [33] *CrysAlisPro 1.171.35.11*, Agilent Technologies, **2011**.
- [34] A. Altomare, G. Cascarano, C. Giacovazzo, A. Guagliardi, *J. Appl. Crystallogr.* **1993**, 26, 343-350.
- [35] G. M. Sheldrick, *Acta Cryst.* **2008**, A64, 112-122.
- [36] L. Farrugia, *J. Appl. Crystallogr.* **1999**, 32, 837-838.
- [37] A. L. Spek, *Platon, A Multipurpose Crystallographic Tool*, Utrecht University, Utrecht, The Netherlands, **2012**.

10. A STUDY OF 5-(1,2,4-TRIAZOL-C-YL)TETRAZOL-1-OLS: COMBINING THE BENEFITS OF DIFFERENT HETEROCYCLES FOR THE DESIGN OF ENERGETIC MATERIALS

As published in: Chemistry – A European Journal 2013, in press.



ABSTRACT:

This study features the synthesis and full structural as well as spectroscopic characterization of three 5-(1,2,4-triazol-C-yl)tetrazol-1-ol compounds along with selected energetic moieties like nitrimino (**5**), nitro (**6**) and azido (**7**) groups. The influence of those variable energetic moieties as well as the C–C connection of a tetrazol-1-ol and a 1,2,4-triazole on structural and energetic properties is investigated. All compounds were well characterized by various means, including IR and multinuclear NMR spectroscopy, mass spectrometry, and DSC. The molecular structures of **5–8** in the solid state were determined by single-crystal X-ray diffraction. The standard heats of formation were calculated on the CBS-4M level of theory utilizing the atomization energy method, revealing highly positive values for all compounds. The detonation parameters were calculated using the EXPLO5 program and compared to the common secondary explosive RDX. Additionally, the sensitivities towards impact, friction and electrostatic discharge were determined. The potential application of the synthesized compounds as energetic materials will be studied and evaluated using the experimentally obtained values for the thermal decomposition, the sensitivity data, as well as the calculated performance characteristics.

INTRODUCTION

The chemistry of explosives, their development and application are as old as 220 years BC, when blackpowder was discovered accidentally by the Chinese. Nowadays, not only the application for military purposes is studied, but the utilization of energetic materials for civilian use in mining, construction, demolition and safety equipment such as airbags, signal flares and fire extinguishing systems is extensively studied. The academic research mainly focuses on the work with novel energetic systems to determine factors affecting stability and performance and to bring new strategies into the design of energetic materials.^[1,2] Compared to typical explosives in current use, like 2,4,6-trinitrotoluene (TNT) or 1,3,5-trinitro-1,3,5-triazinane (RDX), they derive their energy upon detonation not from the oxidation of a carbon backbone but rather from their high heats of formation. This is especially the result of the contained nitrogen single and double bonds, with the formation of molecular dinitrogen and its very stable N–N triple bond as the main driving force.^[3] A prominent family of novel high-energy-density materials (HEDMs) are azole-based compounds, since they are generally highly endothermic with high densities and low sensitivities towards outer stimuli. Owing to the high positive heats of formation and the high level of environmental compatibility, those compounds have been studied in numerous research groups over the last couple of years with growing interest.

Triazoles and tetrazoles have been used for the preparation of high-performance primary^[4] and secondary^[5] explosives, owing to the fact that energetic materials based on those heterocycles show the desirable compromise between a high nitrogen content on the one hand and excellent kinetic and thermal stabilities due to aromaticity on the other. Many research has been done on the combination of those heterocycles to bistetrazoles^[6] and bistriazoles,^[7] resulting in numerous compounds with outstanding properties as energetic materials. The recently published C–C connection of a tetrazole and a 1,2,4-triazole leads to energetic materials with variable properties.^[8]

The introduction of *N*-oxides is a recently reintroduced method to raise the densities of the compounds for an even greater energy output^[9]. One method for achieving this is the oxidation of the nitrogen-rich heterocycles with oxidizing agents like tri-fluoroperacetic acid,^[10] potassium peroxomonosulfate (Oxone®),^[11] or hypofluorous acid.^[12] The often low selectivity and high oxidation potential of those compounds can lead to several isomers or even a complete decomposition of the starting material, especially when thinking of compounds with several oxidizable nitrogen atoms. An appropriate alternative

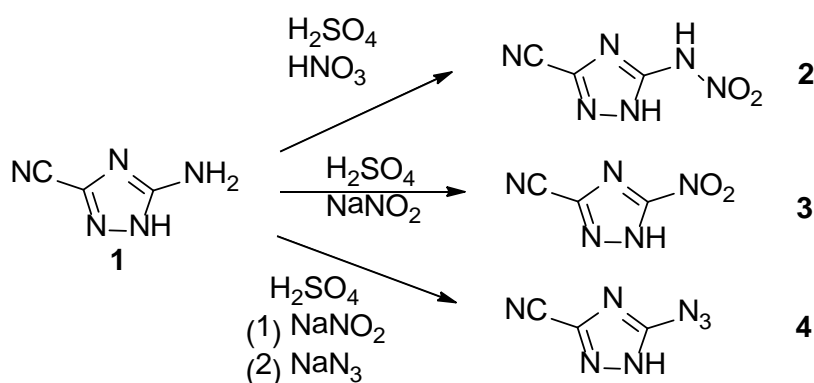
are 1-hydroxytetrazoles, owing to the fact that the oxygen atom is introduced during the synthesis of the tetrazole ring instead of subsequent oxidation.^[13]

RESULTS AND DISCUSSION

SYNTHESIS

The synthesis of the starting material 5-amino-1*H*-1,2,4-triazole-3-carbonitrile (**1**) was accomplished by dehydration of the corresponding carboxamide using phosphorus pentoxide in acetonitrile as published recently.^[8]

The energetic moieties were introduced by modification of the amine group of compound **1** as shown in Scheme 1.



Scheme 1: Synthesis of 5-nitramino-1*H*-1,2,4-triazole-3-carbonitrile (**2**), 5-nitro-1*H*-1,2,4-triazole-3-carbonitrile (**3**) and 5-azido-1*H*-1,2,4-triazole-3-carbonitrile (**4**).

The treatment of 5-amino-1*H*-1,2,4-triazole-3-carbonitrile with a mixture of sulfuric acid/nitric acid (6:1) leads to 5-nitramino-1*H*-1,2,4-triazole-3-carbonitrile (**2**). 5-Nitro-1*H*-1,2,4-triazole-3-carbonitrile (**3**) was obtained by the well-known Sandmeyer reaction via diazotization in sulfuric acid and subsequent reaction with the excess of sodium nitrite. The azido compound (**4**) was as well synthesized via diazotization in sulfuric acid and subsequent reaction with an excess of sodium azide.

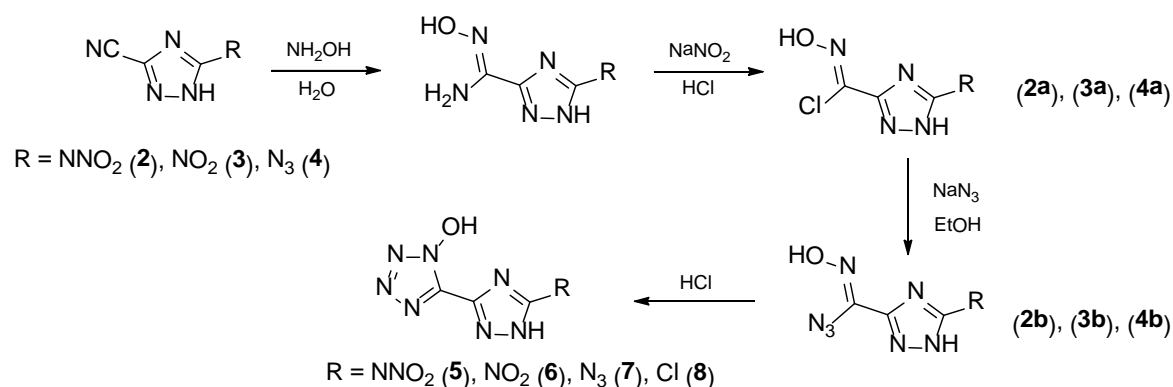
The synthesis of the 1-hydroxytetrazole moiety was accomplished according to the literature known methods used for similar compounds.^[13] As shown in Scheme 2, the reaction of hydroxylamine with the nitrile moiety of **2–4** leads to the formation of the corresponding amidoxime. Those intermediate compounds were not isolated but subsequently reacted with sodium nitrite after addition of hydrochloric acid. The diazotization in hydrochloric acid causes the formation of the chloroxime compounds **2a–**

4a, which were collected by filtration to remove traces of unreacted nitrile. The following chlorine to azide exchange readily takes place in ethanol and leads to the azidoxime compounds **2b–4b**. The final cyclisation works best for compounds **2b** and **3b** in concentrated hydrochloric acid within 12 h and the energetic 1-hydroxytetrazole compounds **5–6** were isolated in excellent yields.

Due to the high sensitivity of compound **4b**, a different cyclization method was chosen in comparison to **2b** and **3b**. The extraction of the azidoxime with diethyl ether after the chlorine to azide exchange without evaporation of the ether avoids isolation of the pure and highly sensitive compound. Subsequent saturation of the ether solution with HCl gas and stirring for two days also leads to the formation of compound **7**. After removal of the ether and the excess of HCl gas, **7** could also be isolated nearly quantitatively.

Surprisingly, in the case of the azidoxime **3b**, the utilization of this method selectively leads to the chlorine compound **8**. Apparently, a nitro to chlorine exchange occurs while stirring **3b** in a saturated solution of HCl in ether and leads to the formation of the less-energetic, undesired chlorine compound.

All three main 5-(1,2,4-triazol-C-yl)tetrazole-1-ol compounds **5–7** were fully characterized by IR and Raman as well as multinuclear NMR spectroscopy and mass spectrometry. The molecular structures of **5–8** in the solid state were determined by single-crystal X-ray diffraction.



Scheme 2: Synthesis of 5-(5-nitrimino-1,4*H*-1,2,4-triazol-3-yl)tetrazol-1-ol (NATTO, **5**), 5-(3-nitro-1*H*-1,2,4-triazol-5-yl)tetrazol-1-ol (NTTO, **6**), 5-(5-azido-1*H*-1,2,4-triazol-3-yl)tetrazol-1-ol (AzTTO, **7**) and 5-(5-chloro-1*H*-1,2,4-triazol-3-yl)tetrazol-1-ol (**8**).

SINGLE CRYSTAL X-RAY STRUCTURE ANALYSIS

Single-crystal X-ray measurements were performed for compounds **5–8** and are discussed in the following. The crystal structure of the undesired side compound **8** can be found in the supporting information. The bond lengths and torsion angles within theazole ring of compounds **5–8** are all in the expected range in comparison to similar triazole and tetrazole compounds.^[6a,14] The bond lengths within the triazole and the tetrazole ring in the crystal structures are all between the length of formal C–N and N–N single and double bonds (C–N: 1.47 Å, 1.22 Å; N–N: 1.48 Å, 1.20 Å).^[15] As expected,^[7f,16] the bistriazole moiety shows a completely planar assembly due to the electron delocalization in the molecule, the nitrimino moiety is pointing towards the nitrogen atom N1 and participates in an intramolecular hydrogen bond N1–H1···O3 with a D···A length of 2.555(2) Å and a D–H···A angle of 111.7(17)° (Figure 1). In comparison to the recently published 5-(5-nitrimino-1,4*H*-1,2,4-triazol-3-yl)-1*H*-tetrazole, the density is increased from 1.618 g cm^{−3} to 1.741 g cm^{−3} by introduction of the 1-hydroxytetrazole. The molecular structure of **5** together with the atom labeling is presented in Figure 1.

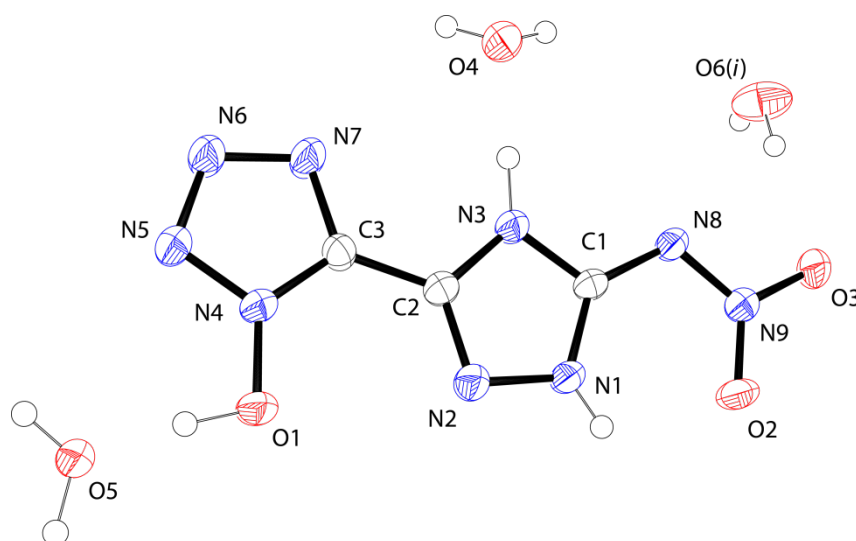


Figure 1. Molecular structure of 5-(5-nitrimino-1,4*H*-1,2,4-triazol-3-yl)tetrazol-1-ol (NATTO, **5**). Thermal ellipsoids are set to 50 % probability. Symmetry code: (i) $-x, y, 3/2-z$.

The structure is dominated by chains along the *a*-axis, established by the threefold hydrogen bond of the oxygen atom O5 acting both as acceptor and donor. Four further nitrogen atoms N1, N2, N3 and N6 are involved in additional hydrogen bonds (Table 1), resulting in strong interactions with surrounding molecules within the chains. The water molecule O4 at the edge acts as linker between two chains, which are arranged in a zigzag

row including an angle of 141° . The rows are stacked along the b -axis with a layer distance $d = 3.31 \text{ \AA}$ and stabilized by the intermolecular hydrogen bonds $\text{O6}^i\text{--H6A}\cdots\text{O3}$ and $\text{O6}^i\text{--H6B}\cdots\text{O4}$.

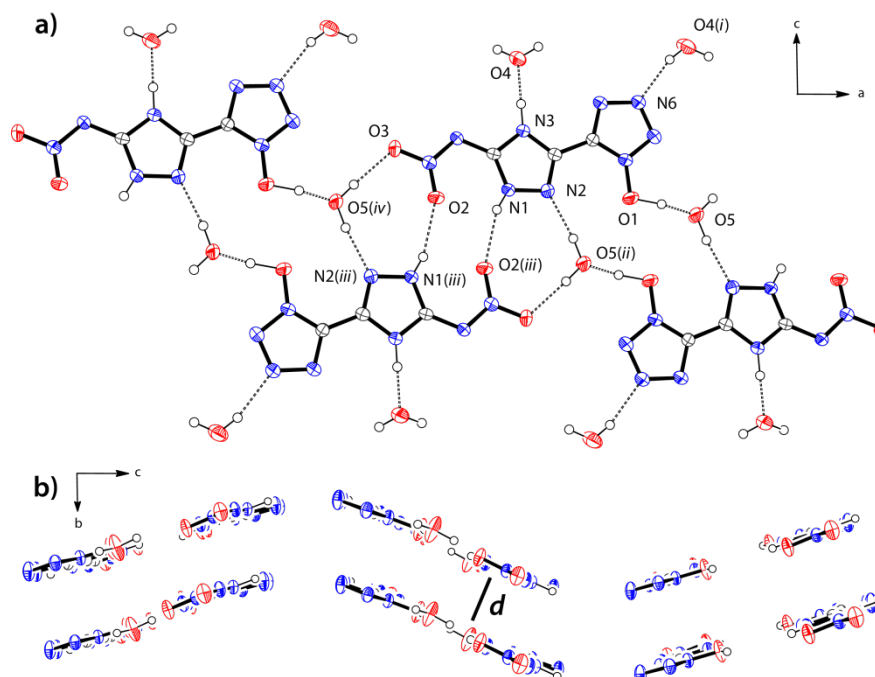


Figure 2. a) Formation of chains along the a -axis in the crystal structure of **5**; b) zigzag arrangement of chains (layer distance $d = 3.31 \text{ \AA}$, water molecules are omitted for clarity). Thermal ellipsoids are set to 50 % probability Symmetry codes: (i) $1-x, y, 3/2-z$; (ii) $1-x, -y, 1-z$; (iii) $-x, -y, 1-z$; (iv) $-1+x, y, z$.

Table 1. Hydrogen bonds present in the crystal structure of **5**.

D–H \cdots A	$d(\text{D–H}) [\text{\AA}]$	$d(\text{H}\cdots\text{A}) [\text{\AA}]$	$d(\text{D–H}\cdots\text{A}) [\text{\AA}]$	$\angle (\text{D–H}\cdots\text{A}) [^\circ]$
N1–H1 \cdots O2	0.82(2)	2.14(2)	2.555(2)	112(2)
N1–H1 \cdots O2 ⁱⁱⁱ	0.82(2)	2.10(2)	2.890(2)	162(2)
N3–H3 \cdots O4	0.96(2)	1.62(2)	2.576(2)	179(5)
O1–H1 \cdots O5	1.12(3)	1.31(3)	2.422(2)	173(2)
O4 ⁱ –H4B \cdots N6	0.83(2)	1.95(2)	2.752(2)	165(2)
O5 ⁱⁱ –H5B \cdots N2	0.95(3)	1.87(3)	2.813(2)	173(2)
O5 ^{iv} –H5A \cdots O3	0.86(3)	1.90(3)	2.750(2)	177(3)
O6 ⁱ –H6A \cdots O3	0.85(2)	1.98(2)	2.796(4)	160(5)
O6 ⁱ –H6B \cdots O4	0.84(2)	2.36(4)	3.018(5)	136(4)

Symmetry codes: (i) $1-x, y, 3/2-z$; (ii) $1-x, -y, 1-z$; (iii) $-x, -y, 1-z$; (iv) $-1+x, y, z$.

5-(3-Nitro-1*H*-1,2,4-triazol-5-yl)tetrazol-1-ol (NTTO, **6**) crystallizes as dihydrate in the triclinic space group *P*−1 with a cell volume of 429.8(1) Å³ and two molecular moieties in the unit cell. As expected, the torsion angle between the two heterocycles is very small (7.5(3)°), the nitro group is also only slightly twisted out of the triazole plane (−2.4(3)°). As it is also the case for the nitrmino compound **5**, the density is increased from 1.661 g cm^{−3} to 1.809 g cm^{−3} in comparison to 5-(3-nitro-1*H*-1,2,4-triazol-5-yl)-2*H*-tetrazole. The formula unit of **6** together with the atom labeling is presented in Figure 3.

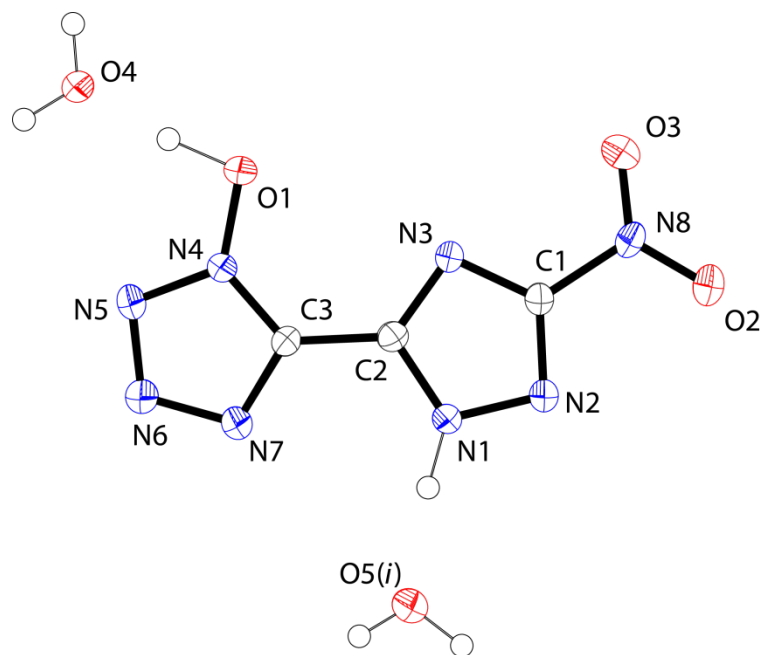


Figure 3. Molecular structure of 5-(3-nitro-1*H*-1,2,4-triazol-5-yl)tetrazole-1-ol (NTTO, **6**). Thermal ellipsoids are set to 50 % probability. Symmetry code: (i) 1−*x*, −*y*, 1−*z*.

In the crystal structure of **6**, the NTTO molecules are arranged in planes and are kept together by several threefold hydrogen bonds with the water molecules (Figure 4a). A direct interaction between two NTTO molecules could not be observed, in contrast to the crystal structure of compound **5**. A strong network of hydrogen bonds is built up by the Oxygen atoms O4 and O5, which act both as donor and acceptor. The layers are connected by a short contact O₁⋯N₈ (*d*(O⋯N) = 3.03 Å) between the hydroxy group and the nitrogen atom of the nitro group and stacked above each other with a layer distance of *d* = 2.99 Å. The stacking of the layers is displayed in Figure 4b together with the distance *d* between the layers.

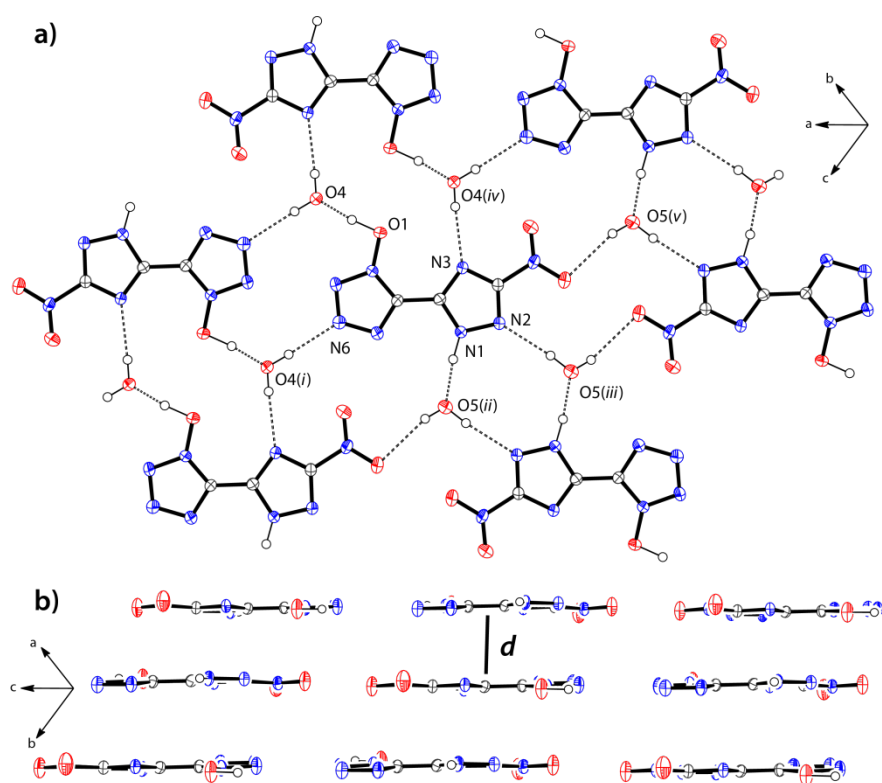


Figure 4. a) Formation of planes in the crystal structure of **6**; b) stacking of layers (layer distance $d = 2.99 \text{ \AA}$, water molecules are omitted for clarity). Thermal ellipsoids are set to 50 % probability. Symmetry codes: (i) $2-x, 1-y, 1-z$; (ii) $1-x, -y, 1-z$; (iii) $x, -1+y, z$; (iv) $2-x, 1-y, -z$; (v) $1-x, -y, -z$.

Table 2. Hydrogen bonds present in the crystal structure of **6**.

D–H...A	$d(\text{D–H}) [\text{\AA}]$	$d(\text{H...A}) [\text{\AA}]$	$d(\text{D–H...A}) [\text{\AA}]$	$\angle(\text{D–H...A}) [^\circ]$
N1–H1...O5 ⁱⁱ	0.97(3)	1.70(3)	2.663(2)	170(2)
O1–H1...O4	1.06(3)	1.42(3)	2.471(2)	173(3)
O4 ^{iv} –H4A...N3	0.85(3)	2.11(3)	2.948(2)	170(3)
O4 ⁱ –H4B...N6	0.86(3)	2.07(3)	2.922(3)	176(3)
O5 ^v –H5A...O2	0.82(3)	2.28(3)	3.065(2)	160(3)
O5 ⁱⁱⁱ –H5B...N2	0.89(3)	2.09(3)	2.971(3)	171(2)

Symmetry codes: (i) $2-x, 1-y, 1-z$; (ii) $1-x, -y, 1-z$; (iii) $x, -1+y, z$; (iv) $2-x, 1-y, -z$; (v) $1-x, -y, -z$.

Finally, 5-(5-azido-1*H*-1,2,4-triazol-3-yl)tetrazol-1-ol (AzTTO, **7**) crystallizes as a monohydrate in the triclinic space group $P\bar{1}$ with two molecules in the unit cell and a cell volume of $416.35(9) \text{ \AA}^3$. The formula unit of **7** together with the atom labeling is presented in Figure 5. The structure of the 5-azido-1,2,4-triazole moiety is similar to that

of the recently published 5-(5-azido-1*H*-1,2,4-triazol-3-yl)tetrazole.^[8] The molecule shows a nearly planar assembly with a torsion angle between the two heterocycles of 2.9(2)°. The azide group is bent with an angle of 172.1(2)° and slightly twisted out of the triazole plane by −7.3(2)°. In contrast to the nitro derivative **6** the proton is located at the nitrogen atom next to the C–N bond, similar to **5** and **4**. The oxygen and the azide are pointing into the same direction, similar to the chloroxime precursor **4a**.^[17]

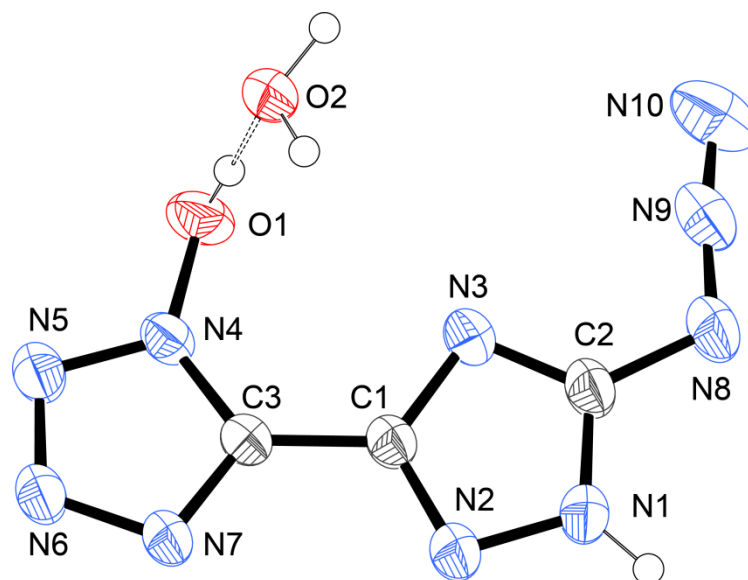


Figure 5. Molecular structure of 5-(5-azido-1*H*-1,2,4-triazol-3-yl)tetrazol-1-ol (AzTTO, **7**). Thermal ellipsoids are set to 50 % probability. Symmetry code: (i) $x, y, 1+z$.

The molecules are forming dimers between two triazole rings with a very weak and mostly electrostatic N1–H1⋯N2ⁱⁱ hydrogen bond ($d(\text{N1} \cdots \text{N2}^{ii})$: 3.175(2) Å). This is similar to the precursor **4**, but there the bond is much stronger ($d(\text{N1} \cdots \text{N2}^i)$: 2.993(2) Å).^[17] The dimers in turn are forming endless parallel chains utilizing the water molecule and with N6 and N7 of the tetrazole ring acting as additional acceptors. The connection between the chains is established by a directed N_γ⋯O interaction between the terminal nitrogen atom of the azide and the hydroxyl group ($d(\text{N10} \cdots \text{O1}^{iv})$: 2.879(2) Å; $d(\text{N9} \cdots \text{N10} \cdots \text{O1}^v)$: 166.7(1)°) well below the sum of the van der Waals radii. The primary hydrogen bonding network and the short contact are illustrated in Figure 6 and the parameters are compiled in Table 3. Finally, the planes are connected by a strong hydrogen bond O1–H1O⋯O2ⁱ between the hydroxyl proton and the water molecule.

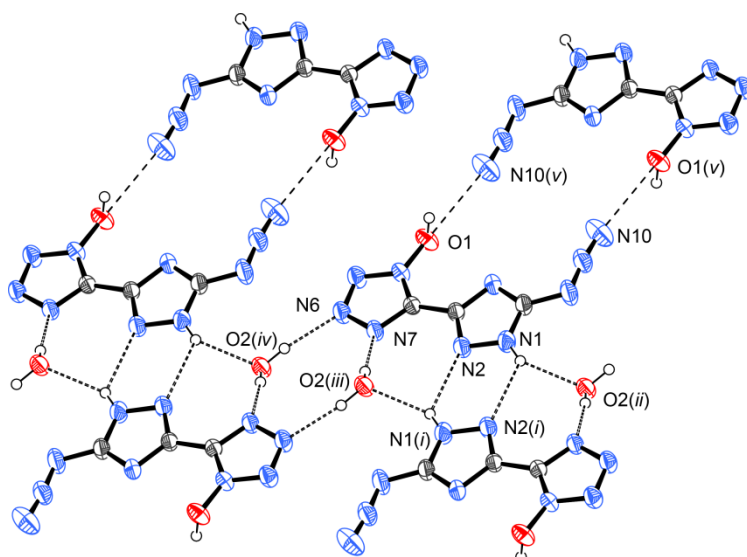


Figure 6: Formation of planes in the crystal structure of **7**, made up from infinite parallel chains. Thermal ellipsoids at 50 % probability. Symmetry codes: (ii) $-x, 1-y, 1-z$; (iii) $x, 1+y, 1+z$; (iv) $1-x, -y, 2-z$.

Table 3. Hydrogen bonds present in the crystal structure of **7**.

D–H...A	$d(\text{D–H})$ [Å]	$d(\text{H...A})$ [Å]	$d(\text{D–H...A})$ [Å]	$\angle (\text{D–H...A})$ [°]
N1–H1...O2	0.91(2)	2.07(2)	2.824(2)	140(2)
N1–H1...N2 ⁱⁱ	0.91(2)	2.51(2)	3.175(2)	130(2)
O1–H1O...O2 ⁱ	0.97(3)	1.61(3)	2.574(2)	175(3)
O2–H2A...N7 ⁱⁱ	0.87(2)	1.94(2)	2.805(2)	170(2)
O2–H2B...N6 ^v	0.85(2)	1.99(2)	2.838(2)	177(2)

Symmetry code: (ii) $-x, 1-y, 1-z$; (iii) $x, 1+y, 1+z$; (iv) $1-x, -y, 2-z$. (v) $x, -1+y, -1+z$.

MULTINUCLEAR NMR SPECTROSCOPY

All title compounds were investigated using ^1H , ^{13}C and ^{14}N NMR spectroscopy. Due to insufficient solubility of compound **5** ^{15}N NMR spectra could only be obtained for compounds **6** and **7**. Compounds **5–8** show two singlets for the carbon atoms of the C–C bridge in the expected range.^[5c,14b] The signal of the carbon atom connected to the energetic moieties is observed at lower field in the range of 148.9 ppm (**8**) to 163.2 ppm (**6**). While the nitro group of compounds **5** and **6** can be identified by a sharp singlet at -24 ppm (**6**) and -25 ppm (**5**) in the ^{14}N NMR spectra, the azido moiety of compound **7** shows a broad singlet at -136 ppm. The NMR signals of all compounds are summarized in Table 4.

Table 4. NMR signals of compounds **4–8** in DMSO-*d*₆.

compound	δ [ppm]			
	$^{13}\text{C}\{^1\text{H}\} \text{C}_{\text{Triazole}}$	$^{13}\text{C}\{^1\text{H}\} \text{C}_{\text{Tetrazole}}$	^{14}N	^1H
5	152.5, 140.5	138.7	−25	7.10
6	163.2, 143.3	138.0	−24	8.09
7	155.2, 144.6	139.7	−136	9.51
8	148.9, 144.8	139.0	/	9.62

Due to the insufficient solubility of compound **5**, ^{15}N NMR spectra could only be obtained for compounds **6** and **7**, as illustrated in Figure 7. Eight well resolved resonances are observed in the ^{15}N NMR spectrum of the nitro-compound **6**. The assignments were based on comparison with theoretical calculations using Gaussian 09 (MPW1PW91/aug-cc-pVDZ).^[18]

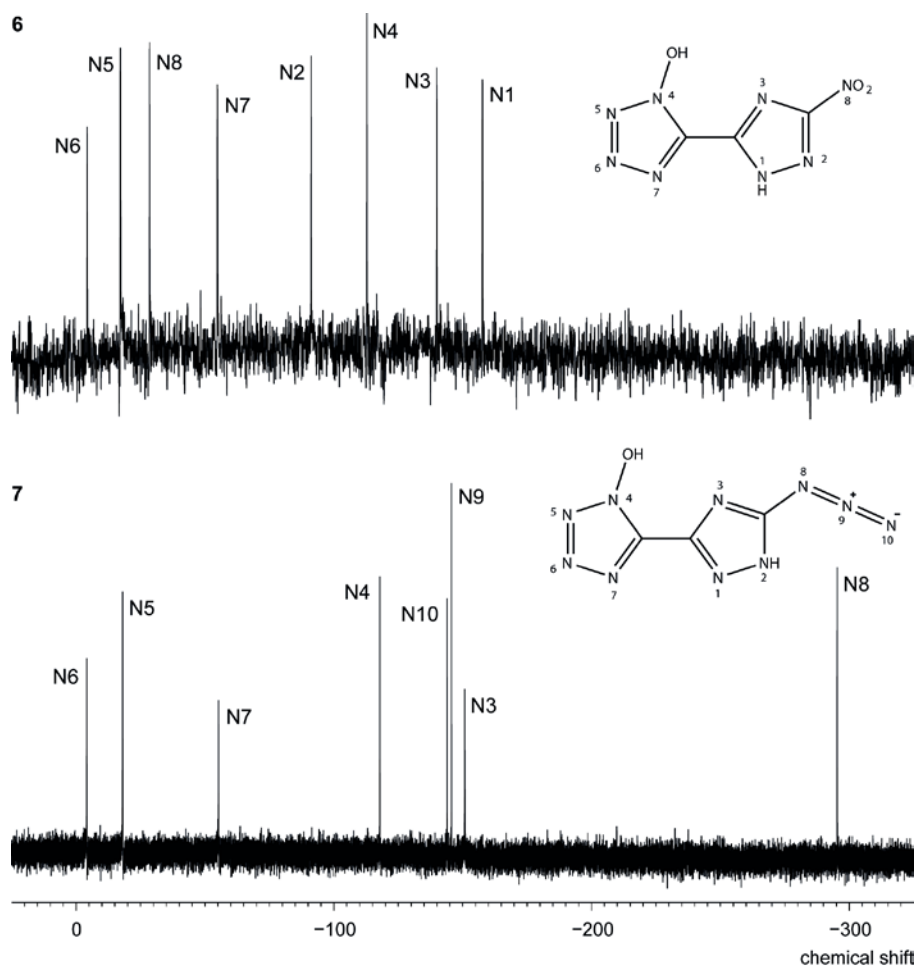


Figure 7. ^{15}N NMR spectra of 5-(3-nitro-1*H*-1,2,4-triazol-5-yl) tetrazol-1-ol (**6**) and 5-(5-azido-1*H*-1,2,4-triazol-3-yl) tetrazol-1-ol (**7**) recorded in DMSO-*d*₆. The *x*-axis represents the chemical shift δ in ppm.

The signals of the triazole nitrogen atoms as well as the nitro group can be found in the expected range similar to the recently published 5-(3-nitro-1*H*-1,2,4-triazol-5-yl)-2*H*-tetrazole,^[8] at shifts of −157.7 (N1), −91.2 (N2), −139.9 (N3), and −28.5 ppm (NO₂). In contrast to this, the azido-compound **7** shows only eight well resolved resonances instead of the expected ten, similar to 5-(5-azido-1*H*-1,2,4-triazol-3-yl)tetrazole.^[8] The two missing signals are the triazole nitrogen atoms N1 and N2, probably resulting from a fast proton exchange. The remaining signals are at shifts of −150.8 (N3), −295.3 (N8), −145.6 (N9), and −144.0 ppm (N10). The signals of the tetrazol-1-ol are similar for both compounds and to 5,5'-bis(tetrazol-1-ol),^[19] and found at −112.8 (N4), −17.2 (N5), −4.2 (N6), and −54.8 ppm (N7) for **6** and at −117.8 (N4), −18.1 (N5), −4.1 (N6), and −55.3 ppm (N7) for **7**, respectively.

THEORETICAL CALCULATIONS, PERFORMANCE CHARACTERISTICS AND STABILITIES

The heats of formation of **5–7** and RDX have been calculated on the CBS-4M level of theory using the atomization energy method and utilizing experimental data (for further details and results refer to the Supporting Information). The results are summarized in Table 5. All compounds show highly endothermic enthalpies of formation with 446 kJ mol^{−1} (**6**), 515 kJ mol^{−1} (**5**) and 795 kJ mol^{−1} (**7**), all by far outperforming RDX (85 kJ mol^{−1}). To estimate the detonation performances of the prepared compounds selected key parameters were calculated with EXPLO5 (version 5.05),^[20] and compared to RDX. The calculated detonation parameters using experimentally determined densities (gas pycnometry at 25 °C with dried compounds) and above mentioned heats of formation are summarized in Table 5. All three compounds **5–7** show lower detonation velocities and pressures than RDX, although all have (much) higher heats of formation and comparable densities.

The thermal stabilities of the title compounds **5–7** were analyzed by differential scanning calorimetry with a heating rate of 5 °C min^{−1} (Figure 8). The compounds were dried before the measurements at 60 °C (**5**, **7**) or 110 °C (**6**), respectively, to remove moisture and crystal water. The determined thermal stabilities are rather low with decomposition beginning at 116 °C (**5**), 144 °C (**7**) and 152 °C (**6**). The azide derivative **7** is the only one to feature a melting point, starting at 83 °C. While the decomposition point of **7** is almost identical to the derivative lacking the nitrogen bound hydroxyl group, except for the missing melting point of the latter, **6** and especially **5** are much less thermally stable (NTT: 211 °C; NATT: 215 °C).^[8] This trend is similar to those reported for 5-nitro-2*H*-

tetrazole vs. 5-nitrotetrazol-2-ol,^[21] and 5,5'-bistetrazole vs. 5,5'-bis(tetrazol-1-ol) and 5,5'-bis(tetrazol-2-ol).^[22] As with the bistetrazoles, deprotonation of the hydroxyl group should clearly raise the thermal stabilities if paired with the right cation. For example while neutral 5,5'-bis(tetrazol-2-ol) decomposes at 165 °C its ammonium salt is stable up to 265 °C and the guanidinium salt even until 331 °C.^[22]

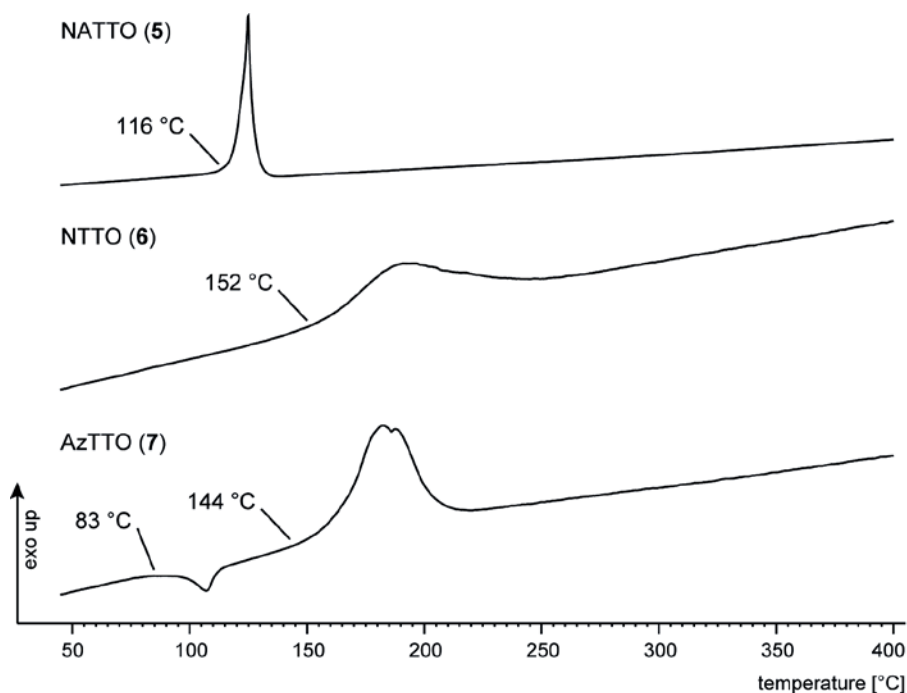


Figure 8. DSC plots of NATTO (**5**), NTTO (**6**) and AzTTO (**7**) with a heating rate of 5 °C min⁻¹.

For an initial safety testing the impact and friction sensitivities as well as the sensitivity towards electrostatic discharge of compounds **5–7** were determined and assigned according to the UN recommendations on the transport of dangerous goods.^[23] All compounds have been dried beforehand (same temperatures as before). Interestingly, the nitrimino derivative **5** is the most sensitive of the three compounds and has to be classified as very sensitive against both impact (< 1 J) and friction (60 N). While the azido derivative **7** is sensitive against both impact (4 J) and friction (120 N), the nitro derivative is almost insensitive (35 J, 360 N). Concerning the sensitivities towards electrostatic discharge both nitro substituted compounds **5** and **6** are more sensitive than **7**, with 130 mJ (**5** and **6**) and 260 mJ (**7**), respectively.

Table 5. Physicochemical properties of compounds **5–7** and hexogen (RDX).

	NATTO (5)	NTTO (6)	AzTTO (7)	RDX ^[o]
Formula	C ₃ H ₃ N ₉ O ₃	C ₃ H ₂ N ₈ O ₃	C ₃ H ₂ N ₁₀ O	C ₃ H ₆ N ₆ O ₆
M [g mol ⁻¹]	213.11	198.10	194.11	222.10
IS [J] ^[a]	< 1	35	4	7.4
FS [N] ^[b]	60	360	120	120
ESD [mJ] ^[c]	130	130	260	200
N [%] ^[d]	59.2	56.6	72.2	37.8
Ω [%] ^[e]	−33.8	−32.3	−49.4	−21.6
T _{dec.} [°C] ^[f]	116	152	144	204
ρ [g cm ⁻³] ^[g]	1.85	1.86	1.69	1.80
Δ _f H° [kJ mol ⁻¹] ^[h]	515	446	795	85
Δ _f U° [kJ kg ⁻¹] ^[i]	2502	2335	4180	481
Calculated detonation parameters (EXPLO5 V5.05)				
−Q _v [kJ kg ⁻¹] ^[j]	5470	5407	5360	6186
T _{ex.} [°C] ^[k]	4126	4217	4207	4260
p _{C-J} [kbar] ^[l]	342	337	275	353
D [m s ⁻¹] ^[m]	8776	8655	8239	8787
V ₀ [L mol ⁻¹] ^[n]	708	677	693	738

[a] Impact sensitivity; [b] friction sensitivity; [c] sensitivity against electrostatic discharge; [d] nitrogen content; [e] oxygen balance; [f] decomposition temperature (DSC, 5 °C min⁻¹); [g] density (25 °C); [h] calculated solid state enthalpy of formation; [i] calculated solid state energy of formation; [j] energy of explosion; [k] explosion temperature; [l] detonation pressure; [m] detonation velocity; [n] volume of gaseous detonation products; [o] taken from the literature.^[24]

The calculated detonation velocities are 8776 m s⁻¹ (**5**), 8655 m s⁻¹ (**6**) and 8239 m s⁻¹ (**7**). In comparison to the corresponding compounds bearing no hydroxyl group at the tetrazole ring,^[8] a marked performance increase is seen. The detonation velocities increase in the range from 350 ms⁻¹ (**7**) to about 650 ms⁻¹ (**5** and **6**). The introduction of the *N*-Oxide also positively influences other detonation parameters like the detonation pressure or the energy of explosion, which are also a remarkably increased.

CONCLUSION

The recently introduced 5-amino-1*H*-1,2,4-triazole-3-carbonitrile (**1**) was further derivatized to the nitrimino (**2**), nitro (**3**) and azido (**4**) compounds, which in turn were cyclized to the respective tetrazol-1-ols **5–7** via the amidoxime, chloroxime and azidoxime intermediates, utilizing adapted literature-known methods. This innovative synthesis leads to the previously unknown C–C connection of a triazole ring with a tetrazol-1-ol ring.

Those different energetic groups containing oxygen or nitrogen and the concept of combining the benefits of two different azoles lead to variable energetic properties. In general, the combination of a triazole ring with its opportunity to introduce a large variety of energetic moieties and a 1-hydroxytetrazole ring implying a large energy content leads to the selective synthesis of precursors for nitrogen-rich ionic primary and secondary explosives. All energetic compounds have been fully characterized by means of vibrational and multinuclear NMR spectroscopy, mass spectrometry and differential scanning calorimetry. Single-crystal X-ray measurements were accomplished for compounds **5–8** and deliver insight into structural characteristics as well as inter- and intramolecular interactions.

As expected, the nitrimino (**5**) as well as the azido-compound (**7**) are the most sensitive derivatives with an impact sensitivity of less than 1 J and 4 J, respectively, and friction sensitivities of 60 N (**5**) and 120 N (**7**). In contrast, the nitro-derivative (**6**) shows moderate sensitivities towards friction (360 N) and impact (35 J). Compounds **5–7** are able to compete with commonly used TNT regarding their detonation parameters, however, the performance data for RDX are not reached. But, taking into account the high nitrogen contents of 59.2 % (**5**), 56.6 % (**6**) and 72.2 % (**7**) and high heats of formation, those compounds could be considered as nitrogen-rich environmentally-friendly primary explosives with proper metal cations (**7**), or be of interest as secondary explosive or propellant ingredient in combination with nitrogen-rich cations (**5** and **6**), respectively.

EXPERIMENTAL SECTION

Caution! Due to the fact that energetic triazole- and tetrazole compounds are to some extent rather unstable against outer stimuli, proper safety precautions should be taken when handling the dry materials. Especially derivatives of azido- and nitrimino-triazoles are energetic primary materials and tend to explode under the influence of impact or friction. Lab personnel and the equipment should be properly grounded and protective equipment like earthed shoes, leather coat, Kevlar[®] gloves, ear protection and face shield is recommended for the handling of any energetic material.

General. All chemical reagents and solvents were obtained from Sigma-Aldrich Inc. or Acros Organics (analytical grade) and were used as supplied without further purification. ¹H, ¹³C{¹H}, ¹⁴N and ¹⁵N NMR spectra were recorded on a JEOL Eclipse 400 instrument in DMSO-*d*₆ at 25 °C. The chemical shifts are given relative to tetramethylsilane (¹H, ¹³C) or nitro methane (¹⁴N, ¹⁵N) as external standards and coupling constants are given in Hertz (Hz). Infrared (IR) spectra were recorded on a PerkinElmer BX FT IR spectrometer equipped with a Smiths DuraSamplIR II diamond ATR unit. Transmittance values are qualitatively described as “very strong” (vs), “strong” (s), “medium” (m), “weak” (w) and “very weak” (vw). Raman spectra were recorded on a Bruker RAM II spectrometer equipped with a Nd:YAG laser (200 mW) operating at 1064 nm and a reflection angle of 180°. The intensities are reported as percentages of the most intense peak and are given in parentheses. Low resolution mass spectra were recorded on a JEOL MStation JMS-700 with 4-nitrobenzyl alcohol as matrix for FAB measurements. Elemental analyses (CHN) were performed with an Elementar Vario EL. Melting and decomposition points were determined by differential scanning calorimetry (Linseis DSC-PT10, calibrated with standard pure indium and zinc). Measurements were performed at a heating rate of 5 °C min⁻¹ in closed aluminum sample pans with a 0.1 mm hole in the lid for gas release to avoid an unsafe increase in pressure under a nitrogen flow of 20 mL min⁻¹ with an empty identical aluminum sample pan as a reference. Melting points were checked with a Büchi Melting Point B-540 in open glass capillaries.

For initial safety testing, the impact and friction sensitivities as well as the electrostatic sensitivities were determined. The impact sensitivity tests were carried out according to STANAG 4489,^[25] modified according to WIWeB instruction 4-5.1.02^[26] using a BAM^[27] drop hammer. The friction sensitivity tests were carried out according to STANAG 4487^[28] and modified according to WIWeB instruction 4-5.1.03^[29] using the

BAM friction tester. The electrostatic sensitivity tests were accomplished according to STANAG 4490^[30] using an electric spark testing device ESD 2010 EN (OZM Research).

Crystallographic measurements. The single-crystal X-ray diffraction data of **5–8** were collected using an Oxford Xcalibur3 diffractometer equipped with a Spellman generator (voltage 50 kV, current 40 mA), Enhance molybdenum K_α radiation source ($\lambda = 71.073$ pm), Oxford Cryosystems Cryostream cooling unit, four circle kappa platform and a Sapphire CCD detector. Data collection and reduction were performed with CrysAlisPro.^[31] The structures were solved with SIR97,^[32] refined with SHELXL-97,^[33] and checked with PLATON,^[34] all integrated into the WinGX software suite.^[35] The finalized CIF files were checked with checkCIF.^[36] Intra- and intermolecular contacts were analyzed with Mercury.^[37] CCDC 926336 (**5**), 926337 (**6**), 926338 (**7**, 173 K), 926339 (**7**, 298 K) and 926340 (**8**) contain the supplementary crystallographic data for this paper. These data can be obtained free of charge from the Cambridge Crystallographic Data Centre via www.ccdc.cam.ac.uk/data_request/cif.

5-Amino-1*H*-1,2,4-triazole-3-carbonitrile (**1**),^[8] 5-azido-1*H*-1,2,4-triazole-3-carbonitrile (**4**) and 5-azido-1*H*-1,2,4-triazole-3-chloroxime (**4a**) were prepared according to the literature.^[17]

5-Nitramino-1*H*-1,2,4-triazole-3-carbonitrile (2): Nitric acid (100 %, 3.3 mL) was added slowly to a solution of 5-amino-1*H*-1,2,4-triazole-3-carbonitrile (**1**, 2.2 g, 20 mmol) in concentrated sulfuric acid (20 mL) at 0 °C. The mixture was stirred at 0 °C for one hour, poured on ice (250 g) and extracted with ethyl acetate (3 × 100 mL). The combined organic phases were dried over magnesium sulfate and the solvent was removed in vacuum to yield a colorless powder (2.7 g, 18 mmol, 87 %). **¹H nmr** (DMSO-*d*₆): $\delta = 14.40$ (s, H_{triazole}) ppm. **¹³C nmr** (DMSO-*d*₆): $\delta = 151.1$ (C–NNO₂), 135.7 (C–CN), 112.9 (CN) ppm. **¹⁴N nmr** (DMSO-*d*₆): $\delta = -32$ (NNO₂) ppm. **IR:** ν (rel. int.) = 3137(w), 2797(w), 2265(vw), 1716(w), 1614(m), 1569(m), 1516(m), 1468(w), 1354(w), 1323(s), 1263(vs), 1185(w), 1144(m), 1099(s), 1032(w), 1015(w), 1005(m), 868(m), 864(m), 838(w), 769(m), 758(m), 733(vs), 733(vs), 721(s), 679(s) cm⁻¹. **Raman** (200 mW): ν (rel. int.) = 2266(43), 1722(1), 1641(2), 1565(20), 1535(9), 1473(15), 1367(6), 1324(4), 1268(4), 1147(4), 1116(2), 1094(2), 1041(12), 1017(3), 1005(6), 847(1), 758(2), 684(1), 625(2), 567(1), 487(6), 432(4), 362(3), 362(3), 220(3) cm⁻¹.

Elemental analysis ($\text{C}_3\text{H}_2\text{N}_6\text{O}_2$): calc.: C 23.38, H 1.31, N 54.54 %; found: C 23.17, H 1.49, N 51.78 %. **Mass spectrometry**: m/z (DEI+) = 154.1 ($[\text{C}_3\text{H}_2\text{N}_6\text{O}_2]^+$). **Sensitivities** (grain size < 100 μm): friction: 360 N; impact: 6 J; ESD: 0.2 J. **DSC** (5 $^\circ\text{C min}^{-1}$): $T_{\text{dec.}}$ = 130 $^\circ\text{C}$.

5-Nitramino-1H-1,2,4-triazole-3-chloroxime (2a): Hydroxylamine (50 wt% in water, 1.2 eq., 1.4 mL) was added to a solution of **2** (2.7 g, 18 mmol) in water (30 mL). The clear solution was stirred at 70 $^\circ\text{C}$ for 30 minutes. The mixture was acidified with hydrochloric acid (37 %, 30 mL) and cooled to 0 $^\circ\text{C}$. A solution of sodium nitrite (1.5 eq., 1.9 g, 27 mmol) in water (15 mL) was added dropwise and the solution was subsequently stirred for two hours at room temperature. The precipitate was collected by filtration, washed with cold water and dried in air to yield a pale yellow powder (3.1 g, 15 mmol, 83 %). **^1H nmr** ($\text{DMSO-}d_6$): δ = 14.44 (s, 1H, $\text{H}_{\text{triazole}}$), 13.31 (s, 1H, NHNO_2), 6.16 (s, 1H, NOH) ppm. **^{13}C nmr** ($\text{DMSO-}d_6$): δ = 153.5 (C– NNO_2), 144.5 (C– CNOHCl), 125.4 (CNOHCl) ppm. **^{14}N nmr** ($\text{DMSO-}d_6$): δ = –19 (NNO_2) ppm. **IR**: ν (rel. int.) = 3430(w), 3336(w), 2987(w), 2836(w), 2604(w), 1616(m), 1585(m), 1547(m), 1503(w), 1451(w), 1420(w), 1289(s), 1220(vs), 1131(m), 1089(w), 1049(w), 1024(m), 1015(m), 998(s), 925(s), 853(m), 777(m), 759(w), 759(w), 745(w), 729(m), 669(m) cm^{-1} . **Raman** (200 mW): ν (rel. int.) = 1614(47), 1586(48), 1557(100), 1507(9), 1463(3), 1297(5), 1219(8), 1137(11), 1118(6), 1057(4), 993(37), 922(3), 875(4), 857(11), 759(25), 673(6), 518(3), 489(3), 430(2), 407(2), 318(4), 246(5), 226(5), 226(5), 219(5) cm^{-1} . **Mass spectrometry**: m/z (FAB–) = 205.2 ($[\text{C}_3\text{H}_2\text{N}_6\text{O}_3\text{Cl}]^-$). **Sensitivities** (grain size < 100 μm): friction: 240 N; impact: 5 J. **DSC** (5 $^\circ\text{C min}^{-1}$): $T_{\text{dec.}}$ = 126 $^\circ\text{C}$.

5-Nitramino-1H-1,2,4-triazole-3-azidoxime (2b): A solution of sodium azide (1.3 g, 20 mmol) in water (8 mL) was added dropwise to a solution of **2a** (3.1 g, 15 mmol) in ethanol (100 mL). The suspension was stirred at room temperature for 12 hours and subsequently poured on 2 M HCl (400 mL). The clear solution was extracted with ethyl acetate (3 \times 100 mL), the combined organic phases were dried over magnesium sulfate and the solvent was removed in vacuum to yield a colorless powder (3.0 g, 14 mmol, 93 %). **^1H nmr** ($\text{DMSO-}d_6$): δ = 14.23 (s, 1H, $\text{H}_{\text{triazole}}$), 12.46 (s, 1H, NHNO_2), 10.00 (s, 1H, NOH) ppm. **^{13}C nmr** ($\text{DMSO-}d_6$): δ = 153.6 (C– NNO_2), 143.3 (C– CNOHN_3), 133.6 (CNOHN_3) ppm. **^{14}N nmr** ($\text{DMSO-}d_6$): δ = –18 (NO_2), –147 (N_3) ppm. **IR**: ν (rel. int.) =

3426(w), 3199(w), 2153(m), 2102(w), 1695(w), 1621(m), 1595(m), 1557(s), 1512(m), 1462(m), 1388(w), 1305(s), 1266(m), 1253(m), 1218(vs), 1131(m), 1094(w), 1044(m), 1007(s), 996(s), 987(m), 940(w), 924(m), 924(m), 862(m), 773(w), 730(w), 688(w), 667(w) cm^{-1} . **Raman** (200 mW): ν (rel. int.) = 2263(3), 2157(4), 2107(2), 1622(59), 1600(16), 1559(100), 1514(9), 1473(5), 1308(7), 1222(5), 1134(8), 1076(6), 1058(3), 1052(2), 998(13), 985(18), 943(2), 864(12), 761(15), 520(2), 486(3), 419(3), 332(4), 332(4), 280(4), 236(6) cm^{-1} . **Mass spectrometry**: m/z (FAB $^-$) = 212.1 ($[\text{C}_3\text{H}_2\text{N}_9\text{O}_3]^-$). **Sensitivities** (grain size < 100 μm): friction: 80 N; impact: 4 J; ESD: 0.13 J. **DSC** (5 $^\circ\text{C min}^{-1}$): $T_{\text{dec.}}$ = 66 $^\circ\text{C}$.

5-(5-Nitrimino-1,4H-1,2,4-triazol-3-yl)tetrazol-1-ol (NATTO, 5): A solution of **2b** (3.0 g, 14 mmol) in concentrated hydrochloric acid (50 mL) was stirred at room temperature for 10 hours. The clear solution was poured on ice and extracted with ethyl acetate (3 \times 100 mL), the combined organic phases were dried over magnesium sulfate and the solvent was removed in vacuum to yield a colorless solid (2.8 g, 13 mmol, 94 %). **^1H nmr** (DMSO- d_6): δ = 7.10 (s, $\text{H}_{\text{triazole}}$) ppm. **^{13}C nmr** (DMSO- d_6): δ = 152.5 (C-NNO_2), 140.5 ($\text{C}_{\text{triazole}}$), 138.7 ($\text{C}_{\text{tetrazole}}$) ppm. **^{14}N nmr** (DMSO- d_6): δ = -25 (NNO_2) ppm. **IR**: ν (rel. int.) = 3607(w), 3398(w), 3186(w), 1650(w), 1605(m), 1583(m), 1550(w), 1519(m), 1469(m), 1407(w), 1317(s), 1243(vs), 1202(s), 1138(w), 1089(w), 1061(w), 999(w), 958(m), 923(w), 868(w), 799(w), 774(m), 717(m), 717(m), 684(m) cm^{-1} . **Raman** (200 mW): ν (rel. int.) = 1648(100), 1596(48), 1579(47), 1532(11), 1521(12), 1481(3), 1420(2), 1336(2), 1267(7), 1154(4), 1129(15), 1115(16), 1012(28), 973(4), 877(5), 775(2), 762(7), 746(4), 738(7), 499(2), 446(2), 423(3), 292(2), 292(2), 257(8) cm^{-1} . **Elemental analysis** ($\text{C}_3\text{H}_3\text{N}_9\text{O}_3$): calc.: C 16.91, H 1.42, N 59.15 %; found: C 17.32, H 1.59, N 56.77 %. **Mass spectrometry**: m/z (FAB $^-$) = 212.2 ($[\text{C}_3\text{H}_2\text{N}_9\text{O}_3]^-$). **Sensitivities** (grain size: < 100 μm): friction: 60 N; impact: < 1 J; ESD: 0.13 J. **DSC** (5 $^\circ\text{C min}^{-1}$): $T_{\text{dec.}}$ = 116 $^\circ\text{C}$.

3-Nitro-1H-1,2,4-triazole-5-carbonitrile (3): A solution of 5-amino-1H-1,2,4-triazole-3-carbonitrile (**1**, 2.2 g, 20 mmol) in 20 % sulfuric acid (40 mL) was added dropwise to a solution of sodium nitrite (10 eq., 14 g, 22 mmol) in water (40 mL) at 0 $^\circ\text{C}$. The mixture was subsequently stirred at 40 $^\circ\text{C}$ for 30 minutes. After cooling down to room temperature the mixture was acidified with sulfuric acid (20 %) until no evolution of

nitrogen dioxide could be observed. The aqueous solution was extracted with ethyl acetate (3 × 50 mL), the combined organic phases were dried over magnesium sulfate and the solvent was removed in vacuum to yield an orange solid (2.6 g, 18 mmol, 92 %). **¹H nmr** (DMSO-*d*₆): δ = 15.56 (s, 1H, H_{triazole}) ppm. **¹³C nmr** (DMSO-*d*₆): δ = 161.3 (C–NO₂), 135.2 (C–CN), 111.6 (CN) ppm. **¹⁴N nmr** (DMSO-*d*₆): δ = –29 (NO₂) ppm. **IR**: ν (rel. int.) = 3141(w), 2263(vw), 1692(w), 1561(vs), 1530(m), 1484(w), 1427(s), 1374(m), 1314(vs), 1258(w), 1176(w), 1048(m), 1013(m), 838(vs), 708(m) cm^{–1}. **Raman** (200 mW): ν (rel. int.) = 2266(100), 2212(1), 1577(5), 1566(5), 1527(3), 1486(3), 1451(81), 1419(13), 1380(19), 1319(13), 1188(14), 1059(15), 1017(4), 841(4), 775(3), 712(5), 639(1), 569(1), 504(3), 472(7), 406(5), 264(3), 255(4), 255(4) cm^{–1}. **Elemental analysis** (C₃HN₅O₂): calc.: C 25.91, H 0.72, N 50.36 %; found: C 26.40, H 0.88, N 49.86 %. **Mass spectrometry**: m/z (DEI+) = 139.0 ([C₃HN₅O₂]⁺). **Sensitivities** (grain size < 100 μ m): friction: 360 N; impact: 40 J. **DSC** (5 °C min^{–1}): $T_{\text{dec.}}$ = 196 °C.

3-Nitro-1H-1,2,4-triazole-5-chloroxime (3a): Hydroxylamine (50 wt% in water, 1.2 eq., 1.4 mL) was added to a solution of **3** (2.6 g, 18 mmol) in water (20 mL). The clear solution was stirred at 70 °C for 30 minutes. The mixture was acidified with hydrochloric acid (37 %, 20 mL) and cooled to 0 °C. A solution of sodium nitrite (1.5 eq., 1.9 g, 27 mmol) in water (10 mL) was added dropwise and the solution was subsequently stirred for two hours at room temperature. The precipitate was collected by filtration, washed with cold water and dried in air to yield a pale yellow powder (2.8 g, 15 mmol, 82 %). **¹H nmr** (DMSO-*d*₆): δ = 13.39 (s, 1H, H_{triazole}), 6.04 (s, 1H, NOH) ppm. **¹³C nmr** (DMSO-*d*₆): δ = 162.3 (C–NO₂), 149.9 (C–CNOHCl), 125.3 (CNOHCl) ppm. **¹⁴N nmr** (DMSO-*d*₆): δ = –27 (NO₂) ppm. **IR**: ν (rel. int.) = 3575(w), 3358(w), 3215(w), 2454(w), 1845(w), 1578(w), 1555(m), 1482(s), 1400(m), 1336(w), 1322(m), 1178(w), 1100(s), 1040(m), 1023(vs), 920(s), 844(m), 751(m), 728(m), 662(w) cm^{–1}. **Raman** (200 mW): ν (rel. int.) = 1609(76), 1587(26), 1556(22), 1506(14), 1485(100), 1468(55), 1425(46), 1403(28), 1339(15), 1324(27), 1179(24), 1104(3), 1041(35), 1025(14), 924(12), 848(8), 775(6), 731(7), 662(12), 580(5), 544(8), 455(14), 373(5), 373(5), 349(10), 270(7), 251(12), 225(28) cm^{–1}. **Mass spectrometry**: m/z (DEI+) = 191.1 ([C₃H₂N₅O₃Cl]⁺). **Sensitivities** (grain size < 100 μ m): friction: 360 N; impact: 40 J; ESD: 0.2 J. **DSC** (5 °C min^{–1}): $T_{\text{dec.}}$ = 195 °C.

3-Nitro-1H-1,2,4-triazole-5-azidoxime (3b): A solution of sodium azide (1.3 g, 20 mmol) in water (8 mL) was added dropwise to a solution of **3a** (2.8 g, 15 mmol) in ethanol (50 mL). The suspension was stirred at room temperature for two hours and subsequently poured on 2 M HCl (200 mL). The clear solution was extracted with ethyl acetate (3 × 80 mL), the combined organic layers were dried over magnesium sulfate and the solvent was removed in vacuum to yield a colorless powder (2.8 g, 14 mmol, 93 %). **¹H nmr** (DMSO-*d*₆): δ = 12.61 (s, H_{triazole}) ppm. **¹³C nmr** (DMSO-*d*₆): δ = 162.5 (C–NO₂), 148.7 (C–CNOHN₃), 133.4 (CNOHN₃) ppm. **¹⁴N nmr** (DMSO-*d*₆): δ = –26 (NO₂), –146 (N₃) ppm. **IR:** ν (rel. int.) = 3391(w), 3192(w), 2568(w), 2488(w), 2162(m), 2115(m), 1886(w), 1684(m), 1620(m), 1587(w), 1556(s), 1478(m), 1401(m), 1378(m), 1339(m), 1317(m), 1292(s), 1275(s), 1178(m), 1120(s), 1038(m), 1013(m), 938(vs), 938(vs), 861(m), 834(m), 777(w), 749(w), 733(m) cm^{–1}. **Raman** (200 mW): ν (rel. int.) = 2988(8), 2977(7), 2946(18), 2170(9), 2122(7), 1689(7), 1623(84), 1591(33), 1567(25), 1514(8), 1489(99), 1415(31), 1320(23), 1280(16), 1185(17), 1116(5), 1040(23), 1008(14), 943(13), 864(8), 852(5), 841(7), 777(4), 777(4), 739(5), 637(4), 458(12), 383(5), 369(9), 361(9), 293(18), 253(10), 207(3) cm^{–1}. **Mass spectrometry:** *m/z* (DEI+) = 198.1 ([C₃H₂N₈O₃]⁺). **Sensitivities** (grain size < 100 μ m): friction: 240 N; impact: 20 J. **DSC** (5 °C min^{–1}): *T*_{dec.} = 124 °C.

5-(3-Nitro-1,2,4-1H-triazol-5-yl)tetrazol-1-ol (NTTO, 6): A solution of **3b** (2.8 g, 14 mmol) in concentrated hydrochloric acid (50 mL) was stirred at room temperature for 10 hours. The clear solution was poured on ice and extracted with ethyl acetate (3 × 100 mL). The combined organic layers were dried over magnesium sulfate and the solvent was removed in vacuum to yield a colorless solid (2.6 g, 13 mmol, 94 %). **¹H nmr** (DMSO-*d*₆): δ = 14.15 (s, 1H, H_{triazole}), 8.30 (s, 1H, OH) ppm. **¹³C nmr** (DMSO-*d*₆): δ = 163.2 (C–NO₂), 143.3 (C_{triazole}), 138.0 (C_{tetrazole}) ppm. **¹⁴N nmr** (DMSO-*d*₆): δ = –24 (NO₂) ppm. **¹⁵N nmr** (DMSO-*d*₆): δ = –4.2 (N6), –17.2 (N5), –28.5 (N8), –54.8 (N7), –91.2 (N2), –112.8 (N4), –139.9 (N3), –157.7 (N1) ppm. **IR:** ν (rel. int.) = 3585(w), 3144(w), 2916(w), 2848(w), 2608(w), 1908(vw), 1691(m), 1620(w), 1555(s), 1520(m), 1472(m), 1411(s), 1309(vs), 1239(m), 1188(m), 1092(w), 1028(w), 1011(w), 983(s), 931(m), 836(s), 737(w), 709(w), 709(w), 666(w) cm^{–1}. **Raman** (200 mW): ν (rel. int.) = 1674(41), 1622(100), 1610(92), 1556(19), 1521(33), 1513(38), 1488(29), 1477(29), 1442(61), 1414(76), 1359(27), 1338(10), 1312(15), 1292(8), 1277(12),

1246(44), 1202(23), 1191(59), 1161(5), 1147(21), 1098(38), 1031(12), 1015(34), 1015(34), 984(8), 847(4), 773(7), 747(20), 739(18), 563(5), 503(3), 398(12), 337(6), 303(5), 247(4), 230(6), 216(4) cm^{-1} . **Elemental analysis** ($\text{C}_3\text{H}_2\text{N}_8\text{O}_3 \times \text{H}_2\text{O}$): calc.: C 16.67, H 1.87, N 51.58 %; found: C 19.47, H 1.87, N 50.13 %. **Mass spectrometry**: m/z (FAB $^-$) = 197.3 ($[\text{C}_3\text{HN}_8\text{O}_3]^-$). **Sensitivities** (anhydrous, grain size < 100 μm): friction: 360 N; impact: 35 J; ESD: 0.13 J. **DSC** (5 $^\circ\text{C min}^{-1}$): $T_{\text{dec.}}$ = 152 $^\circ\text{C}$.

5-(5-Azido-1H-1,2,4-triazol-3-yl)tetrazol-1-ol (AzTTO, 7): Sodium azide (1.95 g, 30.0 mmol) was dissolved in water (27 mL) and added to a solution of **4b** (3.75 g, 20.0 mmol) in ethanol (33 mL) at 0 $^\circ\text{C}$. The solution was stirred for 15 minutes at that temperature, then for two hours at room temperature. The suspension was acidified with hydrochloric acid (2 m, 20 mL), stirred for 30 minutes, extracted with diethyl ether (5 \times 300 mL) and the combined organic phases were dried over magnesium sulfate. Hydrogen chloride gas was passed into the stirred solution at 0 $^\circ\text{C}$ for 75 minutes, whereby the temperature rose up to 19 $^\circ\text{C}$ (it should not rise higher!). The flask was stoppered and the resulting solution was stirred for two days at room temperature under a hydrogen chloride overpressure. After evaporation of the solvent to almost complete dryness water was added and completely evaporated at ambient conditions to yield a colorless solid (3.71 g, 17.5 mmol, 80 %). **^1H nmr** (DMSO- d_6): δ = 9.51 (br). **^{13}C nmr** (DMSO- d_6): δ = 155.2 ($\text{C}_{\text{triazole}}$), 144.6 (C-N_3), 139.7 ($\text{C}_{\text{tetrazole}}$). **^{14}N nmr** (DMSO- d_6): δ = -136 (N9). **^{15}N nmr** (DMSO- d_6): δ = -4.1 (N6), -18.1 (N5), -55.3 (N7), -117.8 (N4), -144.0 (N10), -145.6 (N9), -150.8 (N3), -295.3 (N8). **IR**: ν (rel. int.) = 3233(s), 2477(w), 2375(w), 2232(w), 2154(vs), 1604(m), 1535(vs), 1479(s), 1336(s), 1296(m), 1275(m), 1223(m), 1190(m), 1152(w), 1129(m), 1071(w), 1046(w), 1014(w), 982(m), 855(w), 781(m), 753(w), 712(w), 696(w), 658(w) cm^{-1} . **Raman** (200 mW): ν (rel. int.) = 2154(8), 1605(100), 1537(20), 1485(10), 1422(8), 1397(4), 1336(12), 1276(17), 1191(2), 1130(5), 1062(2), 1045(6), 1015(5), 980(7), 805(3), 757(3) cm^{-1} . **Mass spectrometry**: m/z (FAB $^-$) = 193.3 ($[\text{C}_3\text{HN}_{10}\text{O}]^-$). **Elemental analysis** ($\text{C}_3\text{H}_4\text{N}_{10}\text{O}_2$): calc.: C 16.99, H 1.90, N 66.03 %; found C 17.53, H 1.87, N 65.16 %. **Sensitivities** (anhydrous, grain size < 100 μm): friction: 120 N; impact: 4 J; ESD: > 260 mJ. **DSC** (5 $^\circ\text{C min}^{-1}$): $T_{\text{melt.}}$ = 83 $^\circ\text{C}$, $T_{\text{dec.}}$ = 144 $^\circ\text{C}$.

REFERENCES

- [1] a) T. M. Klapötke, *Chemistry of High-Energy Materials*, 2nd edition, Walter de Gruyter, Berlin, **2012**; b) K.-Y. Lee, L. B. Chapman, M. D. Coburn, *J. Energ. Mater.* **1987**, *5*, 27–33; c) K.-Y. Lee, C. B. Storm, M. A. Hiskey, M. D. Coburn, *J. Energ. Mater.* **1991**, *9*, 415–428; d) M. A. Hiskey, N. Goldman, J. R. Stine, *J. Energ. Mater.* **1998**, *16*, 119–127; e) P. F. Pagoria, G. S. Lee, A. R. Mitchell, R. D. Schmidt, *Thermochimica Acta* **2002**, *384*, 187–204; f) R. P. Singh, R. D. Verma, D. T. Meshri, J. Shreeve, *Angew. Chem. Int. Ed.* **2006**, *45*, 3584–3601; g) M. B. Talawar, R. Sivabalan, T. Mukundan, H. Muthurajan, A. K. Sikder, B. R. Gandhe, A. S. Rao, *J. Hazard. Mater.* **2009**, *161*, 589–607; h) K. Wang, D. A. Parrish, J. M. Shreeve, *Chem. Eur. J.* **2011**, *17*, 14485–14492; i) J. W. Fronabarger, M. D. Williams, W. B. Sanborn, D. A. Parrish, M. Bichay, *Propellants Explos. Pyrotech.* **2011**, *36*, 459–470; j) D. E. Chavez, D. A. Parrish, *Propellants Explos. Pyrotech.* **2012**, *37*, 536–539; k) L. Liang, H. Huang, K. Wang, C. Bian, J. Song, L. Ling, F. Zhao, Z. Zhou, *J. Mater. Chem.* **2012**, *22*, 21954–21964; l) Y. Zhang, D. A. Parrish, J. M. Shreeve, *J. Mater. Chem. A* **2013**, *1*, 585–593.
- [2] a) T. M. Klapötke, J. Stierstorfer, A. U. Wallek, *Chemistry of Materials* **2008**, *20*, 4519–4530; b) T. M. Klapötke, C. M. Sabaté, *Chemistry of Materials* **2008**, *20*, 3629–3637; c) D. E. Chavez, M. A. Hiskey, D. L. Naud, *Propellants Explos. Pyrotech.* **2004**, *29*, 209–215; d) Y. Huang, H. Gao, B. Twamley, J. M. Shreeve, *Eur. J. Inorg. Chem.* **2008**, 2560–2568; e) H. Gao, J. M. Shreeve, *Chem. Rev.* **2011**, *111*, 7377–7436.
- [3] T. M. Klapötke, in *Structure and bonding* (Ed.: D. M. P. Mingos), Springer, Berlin - Heidelberg, **2007**.
- [4] M. H. V. Huynh, M. A. Hiskey, T. J. Meyer, M. Wetzler, *Proceedings of the National Academy of Sciences* **2006**, *103*, 5409–5412.
- [5] a) T. M. Klapötke, J. Stierstorfer, *Helvetica Chimica Acta* **2007**, *90*, 2132–2150; b) T. M. Klapötke, C. M. Sabaté, J. Stierstorfer, *New Journal of Chemistry* **2009**, *33*, 136–147; c) A. Dippold, T. M. Klapötke, F. A. Martin, *Z. Anorg. Allg. Chem.* **2011**, *637*, 1181–1193.
- [6] a) N. Fischer, D. Izsák, T. M. Klapötke, S. Rappenglück, J. Stierstorfer, *Chem. Eur. J.* **2012**, *18*, 4051–4062; b) N. Fischer, T. M. Klapötke, K. Peters, M. Rusan,

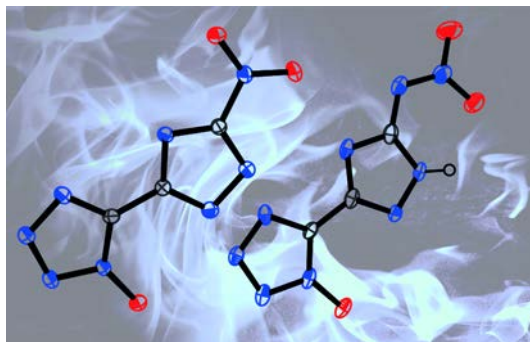
- J. Stierstorfer, *Z. Anorg. Allg. Chem.* **2011**, 637, 1693–1701; c) Y. Guo, G.-H. Tao, Z. Zeng, H. Gao, D. A. Parrish, J. M. Shreeve, *Chem. Eur. J.* **2010**, 16, 3753–3762; d) E. Oliveri-Mandala, T. Passalacqua, *Gazz. Chim. Ital.* **1914**, 43, 465–475; e) D. E. Chavez, M. A. Hiskey, D. L. Naud, *J. Pyrotech.* **1999**, 17–36.
- [7] a) E. L. Metelkina, T. A. Novikova, S. N. Berdonosova, D. Y. Berdonosov, V. S. Grineva, *Russ. J. Org. Chem.* **2004**, 40, 1412–1414; b) E. L. Metelkina, T. A. Novikova, S. N. Berdonosova, D. Y. Berdonosov, *Russ. J. Org. Chem.* **2005**, 41, 440–443; c) E. Metelkina, T. Novikova, *Russ. J. Org. Chem.* **2004**, 40, 1737–1743; d) A. M. Astachov, V. A. Revenko, L. A. Kruglyakova, E. S. Buka, in *New Trends in Research of Energetic Materials, Proceedings of the 10th Seminar, Pardubice, Czech Republic, Apr. 25–27, 2007*, 505–511; e) A. M. Astachov, V. A. Revenko, E. S. Buka, in *New Trends in Research of Energetic Materials, Proceedings of the 12th Seminar, Pardubice, Czech Republic, Apr. 1–3, 2009*, 396–404; f) R. Wang, H. Xu, Y. Guo, R. Sa, J. M. Shreeve, *J. Am. Chem. Soc.* **2010**, 132, 11904–11905; g) Y. V. Serov, M. S. Pevzner, T. P. Kofman, I. V. Tselinskii, *Russ. J. Org. Chem.* **1990**, 26, 773–777; h) L. I. Bagal, M. S. Pevzner, A. N. Frolov, N. I. Sheludyakova, *Chem. Heterocyc. Comp.* **1970**, 6, 240–244; i) A. A. Dippold, T. M. Klapötke, N. Winter, *Eur. J. Inorg. Chem.* **2012**, 3474–3484.
- [8] A. A. Dippold, T. M. Klapötke, *Chem. Asian J.* **2013**, in press, DOI: 10.1002/asia.201300063.
- [9] a) M. S. Molchanovaa, T. S. Pivinaa, E. A. Arnautovab, N. S. Zefirovb, *J. Mol. Struct. THEOCHEM* **1999**, 465, 11–24; b) M. Göbel, K. Karaghiosoff, T. M. Klapötke, D. G. Piercey, J. Stierstorfer, *J. Am. Chem. Soc.* **2010**, 132, 17216–17226.
- [10] D. Rong, V. A. Phillips, R. S. Rubio, M. A. Castro, R. T. Wheelhouse, *Tetrahedron Lett.* **2008**, 49, 6933–6935.
- [11] T. M. Klapötke, D. G. Piercey, J. Stierstorfer, *Chem. Eur. J.* **2011**, 17, 13068–13077.
- [12] T. Harel, S. Rozen, *J. Org. Chem.* **2010**, 75, 3141–3143.
- [13] a) I. V. Tselinskii, S. F. Mel'nikova, T. V. Romanova, *Russ. J. Org. Chem.* **2001**, 37, 430–436; b) I. V. Tselinskii, S. F. Mel'nikova, T. V. Romanova, *Russ. J. Org. Chem.* **2001**, 37, 1638–1642; c) N. Fischer, D. Fischer, T. M. Klapötke, D. G.

- Piercey, J. Stierstorfer, *J. Mater. Chem.* **2012**, 22, 20418–20422; d) D. Fischer, T. M. Klapötke, D. G. Piercey, J. Stierstorfer, *Chem. Eur. J.* **2013**, 19, 4602–4613.
- [14] a) D. E. Chavez, B. C. Tappan, B. A. Mason, D. Parrish, *Propellants Explos. Pyrotech.* **2009**, 34, 475–479; b) D. L. Naud, M. A. Hiskey, H. H. Harry, *J. Energ. Mater.* **2003**, 21, 57–62; c) T. P. Kofman, *Russ. J. Org. Chem.* **2002**, 38, 1231–1243; d) E. V. Nikitina, G. L. Starova, O. V. Frank-Kamenetskaya, M. S. Pevzner, *Kristallografiya* **1982**, 27, 485–488; e) A. A. Dippold, T. M. Klapötke, *Chem. Eur. J.* **2012**, 18, 16742–16753.
- [15] a) A. F. Hollemann, E. Wiberg, N. Wiberg, *Lehrbuch der anorganischen Chemie*, de Gruyter, New York, **2007**; b) F. H. Allen, O. Kennard, D. G. Watson, L. Brammer, A. G. Orpen, R. Taylor, *J. Chem. Soc. Perkin Trans. 2* **1987**, S1–S19.
- [16] A. A. Dippold, T. M. Klapötke, F. A. Martin, S. Wiedbrauk, *Eur. J. Inorg. Chem.* **2012**, 2429–2443.
- [17] D. Izsák, T. M. Klapötke, S. Reuter, T. Rösener, *Z. Anorg. Allg. Chem.* **2013**, 639, 899–905.
- [18] M. J. Frisch, G. W. Trucks, H. B. Schlegel, G. E. Scuseria, M. A. Robb, J. R. Cheeseman, G. Scalmani, V. Barone, B. Mennucci, G. A. Petersson, H. Nakatsuji, M. Caricato, X. Li, H. P. Hratchian, A. F. Izmaylov, J. Bloino, G. Zheng, J. L. Sonnenberg, M. Hada, M. Ehara, K. Toyota, R. Fukuda, J. Hasegawa, M. Ishida, T. Nakajima, Y. Honda, O. Kitao, H. Nakai, T. Vreven, J. A. Montgomery, Jr., J. E. Peralta, F. Ogliaro, M. Bearpark, J. J. Heyd, E. Brothers, K. N. Kudin, V. N. Staroverov, T. Keith, R. Kobayashi, J. Normand, K. Raghavachari, A. Rendell, J. C. Burant, S. S. Iyengar, J. Tomasi, M. Cossi, N. Rega, J. M. Millam, M. Klene, J. E. Knox, J. B. Cross, V. Bakken, C. Adamo, J. Jaramillo, R. Gomperts, R. E. Stratmann, O. Yazyev, A. J. Austin, R. Cammi, C. Pomelli, J. W. Ochterski, R. L. Martin, K. Morokuma, V. G. Zakrzewski, G. A. Voth, P. Salvador, J. J. Dannenberg, S. Dapprich, A. D. Daniels, O. Farkas, J. B. Foresman, J. V. Ortiz, J. Cioslowski, and D. J. Fox, *Gaussian 09 Revision C.01*, Gaussian, Inc., Wallingford, CT, USA, **2010**.
- [19] N. Fischer, T. M. Klapötke, M. Reymann, J. Stierstorfer, *Eur. J. Inorg. Chem.* **2013**, 2167–2180.
- [20] M. Sućeska, *EXPLO5 5.05*, Zagreb, Croatia, **2011**.
- [21] M. Göbel, K. Karaghiosoff, T. M. Klapötke, D. G. Piercey, J. Stierstorfer, *J. Am. Chem. Soc.* **2010**, 132, 17216–17226.

- [22] N. Fischer, L. Gao, T. M. Klapötke, J. Stierstorfer, *Polyhedron* **2013**, *51*, 201–210.
- [23] Impact: insensitive > 40 J, less sensitive ≥ 35 J, sensitive ≥ 4 J, very sensitive ≤ 3 J; Friction: insensitive > 360 N, less sensitive = 360 N, sensitive < 360 N and > 80 N, very sensitive ≤ 80 N, extremely sensitive ≤ 10 N; According to: *Recommendations on the Transport of Dangerous Goods, Manual of Tests and Criteria*, 4th edition, United Nations, New York - Geneva, **1999**.
- [24] J. Köhler, R. Meyer, A. Homburg, *Explosivstoffe*, 10. Auflage, Wiley-VCH, Weinheim, **2008**.
- [25] *NATO Standardization Agreement 4489*, September 17, **1999**.
- [26] *WIWeB-Standardarbeitsanweisung 4-5.1.02*, November 8, **2002**.
- [27] Bundesanstalt für Materialforschung und -prüfung, www.bam.de.
- [28] *NATO Standardization Agreement 4487*, August 22, **2002**.
- [29] *WIWeB-Standardarbeitsanweisung 4-5.1.03*, November 8, **2002**.
- [30] *NATO Standardization Agreement 4490*, February 19, **2001**.
- [31] *CrysAlisPro 1.171.36.24*, Agilent Technologies, Santa Clara, CA, USA, **2012**.
- [32] A. Altomare, M. C. Burla, M. Camalli, G. L. Cascarano, C. Giacovazzo, A. Guagliardi, A. G. G. Moliterni, G. Polidori, R. Spagna, *J. Appl. Cryst.* **1999**, *32*, 115–119.
- [33] G. M. Sheldrick, *Acta Cryst.* **2008**, *A64*, 112–122.
- [34] L. Spek, *PLATON*, Utrecht University, Utrecht, Netherlands, **2012**.
- [35] L. J. Farrugia, *J. Appl. Cryst.* **1999**, *32*, 837–838.
- [36] <http://journals.iucr.org/services/cif/checkcif.html>
- [37] C. F. Macrae, P. R. Edgington, P. McCabe, E. Pidcock, G. P. Shields, R. Taylor, M. Towler, J. van de Streek, *J. Appl. Crystallogr.* **2006**, *39*, 453–457.

11. A COMPARATIVE STUDY ON INSENSITIVE ENERGETIC DERIVATIVES OF 5-(1,2,4-TRIAZOL-C-YL)-TETRAZOLES AND THEIR 1-HYDROXY-TETRAZOLE ANALOGUES

As published in: Zeitschrift für Anorganische und Allgemeine Chemie 2013, in press.



ABSTRACT:

In this contribution, the synthesis and characterization of selected nitrogen-rich salts based on 5-(1,2,4-Triazol-C-yl)tetrazoles and their 1-hydroxy-tetrazole analogues is presented. The combination with guanidinium, triaminoguanidinium and hydroxylammonium cations leads to enhanced performance and sensitivities. The main focus of this work is on the energetic properties of those ionic derivatives in comparison to the neutral compounds. Additionally, the positive influence of the introduction of *N*-oxides in energetic materials is shown. Structural characterization was accomplished by means of Raman, IR and multinuclear NMR spectroscopy. The standard enthalpies of formation were calculated for selected compounds at the CBS-4M level of theory, the detonation parameters were calculated using the EXPLO5.05 program. Additionally, thermal stability was measured via DSC and sensitivities against impact, friction and electrostatic discharge were determined.

INTRODUCTION

In the last decades, research in the field of energetic materials faced a profound change. Numerous studies raised awareness of the toxicity of widely-used substances like TNT, RDX and HMX and their degradation products towards humans and the environment.^[1] Additionally, modern safety requirements of the armed forces^[2] cause a growing demand for material less vulnerable to stimuli like shock, heat and bullet impact. Research around the globe focuses strongly on compounds based on nitrogen-rich heterocycles, since those liberate mostly molecular nitrogen as innocuous product of combustion or explosion. Furthermore, attractive energetic properties due to substantial ring strain and highly positive heats of formation attract notice to the research of environmentally friendly high-power energetic materials^[3].

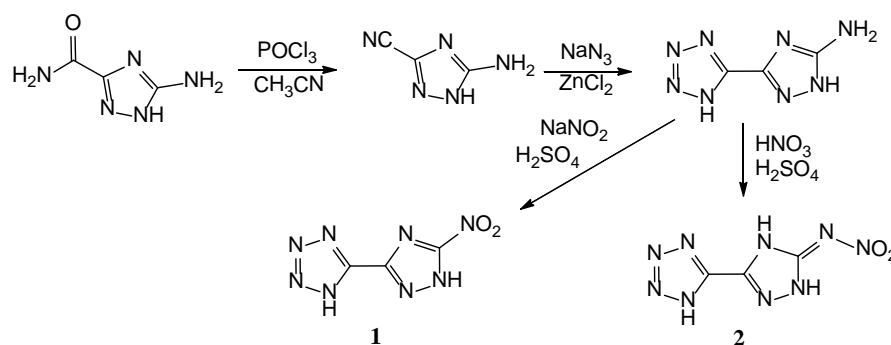
Recent studies on C–C connected heterocycles like bistriazoles and bistetrazoles revealed excellent characteristics regarding stability and detonation properties.^[3a, 4] The connection via C–C bond of a triazole ring with its opportunity to introduce a large variety of energetic moieties and a tetrazole or a *N*-hydroxy-tetrazole ring implying a large energy content leads to energetic materials with tunable properties.^[5] Due to the fact that nitrogen-rich salts of energetic compounds show an increased stability compared to the uncharged compounds, we present the treatment of energetic triazole compounds with several nitrogen-rich bases to form the corresponding salts. Cations like guanidinium, triaminoguanidinium or hydroxylammonium not only increase the overall nitrogen content and thus the heat of formation, but also improve the performance characteristics.^[4a, 6]

The focus of this study is on the synthesis and full characterization of energetic salts of 5-(1,2,4-Triazol-C-yl)tetrazoles (**1,2**) and their 1-hydroxy-tetrazole analogues (**3,4**). The energetic performance and sensitivity data of the ionic compounds are presented and compared to the neutral precursors. Additionally, the positive influence of the introduction of *N*-oxides in energetic materials is shown.

RESULTS AND DISCUSSION

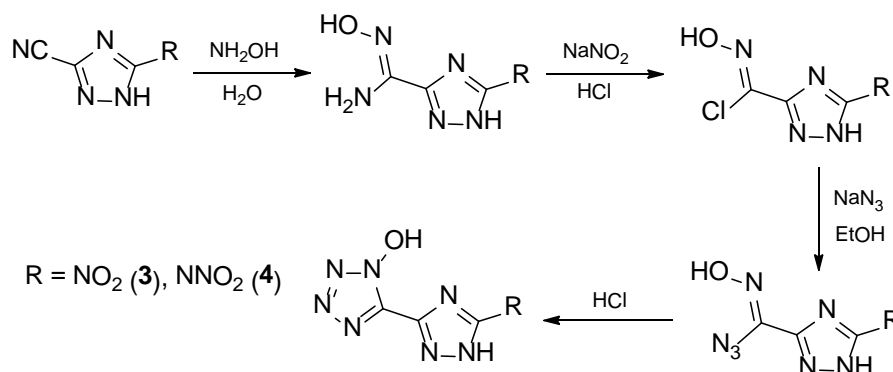
SYNTHESIS

All four neutral 5-(1,2,4-Triazol-C-yl)tetrazoles (**1**, **2**) and 5-(1,2,4-Triazol-C-yl)tetrazol-1-oles (**3**, **4**) were synthesized as published recently starting from 5-amino-1*H*-1,2,4-triazole-3-carbonitrile.^[5] In the case of compounds **1** and **2**, first of all the tetrazole ring was built up by a cycloaddition with sodium azide, followed by introduction of the energetic moieties via Sandmeyer reaction or nitration with nitric acid. (Scheme 1).^[5a]



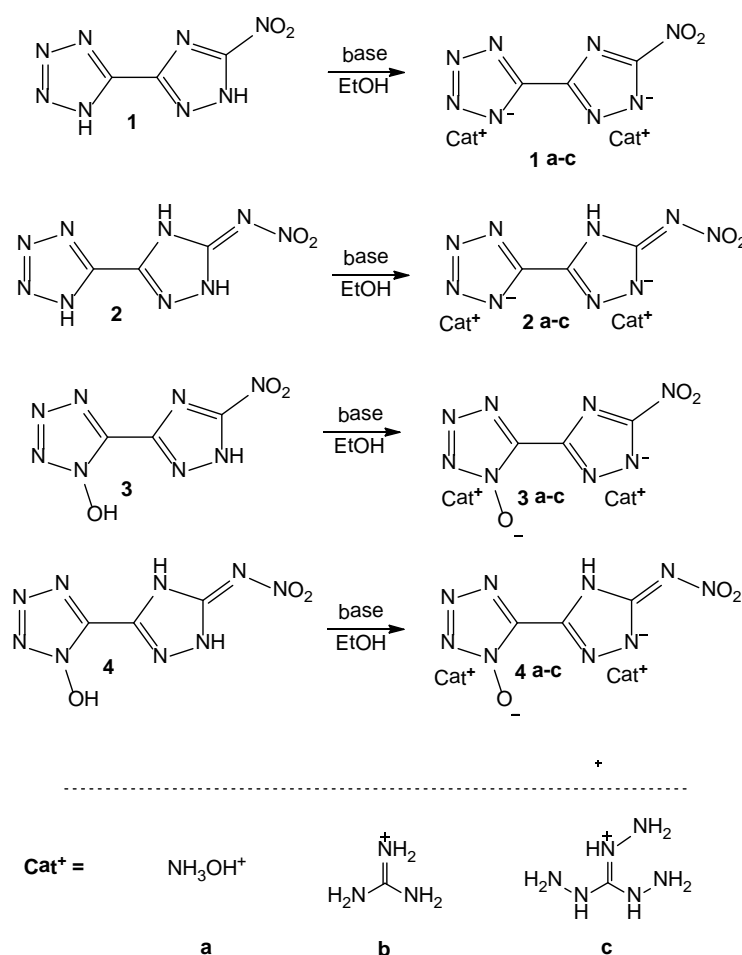
Scheme 1: Synthesis of NTT (**1**) and NATT (**2**).

A different approach was used for the synthesis of compounds **3** and **4**. The energetic moieties were primarily introduced by modification of the amine group of 5-amino-1*H*-1,2,4-triazole-3-carbonitrile. Multiple reaction steps including the formation of an amidoxime, chlorination, chlorine to azide exchange and finally cyclization lead to the 1-hydroxy-tetrazole compounds **3** and **4** (Scheme 2).^[5b]



Scheme 2: Synthesis of 5-(3-nitro-1*H*-1,2,4-triazol-5-yl)tetrazol-1-ol (NTTO, **3**) 5-(5-nitrimino-1,4*H*-1,2,4-triazol-3-yl)tetrazol-1-ol (NATTO, **4**).

Preparation of the corresponding salts of compounds **1–4** was accomplished by diluting the neutral compound in ethanol and addition of two equivalents of the corresponding organic base. This step benefits from the very poor solubility of the ionic target molecules, contrary to the neutral ones which dissolve readily in ethanol. Precipitation of the desired ionic compounds occurred almost quantitative and led to high purities.



Scheme 3: Synthetic route to the nitrogen-rich salts derived from **1–4** using the corresponding nitrogen-rich bases (hydroxylamine, guanidinium carbonate, triaminoguanidine).

MULTINUCLEAR NMR SPECTROSCOPY

All compounds were investigated using ^1H , ^{13}C and ^{14}N NMR spectroscopy. The $^{13}\text{C}\{^1\text{H}\}$ -spectra show three signals for the carbon atoms in the expected range, deprotonation with nitrogen-rich bases shifts the signals of all carbon atoms to lower field in comparison to the uncharged compounds. The signal of the carbon atom next to the energetic moiety is shifted furthest downfield for all compounds in the range of 157.3 ppm (**2c**) and 165.9 ppm (**3b**).

The signal of the bridging carbon of the triazole ring can be observed in the range of 151.4 ppm (**2a**) to 157.3 ppm (**1c**) and the corresponding signal of the tetrazole carbon atom is located in the range of 148.4 ppm (**2a**) to 156.4 ppm (**1c**) for the triazolyt-tetrazole compounds. In the case of the tetrazole-1-*N*-oxide compounds, all signals of the bridging carbon atoms are shifted to higher field. The signal of the triazole ring can be observed in the range of 147.8 ppm (**4a**) to 152.8 ppm (**3c**) and the corresponding signal of the tetrazole carbon atom is located in the range of 137.7 ppm (**4c**) to 139.2 ppm (**3a**). The $^{14}\text{N}\{^1\text{H}\}$ NMR spectra of all compounds show a broad signal for the nitro group between -10 ppm and -25 ppm. Based on comparable ionic compounds^[4a, 6], the proton signals of all cations can be found in the expected range.

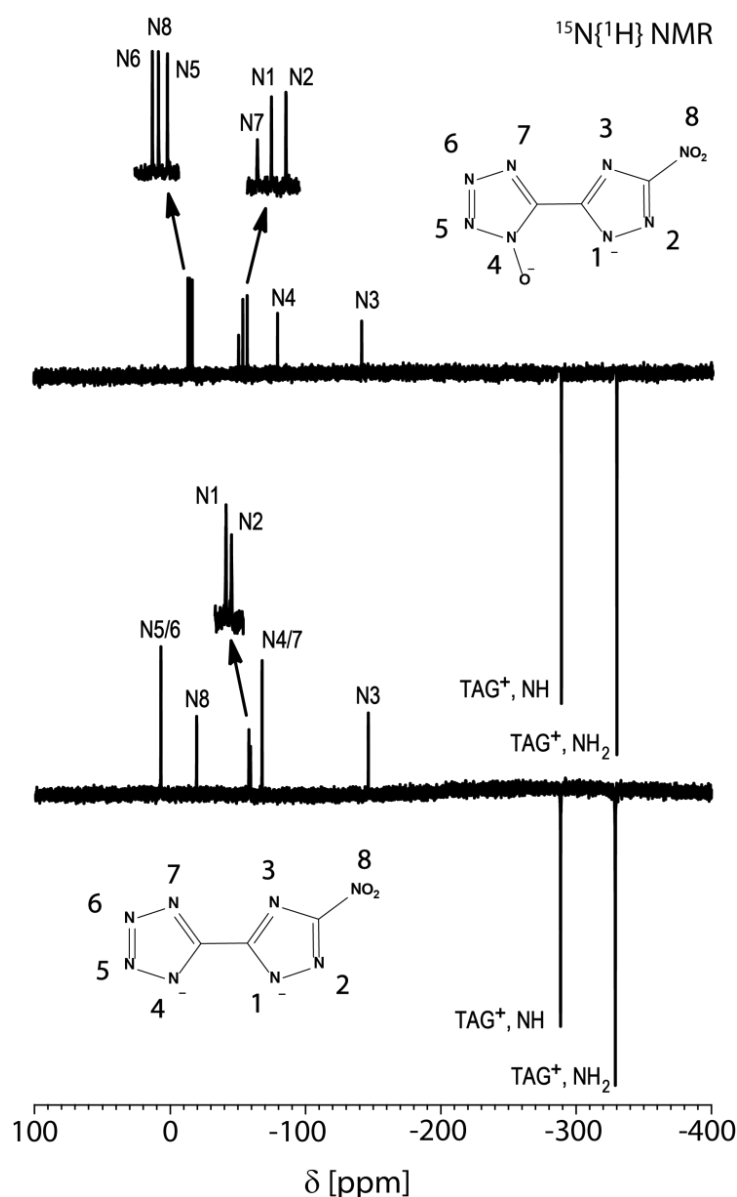


Figure 1: $^{15}\text{N}\{^1\text{H}\}$ NMR spectra of compounds **1c** (bottom) and **3c** (top) recorded in DMSO-*d*₆. The *x*-axis represents the chemical shift δ in ppm.

Due to the insufficient solubility of compound **2a–c** and **4a–c**, $^{15}\text{N}\{^1\text{H}\}$ NMR spectra were recorded for compounds **1c** and **3c**, as illustrated in Figure 1. The assignments are based on comparison with similar molecules and additional theoretical calculations using Gaussian 09 (MPW1PW91/aug-cc-pVDZ).^[7] The signals of the triazole nitrogen atoms as well as the nitro group can be found in both cases in the expected range very similar to the recently published 3,3'-dinitro-5-5'-bistriazolate anion.^[8] Two well resolved resonances are observed in the ^{15}N NMR spectrum of the tetrazolate-compound **1c** at -7.3 (N5/6), and -67.6 ppm (N4/7), which is in good agreement with the resonances of the 5-5'-bistetrazolate anion (-3.0 , -66.0).^[3a] The tetrazole-*N*-oxide ring of compound **3c** shows four well resolved resonances. The signals can be observed at shifts of -82.4 (N4), -20.2 (N5), -17.0 (N6), and -54.0 ppm (N7), comparable with the signals of the similar 5,5'-bistetrazole-1,1'-diolate anion.^[9]

SINGLE CRYSTAL X-RAY STRUCTURE ANALYSIS

All compounds were recrystallized from water, which mainly led to the formation of microcrystalline material not suitable for X-ray analysis. Only crystals of compounds **3b** were appropriate and the crystal structure is discussed in the following. The bond lengths and torsion angles within the azole rings are all in the range of formal C–N and N–N single and double bonds (C–N: 1.47 \AA , 1.22 \AA ; N–N: 1.48 \AA , 1.20 \AA).^[10] The $\text{C}_3\text{--N}_5\text{--N}_6$ angle of the *N*-oxide anion has an value of $108.7(1)^\circ$ as compared to $109.9(2)^\circ$ for the neutral compound **3**. As expected the N5–O3 bond length is shortened to $1.317(2)\text{ \AA}$ upon deprotonation ($1.345(2)\text{ \AA}$ in **3**). The torsion angle between both heterocycles and the one of the nitro group is very small ($2.7(2)^\circ$ and $0.8(2)^\circ$), which leads to a nearly planar assembly. Compound **3b** crystallizes as a monohydrate in the monoclinic space group $P2_1/n$ with a density of 1.639 g cm^{-3} , the formula unit is shown in Figure 2.

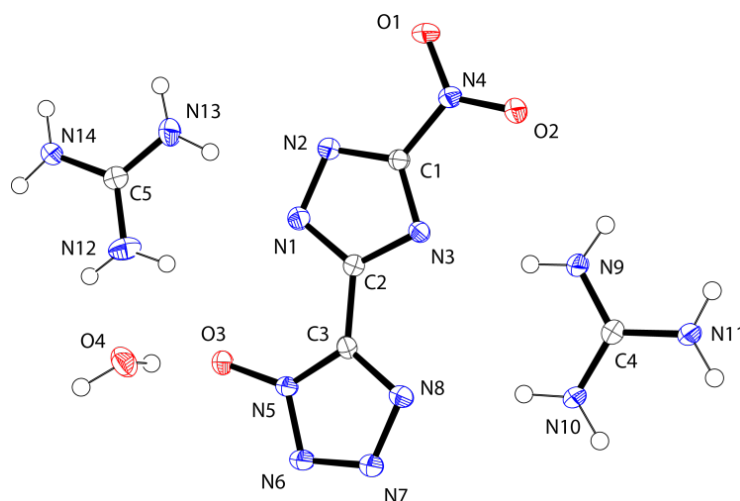


Figure 2: Molecular structure of Guanidinium 5-(3-Nitro-1,2,4-triazolate-5-yl)tetrazol-1-olate (**3b**). Thermal ellipsoids are set to 50 % probability.

Due to the planarity of both cation and anion, the crystal structure of **3b** is built up by planes that are kept together by a strong network of hydrogen bonds. As shown in Figure 3, each NTTO^{2-} anion is surrounded by five guanidinium cations via strong hydrogen bonds towards the atoms of the azole rings and the oxygen O1 of the nitro group (Table 1).

Table 1: Hydrogen bonds present in **3b**.

D–H...A	d (D–H) [Å]	d (H...A) [Å]	d (D–A) [Å]	< (D–H...A) [°]
O4 ⁱ –H4b...N2	0.87(2)	2.06(2)	2.916(2)	169(2)
N9 ⁱⁱ –H9a...O4	0.86 (2)	1.98(2)	2.801(2)	158(2)
N9 ^{iv} –H9b...N3	0.85(2)	2.10(2)	2.920(2)	165(2)
N10 ^{iv} –H10a...N8	0.90(2)	2.20(2)	3.095(2)	175(2)
N11–H11a...N6	0.86 (2)	2.32(2)	3.175(2)	173(2)
N11 ⁱⁱ –H11b...O4	0.86(2)	2.32(2)	3.053(2)	143(1)
N12 ⁱ –H12a...O3	0.86(2)	2.10(2)	2.814(2)	140 (2)
N12 ^v –H12b...N7	0.86(2)	2.40(2)	3.199(2)	155(2)
N13 ⁱ –H13a...N1	0.89(2)	2.16(2)	3.040(2)	170(2)
N13 ⁱ –H13b...N2	0.89(2)	2.32(2)	3.152(2)	154(2)
N14 ⁱⁱⁱ –H14a...O1	0.87(2)	2.19(2)	3.044(2)	164(2)
N14 ^v –H14b...N7	0.87(2)	2.37(2)	3.172(2)	154(2)

Symmetry Operators: (i) $1/2-x, 1/2+y, 1/2-z$; (ii) $x, -1+y, z$; (iii) $1-x, -y, -z$; (iv) $1/2+x, 1/2-y, -1/2+z$; (v) $1-x, 1-y, -z$.

It is remarkable to note that all accessible nitrogen atoms (and the *N*-oxide O3) act as acceptor for hydrogen bonds, which is merely possible due to the several N-H groups of the surrounding guanidinium cations. All contacts lie well within the sum of van der Waals radii ($r_w(\text{O}) + r_w(\text{N}) = 3.07 \text{ \AA}$, $r_w(\text{N}) + r_w(\text{N}) = 3.20 \text{ \AA}$)^[11] with a D...A length between 2.801(2) Å and 3.199(2) Å. Most of the hydrogen bonds are strongly directed with D-H...A angles between 155(2)° and 175(2)°. In addition, the oxygen atom O1 is involved in a electrostatic interaction with the π -electrons of the overlying tetrazole ring, which supports the stacking of the layers.

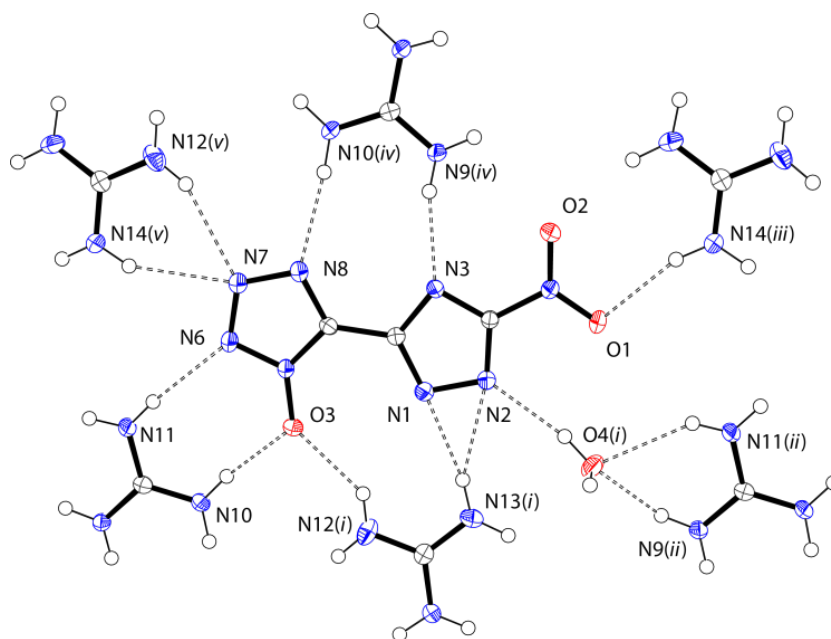


Figure 3: Formation of planes in the crystal structure of **3b**; Thermal ellipsoids are set to 50 % probability. Symmetry codes: (i) $1/2-x, 1/2+y, 1/2-z$; (ii) $x, -1+y, z$; (iii) $1-x, -y, -z$; (iv) $1/2+x, 1/2-y, -1/2+z$; (v) $1-x, 1-y, -z$.

THEORETICAL CALCULATIONS, PERFORMANCE CHARACTERISTICS AND STABILITIES

The heats of formation of all compounds have been calculated on the CBS-4M level of theory using the atomization energy method and utilizing experimental data (for further details and results refer to the Supporting Information). All compounds show highly endothermic enthalpies of formation in the range of 234 kJ mol⁻¹ (**1b**) to 1009 kJ mol⁻¹ (**4c**), all by far outperforming RDX (70 kJ mol⁻¹).

In order to estimate the detonation performances of the prepared compounds selected key parameters were calculated with EXPLO5 (version 5.05)^[20] and compared to RDX. The calculated detonation parameters using experimentally determined densities (gas

pycnometry at 25 °C with dried compounds) and calculated heats of formation are summarized in Table 2.

Sensitivity

Regarding the precursor compounds NATT (**2**) and NATTO (**4**), both show very high sensitivity towards impact, friction and electrostatic discharge. One of the key aspects of this study was the synthesis of ionic derivatives that are safer to handle, while being at least equally energetic. In the case of compounds **2a–c**, the sensitivity towards impact is reduced from 1 J to 40 J and the sensitivity towards friction could be lowered to 160 N (**2a**), 324 N (**2b**) and 360 N (**2c**). Compounds **4a–c** also show lower sensitivity values (8 J (**4a**), 40 J (**4b**), 10 J (**4c**)) in comparison to the neutral compound **4**, however the low sensitivities of the corresponding compounds bearing no *N*-oxide are only reached for compound **4b**. Figure 1 shows the thermal decomposition of the ionic derivatives **2a–c** (solid lines) and **4a–c** (dashed lines). As expected, the thermal stability of all ionic compounds mostly depends on the cation, however the ionic *N*-oxide compounds (**4a–c**) all show a lower decomposition temperature in comparison to compounds **2a–c** as it is expected for *N*-hydroxy azoles.^[12] With a decomposition temperature of 238 °C (**2b**) and 212 °C (**4b**), only the guanidinium salts show a higher onset temperature compared to RDX (Figure 4).

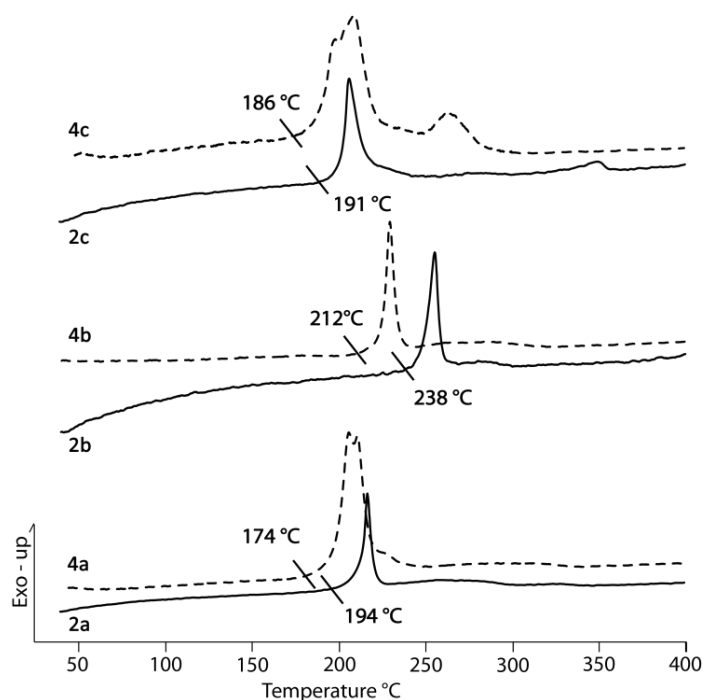


Figure 4: DSC plots of ionic derivatives **2a–c** (solid lines) and **4a–c** (dashed lines). DSC plots were recorded with a heating rate of 5 °C min⁻¹.

The sensitivity of the neutral NTT (**1**) and NTTO (**3**) towards external stimuli could also be further decreased by deprotonating with organic bases. All compounds (except **3a**) show an impact sensitivity of 40 J and friction sensitivity of 360 N. As shown in Figure 3, the guanidinium salt (**3b**) shows a remarkably high decomposition temperature (296 °C) in comparison to the neutral compound **1**, whereas compound **3c** starts to decompose at 190 °C and **3a** at 182 °C. Again, the ionic *N*-oxide compounds (**3a–c**) show lower decomposition temperatures in comparison to compounds **1a–c**, only the guanidinium salt **3b** exceeds 200 °C with a thermal stability of 269 °C (Figure 5).

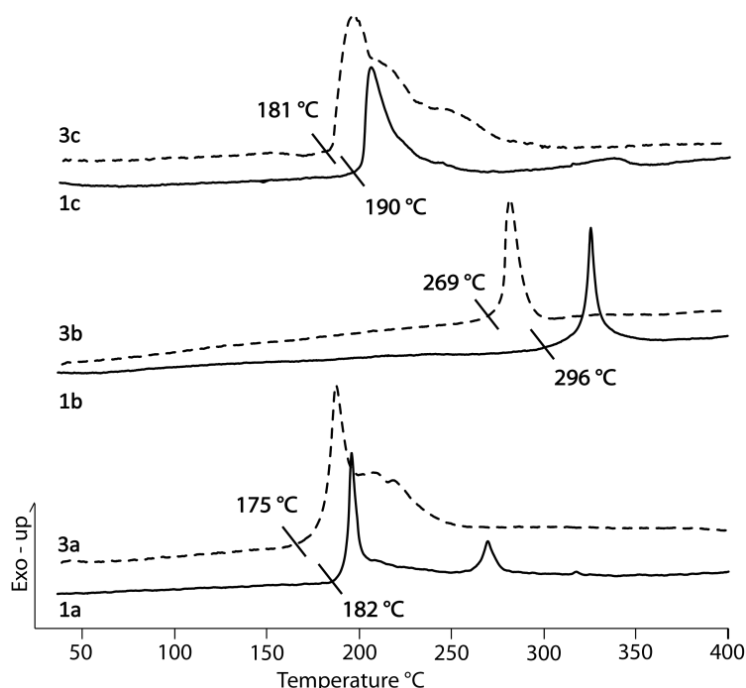


Figure 5: DSC plots of ionic derivatives **1a–c** (solid lines) and **3a–c** (dashed lines). DSC plots were recorded with a heating rate of 5 °C min⁻¹.

Performance

The results of theoretical calculations regarding performance are summarized in Tables 2a and 2b. In general, the triazol-C-yl-tetrazoles show lower performance values in comparison to their 1-hydroxy-tetrazole analogues. As expected, the additional oxygen atom generally leads to increased energetic properties due to a higher density and an even greater energy output.^[12b, 14] In comparison to the ionic derivatives of compounds **1** and **2**, a marked performance increase is seen. The detonation velocities of the hydroxylammonium salts **3a** and **4a** are increased by about 500 ms⁻¹. For the guanidinium salts **3b** and **4b**, the influence of the additional oxygen is slightly lower, however the detonation velocity is still increased by about 270 ms⁻¹. The introduction of

the *N*-oxide also positively influences other detonation parameters like the detonation pressure or the energy of explosion (increased by appr. 500 kJ kg⁻¹).

Table 2a: Physico-chemical properties of compounds **1** and **3** and their corresponding ionic derivatives (a–c) in comparison to hexogen (RDX).

	1 NTT	3 NTTO	1a	1b	1c	3a	3b	3c	RDX ^[n]
Formula	C ₃ H ₂ N ₈ O ₂	C ₃ H ₂ N ₈ O ₃	C ₃ H ₈ N ₁₀ O ₄	C ₃ H ₁₂ N ₁₄ O ₂	C ₃ H ₁₈ N ₂₀ O ₂	C ₃ H ₈ N ₁₀ O ₅	C ₃ H ₁₂ N ₁₄ O ₃	C ₃ H ₁₈ N ₂₀ O ₃	C ₃ H ₆ N ₆ O ₆
Molecular Mass [g mol ⁻¹]	182.1	198.10	248.16	300.24	390.33	264.15	316.24	406.32	222.12
Impact sensitivity [J] ^a	25	35	40	40	40	8	40	10	7
Friction sensitivity [N] ^b	288	360	360	>360	>360	360	360	360	120
ESD–test [J]	0.85	0.13	0.15	0.6	0.4	0.2	0.5	0.35	--
<i>N</i> [%] ^c	61.5	56.6	56.44	65.3	71.8	53.0	62.0	68.9	37.8
<i>Q</i> [%] ^d	-43.9	-32.3	-38.7	-74.6	-69.7	-30.3	-65.8	-63.0	-21.6
<i>T</i> _{dec.} [°C] ^e	211	152	182	296	190	175	269	181	210
<i>ρ</i> [g cm ⁻³] ^f	1.70	1.86	1.78	1.71	1.68	1.81	1.72	1.70	1.82
$\Delta_f H_m^\circ$ [kJ mol ⁻¹] ^g	518	446	316	234	958	356	260	977	70
$\Delta_f U^\circ$ [kJ kg ⁻¹] ^h	2430	2335	1385	896	2582	1456	936	2529	417
EXPLO5 (V5.05) values:									
$-\Delta_E U^\circ$ [kJ kg ⁻¹] ⁱ	4730	5407	5201	2866	4285	5750	3471	4688	6128
<i>T</i> _E [K] ^j	3833	4217	3651	2259	2830	3939	2593	3073	4207
<i>p</i> _{C-J} [kbar] ^k	254	337	291	219	290	352	244	299	349
<i>V</i> _{Det.} [m s ⁻¹] ^l	7919	8655	8473	7682	8644	8996	7974	8728	8749
Gas vol. [L kg ⁻¹] ^m	682	677	808	773	826	799	781	831	740

Of all described compounds, the triaminoguanidinium salt **3c** and the hydroxylamonium salt **4a** exhibit the best calculated performance values regarding the detonation parameters, sensitivities and thermal stability. Compound **4a** displays the best performance with a calculated detonation velocity of 9014 ms⁻¹, a detonation pressure of 348 kbar and a decomposition temperature of 179 °C. The triaminoguanidinium compound exhibits energetic properties in the range of RDX with 8728 m s⁻¹, a detonation pressure of 299 kbar and a decomposition temperature of 181 °C, along with a very high nitrogen content of 68.9 %.

Although lower performance values (*v*_{det} = 7974 m s⁻¹ and 7970 m s⁻¹) were calculated for the guanidinium salts **3b** and **4b**, these compounds displays the highest decomposition temperatures of 269 °C and 212 °C together with an insensitivity towards friction and impact.

The most interesting compounds regarding the energetic properties are the hydroxylammonium and triaminoguanidinium compounds (**4a** and **3c**). Those compounds exhibit decomposition temperatures slightly below 200 °C and performance values in the range of RDX (8728 m s⁻¹ (**3c**)) or even well above (9014 m s⁻¹ (**4a**)).

Table 2b: Physico-chemical properties of compounds **2** and **4** and their corresponding ionic derivatives (a–c) in comparison to hexogen (RDX).

	2 NATT	4 NATT O	2a	2b	2c	4a	4b	4c	RDX ^[n]
Formula	C ₃ H ₃ N ₉ O ₂	C ₃ H ₃ N ₉ O ₃	C ₃ H ₉ N ₁₁ O ₄	C ₅ H ₁₃ N ₁₅ O ₂	C ₅ H ₁₉ N ₂₁ O ₂	C ₃ H ₉ N ₁₁ O ₅	C ₅ H ₁₃ N ₁₅ O ₃	C ₅ H ₁₉ N ₂₁ O ₃	C ₃ H ₆ N ₆ O ₆
Molecular Mass [g mol ⁻¹]	197.1	213.11	263.2	315.26	405.34	279.17	331.25	421.34	222.12
Impact sensitivity [J] ^a	<1	< 1	40	40	40	8	40	10	7
Friction sensitivity [N] ^b	18	60	160	>360	324	288	360	288	120
ESD–test [J]	0.07	0.13	0.15	0.6	0.2	0.1	0.8	0.3	--
N [%] ^c	64.0	59.2	58.5	66.6	72.6	55.2	63.4	69.8	37.8
Ω [%] ^d	-44.6	-33.8	-38.7	-74.6	-69.7	-31.5	-65.2	-62.6	-21.6
T _{dec.} [°C] ^e	215	116	194	238	191	179	212	186	210
ρ [g cm ⁻³] ^f	1.70	1.85	1.75	1.68	1.66	1.79	1.70	1.67	1.82
Δ _f H _m ^o [kJ mol ⁻¹] ^g	576	515	354	261	978	418	304	1009	70
Δ _f U ^o [kJ kg ⁻¹] ^h	2549	2502	1458	946	2542	1607	1033	2521	417
EXPLO5 (V5.05) values:									
-Δ _E U ^o [kJ kg ⁻¹] ⁱ	4804	5470	5273	2915	4246	5769	3495	4643	6128
T _E [K] ^j	3781	4126	3684	2281	2814	3898	2600	3033	4207
p _{C-J} [kbar] ^k	262	342	293	221	289	348	242	288	349
V _{Det.} [m s ⁻¹] ^l	8062	8776	8500	7709	8628	9014	7970	8628	8749
Gas vol. [L kg ⁻¹] ^m	712	708	807	773	827	818	791	836	740

^[a] BAM drophammer, grain size (75–150 μm); ^[b] BAM friction tester, grain size (75–150 μm); ^[c] Nitrogen content;

^[d] Oxygen balance; ^[e] Temperature of decomposition by DSC ($\beta = 5$ °C, Onset values); ^[f] densities based on gas-pycnometer measurements of anhydrous compounds at 25 °C; ^[g] Molar enthalpy of formation; ^[h] Energy of formation;

^[i] Energy of Explosion; ^[j] Explosion temperature; ^[k] Detonation pressure; ^[l] Detonation velocity;

^[m] Assuming only gaseous products; ^[n] values based on Ref. ^[13].

CONCLUSION

By reacting the nitro- and nitrimino triazolyl-tetrazole compounds (**1**, **2**) and their 1-hydroxy-tetrazole analogues (**3,4**) with nitrogen-rich organic bases, twelve ionic nitrogen rich energetic materials were synthesized and fully characterized by means of vibrational and NMR spectroscopy as well as sensitivity towards impact and friction. Their thermal behavior was investigated with differential scanning calorimetry and their energetic properties calculated theoretically. The ionic *N*-oxide compounds (**3a-c**, **4a-c**) show lower decomposition temperature in comparison to the compounds bearing no *N*-oxide, however the stability is mainly influenced by the corresponding cation. Most of the compounds show reduced sensitivities in comparison to their neutral precursors, especially the ionic compounds based on NATT (**2a-c**) and NATTO (**4a-c**) are much safer to handle, since the stability towards friction and impact was considerably increased.

Regarding the detonation properties, the performance is mostly affected by the cation. The guanidinium salts always show the lowest detonation velocities, the hydroxylammonium and triaminoguanidinium salts are basically in the same range. In general, the triazol-C-yl-tetrazoles show lower performance values in comparison to their 1-hydroxy-tetrazole analogues. The detonation velocities of the hydroxylammonium salts are increased by about 500 ms^{-1} due to the *N*-oxide. For the guanidinium salts, the influence of the additional oxygen is slightly lower, however the detonation velocity is still increased by about 270 ms^{-1} . The introduction of an *N*-oxide in tetrazole based energetic materials obviously positively influences the detonation parameters due to a higher density and an even greater energy output, however this advantage comes along with lower decomposition temperatures.

EXPERIMENTAL SECTION

Caution: Although all presented nitroazoles are rather stable against outer stimuli, proper safety precautions should be taken when handling the dry materials. The neutral nitraminoazole is of high sensitivity and tends to explode under the influence of heat, impact or friction. Lab personnel and the equipment should be properly grounded and protective equipment like earthed shoes, leather coat, Kevlar[®] gloves, ear protection and face shield is recommended.

General. All chemical reagents and solvents were obtained from Sigma-Aldrich Inc. or Acros Organics (analytical grade) and were used as supplied without further purification. ^1H , $^{13}\text{C}\{^1\text{H}\}$, $^{14}\text{N}\{^1\text{H}\}$ and NMR spectra were recorded on a JEOL Eclipse 400 instrument in $\text{DMSO-}d_6$ at 25 °C. The chemical shifts are given relative to tetramethylsilane (^1H , ^{13}C) or nitro methane (^{14}N) as external standards and coupling constants are given in Hertz (Hz). Infrared (IR) spectra were recorded on a Perkin-Elmer Spectrum BX FT-IR instrument equipped with an ATR unit at 25 °C. Transmittance values are qualitatively described as “very strong” (vs), “strong” (s), “medium” (m), “weak” (w) and “very weak” (vw). Raman spectra were recorded on a Bruker RAM II spectrometer equipped with a Nd:YAG laser (200 mW) operating at 1064 nm and a reflection angle of 180°. The intensities are reported as percentages of the most intense peak and are given in parentheses. Elemental analyses (CHNO) were performed with a Netzsch Simultaneous Thermal Analyzer STA 429. Melting and decomposition points were determined by differential scanning calorimetry (Linseis PT 10 DSC, calibrated with standard pure indium and zinc). Measurements were performed at a heating rate of 5 °C min⁻¹ in closed aluminum sample pans with a 1 µm hole in the lid for gas release to avoid an unsafe increase in pressure under a nitrogen flow of 20 mL min⁻¹ with an empty identical aluminum sample pan as a reference.

For initial safety testing, the impact and friction sensitivities as well as the electrostatic sensitivities were determined. The impact sensitivity tests were carried out according to STANAG 4489,^[15] modified according to WIWEB instruction 4-5.1.02^[16] using a BAM^[17] drop hammer. The friction sensitivity tests were carried out according to STANAG 4487^[18] and modified according to WIWEB instruction 4-5.1.03^[19] using the BAM^[17] friction tester. The electrostatic sensitivity tests were accomplished according to STANAG 4490^[20] using an electric spark testing device ESD 2010EN (OZM Research).

Crystallographic measurements. The single-crystal X-ray diffraction data of **3b** was collected using an Oxford Xcalibur3 diffractometer equipped with a Spellman generator (voltage 50 kV, current 40 mA), Enhance molybdenum K_{α} radiation source ($\lambda = 71.073$ pm), Oxford Cryosystems Cryostream cooling unit, four circle kappa platform and a Sapphire CCD detector. Data collection and reduction was performed with CrysAlisPro.^[21] The structure was solved with SIR97^[22], refined with SHELXL-97^[23], and checked with PLATON^[24], all integrated into the WinGX software suite^[25]. The finalized CIF file was checked with checkCIF.^[26] Intra- and intermolecular contacts were analyzed with Mercury.^[27] CCDC 946356 (**3b**), contains the supplementary crystallographic data for this paper. These data can be obtained free of charge from the Cambridge Crystallographic Data Centre via www.ccdc.cam.ac.uk/data_request/cif.

The precursors **1** and **2** as well as **3** and **4** were synthesized according to literature.^[5]

Hydroxylammonium 5-(5-nitro-1,2,4-triazolate-3-yl)-tetrazolate (1a)

5-(5-nitro-1,2,4-triazol-3-yl)-tetrazole (NTT, **1**) (0.5 g, 2.7 mmol) was diluted in 25 ml of EtOH and hydroxylamine (50 wt% in water, 0.32 mL, 5.5 mmol) was added. The precipitate was filtered off and washed with EtOH and Et₂O to yield **3a** (0.51 g, 2.0 mmol, 74%) as slightly yellow powder.

¹H NMR (DMSO-*d*₆): δ (ppm) = 9.43 (s, 3H, NH₃-OH); **¹³C NMR** (DMSO-*d*₆): δ (ppm) = 164.7, 153.5, 153.3; **¹⁴N NMR** (DMSO-*d*₆): δ (ppm) = -18 (NO₂); **IR**: 3624(w), 3562(w), 3016(m), 2699(s), 1643(m), 1617(m), 1513(s), 1480(m), 1469(vs), 1407(s), 1393(vs), 1321(m), 1308(s), 1292(m), 1284(m), 1252(s), 1236(s), 1191(m), 1144(m), 1114(m), 1102(s), 1047(w), 1011(m), 1011(m), 1001(s), 842(s), 777(s), 764(s), 730(m), 716(m), 655(m); **Raman** (200 mW): ν (cm⁻¹) (rel. int.): 1583(95), 1522(5), 1513(4), 1473(9), 1410(45), 1399(49), 1323(35), 1293(8), 1285(16), 1194(7), 1145(5), 1115(100), 1105(22), 1087(11), 1047(9), 1040(11), 1006(13), 847(12), 778(4), 765(4), 395(6), 343(5); **Elemental analysis** (C₃H₈N₁₀O₄): calc.: C 14.25, H 3.25, N 56.44; found: C 14.68, H 3.44, N 52.38. **Mass spectrometry**: m/z (FAB⁻): 181.0 [C₃HN₈O₂⁻]; (FAB⁺): 34.1 [NH₄OH⁺]; **DSC** (Onset, 5 °C/min): T_{Dec}: 190 °C. **Sensitivities** (grain size: < 100 μ m): FS: > 360 N, IS: 40, ESD: 0.15 J.

Guanidinium 5-(5-nitro-1,2,4-triazolate-3-yl)-tetrazolate (1b)

5-(5-nitro-1,2,4-triazol-3-yl)-tetrazole (NTT, **1**) (0.5 g, 2.7 mmol) was diluted in 20 ml of EtOH. A solution of guanidinium carbonate (0.49 g, 2.7 mmol) in water (5 mL) was added, the mixture was refluxed for 15 min and subsequently cooled to room temperature. The precipitate was filtered off and washed with EtOH and Et₂O to yield **3b** (0.75 g, 2.5 mmol, 91%) as yellow powder.

¹H NMR (DMSO-d₆): δ (ppm) = 7.46 (s, 6H, NH₂, G⁺). **¹³C NMR** (DMSO-d₆): δ (ppm) = 165.6, 158.8, 156.3, 155.9; **¹⁴N NMR** (DMSO-d₆): δ (ppm) = -25 (NO₂); **IR**: 3428(m), 3343(m), 3084(m), 1680(s), 1653(s), 1635(s), 1582(m), 1503(m), 1465(s), 1398(s), 1377(vs), 1302(s), 1276(m), 1187(m), 1148(m), 1141(m), 1091(s), 1035(w), 1010(w), 1002(m), 838(m), 781(w), 775(w), 775(w), 716(w), 657(w); **Raman** (200 mW): ν (cm⁻¹) (rel. int.): 1585(76), 1556(7), 1520(6), 1471(7), 1399(50), 1391(66), 1310(33), 1278(39), 1190(2), 1105(100), 1094(79), 1061(4), 1043(10), 1037(10), 1013(19), 841(14), 778(3), 765(2), 536(10), 507(2), 474(2), 394(3); **Elemental analysis** (C₅H₁₂N₁₄O₂): calc.: C 20.00, H 4.03, N 65.31; found: C 20.60, H 4.13, N 62.96. **Mass spectrometry**: *m/z* (FAB⁺): 60.0 [CH₆N₃⁺]; (FAB⁻): 181.1 [C₃HN₈O₂]; **DSC** (Onset, 5 °C/min): T_{Dec}: 286 °C. **Sensitivities** (grain size: < 100 μm): FS: > 360 N, IS: 40 J, ESD: 0.6 J.

Triaminoguanidinium 5-(5-nitro-1,2,4-triazolate-3-yl)-tetrazolate (1c)

Triaminoguanidine (0.57 g, 5.5 mmol) was added to a solution of 5-(5-nitro-1,2,4-triazol-3-yl)-tetrazole (NTT, **1**) (500 mg, 2.746 mmol) in ethanol (20 mL) and the mixture was refluxed for 15 minutes. After cooling to room temperature, the precipitate was collected by filtration, washed with EtOH and Et₂O to yield **3c** (0.98 g, 2.5 mmol, 91 %) as yellow powder.

¹H NMR (DMSO-d₆): δ (ppm) = 8.79 (s, 3H, NH, TAG⁺), 4.61 (s, 6H, NH₂, TAG⁺); **¹³C NMR** (DMSO-d₆): δ (ppm) = 165.6, 159.3, 157.3, 156.4; **¹⁴N NMR** (DMSO-d₆): δ (ppm) = -14 (NO₂); **¹⁵N NMR** (DMSO-d₆): δ (ppm) = -7.3 (N5/6), -19.2 (N8), -57.8 (N1), -59.0 (N2), -67.6 (N4/7), -146.2 (N3), -288.3 (TAG⁺, NH), -328.8 (TAG⁺, NH₂); **IR**: 3367(m), 3299(m), 3155(m), 1685(vs), 1671(vs), 1601(w), 1509(s), 1462(m), 1380(s), 1336(m), 1293(m), 1264(m), 1219(w), 1194(w), 1141(s), 1083(s), 1013(m), 994(s), 936(s), 834(m), 721(m), 662(w), 641(m), 641(m); **Raman** (200 mW): ν (cm⁻¹) (rel. int.): 1574(81), 1559(30), 1513(4), 1464(9), 1393(32), 1379(79), 1305(32), 1277(20), 1265(24), 1193(3), 1096(99), 1087(95), 1038(8), 1031(11), 996(2), 885(8), 836(10), 781(4), 640(2), 405(5); **Elemental analysis** (C₅H₁₈N₂₀O₂): calc.: C 15.39,

H 4.65, N 71.77; found: C 17.55, H 4.25, N 71.58. **Mass spectrometry:** m/z (FAB⁺): 105.1 [CH₉N₆⁺], (FAB⁻): 181.1 [C₃HN₈O₂⁻]; **DSC** (Onset, 5 °C/min): T_{Dec}: 192 °C; **Sensitivities** (grain size: < 100 µm): FS: > 360 N, IS: 40 J, ESD: 0.4 J.

Hydroxylammonium 5-(5-nitrimino-1,2,4-triazolate-3-yl)-tetrazolate (2a)

Hydroxylamine (50 wt% in water, 0.26 mL, 4.5 mmol) was added to a solution of 5-(3-nitrimino-1,2,4-triazol-3-yl)-tetrazole (**2**) (0.5 g, 2.2 mmol) in ethanol (30 mL). The precipitate was collected by filtration and washed with EtOH and Et₂O to yield **4a** (0.30 g, 1.2 mmol, 54 %) as slightly yellow solid.

¹H NMR (DMSO-d₆): δ (ppm) = 10.64 (s, 3H, NH₃OH); **¹³C NMR** (DMSO-d₆): δ (ppm) = 157.7, 151.4, 148.4; **¹⁴N NMR** (DMSO-d₆): δ (ppm) = -16 (NO₂); **IR**: 3187(w), 2938(m), 2698(m), 2691(m), 1627(w), 1573(m), 1532(m), 1512(m), 1486(m), 1450(m), 1445(m), 1417(m), 1390(m), 1370(m), 1341(s), 1333(s), 1306(m), 1263(vs), 1239(s), 1209(s), 1185(m), 1164(m), 1137(m), 1137(m), 1114(m), 1104(s), 1091(m), 1079(m), 1060(m), 1007(m), 1000(s), 969(m), 879(w), 850(m), 832(m), 777(m), 761(s), 746(m), 732(m), 720(s), 693(w); **Raman** (200 mW): ν (cm⁻¹) (rel. int.): 1629(91), 1597(94), 1568(68), 1531(28), 1512(16), 1487(19), 1426(5), 1381(6), 1371(6), 1263(7), 1212(5), 1187(6), 1167(4), 1144(22), 1115(31), 1081(13), 1063(8), 1040(7), 1028(28), 999(41), 881(5), 854(8), 756(16), 756(16), 748(12), 428(4), 329(4), 314(4), 235(4); **Elemental analysis** (C₃H₉N₁₁O₄): calc.: C 13.69, H 3.45, N 58.54; found: C 15.04, H 2.99, N 58.67. **Mass spectrometry:** m/z (FAB⁺): 34.0 [NH₄O⁺]; (FAB⁻): 196.1 [C₃H₂N₉O₂⁻]; **DSC** (Onset, 5 °C/min): T_{Dec}: 194 °C. **Sensitivities** (grain size: < 100 µm): FS: 160 N, IS: 40, ESD: 0.15 J.

Guanidinium 5-(5-nitrimino-1,2,4-triazolate-3-yl)-tetrazolate (2b)

5-(5-nitrimino-1,2,4-triazol-3-yl)-tetrazole (**2**) (0.5 g, 2.1 mmol) was dissolved in 30 mL of EtOH. A solution of guanidinium carbonate (0.39 g, 2.2 mmol) in water (5 mL) was added, the mixture was refluxed for 15 min and subsequently cooled to room temperature. The precipitate was collected by filtration and washed with EtOH and Et₂O to yield **4b** (0.60 g, 1.9 mmol, 89 %) as yellow powder.

¹H NMR (DMSO-d₆): δ (ppm) = 7.68 (s, 6H, NH₂, G⁺). **¹³C NMR** (DMSO-d₆): δ (ppm) = 158.3, 157.7, 155.2, 152.3; **¹⁴N NMR** (DMSO-d₆): δ (ppm) = -17 (NO₂); **IR**: 3385(m), 1699(m), 1665(m), 1651(s), 1637(s), 1579(w), 1516(m), 1457(m), 1399(m), 1358(m), 1333(vs), 1280(vs), 1236(m), 1187(m), 1136(m), 1079(s), 1039(w), 1009(w), 982(m),

857(w), 766(m), 750(w), 733(m), 733(m); **Raman** (200 mW): ν (cm^{-1}) (rel. int.): 1593(98), 1561(5), 1512(28), 1461(21), 1357(5), 1279(6), 1189(3), 1141(10), 1132(8), 1062(5), 1013(36), 860(4), 751(6), 550(5), 424(3), 321(3), 258(3); **Elemental analysis** ($\text{C}_5\text{H}_{13}\text{N}_{15}\text{O}_2$): calc.: C 19.05, H 4.16, N 66.64; found: C 19.50, H 4.14, N 64.67. **Mass spectrometry**: m/z (FAB^+): 60.0 [CH_6N_3^+]; (FAB^-): 196.1 [$\text{C}_3\text{H}_2\text{N}_9\text{O}_2^-$]; **DSC** (Onset, 5 $^\circ\text{C}/\text{min}$): T_{Dec} : 238 $^\circ\text{C}$. **Sensitivities** (grain size: < 100 μm): FS: > 360 N, IS: 40, ESD: 0.6 J.

Triaminoguanidinium 5-(5-nitrimino-1,2,4-triazolate-3-yl)-tetrazolate (2c)

Triaminoguanidine (380 mg, 3.65 mmol) was added to a solution of 5-(5-nitrimino-1,2,4-triazol-3-yl)-tetrazole (**2**) (360 mg, 1.83 mmol) in ethanol (30 mL). The mixture was refluxed for 20 minutes and cooled down to room temperature. The precipitate was collected by filtration and washed with EtOH and Et₂O to yield **4c** (0.69 g, 1.7 mmol, 93 %) as colorless powder.

¹H NMR ($\text{DMSO}-d_6$): δ (ppm) = 12.80 (s, 1H, $\text{H}_{\text{Triazole}}$); 8.71 (s, 3H, NH, TAG⁺); 4.57 (s, 6H, NH₂, TAG⁺). **¹³C NMR** ($\text{DMSO}-d_6$): δ (ppm) = 159.2 (TAG⁺), 157.3, 155.3, 153.0; **¹⁴N NMR** ($\text{DMSO}-d_6$): δ (ppm) = -17 (NO_2); **IR**: 1687(vs), 1624(m), 1517(s), 1464(m), 1401(m), 1353(vs), 1272(s), 1210(m), 1179(m), 1140(s), 1061(s), 1047(s), 986(vs), 958(s), 857(w), 778(w), 763(w), 731(m), 716(m), 634(w); **Raman** (200 mW): ν (cm^{-1}) (rel. int.): 1587(100), 1518(55), 1466(17), 1402(10), 1359(14), 1274(11), 1137(19), 1077(6), 1053(7), 1008(50), 859(5); **Elemental analysis** ($\text{C}_5\text{H}_{19}\text{N}_{21}\text{O}_2$): calc.: C 14.28, H 4.72, N 72.57; found: C 16.51, H 4.98, N 70.28. **Mass spectrometry**: m/z (FAB^+): 105.1 [CH_9N_6^+]; (FAB^-): 196.1 [$\text{C}_3\text{HN}_9\text{O}_2^-$]; **DSC** (Onset, 5 $^\circ\text{C}/\text{min}$): T_{Dec} : 191 $^\circ\text{C}$. **Sensitivities** (grain size: < 100 μm): FS: 324 N, IS: 40, ESD: 0.2 J.

Hydroxylamonium 5-(3-Nitro-1,2,4-1H-triazolate-5-yl)tetrazol-1-olate (3a)

Hydroxylamine (50 wt% in water, 0.3 mL, 5.0 mmol) was added to a solution of **5** (0.5 g, 2.5 mmol) in ethanol (50 mL) and stirred at 60 $^\circ\text{C}$ for 5 minutes. After cooling down to room temperature the precipitate was collected by filtration, washed with ethanol and diethyl ether and dried in air to yield **3a** as pale yellow powder. (0.54 g, 2.04 mmol, 81 %). **¹H NMR** ($\text{DMSO}-d_6$): δ = 9.76 (s, 3H, NH₃OH) ppm; **¹³C NMR** ($\text{DMSO}-d_6$): δ = 165.6 (C-NO₂), 150.9 (C_{triazole}), 139.2 (C_{tetrazole}) ppm. **¹⁴N NMR** ($\text{DMSO}-d_6$): δ = -14 (NO_2) ppm; **IR**: ν (rel. int.) = 3204(w), 2953(m), 2707(m), 2703(m), 1623(w), 1540(m), 1508(m), 1478(vs), 1422(m), 1401(m), 1352(m), 1319(m), 1306(m), 1238(m), 1220(s),

1205(vs), 1149(m), 1049(w), 1015(m), 1000(s), 839(s), 758(m), 715(m), 715(m), 658(m) cm^{-1} ; **Raman** (200 mW): ν (rel. int.) = 1586(100), 1477(12), 1402(66), 1355(13), 1320(23), 1239(18), 1208(4), 1149(54), 1139(41), 1116(14), 1050(3), 1031(20), 1016(9), 845(4), 766(4), 753(8), 416(4), 378(3), 333(3), 271(3) cm^{-1} ; **Elemental analysis** ($\text{C}_3\text{H}_2\text{N}_8\text{O}_3$): calc.: C 13.64, H 3.05, N 53.02 %; found: C 14.79, H 3.17, N 54.79 %. **Mass spectrometry**: m/z (FAB^+): 34.2 [NH_3OH^+], m/z (FAB^-): 197.1 [$\text{C}_3\text{HN}_8\text{O}_3^-$]. **Sensitivities** (anhydrous, grain size < 100 μm): friction: 360 N; impact: 8 J. **DSC** (5 $^\circ\text{C min}^{-1}$): $T_{\text{dec.}}$ = 175 $^\circ\text{C}$.

Guanidinium 5-(3-Nitro-1,2,4-1H-triazolate-5-yl)tetrazol-1-olate (3b)

A solution of guanidinium carbonate (0.45 g, 2.5 mmol) in water (5 mL) was added to a solution of **5** (0.5 g, 2.5 mmol) in ethanol (50 mL) and refluxed for 30 minutes. After cooling down to room temperature the precipitate was collected by filtration, washed with ethanol and diethyl ether and dried in air to yield **3b** as yellow powder. (0.6 g, 1.9 mmol, 75 %). **^1H NMR** ($\text{DMSO}-d_6$): δ = 7.33 (s, 6H, NH_2 , G^+) ppm. **^{13}C NMR** ($\text{DMSO}-d_6$): δ = 165.9 ($\text{C}-\text{NO}_2$), 158.7 (C_{Gu}), 151.9 ($\text{C}_{\text{triazole}}$), 138.7 ($\text{C}_{\text{tetrazole}}$) ppm. **^{14}N NMR** ($\text{DMSO}-d_6$): δ = -13.6 (NO_2) ppm; **IR**: ν (rel. int.) = 3478(m), 3423(m), 3303(m), 3116(s), 1679(s), 1648(s), 1634(s), 1580(m), 1507(m), 1468(vs), 1390(vs), 1352(vs), 1304(s), 1241(s), 1213(m), 1149(m), 1075(s), 993(m), 840(vs), 766(s), 711(m), 675(s), 656(vs), 656(vs) cm^{-1} ; **Raman** (200 mW): ν (rel. int.) = 1581(78), 1509(8), 1468(3), 1392(100), 1351(39), 1305(17), 1283(58), 1242(4), 1216(2), 1150(16), 1111(8), 1081(85), 1035(8), 1026(11), 1014(14), 842(9), 767(2), 755(4), 540(4), 494(2), 425(3), 318(2), 249(3), 249(3) cm^{-1} ; **Elemental analysis** ($\text{C}_3\text{H}_2\text{N}_8\text{O}_3$): calc.: C 18.99, H 3.82, N 62.01 %; found: C 19.57, H 3.69, N 60.71 %. **Mass spectrometry**: m/z (FAB^+): 60.0 [C_6HN_3^+], m/z (FAB^-): 197.3 [$\text{C}_3\text{HN}_8\text{O}_3^-$]. **Sensitivities** (anhydrous, grain size < 100 μm): friction: 360 N; impact: 40 J. **DSC** (5 $^\circ\text{C min}^{-1}$): $T_{\text{dec.}}$ = 269 $^\circ\text{C}$.

Triaminoguanidinium 5-(3-Nitro-1,2,4-1H-triazolate-5-yl)tetrazol-1-olate (3c)

Triaminoguanidine (0.52 g, 5.0 mmol) was added to a solution of **5** (0.5 g, 2.5 mmol) in ethanol (50 mL) and the mixture was stirred at 40 $^\circ\text{C}$ for 30 minutes. After cooling down to room temperature the precipitate was collected by filtration, washed with ethanol and diethyl ether and dried in air to yield **3c** as pale yellow powder. (0.67 g, 1.6 mmol, 66 %). **^1H NMR** ($\text{DMSO}-d_6$): δ = 8.7 (s, 3H, NH , TAG^+), 4.5 (s, 6H, NH_2 , TAG^+) ppm. **^{13}C NMR** ($\text{DMSO}-d_6$): δ = 166.3 ($\text{C}-\text{NO}_2$), 159.7 (C_{TAG}), 152.8 ($\text{C}_{\text{triazole}}$), 138.9 ($\text{C}_{\text{tetrazole}}$)

ppm; ^{14}N NMR (DMSO- d_6): $\delta = -10$ (NO_2) ppm; ^{15}N NMR (DMSO- d_6): δ (ppm) = -17.0 (N6), -18.3 (N8), -20.2 (N5), -54.0 (N7), -57.0 (N1), -60.2 (N2), -82.4 (N4), -143.7 (N3), -289.4 (TAG^+ , NH), -329.8 (TAG^+ , NH_2); **IR**: ν (rel. int.) = $3320(\text{m})$, $3175(\text{m})$, $1678(\text{s})$, $1662(\text{s})$, $1530(\text{m})$, $1465(\text{s})$, $1384(\text{s})$, $1343(\text{m})$, $1308(\text{s})$, $1191(\text{s})$, $1132(\text{s})$, $1100(\text{m})$, $987(\text{s})$, $956(\text{s})$, $953(\text{s})$, $907(\text{s})$, $904(\text{s})$, $877(\text{m})$, $839(\text{vs})$, $796(\text{m})$, $756(\text{s})$, $718(\text{m})$, $703(\text{m})$, $703(\text{m})$, $699(\text{s})$, $695(\text{s})$, $684(\text{s})$, $660(\text{s})$, $652(\text{s})$ cm^{-1} ; **Raman** (200 mW): ν (rel. int.) = $3221(2)$, $1891(2)$, $1577(82)$, $1466(11)$, $1413(19)$, $1386(87)$, $1349(7)$, $1308(25)$, $1296(20)$, $1236(23)$, $1195(4)$, $1123(10)$, $1102(100)$, $1032(6)$, $1015(14)$, $883(3)$, $839(5)$, $759(4)$, $639(3)$, $502(2)$, $418(6)$, $370(3)$ cm^{-1} ; **Elemental analysis** ($\text{C}_3\text{H}_2\text{N}_8\text{O}_3$): calc.: C 14.45, H 4.47, N 68.94 %; found: C 14.72, H 4.75, N 64.97 %; **Mass spectrometry**: m/z (FAB^+): 105.1 [CH_9N_3^+], m/z (FAB^-): 197.2 [$\text{C}_3\text{HN}_8\text{O}_3^-$]. **Sensitivities** (anhydrous, grain size < 100 μm): friction: 360 N; impact: 10 J. **DSC** (5 $^\circ\text{C}$ min^{-1}): $T_{\text{dec.}} = 181$ $^\circ\text{C}$.

Hydroxylamonium 5-(5-Nitramino-1H-1,2,4-triazolate-3-yl) tetrazol-1-olate (4a)

Hydroxylamine (50 wt% in water, 0.3 mL, 4.6 mmol) was added to a solution of **3** (0.5 g, 2.3 mmol) in ethanol (50 mL) and the mixture was stirred at 60 $^\circ\text{C}$ for 5 minutes. After cooling down to room temperature the precipitate was collected by filtration, washed with ethanol and diethyl ether and dried in air to yield **4a** as colorless powder. (0.52 g, 1.9 mmol, 80 %). ^1H NMR (DMSO- d_6): $\delta = 8.42$ (s, 3H, NH_3OH^+) ppm. ^{13}C NMR (DMSO- d_6): $\delta = 158.1$ (C-NHNO_2), 147.8 ($\text{C}_{\text{triazole}}$), 138.6 ($\text{C}_{\text{tetrazole}}$) ppm. ^{14}N NMR (DMSO- d_6): $\delta = -10$ (NO_2) ppm; **IR**: ν (rel. int.) = $3464(\text{s})$, $3366(\text{s})$, $3179(\text{s})$, $1644(\text{vs})$, $1523(\text{s})$, $1470(\text{vs})$, $1425(\text{s})$, $1405(\text{m})$, $1375(\text{s})$, $1344(\text{vs})$, $1273(\text{s})$, $1242(\text{s})$, $1209(\text{s})$, $1101(\text{s})$, $1085(\text{s})$, $1003(\text{s})$, $988(\text{s})$, $764(\text{s})$, $724(\text{vs})$ cm^{-1} ; **Raman** (200 mW): ν (rel. int.) = $1606(97)$, $1600(100)$, $1539(20)$, $1491(15)$, $1481(20)$, $1386(12)$, $1359(6)$, $1319(3)$, $1252(9)$, $1152(21)$, $1138(17)$, $1085(3)$, $1030(25)$, $1017(34)$, $985(7)$, $876(7)$, $763(11)$, $755(10)$, $732(3)$, $600(3)$, $442(5)$, $303(2)$, $280(4)$, $280(4)$, $253(2)$ cm^{-1} ; **Elemental analysis** ($\text{C}_3\text{H}_2\text{N}_8\text{O}_3$): calc.: C 12.91, H 3.25, N 55.19 %; found: C 13.19, H 3.33, N 53.72 %; **Mass spectrometry**: m/z (FAB^+): 34.1 [NH_3OH^+], m/z (FAB^-): 212.1 [$\text{C}_3\text{HN}_9\text{O}_3^-$]. **Sensitivities** (anhydrous, grain size < 100 μm): friction: 288 N; impact: 8 J. **DSC** (5 $^\circ\text{C}$ min^{-1}): $T_{\text{dec.}} = 179$ $^\circ\text{C}$.

Guanidinium 5-(5-Nitramino-1H-1,2,4-triazolate-3-yl)tetrazol-1-olate (4b)

A solution of guanidinium carbonate (0.42 g, 2.3 mmol) in water (5 mL) was added to a solution of **3** (0.5 g, 2.3 mmol) in ethanol (50 mL) and the mixture was refluxed for 30 minutes. After cooling down to room temperature the precipitate was collected by filtration, washed with ethanol and diethyl ether and dried in air to yield **4b** as colorless powder. (0.66 g, 2.0 mmol, 85 %). **¹H NMR** (DMSO-*d*₆): δ = 7.23 (s, 6H, NH₂, G⁺) ppm. **¹³C NMR** (DMSO-*d*₆): δ = 158.6 (C, G⁺), 157.9 (C–NHNO₂), 148.8 (C_{triazole}), 138.1 (C_{tetrazole}) ppm; **¹⁴N NMR** (DMSO-*d*₆): δ = –11 (NO₂) ppm; **IR**: ν (rel. int.) = 3548(vw), 3456(m), 3370(m), 3179(m), 3116(m), 1681(m), 1642(vs), 1587(w), 1523(m), 1468(s), 1425(m), 1382(s), 1369(s), 1345(vs), 1259(m), 1243(s), 1210(m), 1159(m), 1100(m), 1084(s), 1010(m), 987(s), 863(w), 863(w), 764(s), 746(m), 723(s), 677(m) cm^{–1}; **Raman** (200 mW): ν (rel. int.) = 3217(2), 1594(100), 1524(34), 1474(21), 1425(5), 1413(4), 1406(4), 1371(19), 1349(6), 1262(3), 1247(4), 1213(5), 1161(8), 1134(7), 1087(3), 1023(52), 1011(34), 988(3), 865(5), 773(6), 748(8), 539(7), 451(5), 451(5), 442(8), 273(4), 247(3) cm^{–1}; **Elemental analysis** (C₃H₂N₈O₃): calc.: C 18.13, H 3.96, N 63.43 %; found: C 17.80, H 4.17, N 59.31 %; **Mass spectrometry**: m/z (FAB⁺): 60.1 [CH₆N₃⁺], m/z (FAB[–]): 212.1 [C₃HN₉O₃[–]]. **Sensitivities** (anhydrous, grain size < 100 μ m): friction: 360 N; impact: 40 J. **DSC** (5 °C min^{–1}): $T_{\text{dec.}}$ = 212 °C.

Triaminoguanidinium 5-(5-Nitramino-1H-1,2,4-triazolate-3-yl)tetrazol-1-olate (4c)

Triaminoguanidine (0.49 g, 4.6 mmol) was added to a solution of **5** (0.5 g, 2.3 mmol) in ethanol (50 mL) and the mixture was stirred at 40 °C for 30 minutes. After cooling down to room temperature the precipitate was collected by filtration, washed with ethanol and diethyl ether and dried in air to yield **4c** as colorless powder. (0.83 g, 2.0 mmol, 84 %). **¹H NMR** (DMSO-*d*₆): δ = 8.59 (s, 3H, NH, TAG⁺), 4.36 (s, 6H, NH₂, TAG⁺) ppm. **¹³C NMR** (DMSO-*d*₆): δ = 159.6 (C_{TAG}), 158.1 (C–NHNO₂), 148.7 (C_{triazole}), 137.7 (C_{tetrazole}) ppm; **¹⁴N NMR** (DMSO-*d*₆): δ = –10 (NO₂) ppm. **IR**: ν (rel. int.) = 3320(m), 3207(s), 1685(vs), 1524(m), 1468(s), 1328(vs), 1237(m), 1198(m), 1133(s), 1076(m), 980(s), 967(s), 856(m), 768(s), 728(m) cm^{–1}; **Raman** (200 mW): ν (rel. int.) = 3321(6), 3236(9), 1682(5), 1592(100), 1524(46), 1469(22), 1370(13), 1236(4), 1187(3), 1140(13), 1084(2), 1009(37), 883(13), 865(9), 749(10), 638(4), 417(6), 270(6) cm^{–1}; **Elemental analysis** (C₃H₂N₈O₃): calc.: C 14.25, H 4.55, N 69.81 %; found: C 13.82, H 4.78, N 64.78 %; **Mass spectrometry**: m/z (FAB⁺): 105.0 [CH₉N₆⁺], m/z (FAB[–]): 212.1

([C₃HN₉O₃⁻]). **Sensitivities** (anhydrous, grain size < 100 μm): friction: 288 N; impact: 10 J. **DSC** (5 °C min⁻¹): T_{dec.} = 186 °C.

REFERENCES

- [1] a) W. D. Won, L. H. DiSalvo, J. Ng, *Appl. Environ. Microb.* **1976**, *31*, 576-580; b) J. A. Steevens, B. M. Duke, G. R. Lotufo, T. S. Bridges, *Environ. Toxicol. Chem.* **2002**, *21*, 1475-1482; c) M. B. Talawar, R. Sivabalan, T. Mukundan, H. Muthurajan, A. K. Sikder, B. R. Gandhe, A. S. Rao, *J. Hazard. Mater.* **2009**, *161*, 589-607; d) P. Richter-Torres, A. Dorsey, C. S. Hodes, *Toxicological Profile for 2,4,6-Trinitrotoluene*, U.S. Department of Health and Human Services, Public Health Service, Agency for Toxic Substances and Disease Registry, **1995**; e) W. McLellan, W. R. Hartley, M. Brower, *Health advisory for hexahydro-1,3,5-trinitro-1,3,5-triazine*, Technical report PB90-273533; Office of Drinking Water, U.S. Environmental Protection Agency: Washington, DC, **1988**; f) P. Y. Robidoux, J. Hawari, G. Bardai, L. Paquet, G. Ampleman, S. Thiboutot, G. I. Sunahara, *Arch. Environ. Con. Tox.* **2002**, *43*, 379-388; g) A. Esteve-Núñez, A. Caballero, J. L. Ramos, *Microbiol. Mol. Biol. Rev.* **2001**, *65*, 335-352; h) B. Van Aken, J. M. Yoon, J. L. Schnoor, *Appl. Environ. Microbiol.* **2004**, *70*, 508-517.
- [2] *NATO standardization agreement (STANAG) - Policy for introduction and assessment of Insensitive Munitions (MURAT) no.4439, 3rd ed., Mar. 17, 2010.*
- [3] a) N. Fischer, D. Izsák, T. M. Klapötke, S. Rappenglück, J. Stierstorfer, *Chem-Eur. J.* **2012**, *18*, 4051-4062; b) T. M. Klapötke, *Chemistry of high-energy materials*, 2nd ed., De Gruyter: Berlin **2012**; c) C. M. Sabate, T. M. Klapötke, *New Trends in Research of Energetic Materials, Proceedings of the 12th Seminar, University of Pardubice, Czech Republic*, **2009**, 172-194; d) S. Yang, S. Xu, H. Huang, W. Zhang, X. Zhang, *Prog. Chem.* **2008**, *20*, 526-537; e) D. E. Chavez, M. A. Hiskey, D. L. Naud, *Prop. Explos. Pyrot.* **2004**, *29*, 209-215; f) P. F. Pagoria, G. S. Lee, A. R. Mitchell, R. D. Schmidt, *Thermochim. Acta* **2002**, *384*, 187-204.
- [4] a) A. A. Dippold, T. M. Klapötke, N. Winter, *Eur. J. Inorg. Chem.* **2012**, *2012*, 3474-3484; b) A. A. Dippold, T. M. Klapötke, *Chem-Eur. J.* **2012**, *18*, 16742-16753; c) A. A. Dippold, M. Feller, T. M. Klapötke, *Centr. Eur. J. Energ. Mat.* **2011**, *8*, 261-278.

- [5] a) A. A. Dippold, T. M. Klapötke, *Chem-Asian J.* **2013**, 8, 1463-1471; b) A. A. Dippold, T. M. Klapötke, d. Izsak, *Chem-Eur. J.* **2013**, *in press*, DOI: chem.201301339.
- [6] A. A. Dippold, T. M. Klapötke, F. A. Martin, *Z. Anorg. Allg. Chem.* **2011**, 637, 1181-1193.
- [7] M. J. Frisch, G. W. Trucks, H. B. Schlegel, G. E. Scuseria, M. A. Robb, J. R. Cheeseman, G. Scalmani, V. Barone, B. Mennucci, G. A. Petersson, H. Nakatsuji, M. Caricato, X. Li, H. P. Hratchian, A. F. Izmaylov, J. Bloino, G. Zheng, J. L. Sonnenberg, M. Hada, M. Ehara, K. Toyota, R. Fukuda, J. Hasegawa, M. Ishida, T. Nakajima, Y. Honda, O. Kitao, H. Nakai, T. Vreven, J. A. J. Montgomery, J. E. Peralta, F. Ogliaro, M. Bearpark, J. J. Heyd, E. Brothers, K. N. Kudin, V. N. Staroverov, R. Kobayashi, J. Normand, K. Raghavachari, A. Rendell, J. C. Burant, S. S. Iyengar, J. Tomasi, M. Cossi, N. Rega, J. M. Millam, M. Klene, J. E. Knox, J. B. Cross, V. Bakken, C. Adamo, J. Jaramillo, R. Gomperts, R. E. Stratmann, O. Yazyev, A. J. Austin, R. Cammi, C. Pomelli, J. W. Ochterski, R. L. Martin, K. Morokuma, V. G. Zakrzewski, G. A. Voth, P. Salvador, J. J. Dannenberg, S. Dapprich, A. D. Daniels, Ö. Farkas, J. B. Foresman, J. V. Ortiz, J. Cioslowski, D. J. Fox, *Wallingford CT* **2009**.
- [8] A. A. Dippold, T. M. Klapötke, N. Winter, *Eur. J. Inorg. Chem.* **2012**, 2012, 3474-3484.
- [9] N. Fischer, T. M. Klapötke, M. Reymann, J. Stierstorfer, *Eur. J. Inorg. Chem.* **2013**, 2167-2180.
- [10] a) A. F. Hollemann, E. Wiberg, N. Wiberg, *Lehrbuch der anorganischen Chemie*, de Gruyter: New York, **2007**; b) F. H. Allen, O. Kennard, D. G. Watson, L. Brammer, A. G. Orpen, R. Taylor, *J. Chem. Soc., Perkin Trans. 2* **1987**, 1-19.
- [11] A. Bondi, *J. Phys. Chem.* **1964**, 68, 441-451.
- [12] a) M. Göbel, K. Karaghiosoff, T. M. Klapötke, D. G. Piercey, J. Stierstorfer, *J. Am. Chem. Soc.* **2010**, 132, 17216-17226; b) N. Fischer, D. Fischer, T. M. Klapötke, D. G. Piercey, J. Stierstorfer, *J. Mat. Chem.* **2012**, 22, 20418-20422.
- [13] R. Meyer, J. Köhler, A. Homburg, *Explosives*, 6th ed., Wiley-VCH Verlag GmbH & Co. KGaA, Weinheim, **2007**.
- [14] a) M. S. Molchanovaa, T. S. Pivinaa, E. A. Arnautovab, N. S. Zefirovb, *J. Mol. Struct. THEOCHEM* **1999**, 465, 11-24; b) M. Goebel, K. Karaghiosoff, T. M. Klapötke, D. G. Piercey, J. Stierstorfer, *J. Am. Chem. Soc.* **2010**, 132, 17216-

- 17226; c) H. Singh, U. Mukherjee, R. S. Saini, *J. Energ. Mater.* **2012**, 30, 265-281; d) T. M. Klapötke, D. G. Piercey, J. Stierstorfer, *Chem-Eur. J.* **2011**, 17, 13068-13077.
- [15] *NATO standardization agreement (STANAG) on explosives and impact tests, no.4489, 1st ed., Sept. 17, 1999.*
- [16] *WIWEB-Standardarbeitsanweisung 4-5.1.02, Ermittlung der Explosionsgefährlichkeit, hier: der Schlagempfindlichkeit mit dem Fallhammer, Nov. 08, 2002.*
- [17] <http://www.bam.de>.
- [18] *NATO standardization agreement (STANAG) on explosives, friction tests, no.4487, 1st ed., Aug. 22, 2002.*
- [19] *WIWEB-Standardarbeitsanweisung 4-5.1.03, Ermittlung der Explosionsgefährlichkeit, hier: der Reibempfindlichkeit mit dem Reibeapparat, Nov. 08, 2002.*
- [20] *NATO standardization agreement (STANAG) on explosives, electrostatic discharge sensitivity tests, no.4490, 1st ed., Feb. 19, 2001.*
- [21] *CrysAlisPro 1.171.36.21, Agilent Technologies, 2012.*
- [22] A. Altomare, M. C. Burla, M. Camalli, G. L. Cascarano, C. Giacovazzo, A. Guagliardi, A. G. G. Moliterni, G. Polidori, R. Spagna, *J. Appl. Cryst.* **1999**, 32, 115-119.
- [23] G. M. Sheldrick, *Acta Crystallogr. Sect. A* **2008**, 64, 112–122.
- [24] A. L. Spek, *Platon, A Multipurpose Crystallographic Tool, Utrecht University, Utrecht, The Netherlands, 2012.*
- [25] L. J. Farrugia, *J. Appl. Crystallogr.* **1999**, 32, 837-838.
- [26] <http://journals.iucr.org/services/cif/checkcif.html>
- [27] C. F. Macrae, P. Edgington, P. McCabe, E. Pidcock, G. P. Shields, R. Taylor, M. Towler, J. van de Streek, *J. Appl. Crystallogr.* **2006**, 39, 565.

12. APPENDIX

LIST OF ABBREVIATIONS

Å	Angström (10^{-10} m)
ADN	Ammonium dinitramide
AG	Aminoguanidinium cation
ANTA	5-Amino-3-nitro-1 <i>H</i> -1,2,4-triazole
AP	Ammonium perchlorate
ATR	Attenuated total reflection
d	doublet
δ	Chemical shift
DCI	Desorption chemical ionization (MS)
DCT	4,5-Dicyano-1,2,3-triazolate anion
dec.	Decomposition
DEI	Desorption electron impact (MS)
DSC	Differential Scanning Calorimetry
EI	Electron impact (MS)
FAB	Fast atom bombardment (MS)
FW	Formula weight
G	Guanidinium cation
HMX	1,3,5,7-tetranitro-1,3,5,7-tetrazocane
Hz	Hertz
IR	Infrared
J	Coupling constant (NMR); Joule (Sensitivity)
KDN	Potassium dinitramide
m	medium (IR); multiplett (NMR)
<i>m/z</i>	mass per charge (MS)
MeNO ₂	Nitromethane
MS	Mass spectrometry
N	Newton
NMR	Nuclear Magnetic Resonance
NQ	Nitroguanidine
<i>P</i> _{C-J}	Detonation pressure at the Chapman-Jouguet point
ppm	parts per million (NMR)
q	quartet
ρ	Density (g cm ⁻³)
RDX	1,3,5-trinitro-1,3,5-triazinane
<i>r</i> _w	van der Waals radii
<i>S</i>	Goodness of Fit
s	strong (IR); singlet (NMR)

STANAG	Standardization agreement
t	triplet
T	Temperature
TATB	Trinitrotriaminobenzene
T _{ex}	Temperature of explosion
TAG	Triaminoguanidinium cation
TLC	Thin layer chromatography
TMS	Tetramethylsilyl
TNT	Trinitrotoluene
vs	very strong (IR)
Ω	Oxygen balance
w	weak (IR)
Z	Number of asymmetric units in unit cell

SUPPORTING INFORMATION FOR CHAPTER 5

Table S1: Crystallographic data and parameter for compounds **1,2 4** and **5**.

	DABT × DMSO (1)	DNBT (2)	DAzBT (4)	DNMBT (5)
Formula	C ₈ H ₁₈ N ₈ O ₂ S ₂	C ₄ H ₂ N ₈ O ₄	C ₄ H ₆ N ₁₂ O ₂	C ₆ H ₈ N ₁₀ O ₁₀
FW [g mol ⁻¹]	322.4	226.1	254.2	380.2
Crystal system	monoclinic	monoclinic	triclinic	monoclinic
Space Group	<i>P</i> 2 ₁ / <i>c</i>	<i>P</i> 2 ₁ / <i>n</i>	<i>P</i> -1	<i>P</i> 2 ₁ / <i>c</i>
Color / Habit	colorless block	colorless block	colorless rod	colorless block
Size [mm]	0.35x0.20x0.10	0.2x0.2x0.1	0.58x0.07x0.06	0.31x0.19x0.05
<i>a</i> [Å]	9.530(1)	5.0559(6)	3.5621(7)	5.1144(3)
<i>b</i> [Å]	8.6066(7)	6.3080(7)	7.2277(13)	8.8867(5)
<i>c</i> [Å]	9.958(1)	12.4268(14)	10.509(2)	14.2716(9)
α [°]	90	90	72.298(18)	90
β [°]	113.22(1)	95.136(11)	85.348(17)	93.531(6)
γ [°]	90	90	84.947(15)	90
<i>V</i> [Å ³]	750.55(14)	394.73(8)	256.34(9)	647.41(7)
<i>Z</i>	2	2	1	2
$\rho_{\text{calc.}}$ [g cm ⁻³]	1.4267(3)	1.9024(4)	1.6465(6)	1.9503(2)
μ [mm ⁻¹]	0.370	0.169	0.137	0.184
<i>F</i> (000)	340	228	130	388
$\lambda_{\text{MoK}\alpha}$ [Å]	0.71073	0.71073	0.71073	0.71073
<i>T</i> [K]	173	173	173	173
Theta Min-Max [°]	4.28–28.88	4.23–26.50	4.25–32.21	4.15–33.45
Dataset h	-11; 5	-6; 6	-5; 4	-6; 6
Dataset k	-10; 9	-7; 7	-8; 8	-10; 11
Dataset l	-12; 12	-15; 8	-12; 12	-12; 18
Reflections collected	1460	2036	2576	3565
Independent reflections	1251	809	996	1406
Observed reflections	1088	678	798	1170
No. parameters	144	77	94	134
<i>R</i> _{int}	0.0220	0.0283	0.0337	0.0290
<i>R</i> ₁ , w <i>R</i> ₂ (I> σ I ₀)	0.0397; 0.0927	0.0347; 0.0827	0.0335; 0.0739	0.0353; 0.0902
<i>R</i> ₁ , w <i>R</i> ₂ (all data)	0.0481; 0.0976	0.0434; 0.0891	0.0480; 0.0811	0.0457; 0.0972
<i>S</i>	1.143	1.036	1.051	1.064
Resd. Dens. [e Å ⁻³]	0.225; -0.316	0.201; -0.281	0.155; -0.162	0.376; -0.254
Device type	Oxford Xcalibur3 CCD	Oxford Xcalibur3 CCD	Oxford Xcalibur3 CCD	Oxford Xcalibur3 CCD
Solution	SHELXS-97	SHELXS-97	SHELXS-97	SHELXS-97
Refinement	SHELXL-97	SHELXL-97	SHELXL-97	SHELXL-97
Absorption correction	multi-scan	multi-scan	multi-scan	multi-scan
CCDC	887530	864398	887531	887532

SUPPORTING INFORMATION FOR CHAPTER 6

Table S1: Crystallographic data and parameter for DNBT and the corresponding salts.

	DNBT (2)	NH ₄ -DNBT x 2 H ₂ O (3a)	Hx-DNBT (3c)	AG-DNBT x 2 H ₂ O (3e)	TAG-DNBT (3f)
Measurement	hx016	gx391	qn034	gx384	gx380
Formula	C ₄ H ₂ N ₈ O ₄	C ₄ H ₁₂ N ₁₀ O ₆	C ₄ H ₈ N ₁₀ O ₆	C ₆ H ₁₈ N ₁₆ O ₆	C ₆ H ₁₈ N ₂₀ O ₄
FW [g mol ⁻¹]	226.110	296.202	292.170	410.311	434.340
Crystal system	monoclinic	monoclinic	monoclinic	triclinic	triclinic
Space Group	<i>P</i> 2 ₁ / <i>n</i>	<i>P</i> 2 ₁ / <i>n</i>	<i>P</i> 2 ₁ / <i>c</i>	<i>P</i> -1	<i>P</i> -1
Color / Habit	colorless block	colorless plate	colorless rod	yellow plate	colorless block
Size [mm]	0.2x0.2x0.1	0.59x0.58x0.11	0.25x0.09x0.03	0.42x0.21x0.01	0.44x0.41x0.39
<i>a</i> [Å]	5.0559(6)	7.1796(16)	3.8248(2)	4.7081(6)	7.1460(8)
<i>b</i> [Å]	6.3080(7)	11.736(2)	14.2620(10)	7.5734(10)	7.4574(9)
<i>c</i> [Å]	12.4268(14)	7.6060(15)	9.7288(7)	12.197(2)	8.4596(8)
α [°]	90	90	90	105.107(14)	93.973(9)
β [°]	95.136(11)	104.65(2)	95.014(4)	94.072(12)	101.610(9)
γ [°]	90	90	90	97.894(10)	99.154(9)
<i>V</i> [Å ³]	394.73(8)	620.1(2)	528.67(6)	413.29(10)	433.57(8)
<i>Z</i>	2	2	2	1	1
$\rho_{\text{calc.}}$ [g cm ⁻³]	1.9024(4)	1.5864(5)	1.8354(2)	1.6486(4)	1.6635(3)
μ [mm ⁻¹]	0.169	0.143	0.167	0.142	0.139
<i>F</i> (000)	228	308	300	214	226
$\lambda_{\text{MoK}\alpha}$ [Å]	0.71073	0.71073	0.71073	0.71073	0.71073
<i>T</i> [K]	173	173	173	173	
Theta Min-Max [°]	4.23–26.50	4.44–26.49	3.55–25.31	4.55–26.49	4.24–26.50
Dataset h	-6; 6	-7; 9	-4, 4	-5; 5	-8, 8
Dataset k	-7; 7	-13; 14	-17; 17	-9; 8	-9; 9
Dataset l	-15; 8	-9; 9	-11; 11	-13; 15	-10; 10
Reflections collected	2036	3198	3411	2152	4595
Independent reflections	809	1266	962	1660	1791
Observed reflections	678	1119	805	947	1376
No. parameters	77	115	107	161	163
<i>R</i> _{int}	0.0283	0.0200	0.0348	0.0166	0.0219
<i>R</i> ₁ , w <i>R</i> ₂ (<i>I</i> > σ <i>I</i> ₀)	0.0347; 0.0827	0.0588; 0.1351	0.0400; 0.0936	0.0408; 0.0827	0.0323; 0.0832
<i>R</i> ₁ , w <i>R</i> ₂ (all data)	0.0434; 0.0891	0.0641; 0.1367	0.0512; 0.0998	0.0819; 0.0892	0.0448; 0.0870
<i>S</i>	1.036	1.208	1.091	0.824	0.982
Resd. Dens. [e Å ⁻³]	0.201; -0.281	0.327; -0.330	0.236; -0.244	0.180; -0.313	0.180; -0.289
Device type	Oxford Xcalibur3 CCD	Oxford Xcalibur3 CCD	Kappa CCD	Oxford Xcalibur3 CCD	Oxford Xcalibur3 CCD
Solution	SHELXS-97	SHELXS-97	SHELXS-97	SHELXS-97	SHELXS-97
Refinement	SHELXL-97	SHELXL-97	SHELXL-97	SHELXL-97	SHELXL-97
Absorption correction	multi-scan	multi-scan	none	multi-scan	multi-scan
CCDC	864398	864400	864399	864397	864401

Table S2: Selected bond lengths[Å], bond angles [°] and torsion angles [°] of compounds **2** and **3a–f**.

	DNBT (2)	(NH ₄) ₂ DNBT 2H ₂ O (3a)	(NH ₃ OH) ₂ × DNBT (3c)	(AG) ₂ × 2H ₂ O (3e)	DNBT (TAG) ₂ DNBT (3f)
bond length [Å]					
N1–N2	1.3497(18)	1.372(3)	1.364(2)	1.358(3)	1.3672(15)
N2–C2	1.315(2)	1.320(4)	1.322(3)	1.323(3)	1.3240(17)
C2–N3	1.3456(18)	1.336(4)	1.338(3)	1.329(3)	1.3337(16)
N3–C1	1.3282(19)	1.352(4)	1.345(3)	1.352(3)	1.3443(17)
C1–C1(<i>i</i>)	1.453(2)	1.471(4)	1.453(3)	1.448(3)	1.4630(18)
C2–N4	1.4533(19)	1.450(4)	1.437(3)	1.447(3)	1.4429(17)
N4–O1	1.2360(17)	1.226(4)	1.218(2)	1.231(2)	1.2318(15)
N4–O2	1.2223(18)	1.223(4)	1.226(3)	1.229(3)	1.2296(14)
bond angles [°]					
N1–N2–C2	100.57(13)	104.3(2)	103.82(16)	102.95(18)	103.35(10)
N2–C2–N3	118.10(13)	116.4(3)	116.65(18)	117.8(2)	117.38(12)
C2–N3–C1	100.57(11)	100.0(3)	99.85(16)	99.25(18)	99.37(10)
N3–C1–N1	110.57(13)	113.8(3)	113.59(17)	113.26(19)	114.01(11)
C1–N1–N2	110.19(13)	105.6(3)	106.09(16)	106.75(17)	105.89(10)
O1–N4–O2	124.39(12)	124.3(3)	123.60(18)	124.87(18)	123.58(11)
torsion angles [°]					
O1–N4–C2–N2	2.9(2)	-1.7(4)	-9.4(3)	-6.2(3)	-2.83(19)
O2–N4–C2–N3	2.9(2)	0.4(5)	-7.6(3)	-7.4(3)	-3.83(19)

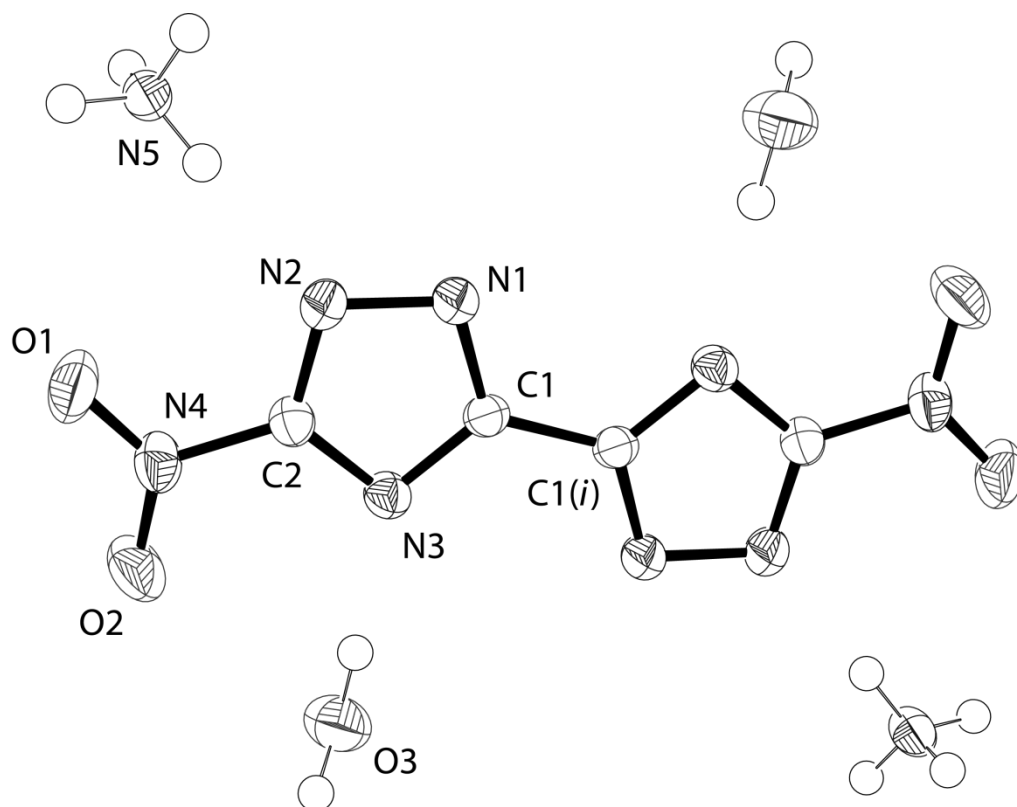


Figure S1: Molecular structure of ammonium 3,3'-dinitro-bis-(1,2,4-triazolate) (**3a**). Thermal ellipsoids present the 50 % probability level; symmetry operator: (i) 1-x, -y, 2-z

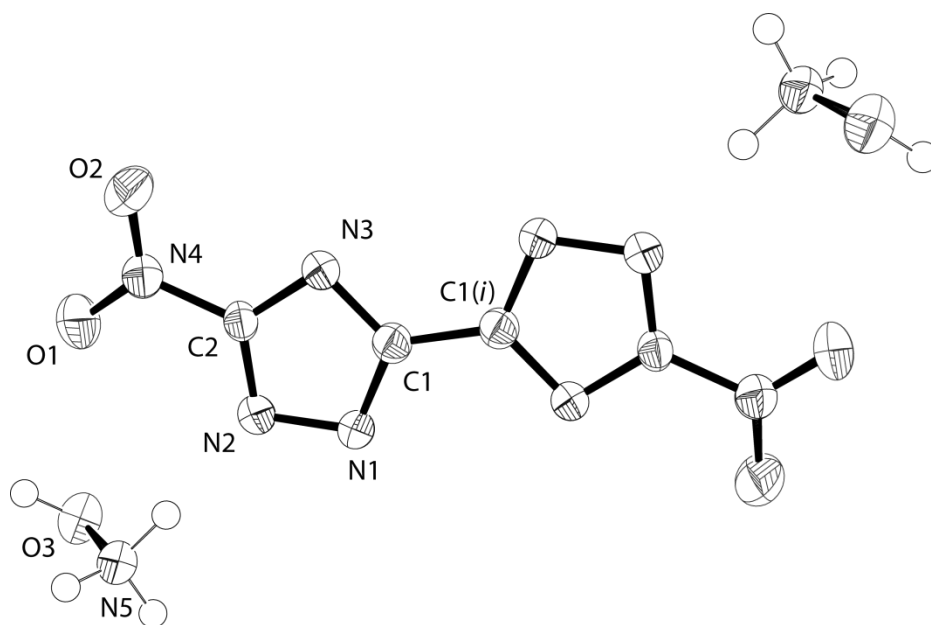


Figure S2: Molecular structure of hydroxylammonium 3,3'-dinitro-bis-(1,2,4-triazolate) (**3c**). Thermal ellipsoids present the 50 % probability level; symmetry operator: (i) 1-x, 1-y, -z.

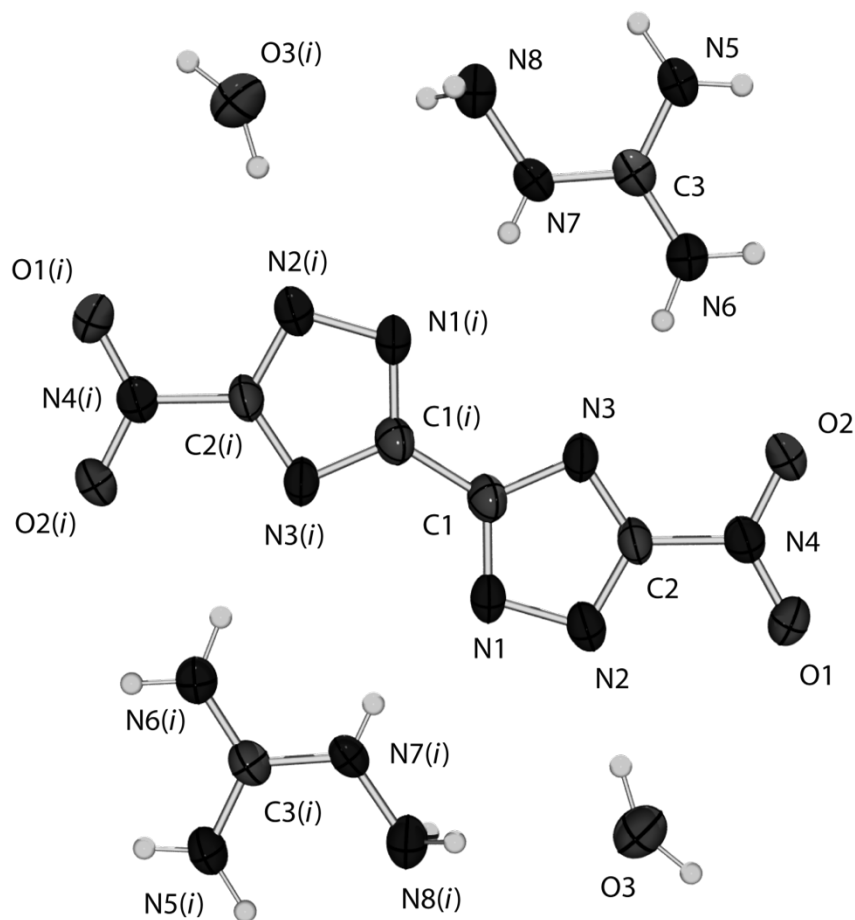


Figure S3: Molecular structure of aminoguanidinium 3,3'-dinitro-bis-(1,2,4-triazolate) (**3e**). Thermal ellipsoids present the 50 % probability level; Symmetry operator: (i) $-1-x, 1-y, 1-z$.

SUPPORTING INFORMATION FOR CHAPTER 7

Heats of Formation

In bomb calorimetric measurements nitrogen-rich highly energetic compounds tend to burn incompletely due to the trend of explosion. Oftentimes wrong heats of combustion ($\Delta_c H$) and finally wrong heats of formation ($\Delta_f H^\circ$) are obtained. Therefore the heats of formation of **5–7** have been calculated on the same level for better comparison. All calculations were carried out using the Gaussian 09 (revision C.01) program package.^[1] The enthalpies (H) were calculated using the complete basis set (CBS) method described by Petersson and coworkers in order to obtain very accurate values. In this study we applied the modified CBS-4M method (M referring to the use of minimal population localization) which is a re-parameterized version of the original CBS-4 method and also includes some additional empirical corrections.^[2]

The enthalpies of the gas-phase species M were calculated by the atomization energy method according to Equation 1,^[3] using literature values for atomic $\Delta_f H^\circ_{(g,A)}$.^[4]

$$\Delta_f H^\circ_{(g,M)} = H^{298}_{(g,M)} - \sum H^{298}_{(g,A)} + \sum \Delta_f H^\circ_{(g,A)} \quad (1)$$

The solid-state enthalpy of formation for neutral compounds can be estimated with Trouton's rule according to Equation 2,^[5] where T is either the melting point or the decomposition temperature (in K) if no melting occurs prior to decomposition.

$$\Delta_f H^\circ_{(s)} = \Delta_f H^\circ_{(g)} - \Delta_{\text{sub}} H = \Delta_f H^\circ_{(g)} - (188 / \text{J mol}^{-1} \text{ K}^{-1} \times T) \quad (2)$$

Finally, the solid-state molar enthalpies of formation ($\Delta_f H^\circ$) were used to calculate the solid-state energies of formation ($\Delta_f U^\circ$) according to Equation 3, with Δn being the change of moles of gaseous components.

$$\Delta U = \Delta H - \Delta n RT \quad (3)$$

Table S1: CBS-4M calculation results.

M	PG ^[a]	$-H$ / a.u. ^[b]	$\Delta_f H^\circ_{(g)}$ / kJ mol ⁻¹ ^[c]	$-\Delta n$ ^[d]
1	C ₁	833.286389	587.7	7.5
2	C ₁	778.023249	526.3	6.5
3	C ₁	737.128110	862.2	6.5
NNBT²⁻	C ₁	945.400176	229.1	–
NH₄O⁺	C _s	131.863249	164.1	–
G⁺	C ₁	205.453192	137.1	–
TAG⁺	C ₃	371.197775	208.8	–
4a	–	–	915.5	13.0
4b	–	–	800.3	16.0
4c	–	–	1102.1	22.0
RDX	C ₁	896.346781	174.2	9.0

[a] Point group, [b] CBS-4M calculated enthalpy, [c] gas-phase enthalpy of formation, [d] change of moles of gaseous components.

Table S2. Literature values for atomic $\Delta H^\circ_f{}^{298}$ / kcal mol⁻¹

	NIST ⁴
H	52.1
C	171.3
N	113.0
O	59.6

Table S3: Molecular volumes, lattice energies and lattice enthalpies.

	V _M / nm ³	U _L / kJ mol ⁻¹	ΔH_L / kJ mol ⁻¹
4a	0.271	1353.8	1358.8
4b	0.345	1235.3	1242.8
4c	0.431	1134.2	1141.6

REFERENCES

- [1] M. J. Frisch, G. W. Trucks, H. B. Schlegel, G. E. Scuseria, M. A. Robb, J. R. Cheeseman, G. Scalmani, V. Barone, B. Mennucci, G. A. Petersson, H. Nakatsuji, M. Caricato, X. Li, H. P. Hratchian, A. F. Izmaylov, J. Bloino, G. Zheng, J. L. Sonnenberg, M. Hada, M. Ehara, K. Toyota, R. Fukuda, J. Hasegawa, M. Ishida, T. Nakajima, Y. Honda, O. Kitao, H. Nakai, T. Vreven, J. A. Montgomery, Jr., J. E. Peralta, F. Ogliaro, M. Bearpark, J. J. Heyd, E. Brothers, K. N. Kudin, V. N. Staroverov, T. Keith, R. Kobayashi, J. Normand, K. Raghavachari, A. Rendell, J. C. Burant, S. S. Iyengar, J. Tomasi, M. Cossi, N. Rega, J. M. Millam, M. Klene, J. E. Knox, J. B. Cross, V. Bakken, C. Adamo, J. Jaramillo, R. Gomperts, R. E. Stratmann, O. Yazyev, A. J. Austin, R. Cammi, C. Pomelli, J. W. Ochterski, R. L. Martin, K. Morokuma, V. G. Zakrzewski, G. A. Voth, P. Salvador, J. J. Dannenberg, S. Dapprich, A. D. Daniels, O. Farkas, J. B. Foresman, J. V. Ortiz, J. Cioslowski, and D. J. Fox, *Gaussian 09 Revision C.01*, Gaussian, Inc., Wallingford, CT, USA, **2010**.
- [2] a) J. W. Ochterski, G. A. Petersson, J. A. Montgomery, *J. Chem. Phys.* **1996**, *104*, 2598–2619; b) J. A. Montgomery, M. J. Frisch, J. W. Ochterski, G. A. Petersson, *J. Chem. Phys.* **2000**, *112*, 6532–6542.
- [3] a) B. M. Rice, S. V. Pai, J. Hare, *Combust. Flame* **1999**, *118*, 445–458; b) B. M. Rice, J. J. Hare, *J. Phys. Chem. A* **2002**, *106*, 1770–1783; c) E. F. C. Byrd, B. M. Rice, *J. Phys. Chem. A* **2006**, *110*, 1005–1013.
- [4] a) P. J. Linstrom, W. G. Mallard (Editors), *NIST Standard Reference Database Number 69*, <http://webbook.nist.gov/chemistry> (accessed December 31, 2012); b) J. D. Cox, D. D. Wagman, V. A. Medvedev, *CODATA Key Values for Thermodynamics*, Hemisphere Publishing Corp., New York, **1984**.
- [5] a) F. Trouton, *Philos. Mag.* **1884**, *18*, 54–57; b) M. S. Westwell, M. S. Searle, D. J. Wales, D. H. Williams, *J. Am. Chem. Soc.* **1995**, *117*, 5013–5015.

SUPPORTING INFORMATION FOR CHAPTER 8

Table S1: Crystal density, selected bond lengths[Å] and bond angles [°] of compounds **2**, **3** and **4a–f**.

	DNBT (2)	DNBTO (3)	(NH ₄) ₂ DNBTO (4a)	(N ₂ H ₅) ₂ DNBTO (4c)	(NH ₃ OH) 2 DNBTO (4c)	(G) ₂ DNBTO (4c)	(AG) ₂ DNBTO (4c)	(TAG) ₂ DNBTO (4c)	DNBT ²⁻ (average)	DNBTO ²⁻ (average)
Crystal density [gcm ⁻³] (173 K)	1.764 (×2 H ₂ O)	1.862 (×2 H ₂ O)	1.696 (×2 H ₂ O)	1.841	1.952	1.788	1.764	1.730 (×2 H ₂ O)	/	/
bond length [Å]										
N1–N2	1.350(2)	1.339(2)	1.351(2)	1.354(3)	1.352(2)	1.349(4)	1.343(3)	1.348(5)	1.36	1.35
N2–C2	1.315(2)	1.328(2)	1.330(2)	1.330(3)	1.333(2)	1.328(5)	1.336(3)	1.336(5)	1.32	1.33
C2–N3	1.346(2)	1.333(2)	1.329(2)	1.339(3)	1.323(2)	1.328(5)	1.329(3)	1.334(5)	1.33	1.33
N3–C1	1.328(2)	1.342(2)	1.347(2)	1.350(3)	1.343(2)	1.348(5)	1.344(3)	1.346(5)	1.35	1.35
C1–C1(<i>i</i>)	1.453(2)	1.451(2)	1.452(3)	1.461(3)	1.443(2)	1.462(5)	1.451(3)	1.438(6)	1.46	1.45
C1–N1	1.349(2)	1.350(2)	1.358(2)	1.358(3)	1.364(2)	1.361(5)	1.363(3)	1.375(5)	1.35	1.36
C2–N4	1.453(2)	1.452(2)	1.448(2)	1.442(3)	1.433(2)	1.454(5)	1.440(3)	1.427(5)	1.45	1.44
N1–O3	/	1.349(2)	1.313(2)	1.294(3)	1.307(2)	1.294(4)	1.302(2)	1.296(4)	/	1.30
bond angles [°]										
N1–N2–C2	100.6(1)	99.8(1)	100.7(1)	101.4(2)	100.5(1)	101.0(3)	100.7(2)	101.0(3)	103.6	100.8
N2–C2–N3	118.1(1)	118.0(1)	118.3(2)	117.6(2)	118.1(2)	118.5(3)	118.0(2)	117.9(4)	117.2	118.3
C2–N3–C1	100.6(1)	101.5(1)	100.9(1)	101.0(2)	101.7(1)	100.6(3)	101.3(2)	101.6(3)	99.7	101.1
N3–C1–N1	110.6(1)	108.6(1)	110.1(2)	110.3(2)	109.4(1)	110.4(3)	109.6(2)	109.4(3)	113.7	109.8
C1–N1–N2	110.2(1)	112.1(1)	110.0(1)	109.7(2)	110.2(1)	109.5(3)	110.5(2)	110.2(3)	106.1	110.0

Heats of Formation

In bomb calorimetric measurements nitrogen-rich highly energetic compounds tend to burn incompletely due to the trend of explosion. Oftentimes wrong heats of combustion ($\Delta_c H$) and finally wrong heats of formation ($\Delta_f H^\circ$) are obtained. Therefore the heats of formation of RDX, **3** and **4a–f** have been calculated on the same level for better comparison. All calculations were carried out using the Gaussian 09 (revision C.01) program package.^[1] The enthalpies (H) were calculated using the complete basis set (CBS) method described by Petersson and coworkers in order to obtain very accurate values. In this study we applied the modified CBS-4M method (M referring to the use of

minimal population localization) which is a re-parameterized version of the original CBS-4 method and also includes some additional empirical corrections.^[2]

The enthalpies of the gas-phase species *M* were calculated by the atomization energy method according to Equation 1,^[3] using literature values for atomic $\Delta_f H^\circ_{(g,A)}$.^[4]

$$\Delta_f H^\circ_{(g,M)} = H^{298}_{(g,M)} - \sum H^{298}_{(g,A)} + \sum \Delta_f H^\circ_{(g,A)} \quad (1)$$

The solid-state enthalpy of formation for neutral compounds can be estimated with Trouton's rule according to Equation 2,^[5] where *T* is either the melting point or the decomposition temperature (in K) if no melting occurs prior to decomposition.

$$\Delta_f H^\circ_{(s)} = \Delta_f H^\circ_{(g)} - \Delta_{\text{sub}} H = \Delta_f H^\circ_{(g)} - (188 / \text{J mol}^{-1} \text{ K}^{-1} \times T) \quad (2)$$

Finally, the solid-state molar enthalpies of formation ($\Delta_f H^\circ$) were used to calculate the solid-state energies of formation ($\Delta_f U^\circ$) according to Equation 3, with Δn being the change of moles of gaseous components.

$$\Delta U = \Delta H - \Delta n RT \quad (3)$$

Table S2: CBS-4M calculation results.

M	Point group	$-H / \text{a.u.}$
3	C_1	1041.39643
DNBTO²⁻	C_1	1040.299863
NH₄⁺	T_d	56.796608
N₂H₅⁺	C_s	112.030523
NH₄O⁺	C_s	131.863249
G⁺, C(NH₂)₃⁺	C_1	205.453192
AG⁺, (H₂N)₂C(NHNH₂)⁺	C_s	260.701802
TAG⁺	C_3	371.197775
RDX	C_1	896.346781

Table S3. Literature values for atomic $\Delta H^\circ_f{}^{298} / \text{kcal mol}^{-1}$

	NIST ⁴
H	52.1
C	171.3
N	113.0
O	59.6

Table S4: Enthalpies of the gas-phase species M.

M	sum formula	$\Delta_f H^\circ_{(g)} / \text{kJ mol}^{-1}$
3	$\text{C}_4\text{H}_2\text{N}_8\text{O}_6$	380.0
DNBTO²⁻	$\text{C}_4\text{N}_8\text{O}_6^{2-}$	192.4
NH₄⁺	NH_4^+	151.9
N₂H₅⁺	N_2H_5^+	185.1
NH₄O⁺	NH_4O^+	164.1
G⁺	CH_6N_3^+	137.1
AG⁺	CH_7N_4^+	161.0
TAG⁺	CH_9N_6^+	208.8
RDX	$\text{C}_3\text{H}_6\text{N}_6\text{O}_6$	174.2
4a	$\text{C}_4\text{H}_8\text{N}_{10}\text{O}_6$	827.7
4b	$\text{C}_4\text{H}_{10}\text{N}_{12}\text{O}_6$	965.8
4c	$\text{C}_4\text{H}_8\text{N}_{10}\text{O}_8$	878.8
4d	$\text{C}_6\text{H}_{12}\text{N}_{14}\text{O}_6$	763.6
4e	$\text{C}_4\text{H}_{14}\text{N}_{16}\text{O}_6$	863.1
4f	$\text{C}_6\text{H}_{18}\text{N}_{20}\text{O}_6$	1065.4

Table S5: Molecular volumes, lattice energies and lattice enthalpies.

	V_M / nm^3	$U_L / \text{kJ mol}^{-1}$	$\Delta H_L / \text{kJ mol}^{-1}$
4a	0.272	1351.9	1359.4
4b	0.291	1318.4	1325.8
4c	0.276	1344.9	1352.3
4d	0.350	1229.2	1236.7
4e	0.383	1187.4	1194.9
4f	0.446	1119.3	1126.7

Table S6: Solid state energies of formation ($\Delta_f U^\circ$).

	$\Delta_f H^\circ(s) /$ kJ mol^{-1}	$\Delta n^{[a]}$	$\Delta_f U^\circ(s) /$ kJ mol^{-1}	$M / \text{g mol}^{-1}$	$\Delta_f U^\circ(s) / \text{kJ kg}^{-1}$
3	290.1	8.0	310.0	258.11	1200.9
4a	103.6	12.0	133.4	292.17	456.5
4b	413.4	14.0	448.1	322.20	1390.8
4c	212.8	13.0	245.1	324.17	756.0
4d	98.1	16.0	137.8	376.25	366.2
4e	338.9	18.0	383.6	406.28	944.1
4f	811.7	22.0	866.3	466.34	1857.6

[a]: n being the change of moles of gaseous components

REFERENCES

- [1] M. J. Frisch, G. W. Trucks, H. B. Schlegel, G. E. Scuseria, M. A. Robb, J. R. Cheeseman, G. Scalmani, V. Barone, B. Mennucci, G. A. Petersson, H. Nakatsuji, M. Caricato, X. Li, H. P. Hratchian, A. F. Izmaylov, J. Bloino, G. Zheng, J. L. Sonnenberg, M. Hada, M. Ehara, K. Toyota, R. Fukuda, J. Hasegawa, M. Ishida, T. Nakajima, Y. Honda, O. Kitao, H. Nakai, T. Vreven, J. A. Montgomery, Jr., J. E. Peralta, F. Ogliaro, M. Bearpark, J. J. Heyd, E. Brothers, K. N. Kudin, V. N. Staroverov, T. Keith, R. Kobayashi, J. Normand, K. Raghavachari, A. Rendell, J. C. Burant, S. S. Iyengar, J. Tomasi, M. Cossi, N. Rega, J. M. Millam, M. Klene, J. E. Knox, J. B. Cross, V. Bakken, C. Adamo, J. Jaramillo, R. Gomperts, R. E. Stratmann, O. Yazyev, A. J. Austin, R. Cammi, C. Pomelli, J. W. Ochterski, R. L. Martin, K. Morokuma, V. G. Zakrzewski, G. A. Voth, P. Salvador, J. J. Dannenberg, S. Dapprich, A. D. Daniels, O. Farkas, J. B. Foresman, J. V. Ortiz, J. Cioslowski, and D. J. Fox, *Gaussian 09 Revision C.01*, Gaussian, Inc., Wallingford, CT, USA, **2010**.
- [2] a) J. W. Ochterski, G. A. Petersson, J. A. Montgomery, *J. Chem. Phys.* **1996**, *104*, 2598–2619; b) J. A. Montgomery, M. J. Frisch, J. W. Ochterski, G. A. Petersson, *J. Chem. Phys.* **2000**, *112*, 6532–6542.
- [3] a) B. M. Rice, S. V. Pai, J. Hare, *Combust. Flame* **1999**, *118*, 445–458; b) B. M. Rice, J. J. Hare, *J. Phys. Chem. A* **2002**, *106*, 1770–1783; c) E. F. C. Byrd, B. M. Rice, *J. Phys. Chem. A* **2006**, *110*, 1005–1013.

- [4] a) P. J. Linstrom, W. G. Mallard (Editors), *NIST Standard Reference Database Number 69*, <http://webbook.nist.gov/chemistry> (accessed December 31, 2012); b) J. D. Cox, D. D. Wagman, V. A. Medvedev, *CODATA Key Values for Thermodynamics*, Hemisphere Publishing Corp., New York, **1984**.
- [5] a) F. Trouton, *Philos. Mag.* **1884**, *18*, 54–57; b) M. S. Westwell, M. S. Searle, D. J. Wales, D. H. Williams, *J. Am. Chem. Soc.* **1995**, *117*, 5013–5015.

SUPPORTING INFORMATION FOR CHAPTER 9

Table S1: Crystallographic data and parameters for compounds **3–7**.

	ACT (3)	ATT*Cl (4*Cl)	NATT * 3H ₂ O (5)	NTT * 2H ₂ O (6)	AzTT * 2H ₂ O (7)
Formula	C ₃ H ₃ N ₅	C ₃ H ₇ N ₈ Cl	C ₃ H ₉ N ₉ O ₅	C ₃ H ₆ N ₈ O ₄	C ₃ H ₆ N ₁₀ O ₂
FW [g mol ⁻¹]	109.1	206.6	251.2	218.1	214.1
Crystal system	monoclinic	monoclinic	monoclinic	triclinic	orthorhombic
Space Group	<i>P</i> 2 ₁ / <i>c</i>	<i>P</i> 2 ₁ / <i>c</i>	<i>P</i> 2 ₁ / <i>c</i>	<i>P</i> -1	<i>Fdd</i> 2
Color / Habit	colorless block	colorless plate	colorless plate	orange block	colorless rod
Size [mm]	0.41x0.35x0.17	0.40x0.40x0.03	0.20x0.20x0.05	0.58x0.50x0.45	0.27x0.08x0.04
<i>a</i> [Å]	5.2690(8)	5.2168(4)	7.2260(5)	5.0703(6)	22.8925(8)
<i>b</i> [Å]	5.4724(6)	9.4832(6)	4.5579(4)	9.0366(9)	42.7552(14)
<i>c</i> [Å]	16.0548(19)	17.0149(10)	31.331(3)	9.9467(11)	3.62200(10)
α [°]	90	90	90	92.601(8)	90
β [°]	90.816(12)	90.685(6)	92.270(7)	102.184(10)	90
γ [°]	90	90	90	100.668(9)	90
<i>V</i> [Å ³]	462.88(10)	841.70(10)	1031.09(15)	436.08(8)	3545.1(2)
<i>Z</i>	4	4	4	2	16
$\rho_{\text{calc.}}$ [g cm ⁻³]	1.5654(3)	1.63033(19)	1.6180(2)	1.6613(3)	1.60493(9)
μ [mm ⁻¹]	0.116	0.431	0.147	0.149	0.135
<i>F</i> (000)	224	424	520	224	1760
$\lambda_{\text{MoK}\alpha}$ [Å]	0.71073	0.71073	0.71073	0.71073	0.71073
<i>T</i> [K]	173	173	173	173	173
Theta Min-Max [°]	4.60–26.47	4.19–26.50	4.52–26.00	4.21–25.99	2.61–27.48
Dataset h	-6; 6	-6; 6	-8; 8	-6; 3	-29; 29
Dataset k	-6; 6	-11; 11	-5; 5	-9; 11	-54; 54
Dataset l	-20; 17	-21; 21	-37; 38	-12; 12	-4; 4
Reflections collected	2333	8601	4958	2252	22687
Independent reflections	954	1746	2024	1689	1177
Observed reflections	649	1481	1466	1430	1102
No. parameters	85	139	190	160	158
<i>R</i> _{int}	0.0413	0.0335	0.0380	0.0083	0.0345
<i>R</i> ₁ , w <i>R</i> ₂ (<i>I</i> > σ <i>I</i> ₀)	0.0435; 0.0888	0.0292; 0.0735	0.0374; 0.0752	0.0332; 0.0830	0.0312; 0.0807
<i>R</i> ₁ , w <i>R</i> ₂ (all data)	0.0746; 0.1061	0.0373; 0.0790	0.0608; 0.0826	0.0332; 0.0830	0.0344; 0.0823
<i>S</i>	1.042	1.059	1.014	1.041	1.080
Resd. Dens. [e Å ⁻³]	0.228; -0.180	0.306; -0.252	0.205; -0.191	0.222; -0.183	0.216; -0.168
Device type	Oxford	Oxford	Oxford	Oxford	Bruker
	Xcalibur3	Xcalibur3	Xcalibur3	Xcalibur3	D8 Quest
	CCD	CCD	CCD	CCD	
Solution	SHELXS-97	SHELXS-97	SHELXS-97	SHELXS-97	SIR-97
Refinement	SHELXL-97	SHELXL-97	SHELXL-97	SHELXL-97	SHELXL-97
Absorption correction	multi-scan	multi-scan	multi-scan	multi-scan	multi-scan
CCDC	906004	906005	906007	906006	906008

Crystals of the chloride salt of **4** suitable for X-Ray analysis could be obtained by slow evaporation of a solution of **4** in 2 M hydrochloric acid. Figure S1 shows the crystal structure of the chloride salt together with the labeling scheme. As it is typical for triazole compounds, the most basic nitrogen atom N3 is protonated, the hydrogen atoms of the amino group are now completely in plane with the triazole ring. Due to the formation of the tetrazole ring, the C2–C3 bond length is increased from 1.438(3) Å (**3**) to 1.451(2) Å in the chloride salt of compound **4**.

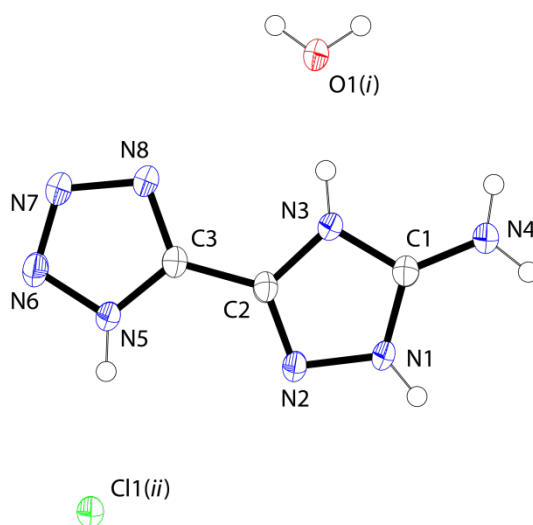


Figure S1: Molecular structure of 5-(5-amino-1,4*H*-1,2,4-triazolium-3-yl)-1*H*-tetrazole chloride, thermal ellipsoids are set to 50 % probability, symmetry codes: (i) $1-x, 1/2+y, 1/2-z$; (ii) $1-x, -y, -z$.

SUPPORTING INFORMATION FOR CHAPTER 10

Table S1: Crystallographic data for **5**, **6** and **7** (173 K).

	5	6	7
Formula	C ₃ H ₉ N ₉ O ₆	C ₃ H ₆ N ₈ O ₅	C ₃ H ₄ N ₁₀ O ₂
<i>M</i> / g mol ⁻¹	267.16	234.13	212.16
Color	colorless	colorless	colorless
Habit	block	plate	block
Crystal size / mm	0.45 × 0.40 × 0.20	0.35 × 0.20 × 0.02	0.40 × 0.21 × 0.12
Crystal system	monoclinic	triclinic	triclinic
Space Group	<i>C</i> 2/ <i>c</i> (15)	<i>P</i> -1 (2)	<i>P</i> -1 (2)
<i>a</i> / Å	12.5692(7)	7.1459(9)	7.3393(8)
<i>b</i> / Å	6.6184(5)	7.1453(9)	7.3888(10)
<i>c</i> / Å	24.9737(13)	9.0182(11)	7.8723(9)
<i>α</i> / °	90	75.900(10)	97.515(10)
<i>β</i> / °	101.062(5)	74.281(10)	95.120(9)
<i>γ</i> / °	90	85.007(10)	98.213(10)
<i>V</i> / Å ³	2038.9(2)	429.78(9)	416.35(9)
<i>Z</i>	8	2	2
<i>ρ</i> _{calc.} / g cm ⁻³	1.741	1.809	1.692
<i>T</i> / K	173(2)	173(2)	173(2)
<i>F</i> (000)	1104	240	216
<i>μ</i> / mm ⁻¹	0.161	0.166	0.143
<i>λ</i> _{MoKα} / Å	0.71073	0.71073	0.71073
<i>θ</i> range / °	4.47–27.00	4.21–26.49	4.29–26.00
Dataset (<i>h</i> ; <i>k</i> ; <i>l</i>)	–14:16; –8:7; –31:26	–8:8; –8:4; –10:11	–8:9; –8:9; –7:9
Reflections collected	5523	2340	2174
Independent reflections	2200	1754	1618
Observed reflections	1646	1287	1409
<i>R</i> _{int.}	0.0280	0.0207	0.0145
Parameters	212	163	152
<i>R</i> ₁ (obs.)	0.0396	0.0430	0.0344
<i>wR</i> ₂ (all data)	0.1000	0.0976	0.0924
<i>S</i>	1.075	1.041	1.034
Res. dens. / e Å ⁻³	–0.221:0.337	–0.291:0.208	–0.212:0.268
Solution	SIR97	SIR97	SHELXS-97
Refinement	SHELXL-97	SHELXL-97	SHELXL-97
Absorption correction	multi-scan	multi-scan	multi-scan
CCDC	926336	926337	926338

Table S2: Crystallographic data for **7** (298 K) and **8**.

	7	8
Formula	C ₃ H ₄ N ₁₀ O ₂	C ₃ H ₄ ClN ₇ O ₂
<i>M</i> / g mol ^{−1}	212.16	205.56
Color	colorless	colorless
Habit	block	rod
Crystal size / mm	0.41 × 0.22 × 0.09	0.54 × 0.19 × 0.03
Crystal system	triclinic	monoclinic
Space Group	<i>P</i> −1 (2)	<i>C</i> 2/ <i>c</i> (15)
<i>a</i> / Å	7.4228(11)	25.021(9)
<i>b</i> / Å	7.4330(11)	3.9720(9)
<i>c</i> / Å	7.9156(13)	19.722(7)
<i>α</i> / °	95.424(13)	90
<i>β</i> / °	97.670(13)	126.96(6)
<i>γ</i> / °	97.908(12)	90
<i>V</i> / Å ³	425.86(11)	1566.2(9)
<i>Z</i>	2	9
<i>ρ</i> _{calc.} / g cm ^{−3}	1.655	1.744
<i>T</i> / K	298(2)	173(2)
<i>F</i> (000)	216	832
<i>μ</i> / mm ^{−1}	0.140	0.469
<i>λ</i> _{MoKα} / Å	0.71073	0.71073
<i>θ</i> range / °	4.24–26.37	4.15–25.99
Dataset (<i>h</i> ; <i>k</i> ; <i>l</i>)	−7:9; −9:9; −8:9	−30:30; −4:4; −21:24
Reflections collected	2308	3689
Independent reflections	1729	1525
Observed reflections	1406	1177
<i>R</i> _{int.}	0.0164	0.0282
Parameters	152	130
<i>R</i> ₁ (obs.)	0.0391	0.0380
<i>wR</i> ₂ (all data)	0.0970	0.1094
<i>S</i>	1.109	1.048
Res. dens. / e Å ^{−3}	−0.209:0.149	−0.211:0.252
Solution	SIR97	SIR97
Refinement	SHELXL-97	SHELXL-97
Absorption correction	multi-scan	multi-scan
CCDC	926339	926340

Crystal Structures

The undesired side-product 5-(5-chloro-1*H*-1,2,4-triazol-3-yl)tetrazol-1-ol (**8**) crystallizes also as monohydrate in the monoclinic space group *C2/c* with two molecules in the unit cell and a cell volume of 1566.2(9) Å³. The formula unit of **8** together with the atom labeling is presented in Figure S1.

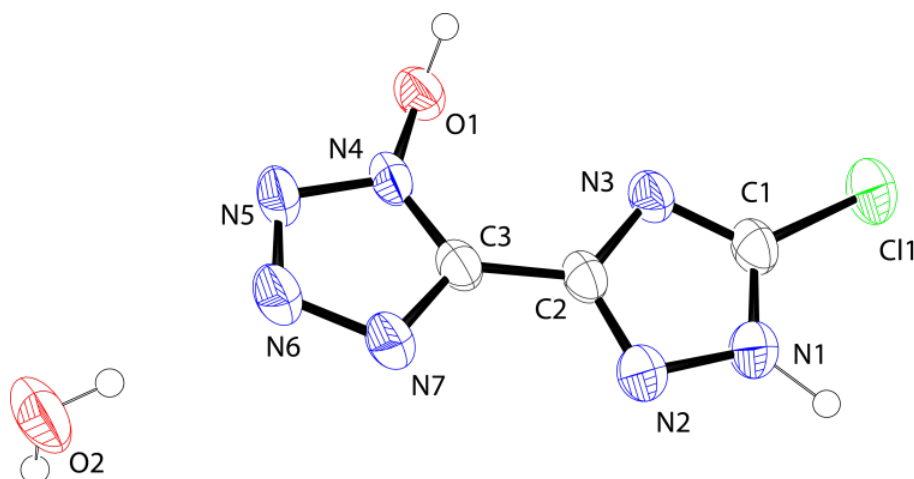


Figure S1: Molecular structure of 5-(5-chloro-1*H*-1,2,4-triazol-3-yl)tetrazol-1-ol (**8**). Thermal ellipsoids are set to 50 % probability.

Heats of Formation

In bomb calorimetric measurements nitrogen-rich highly energetic compounds tend to burn incompletely due to the trend of explosion. Oftentimes wrong heats of combustion ($\Delta_c H$) and finally wrong heats of formation ($\Delta_f H^\circ$) are obtained. Therefore the heats of formation of **5–7** have been calculated on the same level for better comparison. All calculations were carried out using the Gaussian 09 (revision C.01) program package.^[1] The enthalpies (*H*) were calculated using the complete basis set (CBS) method described by Petersson and coworkers in order to obtain very accurate values. In this study we applied the modified CBS-4M method (M referring to the use of minimal population localization) which is a re-parameterized version of the original CBS-4 method and also includes some additional empirical corrections.^[2]

The enthalpies of the gas-phase species M were calculated by the atomization energy method according to Equation 1,^[3] using literature values for atomic $\Delta_f H^\circ_{(g,A)}$.^[4]

$$\Delta_f H^\circ_{(g,M)} = H^{298}_{(g,M)} - \sum H^{298}_{(g,A)} + \sum \Delta_f H^\circ_{(g,A)} \quad (1)$$

The solid-state enthalpy of formation for neutral compounds can be estimated with Trouton's rule according to Equation 2,^[5] where *T* is either the melting point or the decomposition temperature (in K) if no melting occurs prior to decomposition.

$$\Delta_f H^\circ_{(s)} = \Delta_f H^\circ_{(g)} - \Delta_{\text{sub}} H = \Delta_f H^\circ_{(g)} - (188 / \text{J mol}^{-1} \text{K}^{-1} \times T) \quad (2)$$

Finally, the solid-state molar enthalpies of formation ($\Delta_f H^\circ$) were used to calculate the solid-state energies of formation ($\Delta_f U^\circ$) according to Equation 3, with Δn being the change of moles of gaseous components.

$$\Delta U = \Delta H - \Delta n RT \quad (3)$$

Table S3: CBS-4M calculation results.

M	PG ^[a]	$-H / \text{a.u.}$ ^[b]	$\Delta_f H^\circ_{(g)} / \text{kJ mol}^{-1}$ ^[c]	$-\Delta n$ ^[d]
5	C ₁	833.286389	587.7	7.5
6	C ₁	778.023249	526.3	6.5
7	C ₁	737.128110	862.2	6.5
RDX	C ₁	896.346781	174.2	9.0
H		0.500991		
C		37.786156		
N		54.522462		
O		74.991202		

[a] Point group, [b] CBS-4M calculated enthalpy, [c] gas-phase enthalpy of formation, [d] change of moles of gaseous components.

References

- [1] M. J. Frisch, G. W. Trucks, H. B. Schlegel, G. E. Scuseria, M. A. Robb, J. R. Cheeseman, G. Scalmani, V. Barone, B. Mennucci, G. A. Petersson, H. Nakatsuji, M. Caricato, X. Li, H. P. Hratchian, A. F. Izmaylov, J. Bloino, G. Zheng, J. L. Sonnenberg, M. Hada, M. Ehara, K. Toyota, R. Fukuda, J. Hasegawa, M. Ishida, T. Nakajima, Y. Honda, O. Kitao, H. Nakai, T. Vreven, J. A. Montgomery, Jr., J. E. Peralta, F. Ogliaro, M. Bearpark, J. J. Heyd, E. Brothers, K. N. Kudin, V. N. Staroverov, T. Keith, R. Kobayashi, J. Normand, K. Raghavachari, A. Rendell, J. C. Burant, S. S. Iyengar, J. Tomasi, M. Cossi, N. Rega, J. M. Millam, M. Klene, J. E. Knox, J. B. Cross, V. Bakken, C. Adamo, J. Jaramillo, R. Gomperts, R. E. Stratmann, O. Yazyev, A. J. Austin, R. Cammi, C. Pomelli, J. W. Ochterski, R. L. Martin, K. Morokuma, V. G. Zakrzewski, G. A. Voth, P. Salvador, J. J. Dannenberg, S. Dapprich, A. D. Daniels, O. Farkas, J. B. Foresman, J. V. Ortiz, J. Cioslowski, and D. J. Fox, *Gaussian 09 Revision C.01*, Gaussian, Inc., Wallingford, CT, USA, **2010**.

- [2] a) J. W. Ochterski, G. A. Petersson, J. A. Montgomery, *J. Chem. Phys.* **1996**, *104*, 2598–2619; b) J. A. Montgomery, M. J. Frisch, J. W. Ochterski, G. A. Petersson, *J. Chem. Phys.* **2000**, *112*, 6532–6542.
- [3] a) B. M. Rice, S. V. Pai, J. Hare, *Combust. Flame* **1999**, *118*, 445–458; b) B. M. Rice, J. J. Hare, *J. Phys. Chem. A* **2002**, *106*, 1770–1783; c) E. F. C. Byrd, B. M. Rice, *J. Phys. Chem. A* **2006**, *110*, 1005–1013.
- [4] a) P. J. Linstrom, W. G. Mallard (Editors), *NIST Standard Reference Database Number 69*, <http://webbook.nist.gov/chemistry> (accessed December 31, 2012); b) J. D. Cox, D. D. Wagman, V. A. Medvedev, *CODATA Key Values for Thermodynamics*, Hemisphere Publishing Corp., New York, **1984**.
- [5] a) F. Trouton, *Philos. Mag.* **1884**, *18*, 54–57; b) M. S. Westwell, M. S. Searle, D. J. Wales, D. H. Williams, *J. Am. Chem. Soc.* **1995**, *117*, 5013–5015.

SUPPORTING INFORMATION FOR CHAPTER 11

Heats of Formation

In bomb calorimetric measurements nitrogen-rich highly energetic compounds tend to burn incompletely due to the trend of explosion. Oftentimes wrong heats of combustion ($\Delta_c H$) and finally wrong heats of formation ($\Delta_f H^\circ$) are obtained. Therefore the heats of formation of all compounds have been calculated on the same level for better comparison. All calculations were carried out using the Gaussian 09 (revision C.01) program package.^[1] The enthalpies (H) were calculated using the complete basis set (CBS) method described by Petersson and coworkers in order to obtain very accurate values. In this study we applied the modified CBS-4M method (M referring to the use of minimal population localization) which is a re-parameterized version of the original CBS-4 method and also includes some additional empirical corrections.^[2]

The enthalpies of the gas-phase species M were calculated by the atomization energy method according to Equation 1,^[3] using literature values for atomic $\Delta_f H^\circ_{(g,A)}$.^[4]

$$\Delta_f H^\circ_{(g,M)} = H^{298}_{(g,M)} - \sum H^{298}_{(g,A)} + \sum \Delta_f H^\circ_{(g,A)} \quad (1)$$

The solid-state enthalpy of formation for neutral compounds can be estimated with Trouton's rule according to Equation 2,^[5] where T is either the melting point or the decomposition temperature (in K) if no melting occurs prior to decomposition.

$$\Delta_f H^\circ_{(s)} = \Delta_f H^\circ_{(g)} - \Delta_{\text{sub}} H = \Delta_f H^\circ_{(g)} - (188 / \text{J mol}^{-1} \text{ K}^{-1} \times T) \quad (2)$$

Finally, the solid-state molar enthalpies of formation ($\Delta_f H^\circ$) were used to calculate the solid-state energies of formation ($\Delta_f U^\circ$) according to Equation 3, with Δn being the change of moles of gaseous components.

$$\Delta U = \Delta H - \Delta n RT \quad (3)$$

Table S1: CBS-4M calculation results.

M	PG ^[a]	$-H$ / a.u. ^[b]	$\Delta_f H^\circ_{(g)}$ / kJ mol ⁻¹ ^[c]	$-\Delta n$ ^[d]
NTT ²⁻	C ₁	701.815176	405.4	–
NATT ²⁻	C ₁	757.100721	407.9	–
NTTO ²⁻	C ₁	776.901276	405.4	–
NATTO ²⁻	C ₁	832.187768	405.4	–
NH₄O ⁺	C _s	131.863249	164.1	–
G ⁺ , CH₆N₃ ⁺	C ₁	205.453192	137.1	–
TAG ⁺ , CH₉N₆ ⁺	C ₃	371.197775	208.8	–
1a	–	–	1091.7	11.0
1b	–	–	976.6	14.0
1c	–	–	1248.4	20.0
2a	–	–	1094.3	12.0
2b	–	–	979.1	15.0
2c	–	–	1281.0	21.0
3a	–	–	1091.8	11.5
3b	–	–	976.6	14.5
3c	–	–	1278.4	20.5
4a	–	–	1091.8	12.5
4b	–	–	976.6	15.5
4c	–	–	1278.5	21.5
RDX	C ₁	896.346781	174.2	9.0

[a] Point group, [b] CBS-4M calculated enthalpy, [c] gas-phase enthalpy of formation, [d] change of moles of gaseous components.

Table S2. Literature values for atomic $\Delta H_f^{\circ 298}$ / kcal mol⁻¹

	NIST ⁴
H	52.1
C	171.3
N	113.0
O	59.6

Table S3: Molecular volumes, lattice energies and lattice enthalpies.

	V_M /nm ³	U_L /kJ mol ⁻¹	ΔH_L / kJ mol ⁻¹
1a	0.224	1454.3	1461.7
1b	0.298	1306.1	1313.5
1c	0.384	1185.7	1193.2
2a	0.239	1419.4	1426.8
2b	0.313	1282.0	1289.4
2c	0.399	1168.4	1175.8
3a	0.240	1417.2	1422.1
3b	0.314	1280.4	1287.8
3c	0.400	1167.3	1174.7
4a	0.270	1355.7	1360.7
4b	0.344	1236.7	1244.1
4c	0.430	1135.2	1142.7

References

- [1] M. J. Frisch, G. W. Trucks, H. B. Schlegel, G. E. Scuseria, M. A. Robb, J. R. Cheeseman, G. Scalmani, V. Barone, B. Mennucci, G. A. Petersson, H. Nakatsuji, M. Caricato, X. Li, H. P. Hratchian, A. F. Izmaylov, J. Bloino, G. Zheng, J. L. Sonnenberg, M. Hada, M. Ehara, K. Toyota, R. Fukuda, J. Hasegawa, M. Ishida, T. Nakajima, Y. Honda, O. Kitao, H. Nakai, T. Vreven, J. A. Montgomery, Jr., J. E. Peralta, F. Ogliaro, M. Bearpark, J. J. Heyd, E. Brothers, K. N. Kudin, V. N. Staroverov, T. Keith, R. Kobayashi, J. Normand, K. Raghavachari, A. Rendell, J. C. Burant, S. S. Iyengar, J. Tomasi, M. Cossi, N. Rega, J. M. Millam, M. Klene, J. E. Knox, J. B. Cross, V. Bakken, C. Adamo, J. Jaramillo, R. Gomperts, R. E. Stratmann, O. Yazyev, A. J. Austin, R. Cammi, C. Pomelli, J. W. Ochterski, R. L. Martin, K. Morokuma, V. G. Zakrzewski, G. A. Voth, P. Salvador, J. J. Dannenberg, S. Dapprich, A. D. Daniels, O. Farkas, J. B. Foresman, J. V. Ortiz, J. Cioslowski, and D. J. Fox, *Gaussian 09 Revision C.01*, Gaussian, Inc., Wallingford, CT, USA, **2010**.
- [2] a) J. W. Ochterski, G. A. Petersson, J. A. Montgomery, *J. Chem. Phys.* **1996**, *104*, 2598–2619; b) J. A. Montgomery, M. J. Frisch, J. W. Ochterski, G. A. Petersson, *J. Chem. Phys.* **2000**, *112*, 6532–6542.
- [3] a) B. M. Rice, S. V. Pai, J. Hare, *Combust. Flame* **1999**, *118*, 445–458; b) B. M. Rice, J. J. Hare, *J. Phys. Chem. A* **2002**, *106*, 1770–1783; c) E. F. C. Byrd, B. M. Rice, *J. Phys. Chem. A* **2006**, *110*, 1005–1013.
- [4] a) P. J. Linstrom, W. G. Mallard (Editors), *NIST Standard Reference Database Number 69*, <http://webbook.nist.gov/chemistry> (accessed December 31, 2012); b) J. D. Cox, D. D. Wagman, V. A. Medvedev, *CODATA Key Values for Thermodynamics*, Hemisphere Publishing Corp., New York, **1984**.
- [5] a) F. Trouton, *Philos. Mag.* **1884**, *18*, 54–57; b) M. S. Westwell, M. S. Searle, D. J. Wales, D. H. Williams, *J. Am. Chem. Soc.* **1995**, *117*, 5013–5015.

CURRICULUM VITAE

Alexander Armin Dippold
Heinrich-Heine-Str. 10, 80686 München
09.05.1986 in Rosenheim

■ EDUCATION

- | | |
|----------------------------------|---------------------------------------------------------------------------------------------------------------------------------------------------------------------------------------|
| 10/2010 – 09/2013 | Dissertation , Ludwig Maximilian University Munich
Research Group Prof. Thomas M. Klapötke,
<i>Nitrogen-Rich Energetic Materials based on 1,2,4-Triazole Derivatives</i> |
| 10/2008 – 09/2010 | Master of Science (Chemistry) , LMU Munich, Master
Thesis in the research group of Prof. Thomas M. Klapötke, |
| 10/2005 – 09/2008
1996 – 2005 | Bachelor of Science (Chemistry and Biochemistry)
Gymnasiums Miesbach, Abitur |

BIBLIOGRAPHY**PUBLICATIONS**

- [1] Alexander A. Dippold, Thomas M. Klapötke, Franz A. Martin, "Synthesis and Characterization of Bis(triaminoguanidinium) 5,5'-Dinitrimino-3,3'-azo-1*H*-1,2,4-triazolate – A Novel Insensitive Energetic Material", *Z. Anorg. Allg. Chem.* **2011**, 673(9), 1181-1193.
- [2] Alexander A. Dippold, Thomas M. Klapötke; "Synthesis and Characterization of 3,3'-Bis(Dinitromethyl)-5,5'-Azo-1*H*-1,2,4-Triazole", *Z. Anorg. Allg. Chem.* **2011**, 637, 1453-1457.
- [3] Alexander A. Dippold, Michael Feller, Thomas M. Klapötke, 5,5'-Dinitrimino-3,3'-methylene-1*H*-1,2,4-bistriazole - A Metal Free Primary Explosive Combining Excellent Thermal Stability and High Performance, *Centr. Europ. J. Energ. Mat.* **2011**, 8, 261-278.
- [4] Alexander A. Dippold, Thomas M. Klapötke, Franz A. Martin and Sandra Wiedbrauk, Nitraminoazoles Based on ANTA – A Comprehensive Study of Structural and Energetic Properties, *Eur. J. Inorg. Chem.* **2012**, 14, 2429-2443.
- [5] Alexander A. Dippold, Thomas M. Klapötke, Nils Winter,, Insensitive Nitrogen-Rich Energetic Compounds Based on the 5,5'-Dinitro-3,3'-bi-1,2,4-triazol-2-ide Anion, *Eur. J. Inorg. Chem.* **2012**, 21, 3474-3484.
- [6] Alexander A. Dippold, Thomas M. Klapötke, Nitrogen-rich Bistriazoles - A comparative study of structural and energetic properties, *Chem. Eur. J.* **2012**, 18, 16742–16753.
- [7] Alexander A. Dippold, Thomas M. Klapötke, Synthesis and characterization of 5-(1,2,4-Triazol-3-yl)tetrazoles with various functionalities, *Chem. Asian. J.* **2013**, 8, 1463-1471.
- [8] Alexander A. Dippold, Thomas M. Klapötke, Daniel Izsák, A Study of 5-(1,2,4-Triazol-C-yl)tetrazol-1-ols: Combining the Benefits of Different Heterocycles for the Design of Energetic Materials, *Chem. Eur. J.* **2013**, *in press*.
- [9] Alexander A. Dippold, Thomas M. Klapötke, A Study of Dinitro-Bis-1,2,4-triazole-1,1-diol and Derivatives – Design of High Performance Insensitive Energetic Materials by the Introduction of N-Oxides, *J. Am. Chem. Soc.* **2013**, 135, 9931-9938.

- [10] Alexander A. Dippold, Thomas M. Klapötke, Michaela Oswald, Asymmetrically substituted 5,5'-Bistriazoles – Nitrogen Rich materials with various energetic functionalities, *Dalton. T.* **2013**, 42, 11136 - 11145.
- [11] Alexander A. Dippold, Thomas M. Klapötke, “A comparative study on insensitive energetic derivatives of 5-(1,2,4-triazol-C-yl)-tetrazoles and their 1-hydroxy-tetrazole analogues”, *Z. Anorg. Allg. Chem.* **2013**, in press.

PATENT

- [1] Alexander A. Dippold, Thomas M. Klapötke, „*Synthese der neuen Sekundärexplosivstoffe MAD-X1, MAD-X2 und MAD-X3*“, Deutsche Patentanmeldung durch die Bayrische Patentallianz GmbH.

CONFERENCE PROCEEDINGS

- [1] Alexander A. Dippold, Thomas. M. Klapötke, Franz A. Martin; “Synthesis and energetic properties of novel nitramino- and nitrimino azoles and corresponding nitrogen rich salts”, *New Trends in Research of Energetic Materials, Proceedings of the 14th Seminar, University of Pardubice, Czech Republic*, **2011**; Vol. 2, p.579-592.
- [2] Alexander A. Dippold, Thomas. M. Klapötke, Franz. A. Martin; “Synthesis and Characterization of Bis(triaminoguanidinium) 5,5'-Dinitrimino-3,3'-azo-1H-1,2,4-triazolate – A promising RDX replacement”, *New Trends in Research of Energetic Materials, Proceedings of the 14th Seminar, University of Pardubice, Czech Republic*, **2011**; Vol. 2, p.561-578.
- [3] Alexander A. Dippold, T. M. Klapötke, Michael Feller, “Synthesis and energetic properties of 5,5'-dinitrimino-3,3'-methylene-1H-1,2,4-triazole and selected nitrogen rich salts”, *New Trends in Research of Energetic Materials, Proceedings of the 14th Seminar, University of Pardubice, Czech Republic*, **2011**; Vol. 2, p.550-560.

AWARD

Master Stipendium of the Dr. Klaus Römer Stiftung (Dez. 2011) for excellent research during the Master Thesis.